VIBRATION ATTENUATION

BY MASS REDISTRIBUTION

A THESIS

SUBMITTED TO THE COLLEGE OF GRADUATE STUDIES AND RESEARCH

IN PARTIAL FULFILLMENT OF THE REQUIREMENTS

FOR THE DEGREE OF DOCTORATE IN PHILOSOPHY

IN THE

DEPARTMENT OF MECHANICAL ENGINEERING

UNIVERSITY OF SASKATCHEWAN

BY

DENISE S.(DERBY) STILLING
SASKATOON, SASKATCHEWAN, CANADA
SPRING, 2000

Permission to Use

The author has agreed that the library at the University of Saskatchewan may make this freely available for inspection. It is understood that due recognition will be given to the author of this thesis and to the University of Saskatchewan in any use of the material in this thesis. Copying or publication or any other use of the thesis for financial gain without approval by the University of Saskatchewan and author's written permission is prohibited.

Requests for permission to copy or to make other use of material in this thesis in whole or in part should be addressed to:

Head of the Department of Mechanical Engineering
University of Saskatchewan
57 Campus Drive
Saskatoon, Saskatchewan
Canada
S7N 5A9

Acknowledgment

The education, experience and lessons as acquired during the course of this program were multi-faceted. Several organizations and individuals deserve recognition.

The support and encouragement of friends and family made completion possible. Special appreciation is extended to the Vice-president at the University of Saskatchewan, Dr. Pezer for just insight and internal direction in reviewing the conditions of this program.

Gratefully acknowledged is the financial support awarded from national and international organizations: Zonta International Foundation -- Amelia Earhart Fellowship and Canadian Federation of University Women -- Margaret McWilliam Scholarship. Also, funding was received from University of Saskatchewan Graduate Student Scholarships and National Science and Engineering Research Council Awards.

Finally, mention is given to the primary research supervisor, Dr. L.G. Watson for the research direction and experiences, and to the technical thesis documentation supervisors, Dr. W. Szyszkowski and Dr. R. Burton.

Abstract

A nontraditional approach for active structural vibration attenuation was proposed using mass redistribution. The focus was on pendulum structures where the objective was to examine the effectiveness of mass reconfiguration along or within a structure to attenuate its vibrational energy.

The mechanics associated with a translating mass along a rotating structure give rise to a Coriolis inertia force which either opposes or increases angular oscillations, thereby producing positive or negative damping, respectively. A strategy of cycling the mass to maximize attenuation and minimize amplification required the mass be moved at twice the frequency of the structural vibrations and be properly coordinated with the angular oscillations. The desired coordination involved moving the mass away from the pivot as the pendulum nears its vertical position and moving the mass towards the pivot when the pendulum nears its maximum angular excursion.

System mass reconfiguration was analyzed by studying various mass displacement profiles including sinusoidal, piece-wise constant velocity and modified proportional and derivative action patterns. These strategies were optimized for various time intervals to maximize the rate of energy attenuation or minimize the final energy state. For small amplitude oscillations with sinusoidal mass motion, the dynamic behavior was modeled by Mathieu-Hill equations to explain the beating phenomenon that occurred when the frequency of the mass motion remained constant.

Several control systems were designed to generate aforementioned mass reconfiguration profiles. The methodologies included human operator, modified proportional and derivative action, knowledge or rule based and artificial neural network controllers. The human operator system improved with experience and was the most effective. Other systems depended on the chosen parmeterization or the implementation of self-adjusting parameters.

Several unique tools were developed during the course of this research, including simulation, optimization and control software.

Table of Contents

List of Figures

List of Tables

Nomenclature and Abbreviations

The basic symbol, notation and abbreviations as used throughout the thesis are listed below. To facilitate easy reference, the table has been divided into appropriate categories. Also, the section of its first occurrence has been included. As necessary, descriptions appears in the text at the first use of the symbol/notation. To eliminate ambiguity when symbols are used with multiple meanings, the definitions are explicitly stated.

Symbol	Description	First Occurrence
	Text and Abbreviations	
KBS	knowledge based system	2.4
ANN	artificial neural networks	2.4
XOR	exclusive or	6.2
BIOS	Basic Input and Output Systems	6.2.1
	General	
$\vec{x}$	vector notation for variable, x	2.2.1.1
t	time	2.2.1.2
$\dot{x},\ddot{x}$	first and second time derivative of variable, x, respectively	2.2.1.1
$\frac{d}{dt}$	first derivative with respect to time	2.4
∂	partial derivative	Appendix C
$f(t)$	function f that is dependent on time	2.2.1.1
o	initial condition / reference to pivot (subscript)	3.3.3,3.3.3
max	maximum magnitude (subscript)	2.2.1.1
min	minimum magnitude (subscript)	2.2.1.1
REF	reference value (subscript)	2.3
$\in$	"belongs" or is an element of	3.3.3
	Mechanics: Pendulum Modeling	
X-Y-Z	fixed or absolute coordinate system	2.2.1.1
x-y-z	moving, rotational coordinate system	2.2.1.1
$\vec{i},\vec{j},\vec{k}$	unit vectors for moving frame of reference corresponding to x-y and z respectively	2.2.1.1

Symbol	Description	Section
A	arbitrary point of interest	2.2.1.1
$\bar{r}$	position of point A measured in fixed coordinate system	2.2.1.1
$\bar{r}_o$	absolute position of the origin	2.2.1.1
$\bar{r}_A$	position of point A measured in moving frame of reference	2.2.1.1
θ	absolute angular displacement	2.2.1.1
ω	absolute angular velocity	2.2.1.1
α	absolute angular acceleration	2.2.1.1
$\bar{F}_{external}$	external force acting on the system	2.2.1.1
$\bar{F}, F$	cable tension or force to move the auxiliary mass (slider)	2.2.1.1
m	mass	2.2.1.1
m_p	mass of the pendulum structure	3.2.3
m_s	mass of the auxiliary mass or slider	3.2.3
I_o	moment of inertia about point O	3.2.3
I_p	moment of inertia about center of mass of the pendulum, $_p$	3.2.3
c	arbitrary constant	2.2.1.1
r	translational position of the end bob measured from the pivot	2.2.1.1
R_o	average radial distance of slider mass with respect to the pivot	3.3.1
Δr	change in the translational displacement of the end mass	2.2.1.2
ε	normalized amplitude for auxiliary mass motion	3.3.1
t_i	instant in time where i=1,2, ...	2.2.1.2
Δt	change in time or time step	4.2.3
Δs	change in length of the pendulum cable	2.2.1.2
ds	incremental change in pendulum length	2.2.1.2
s_1, s_2	cable position at times 1 and 2, respectively	2.2.1.2
l_p	location of concentrated mass	3.2.3
l_r	length of uniform rod	3.2.3
l_e	effective length	Appendix C
T	kinetic energy of the system	2.2.1.2
U	potential energy of the system	2.2.1.2
W_{1-2}	work done to or by the system between instances 1 to 2.	2.2.1.2
WE	sum for work-energy balance	Appendix G
g	acceleration due to gravity	2.2.1.1
N	contact force between slider and guide	3.2.3
R_x, R_y	reaction forces at the pivot	3.2.3
$p(m_s,\theta,r,t)$	'pseudo' force	3.2.4

Symbol	Description	Section
$F_{Coriolis}$	inertia Coriolis force	6.4
$F_{gravity}$	force due to gravity	6.4
$F_{inertia}$	inertia force	7.4
F_q	generalized nonconservative force	Appendix C
ω_n	natural frequency	2.2.1.1
ω_d	damped natural frequency	4.6.3.4
ϖ	frequency for motion of the auxiliary mass	3.3.1
ξ	damping ratio	3.3.3
y_1 and y_2	variable transformations (θ and $\dot{\theta}$)	4.2.2.1
T	period of an oscillation	4.2.3
W	magnitude of the moving force ($m_p g$)	4.3
n	scalar for multiplying sinusoidal frequency	4.3
ϕ	phase shift related to mass reconfiguration	4.4.2
θ_a or θ_b	limits to define mass reconfiguration profiles for rule based controllers	4.4.3
E_R	residual kinetic energy of pendulum system	8.2.1.2
E_{SS}	steady state energy of the system	8.2.3
$\mathcal{L}$	Lagrangian: $\mathcal{L} = T - U$	Appendix C
q	generalized coordinate	Appendix C
δ	variational	Appendix C
A, B and C	coefficients to represent physical parameters	Appendix C
	Mechanics: Mass-Spring-Damper	
y	direction of motion for one degree of freedom system	3.3.3
c	damping coefficient	3.3.3
k	stiffness or elastic coefficient	3.3.3
E	energy of system (Δ-change of)	3.3.3
A	amplitude of oscillation	3.3.3
ξ_{EQ}	equivalent damping ratio	3.3.3
	Mathieu and/or Hill Equation	
a, q, z	parameters for canonical form of Mathieu Equation	3.3.2
$\psi(t)$	periodic function used in Hill's equation	3.3.2
μ	characteristic index	3.3.2
τ	dependent variable (e.g. normalized time)	3.3.1, 3.3.2
$\phi(\tau)$	periodic function of τ	3.3.2
c_1, c_2	arbitrary constants	3.3.2
κ	viscous damping coefficient	3.3.2
y	independent variable	3.3.2
u	independent variable	3.3.2
$\bar{a}$	parameter transformation	3.3.2

Symbol	Description	Section
a_i and b_i	characterisitc number defining characteristic curves on Mathieu's stability chart	3.3.2
	Optimization	
a_i	design parameters	4.6.2
A	vector of design parameters	4.6.2
J	objective or cost function for optimization; subscripts "*ip*" and "*fp*" indicates initial or final portion of simulated energy profile	4.6.2
e_{MAX}	local maximum structural energy value	4.6.2
n	number of energy peaks examined in cost function	4.6.2
N	total number of energy peaks in simulation	4.6.2
i	summation index	4.6.2
g and h	vectors	Appendix J
λ,γ and A	scalars and scalar matrix, respectively	Appendix J
$F()$	fitness function with F being an evaluation of the fitness function	Appendix J
	Control Nomenclature	
$\rightarrow$	approaches	2.3
k or K	control gain	2.4,7.2
k_p or K_p	proportional gain	2.4, 5.3
k_d or K_d	derivative gain	2.4, 5.3
$e()$	error signal	2.4
$\tilde{e}()$	normalized error signal	5.3
$m()$	control signal	5.3
Θ	bias	5.3
z^{-1}	time delay function	5.6.3
	Neural Network Nomenclature	
y	output from neural net node	5.6.2
v	internal nodal activation level (linear combination of inputs)	5.6.2
$\varphi()$	activation function	5.6.2
N	number of signals for a node	5.6.2
w_i	adjustable weight associated with the ith input	5.6.2
w_{ij}	adjustable weight connecting the ith input node to the jth node of the next layer	5.6.2
x_i	ith input	5.6.2
I-J-K-L	indices used to label number of nodes in each layer of a neural net	5.6.2
$\vec{X}(t)$	input vector for control system	5.6.3
$\vec{Y}(t)$	output vector for control system	5.6.3

Symbol	Description	Section
z	summation variable for nodal output	8.3.4.3
e	error signal between desired (^{d}) and net output	App. J and K
E_p	error for single pattern for entire output vector	App. J and K
E	error for the complete training suite	App. J and K
η	scaling factors (learning rates)	Appendix. J
δ	adjustment to weighting matrix element	Appendix K
P	number of patterns in a training suite	App. J and K
	Initial Value Solver Algorithms	
h	time step	Appendix E
k_i	intermediate evaluation of function for instance, i	Appendix E
x_n	dependent variable at instance n	Appendix E
y_n	independent variable at instance n	Appendix E
y_p	predicted value for independent variable	Appendix E

1. Introduction

1.1 Vibrations and Attenuation Techniques

Vibration is defined as the oscillatory behavior that all bodies possessing mass and stiffness exhibit when disturbed by either an internal or external force. Unchecked vibration in a structure is usually unwanted and may lead to wear, premature failure due to fatigue or even catastrophic failure. A classic example of the latter is the Tacoma Narrows Bridge where failure has been attributed to wind induced vibrations near the resonant torsion frequency.

There are several undesirable features of vibrations. Vibrations generally result in either large displacements and severe stresses in a structure or produce fluctuating moderate stresses causing material fatigue and wear. Oscillations transmit forces and cause noise that result in discomfort or medical complications for human operators. Energy losses and deteriorating performance due to vibrations can reduce service usefulness and service life. Malfunction or destruction of delicate mechanisms or instrumentation attached to a structure may also occur.

Engineering designs continue to increase strength and reduce material consumption which result in structures that are more susceptible to vibrations. Structures are being developed from high strength, light weight materials with low internal damping. These structures tend to be more flexible and possess lower energy dissipation abilities resulting in more intense vibration responses. Secondly, the efficiency and speed of the systems have increased so that vibration exciting forces tend to be relatively high and the

dynamic systems often contain high energy sources that may create intense vibration problems. Thirdly, dynamic performance requirements are increasingly more stringent; for example, automation in robotic motion for medical laser surgery requires precise trajectories with strict tolerance limits. The resulting design geometry often renders the structure more susceptible to vibrations. Lastly, the protection of operators from harmful vibrations remains critical. Human tolerance of vibrations is affected by several factors, such as subject position, vibration direction, amplitude of acceleration and velocity, range frequency spectrum and duration. [Irwin and Graf, 1979, Boswell and D'Mello, 1993].

The potential engineering applications for attenuating unwanted vibrations are numerous. For example, maintaining structural integrity when subjected to excitation forces (such as: space structures in coupling and de-coupling operations, tall buildings in earthquake regions, off-shore rigs in tidal waters and overhead transmission lines subject to wind and environmental disturbances) requires prompt attenuation of the structural, vibrational energy. For these externally excited vibrations, the structure or system must dissipate the unwanted energy and be returned to its stable, static state.

Previous efforts have tackled the problem of vibration attenuation in a variety of ways ranging from applying rigorous, standard control theory or using advanced material science products [Miura, 1989]. Although this thesis is not intended to provide a treatise on all of the techniques used to reduce or eliminate vibrations, a review of a few of the techniques serves to provide an appreciation for the diversity and richness of this field. Traditionally, vibration attenuation or control generally addressed the source [Irwin and Graf, 1979]. Typically, the system parameters were adjusted to prevent unacceptable vibrations thorough designing a more rigid structure, balancing moving parts, employing enhanced manufacturing techniques or using improved leveling of the structures. This type of engineering has had a reasonable range of application in detuning the system and is followed for systems subjected to

known forcing functions so that the frequency of the forcing function does not coincide with the natural frequency of the structure. Alternatively, vibrations may be isolated in a passive mode using isolation pads, elastomeric mounts or other isolation units. The system can be constrained by applying external forces or boundary conditions to limit deformation and motion. Many solutions along this venue have been and continue to be explored.

Another damping mechanism, a dynamic absorber, offers the advantage of being relatively low cost and assures the required reduction in vibration ratios at resonant frequency by generating inertia. By adding damping, the design of a dynamic absorber can be further enhanced; that is, the response spectrum is broadened in forming an auxiliary mass-damper absorber. Early vibration absorbers included masses that swing like a pendulum, elastic structures or containers filled with separate weights or granular material or fluids, and weights attached with elastic elements in the form of steel springs, rubber members or elastic rods/plates [Korenev and Reznikov, 1993]. Another possibility is employing active vibration control using feedback control [Inman, 1996].

Adaptability of structural properties from recent material advances promises further advancement to this field [Librescu, 1997]. Material advances have also led to the development of materials with good energy dissipation properties [Bert, 1980], especially polymeric material [Henderson, 1980]. Also, collocated sensors/actuators have been embedded within structures to control dynamic behavior [Crawley, 1994]. Variable geometric or configurable structures employing advances in sensor and actuator technology may be applied to this field [Wada et al., 1989]. The active, internal members have controlled extension and contraction abilities producing a vibrational damper. Preliminary results indicate improved efficiency, when compared to conventional inertia systems consisting merely of a mass [Lu et al., 1992].

The research reported herein examines the challenging problem of attenuating vibrations in the absence of any physical damping either by internal or external friction. The damping-like effects are achieved by using a technique of mass reconfiguration. By coordinating the motion of an auxiliary mass or slider along or within a structure, the dynamic characteristics of the system are altered and its energy can be dissipated. Several displacement profiles for the slider are discussed along with their optimization.

Integrating the motion of the auxiliary mass with the structure is critical to the success of this approach, thus creating a control challenge. Several strategies to effect appropriate control have been postulated including formulating human performance in terms of rule base logic or knowledge based systems, implementing classical control information and applying artificial neural network technology to replicate a successful control strategy. The energy attenuation for these control techniques are applied to the pendulum example.

1.2 Thesis Overview

The purpose of this thesis is to examine a technique for structural vibration attenuation through mass reconfiguration. The dynamic system consists of an auxiliary mass that is slid along a pendulum to alter the structural vibrations. By examining the mechanics of the translational motion of a mass along a rotating system, a strategy is deduced to dissipate the structural energy.

Various control actions and controllers are used to implement attenuation. The controllers examined include a human operator, fixed and variable frequency motion, knowledge based controller, modified proportional and derivative action and artificial neural networks.

This thesis addresses some of the challenges associated with attenuating vibrations via mass reconfiguration. The research spans several fields including structural and vibrational analysis, numerical simulations and

optimization, controls and artificial intelligence technology. Hence, the terminology as used within the thesis has been summarized and appears in Appendix A.

1.3 Thesis Objective

The objective of this research is to investigate the technique of mass redistribution to attenuate structural vibrations. Specifically, the technique has been applied where a mass traverses a pendulum structure. Various controllers are used to effect the strategy to attenuate the pendulum's oscillations.

1.4 Thesis Organization

The documentation focuses on the investigation of mass redistribution for pendulum systems. First, the research perspective is presented in Chapter 2. Both an overview of the premise of the original vibration attenuation technique is reviewed and the requirements for the controlled system are presented. Chapter 3 examines the physics and unique characteristics associated with the governing differential equation between the radially translating mass on the oscillating pendulum structure. Chapter 4 examines not only the simulation process but investigates various translational motion profiles for the sliding or auxiliary mass. In particular, a technique to achieve stable, parametric attenuation is introduced and optimization of other displacement profiles for the auxiliary mass are examined. Chapter 5 introduces the controllers and presents the foundation for an artificial neural network controller. The energy attenuation for various controllers are next reported with details of the simulated dynamics in chapters 6, 7 and 8. The controllers include a human operator, a modified proportional and derivative, a knowledge based and a neural network controllers. The final chapter presents a discussion of results, summarizes the conclusions and provides insight regarding future extensions.

2. Research Perspective

2.1 Introduction

This thesis investigated a method for active vibration attenuation by changing the mass configuration of the structure. The approach required a background integrating several fields; most prominent were structural dynamics, control engineering, optimization and artificial intelligence technology. The research used a numerical simulation approach to assess the feasibility of the proposed philosophy and its implementation.

The mechanism involved either the redistribution of mass within, or the motion of an auxiliary mass along, the vibrating structure. Using this mechanism, the vibrational energy were altered. The mechanics and the inferred control logic for the mechanism are presented in the following sections using the example of a variable length pendulum. For this system, the variable length of the pendulum controls the motion of the end mass, thus making the mechanism of mass reconfiguration intrinsic to the system.

The essential requirements for a generic controller were based on the control logic of the moving mass attenuation device. When considering plausible extensions and implementations, additional features for the controller were realized. In this manner, the functional requirements and the operation mode were considered for the controller.

Although the research was designed to permit future prototype development and experimentation, the research reported herein is based on numerical simulations of the control systems that were developed through original and customized computer software. The ensuing result was a computer simulation of a system capable of monitoring, assessing and

attenuating its vibration. A brief discussion of the approach and evaluation guidelines conclude this chapter.

2.2 The Vibration Attenuation Mechanism

The vibration attenuation mechanism is based on the philosophy that the structural dynamic behavior can be altered through the redistribution of its mass. This redistribution or reconfiguration of mass within a structure can be achieved by moving the structural mass or moving an auxiliary mass within/along the structure. In this study, this motion of a mass within the system is analyzed from both force and energy perspectives. Next, the attenuation of structural vibrations is shown as a mass traverses the oscillating structure in a special way. By reviewing the mechanics of the interaction of the mass as it traverses the structure, a general strategy for attenuating oscillations is deduced.

2.2.1 Mechanics of a Rotating and Translating Mass

Many vibrating systems involve rotational motion, as depicted in Figure 2.1. This oscillatory motion is often characterized as being periodic, such as sinusoidal motion. If the structure experiences rotational motion, then the inertia force that arises from the rotational and translational auxiliary mass motion is referred to as the *Coriolis Force*. The Coriolis force can be viewed as creating either *positive* or *negative damping*[1] which results in a gain or loss in the structural, vibrational energy.

This effect is examined using planar motion of a variable length pendulum. First, the equations governing such a motion are derived and the Coriolis force is discussed. Next, a work-energy balance is conducted to determine the effects on the structural energy state. Specifically, by examining the action associated with raising and lowering the mass at various

[1] Positive damping refers to the loss or dissipation of energy; conversely, negative damping refers to the gain of energy.

phases during a cycle of vibration illustrates how the vibrational energy of the system can be altered.

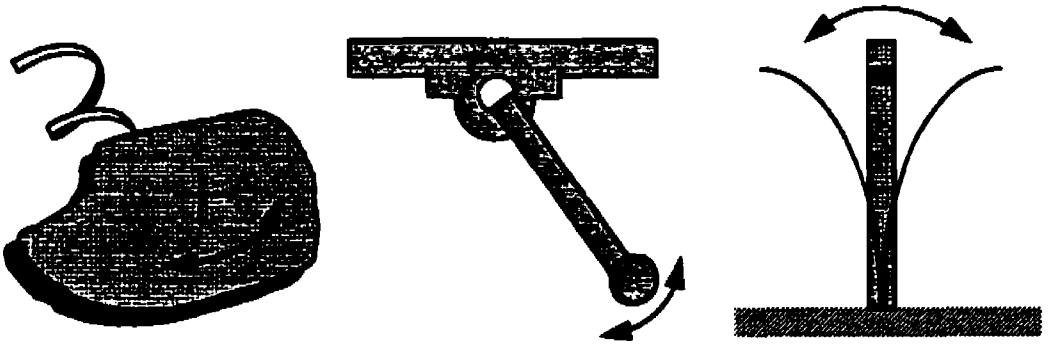

(a) (b) (c)

Figure 2.1 Examples of vibrating systems with rotational motion: (a) disk attached to a rotational spring, (b) simple pendulum and (c) flexural vibration of a beam.

2.2.1.1 Role of Coriolis Inertia Force in Controlling Oscillations

To understand the origin of the Coriolis inertia force, the kinematics of a point mass is considered using a moving, rotational frame of reference. Then, the principles of dynamics in this frame of reference are applied to a variable length pendulum where the action of raising and lowering the mass is analyzed.

The general motion of a point can be defined using a right-handed, absolute or fixed coordinate system, X-Y-Z and the moving reference axis, x-y-z as shown in Figure 2.2. The unit vectors associated with the moving reference frame are $\vec{i}, \vec{j}$ and $\vec{k}$. For clarity, the motion is restricted to the X-Y plane; thus, the Z- and z-axes remain parallel. As shown in Figure 2.2, the absolute position of A is defined as:

$$\vec{r}_A = \vec{r}_O + \vec{r} \tag{2.1}$$

where the position vectors, $\vec{r}_A$ and $\vec{r}_O$, are measured in the fixed frame of reference and the position vector, $\vec{r}$, is measured in the moving coordinate system.

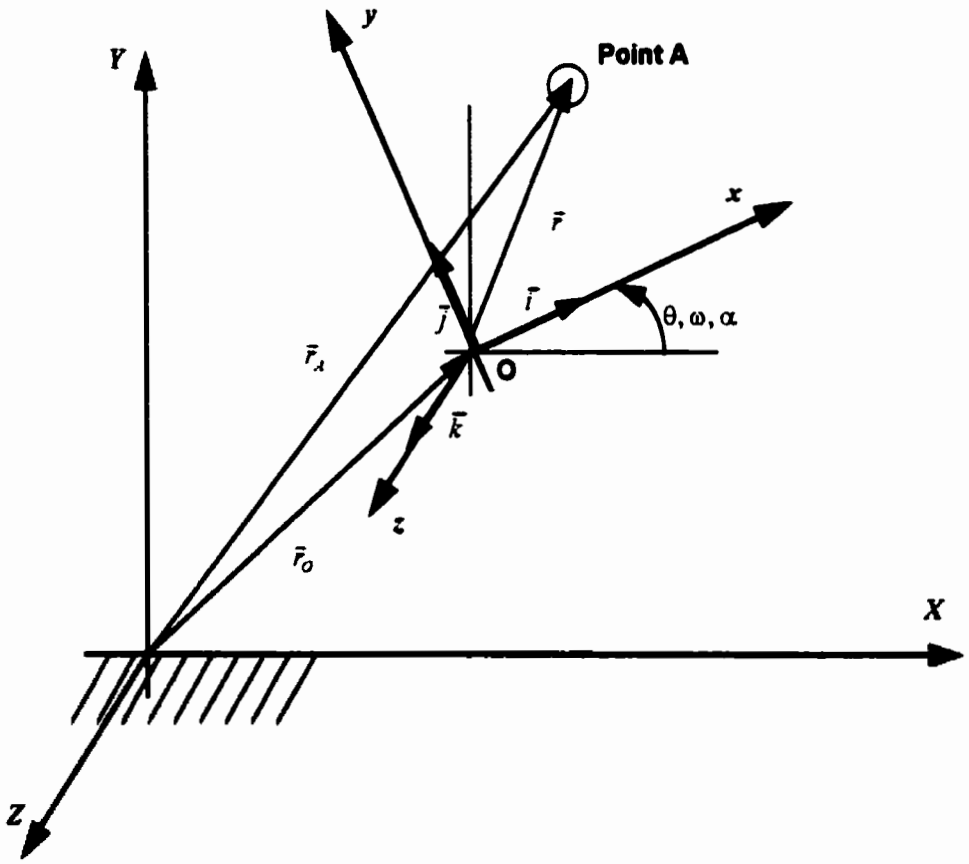

Figure 2.2 Reference frames for locating the point of interest, A.

The velocity and acceleration equations for point A can be derived through successive differentiation of the position vector, Equation 2.1, to give:

$$\dot{\vec{r}}_A = \dot{\vec{r}}_O + \dot{\vec{r}} + \vec{\omega} \times \vec{r} \tag{2.2}$$

and

$$\ddot{\vec{r}}_A = \ddot{\vec{r}}_O + \ddot{\vec{r}} + \vec{\omega} \times (\vec{\omega} \times \vec{r}) + \vec{\alpha} \times \vec{r} + 2\vec{\omega} \times \dot{\vec{r}} \qquad (2.3)$$

where $\vec{\omega} = \omega\vec{k} = \dot{\theta}\vec{k}$ is the angular velocity and $\vec{\alpha} = \alpha\vec{k} = \ddot{\theta}\vec{k}$ is the angular acceleration of the moving coordinate system as measured in the fixed coordinate system.

In Equation 2.2, the term, $\vec{\omega} \times \vec{r}$, represents the velocity due to the difference of rotation between the two frames of reference and is perpendicular to the vector, $\vec{r}$. The term, $\dot{\vec{r}}$, represents the translational motion that is tangential to the path as viewed in the moving system and is referred to as the sliding velocity. Lastly, the term, $\dot{\vec{r}}_O$, represents the absolute velocity of the origin of the moving frame of reference.

In Equation 2.3, the acceleration terms of point A associated with the rotating coordinate system may be referred to as its normal, tangential, Coriolis, sliding and inertia acceleration components. The normal acceleration term, $\vec{\omega} \times (\vec{\omega} \times \vec{r})$, is directed towards the center of the path of motion and the tangential acceleration, $\vec{\alpha} \times \vec{r}$, is perpendicular to this path in the moving coordinate system. These terms represent the relative acceleration of point A as observed from the non-rotating set of axis at the origin, O. The term, $2\vec{\omega} \times \dot{\vec{r}}$, is the Coriolis acceleration with direction normal to the sliding velocity. The Coriolis acceleration is comprised of two effects; one is due to the rate of rotation of the system and other is due to the sliding velocity. The sliding acceleration, $\ddot{\vec{r}}$, has its direction along the path of motion and is referenced to the moving frame of reference. The inertia acceleration of the moving coordinate system is given by $\ddot{\vec{r}}_O$.

When considering the kinetics associated with a mass, m, its motion can be deduced by applying D'Alembert's principle of dynamic equilibrium;

$$\vec{F}_{EXTERNAL} - m\ddot{\vec{r}}_A = 0 \tag{2.4}$$

where $\vec{F}_{EXTERNAL}$ is the resultant of the external forces, and

$-m\ddot{\vec{r}}_A$ is the fictitious inertia force.

Through substitution of Equation 2.3, Equation 2.4 becomes

$$\vec{F}_{EXTERNAL} - m\left(\ddot{\vec{r}}_O + \ddot{\vec{r}} + \dot{\vec{\omega}} \times (\vec{\omega} \times \vec{r}) + \vec{\alpha} \times \vec{r} + 2\vec{\omega} \times \dot{\vec{r}}\right) = 0 \tag{2.5}$$

Thus, in the rotating coordinate system, the inertia force can be divided into several components, including the Coriolis inertia force, $-m\left(2\vec{\omega} \times \dot{\vec{r}}\right)$.

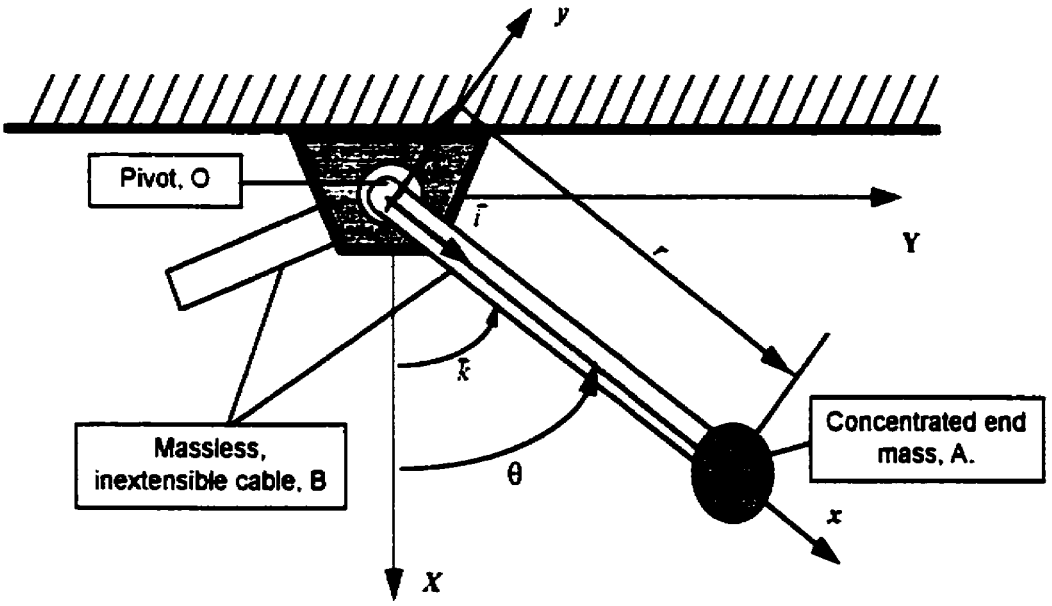

Figure 2.3 Planar motion of a variable length pendulum.

These components will be examined using a simple (or mathematical), variable length pendulum. As shown in Figure 2.3, this pendulum system consists of a concentrated end mass, A, attached to a massless, inextensible

cable, B, that is fed over point O. The origins of the moving and rotating coordinate systems are located at the pivot, O, hence $\bar{r}_O = \dot{\bar{r}}_O = \ddot{\bar{r}}_O = 0$. Also, the moving coordinate system is assumed to be attached to the cable so that the position of the end mass always lies in the $\bar{i}$-direction, $\bar{r} = r \cdot \bar{i}$. Positive angular rotation of the pendulum is assumed counterclockwise, $\bar{\theta} = \theta \cdot \bar{k} > 0$.

According to Equation 2.3, the acceleration for the end mass in terms of this coordinate system, can be described by:

$$\ddot{\bar{r}}_A = \left(\ddot{r} - \omega^2 r\right)\bar{i} + \left(\alpha r + 2\omega\dot{r}\right)\bar{j} \tag{2.6}$$

Upon substituting into Equation 2.4, the components of the fictitious inertia forces acting on the end pendulum can be identified as shown in Figure 2.4. The positive directions of the forces are indicated for the assumed counterclockwise rotation of the pendulum with the end mass moving away from the pivot (that is for $\omega > 0$ and $\dot{r} > 0$). The external forces acting on the end mass include the gravitational force, $m\bar{g}$ and the cable tension, $\bar{F}$ and can be represented as:

$$\bar{F}_{EXTERNAL} = mg\left(\cos\theta\bar{i} - \sin\theta\bar{j}\right) - F\bar{i} \tag{2.7}$$

By substituting Equations 2.6 and 2.7 into Equation 2.4, the differential equations of motion can be defined as:

$$-F + mg\cos\theta - m\ddot{r} + m\omega^2 r = 0 \quad \text{or} \quad mg\cos\theta - m\ddot{r} + m\dot{\theta}^2 r = F \tag{2.8}$$

and

$$mg\sin\theta + m\alpha r + 2m\omega\dot{r} = 0 \quad \text{or} \quad \ddot{\theta} + 2\frac{\dot{r}\dot{\theta}}{r} + \frac{g}{r}\sin\theta = 0. \tag{2.9}$$

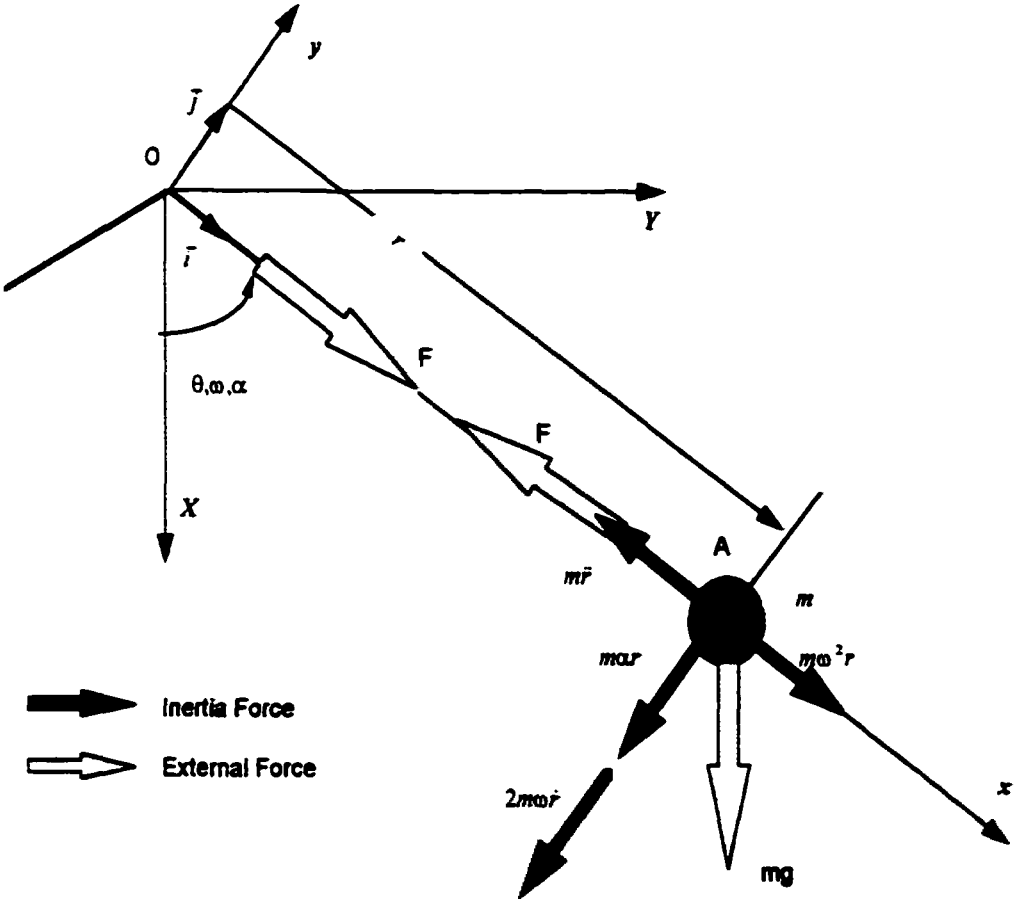

Figure 2.4 Free body diagram of forces acting on a variable length pendulum.

Physically, Equation 2.8 describes the tension, F, in the cable associated with the position and motion of the end mass. The tension is composed of the sliding acceleration that generates the inertia force along the rope, $m\ddot{r}$, the centrifugal force from the oscillations of the end mass, $m\dot{\theta}^2 r$, and a component of the gravitational force, $mg\cos\theta$. The second differential equation, Equation 2.9, describes the angular motion of the pendulum as affected by the position and velocity of the end mass. The term, $2\frac{\dot{r}\dot{\theta}}{r}$, describes the Coriolis effects which are generated by moving the end mass.

Both the Coriolis force and the gravitational force affect the rotation of the pendulum.

The governing differential equation of motion for angular oscillations can be linearized[2] and written in the standard form for damped vibrations,

$$\ddot{\theta} + 2c\dot{\theta} + \omega_n^2\theta = 0 \tag{2.10}$$

where $c = \frac{\dot{r}}{r}$ which represents the viscous damping coefficient when $c > 0$ and is assumed to be a constant, and

$\omega_n = \sqrt{\frac{g}{r}}$ which represents the natural frequency of the pendulum.

Variations in ω_n will be insignificant if the changes in r are negligible.

When the pendulum is being lengthened (that is, $\dot{r} > 0$ which causes the magnitude of r to increase), this action resembles a viscous damper and the oscillation amplitude will be reduced. In contrast, when the pendulum is being shortened, that is $\frac{\dot{r}}{r} = c < 0$; negative damping occurs and the amplitude of the oscillations will be amplified. For the case when $\dot{r} = 0$, the Coriolis effect is eliminated resulting in constant amplitude oscillations. These effects due to varying the pendulum length can be explained by the action of the Coriolis force. When the pendulum is being lengthened as shown in Figure 2.5, regardless of the direction of the velocity, the Coriolis force will always act against the oscillatory motion. The exact opposite effect will be observed when the pendulum is shortened. Therefore, lengthening, $\dot{r} > 0$, or shortening, $\dot{r} < 0$, the pendulum cable creates the Coriolis inertia force which acts to decrease or increase the amplitude of oscillations, respectively.

[2] By assuming small oscillations, then $\sin\theta \approx \theta$.

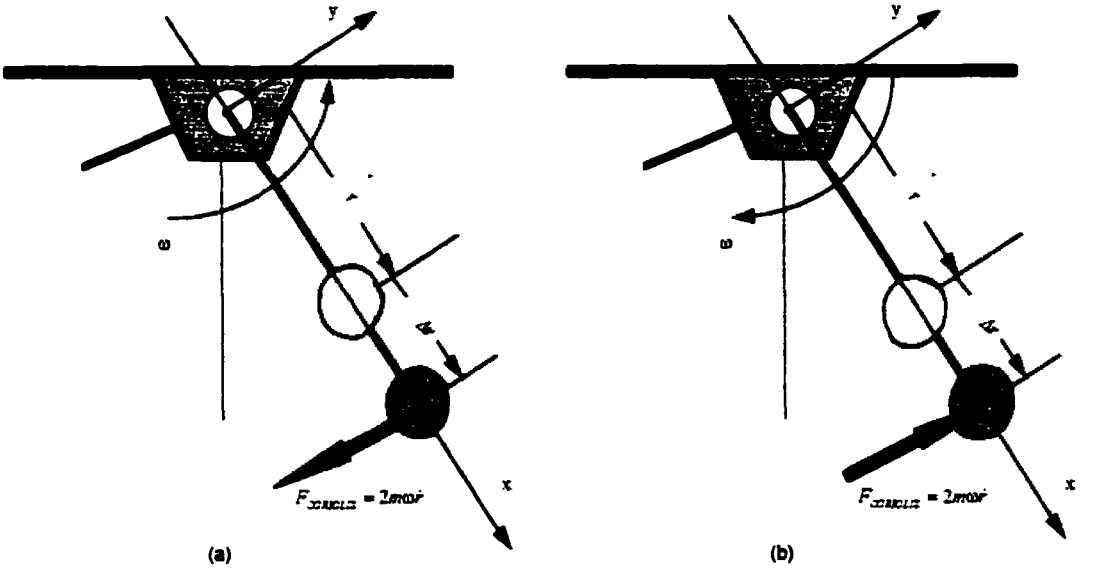

Figure 2.5 The effects of lengthening the pendulum for (a) counterclockwise ($\omega > 0$) or (b) clockwise ($\omega < 0$) pendulum rotation.

Thus, based on these discussions, the intuitive solution for attenuating the structural vibrations would be to continually lengthen the pendulum. Unfortunately, this solution is not feasible as an infinitely long cable or structure would be required to completely attenuate the vibrational energy. Therefore, to ensure practicality, the displacement of the end mass is bounded,

$$r_{min} \le r \le r_{max}. \tag{2.11}$$

As the length of the pendulum cycles between r_{min} and r_{max}, the mass moves towards and away from the pivot, thereby either increasing or decreasing the angular displacement of the pendulum.

If moving the mass both towards and away from the pivot occur during a cycle when the magnitudes of the Coriolis force are identical (but opposite in direction), the angular velocity at the end of the cycle will remain the same as it was at the beginning. However, if a smaller Coriolis force is generated

during the motion towards the pivot than during the motion away from the pivot, the final angular velocity will be decreased and vice versa.

The Coriolis force depends on the current angular velocity and the sliding motion of the end mass. Its magnitude can be regulated through proper coordination between the angular oscillations and the translational motion of the end mass, the pendulum bob. *Therefore, for vibration attenuation, the timing sequence for cycling the end mass (or the translational displacement profiles of the moving mass) should consist of two phases:*

> *Phase 1: The end mass is moved away from the pivot (lengthening the pendulum) when the angular velocity and the Coriolis force are maximum (which occur when the pendulum is near vertical). This should maximize the angular velocity reduction for the next part of the cycle.*
>
> *Phase 2: The end mass is moved towards the pivot (shortening the pendulum) when the angular velocity and the Coriolis force are minimum (which occurs near maximum angular displacement with respect to the vertical, equilibrium position). This should minimize the angular velocity amplification for the next part of the cycle.*

Details of this strategy will be discussed in Chapter 3.[3]

2.2.1.2 Effects of Mass Reconfiguration on A Work-Energy Balance

The attenuation or amplification effects of the redistribution of a system's mass can also be explained using a work-energy balance. For a

---

[3] For the pendulum systems presented herein, moving away from the pivot corresponds to *lowering* the auxiliary or end mass and moving towards the pivot refers to raising this mass.

simple pendulum, the energy consists of kinetic energy, T and gravitational potential energy, U. This energy can be either lost or gained depending on the work done by or on the system. The work-energy balance is defined by the following equality:

$$(T+U)_{t_1} + W_{1-2} = (T+U)_{t_2} \tag{2.12}$$

where the subscripts, t_1 and t_2 represent instances in time and

W_{1-2} is the work done over this interval.

For the variable length pendulum, the work done on the system is associated with moving the end mass. To move the end mass either a force generated internally by a mechanism within the mass or an external force can be applied. The latter is shown in Figure 2.6; the force, $\vec{F}$, pulls the cable over a pivot by a finite distance, Δs, to change the length of the pendulum. The cable is assumed to be inextensible; therefore $\Delta s + \Delta r = 0$. So, the work on the system associated with moving the end mass is the product of the tension in the cable, $\vec{F}$ and the corresponding motion, $\Delta s = -\Delta r$.

If $s_1 = s(t_1)$ and $s_2 = s(t_2)$, for a given interval the work can be defined as:

$$W_{1-2} = \int_{s_1}^{s_2} \vec{F} \cdot d\vec{s}. \tag{2.13}$$

If the tension in the cable is assumed to always be positive and is approximately constant during the lengthening or shortening of the cable, then Equation 2.13 simplifies to:

$$W_{1-2} = F\Delta s \tag{2.14}$$

When the pendulum is being shortened, that is the mass is moved towards the pivot, as shown in Figure 2.6, then

$$\Delta s = s_2 - s_1 > 0 \tag{2.15}$$

and the corresponding work is positive,

$$W_{1-2} \cong F \cdot \Delta s > 0. \tag{2.16}$$

Consequently, according to Equation 2.12, the total energy of the system at time, t_2, increases by the amount, $F \cdot \Delta s$.

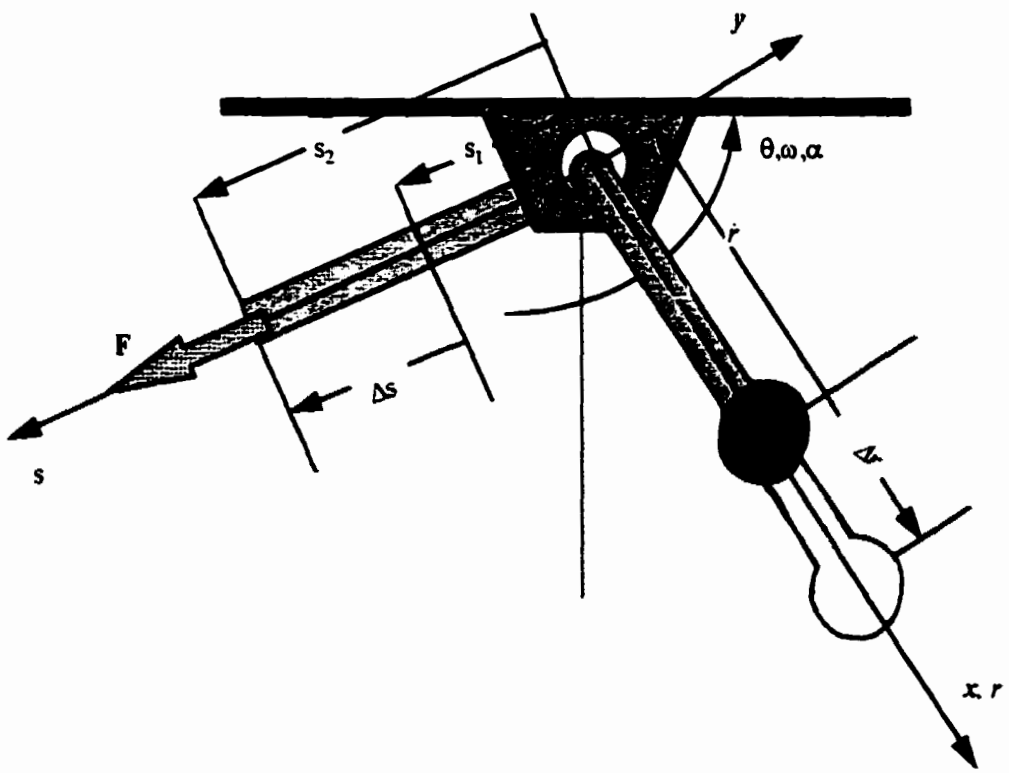

Figure 2.6 Shortening the pendulum increases the system energy.

In contrast, increasing the length of the pendulum, that is moving the mass away from the pivot, results in

$$\Delta s = s_2 - s_1 < 0 \tag{2.17}$$

and the work is negative,

$$W_{1-2} \equiv F \cdot \Delta s < 0, \tag{2.18}$$

resulting in a decrease in the energy of the system.

The continual lengthening of the pendulum generates negative work and decreases the total energy of the system which is in agreement with the previous section. If the mass is allowed to cycle between defined limits, r_{min} and r_{max}, the following scenarios can occur. When the tension in the cable is identical as the mass is moved away from and then back towards the pivot through the same distance, then the net change in energy per cycle will be zero.

However, if the force required to move the mass towards the pivot is different from that to move the mass away from the pivot, then either positive or negative work can be attained during a cycle of motion. Net negative work reduces the energy of the system and attenuates the oscillations of vibration; whereas, net positive work adds energy to the system and amplifies the oscillations.

The net negative work will occur if the force used to move the mass towards the pivot is smaller than the force present when the mass moves away from the pivot over the same distance in one cycle. Since the tension will be maximum when the pendulum passes directly below the pivot and minimum when the pendulum is at points of maximum angular excursion, a strategy for attenuating the vibrations can be deduced. For the pendulum shown in Figure 2.3, the mass should be moving down below the pivot and up at the extremes of its angular displacement. This strategy is consistent with the explanation of the previous section that was based on the Coriolis effect.

2.2.2 Control Logic for Attenuating Vibrations Using a Moving Mass

Considering the physical phenomena associated with the interaction of a moving mass along an oscillating structure, a control strategy can be deduced to attenuate structural vibrations. Periodic motion for the end mass towards and away from the pivot is assumed.

Generally, to decrease the system energy, the end mass should be moved away from the pivot (lowered) between the turning points of the oscillations and moved towards the pivot (raised) at these turning point, as illustrated in Figure 2.7. To maximize the attenuation effects, the lowering of the mass should occur near the central position (when the pendulum is directly below the pivot) as the angular velocity and the cable tension are maximum. This control logic is illustrated in Figure 2.7(b). Note that for this strategy the motion of the mass is at twice the pendulum's angular oscillation frequency.

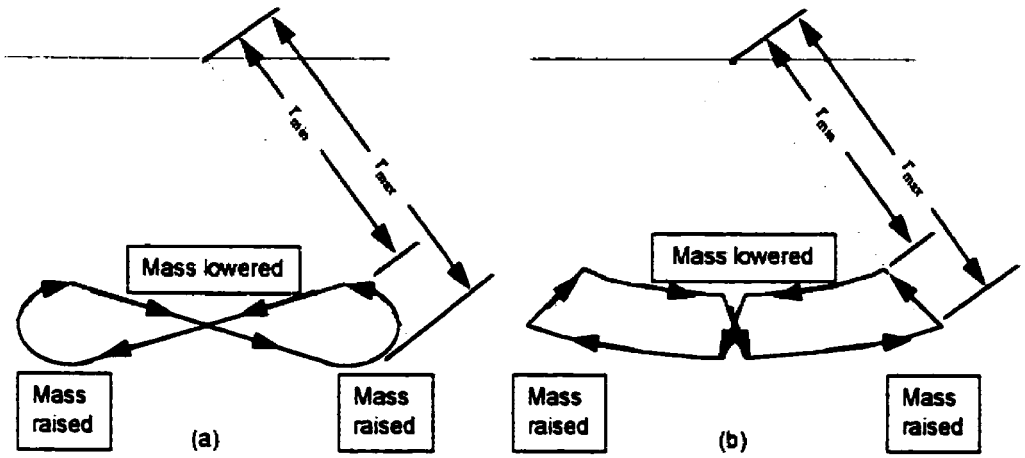

Figure 2.7 Vibration attenuation using (a) a general strategy and (b) a more optimal trajectory for the end mass.

In contrast, to maximize the increase of system energy, the end mass should be raised near the central position when the cable force is large and lowered at extreme excursion points when the cable force is small, as shown in Figure 2.8.

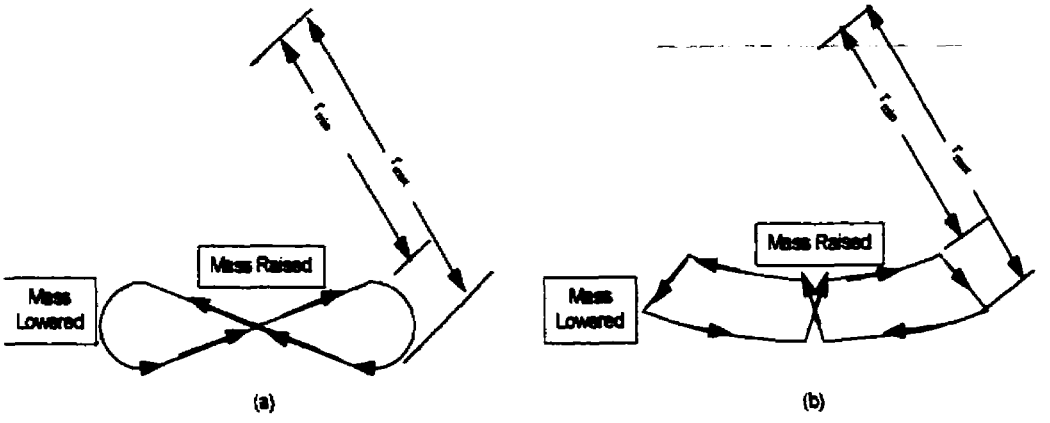

Figure 2.8 Vibration amplification using (a) a general strategy and (b) a more optimal trajectory for the end mass.

To conclude, vibration attenuation can be achieved by moving a mass along a rotating system. As previously discussed, the physical phenomenon can be explained by considering either the Coriolis force or a work-energy balance. Subsequent chapters will discuss the details of mass reconfiguration profiles to effect this control.

2.3 Overview of the Control System

The general requirement of any control system is to achieve the specified objectives in a stable manner, at a reasonable rate and with relative accuracy. Usually, a control system consists of a controller and a plant with operation in either an open loop or closed loop mode, as shown in Figure 2.9. The function of a controller is to generate a signal or signals to modify the performance of the plant to achieve the desired control objective. Controllers possessing feedback monitor parameter(s) or variable(s) to provide appropriate control action. This section examines the control system focusing on the functional requirements for the controller by examining the variable length pendulum, as presented in Section 2.2.

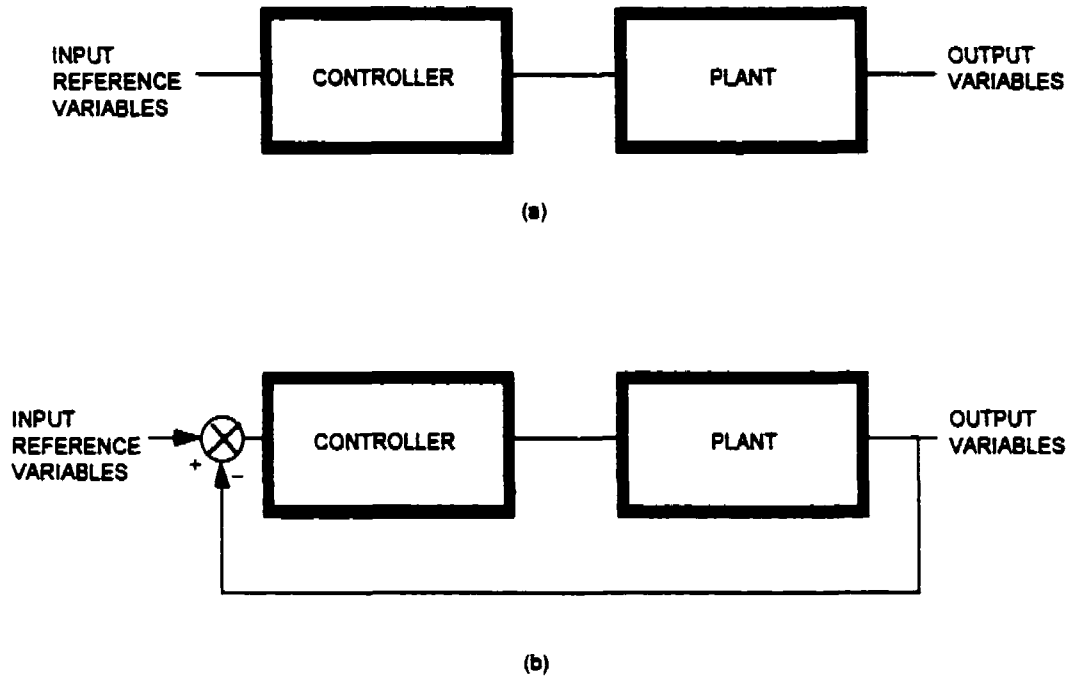

Figure 2.9 Functional block diagram illustrating control operation as either (a) open loop or (b) closed loop.

The control objective for this research is to attenuate the oscillations of a freely vibrating structure. As presented in the preceding section, a method that can alter the vibrational energy of this system is the redistribution of mass within or along the structure. The knowledge and logic applied to direct the motion of the end mass to generate the "damping" mechanism forms the control logic or laws.

As shown for a variable length pendulum, the oscillations can be attenuated either:

(a) by strategically moving the end mass back and forth during a cycle of vibration, or

(b) by continually lengthening the pendulum.

Implementing the latter option suggests an infinitely long pendulum which is physically not plausible. However, the positive damping effects achieved by lengthening the pendulum may be used advantageously as a safety feature to

augment the controller, as to be discussed in a later chapter. So, the selected controller is required to generate the "strategic motion of the end mass".

With reference to the control systems illustrated in Figure 2.8, the variable length pendulum shown in Figure 2.3 and the relevant discussions given in Section 2.2, the plant can be viewed as consisting of two components. The first component is the attenuation mechanism that reconfigures the structural mass; the second component is the freely vibrating structure (the pendulum). For the variable length pendulum, the control mechanism of mass redistribution can be realized by either moving a mass along a massless pendulum strut or changing the length of the pendulum cable.

To quantify the control objective for attenuating the vibrational energy, an input reference variable should be defined. To reduce or ultimately eliminate the structural, vibrational energy, the stable equilibrium state of the angular displacement or velocity for the pendulum structure could serve as the reference signal. As the energy of the system is minimized, the oscillations will be dampened and both $\theta \rightarrow 0$ and $\dot{\theta} \rightarrow 0$. For these conditions ($\theta \rightarrow 0$ and $\dot{\theta} \rightarrow 0$), both the potential energy which is a function of the angular displacement and the kinetic energy which is a function of the angular velocity will be minimized. Since the instantaneous state of either the angular displacement or the angular velocity, independently, is insufficient to quantify a state of zero vibration, both the angular displacement and velocity of the pendulum structure were considered to be the reference input variables ($\theta_{REF} = 0$ and $\dot{\theta}_{REF} = 0$).

Since most vibration problems occur in disturbance prone environments, a closed loop controller was chosen, as these controllers are more adept at handling disturbances. Typically, in a closed loop controller, the actual state data of the structure are monitored and processed. A

comparison between the actual plant behavior and the desired behavior forms the error signal which drives the controller to effect the desired control action.

For this application, the traditional closed loop control system would be a multiple input and multiple output system, as shown in Figure 2.10. A comparison between the reference signals of zero angular displacement and zero angular velocity with the actual corresponding current state of the plant (pendulum) could be made to drive the controller. The objective of the controller is to achieve attenuation, and ideally, cessation of structural vibrations through mass reconfiguration. The plant can be viewed as two components: the attenuation mechanism and the vibrating structure.

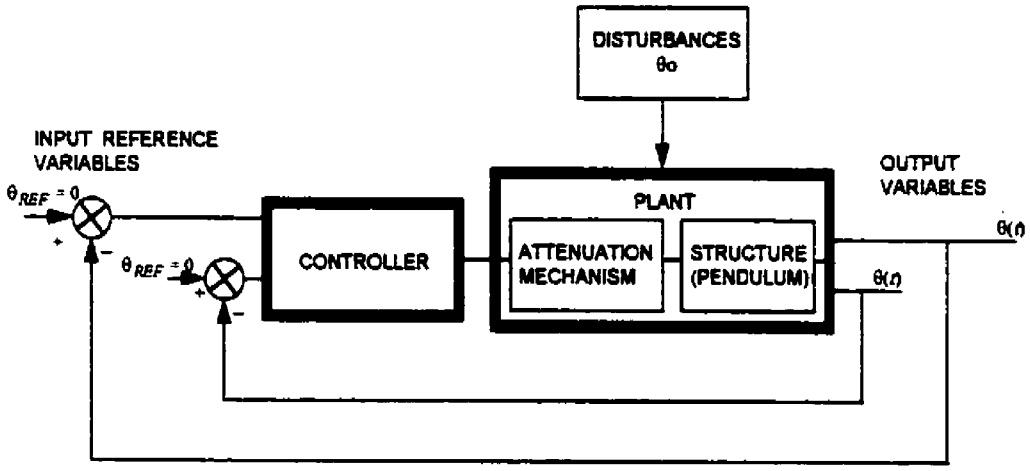

Figure 2.10 Control system based on traditional control theory.

2.4 Rationale Associated With the Controller Implementation

Possible implementations for the controller are based on the overall conception for the control system as presented in Section 2.3. Namely, the underlying architecture is to be a multiple input and multiple output, closed loop control system. Various considerations for implementing the controller are presented with details based not only on examining the pendulum application but also by considering future extensions.

The classic controllers, such as proportional, derivative, integral and/or a combination thereof, were first considered. Classic linear controllers are effectively used with linear, time invariant systems. Implementing one of these types of controllers has the advantage of being well studied with known behavior. Since the identified reference signals of Section 2.3 are the angular displacement and its time derivative, proportional plus derivative control action could be considered. The control algorithm would be mathematically stated as:

$$\dot{r}(t) = k_p\left(\theta_{REF} - \theta(t)\right) + k_d\left(\dot{\theta}_{REF} - \dot{\theta}(t)\right) \tag{2.19}$$

or

$$\dot{r}(t) = k_p\left(e(t)\right) + k_d\left(\frac{de(t)}{dt}\right) \tag{2.20}$$

where k_p and k_d are the proportionality constants;

$e(t)$, the error signal; and

$\dot{r}(t)$, the control signal that physically defines the time derivative of the distance between the pivot and the end mass (the rate of change of the pendulum length).

Details of implementing a controller with similar properties to a proportional and derivative action are presented in Chapter 5.

However, the control process of the interaction of the moving mass along the pendulum is mathematically defined by the nonlinear, coupled, differential equations, Equations 2.9 and 2.10, for which multi-variable, classical control theory appears unsuitable. Selecting the proportionality gains, k_p and k_d, would have to be based on a set operating point or period of operation. The effectiveness of such a controller is related to the accuracy of linearizing this region of operation for the system. If more complex structures are considered, then the mathematical modeling becomes

increasingly intractable. Ideally, the controller must be able to handle multiple, time-varying and nonlinear variables, to operate over a broad set of disturbances (or initial conditions) and to perform well over the entire operating domain.

The next level of intricacy to be considered is enhancing the linear controller by updating or changing the proportionality constants based on the operating requirements of the system. The controller through monitoring error magnitudes, current state conditions or other parameters would "look up" corresponding proportionality constants. Unfortunately, this type of controller would require tabulating the relations between the appropriate proportionality constants and the condition(s) "to be monitored" over the expected operating domain. If the system is not well defined or *a priori* knowledge for quantifying the appropriate control action cannot be discerned, such a table cannot be generated. The effectiveness of the controller would be dependent on each tabulated entry for a region of operation. For nonlinear systems, excessive discretization of the operating domain may be required. This type of controller risks becoming tailored to the specific application and convoluted for complex systems. The adaptive nature of the above controller is a desirable feature. Ideally, the controller should not operate in a simple tracking mode, but rather in an anticipatory manner.

Although for the variable length pendulum, input parameters of angular displacement and angular velocity appear appropriate, these parameters may neither be the most appropriate nor be sufficient in effecting control. Understanding the mechanics of the plant defines important relations among the possible variables and aids in discerning variables to be monitored. For example, the state of the variable length pendulum system may be characterized using the angular displacement or velocity of the vibrating pendulum, the length or change of length of the pendulum, and/or the tension in the cable; these or a subset may serve as the input for the controller. The output from the controller may be either to generated a force on the cable or

to create a displacement profile for the end mass. If the plant were to become more complex, such as possessing multiple masses or being characterized as a continuous mass structure, identifying the fewest, yet pertinent variables becomes increasingly difficult. For the most general case, the controller should be able to handle redundant and perhaps irrelevant data and discern appropriate relations to generate the desired control action. Again, this requirement discourages the use of conventional controllers.

As explained in Section 2.2.2, the control action involves the coordination between structural oscillations and the cyclic, bounded translational motion of an end mass for a finite length pendulum. Then, the controller must either inherently possess appropriate saturation characteristics or have additional control logic to achieve bounded motion. This restriction for the mass reconfiguration may require monitoring additional system parameters. For the variable length pendulum, the position and sliding velocity of the end mass may also need to be fedback to the controller. The complexity of the controller has been increased by introducing the nonlinear phenomena of saturation and by requiring additional logic to ensure compliance with these imposed operating limits.

As the above discussion indicates a nonlinear controller is required, but defining the parameters for its operation is not intuitively obvious. A myriad of parameters within the control strategy for adjusting the mass configuration of the system as suggested in Section 2.2.2 can effect vibration attenuation. The controller must be capable of providing variable output rather than just a proportional signal; control action may be extremely nonlinear, such as a discontinuous relay action or a continuous sinusoidal signal. Furthermore, the representation of the control action may be difficult to quantify.

The controller should be educable[3], since parameters have yet to be identified and defined, and operating points have to be selected. In other words, the "damping term", $2\frac{\dot{r}}{r}$ (see Equation 2.10) has not been explicitly defined nor have the limits for the varying quantities been established. Analyzing various control patterns is integral to understanding and for optimizing the control action. Therefore, a controller should be capable of learning various displacement profiles to effect mass reconfiguration. Perhaps, the controller could evaluate the causal action between various trajectories for the end mass trajectory, $r(t)$, and the dynamics of the system for implementing an efficient displacement profile. Thus, salient features considered for this application were its optimization and learning capabilities. So, if the controller is adaptive and can adjust to unknown parameters, it may self-train for optimal performance.

The computational requirements for monitoring and processing data involve multiple, time-varying parameters, making parallel processing attractive to enhance computational efficiency. Thus, the controller should possess good computational abilities.

Other features of the controller depend in part on the actual implementation, the related instrumentation, the physical components and the control logic. The controller must be easily adapted to handle the chosen implementation of the control logic, flexible in processing various measurements and generating suitable output tailored to the physical design.

In summary, to permit extensibility and flexibility in both application and implementation, the controller must be nonlinear, general purpose, adaptive and educable. Its computational ability must span data storage, processing and advanced logic implementation. The control logic and prior fine tuning of the controller may be based on a priori knowledge, heuristics and self-

[3] For the purpose of this thesis, an educable controller is defined as one that may be trained or instructed for a particular purpose.

assessment. Additional logic to assure safety and compliance with implementation constraints may also be required. To fulfill as many of these criteria as possible, an application of artificial intelligence technology was selected for this work. These methods circumvent many of the shortcomings of conventional control theory. Both knowledge based systems (KBS) and artificial neural networks (ANN) were applied. At the time of initiating this research [Stilling, 1990a] KBS had some proven successes recorded in the literature, yet ANN were in their infancy with few applications and tools being available.

2.5 Synthesis of the Control System

Desirably, the end product is a design for an adaptive, autonomous system consisting of a structure and a controller whose objective is to attenuate its vibrational energy. The feasibility of attenuating vibrational energy through mass reconfiguration had not been previously reported in the literature. Also, mechanisms to effect the technique of mass reconfiguration and controllers to implement the attenuation strategy were neither readily nor commercially available. The research was diverted to numerical simulations rather than towards prototype implementation and experimentation. In addition, the required computer software to implement various components of the proposed system was not available. During the early years of this research, several tools and software packages that were unique and original were developed and evaluated [Stilling, 1993b, 1990a&b; Stilling and Watson, 1994a, 1992, 1991 and 1990; Watson and Stilling, 1994, 1992a&b, 1991a&b and 1990].

The control system was developed as a computer simulation; however, considerations were made to allow physical prototype development. The selection of structural parameters and the control infrastructure were based on the state of the current technology for physically implementing the system. Also, the possibility of extending the proposed thesis technology to more

complex systems affected the formulation, the bounds of variables and subsequent simulations of the systems.

The synthesis began with a numerical simulation of the plant. The dynamic interaction of the moving mass mechanism was investigated in detail. Not only were arbitrary displacement profiles for the auxiliary mass presented for simulating, but also an effort to develop optimal temporal[4] profiles was completed. Based on these plant dynamics, control logic was postulated and necessary knowledge and data to train the controller was generated. The next phase focused on developing and/or training the controller and integrating the controller with the numerical simulation of the plant. As the technology employed was in its infancy, benchmarks and criteria for evaluating the performance were defined for both the components and the integrated control system.

2.6 Summary

The fundamentals that directed the thesis research have been presented, herein. Basically, they included:

- the analysis of the physical phenomenon that is associated with the mass redistribution technique for regulating the angular oscillations,
- an overview of the control architecture for the system that was established to be multi-variable and closed loop,
- a review of the functional requirements and related rationales for implementing a controller, and
- establishing that the approach for investigating the control system for active vibration attenuation was to be by simulations.

The mechanics that describe the vibration attenuation device assume the vibrating system possesses rotational motion, so that a mass which translates along the structure can alter the system energy. The Coriolis

[4] Temporal profile refers to time dependent patterns that are coordinated with the system dynamics.

inertia force that results from the rotational and translational motion of the mass opposes angular motion and serves to "dampen" the oscillations. For a variable length pendulum, mass reconfiguration may be achieved by lengthening or shortening the pendulum. The control logic for attenuating oscillations can be stated as:

(1) lengthen the pendulum as it passes beneath the pivot, and

(2) shorten the pendulum near points of maximum angular excursion.

In selecting a controller, the operation and its possible implementation within the control system were considered. As the control action was to be based on the dynamics of the plant, a closed loop operation mode was favored. Other functional requirements for the variable length pendulum system included the ability to handle multiple, time-varying, nonlinear parameters, to operate in a disturbance-prone environment for a variety of operating set points, to be adaptive and to possess optimizing and learning characteristics. As traditional controllers do not meet these requirements, methods in artificial intelligence were selected for control purposes.

Lastly, computer simulations were chosen as the vehicle of implementation as it provided a forum to investigate multiple aspects of the control system and to examine the overall feasibility of implementation.

3. Modeling of Pendulum Structures With Mass Reconfigurability

3.1 Introduction

In this chapter, the analysis of the simple or mathematical pendulum of the previous chapter is expanded. First, the modeling is advanced by considering a dual mass or physical pendulum system. Such a system more accurately models several applications. Then, the dynamics of the reconfigurable mass-pendulum are analytically reviewed with interesting properties presented. Finally the parameterization for subsequent computer simulations are given.

Vibration attenuation is achieved by mass reconfiguration within a structure. This philosophy is investigated using examples of pendulum structures oscillating in a single plane. Many components and/or structures for both terrestrial and space applications can be modeled by pendulum-based mechanisms and can be retrofitted to incorporate the proposed vibration attenuation mechanism. A few examples of such structures are provided in Section 3.2.1.

The modeling of a pendulum with reconfigurable mass can be simplified to a variable length pendulum[1] as discussed in Section 2.2. Alternately, when modeling a physical pendulum[2] system, the attenuating mass is assumed to be a separate entity that slides along the structure. The governing differential equations are derived for a physical pendulum of fixed

---

[1] The variable length pendulum is referred to as a mathematical pendulum or a simple pendulum where the pendulum structure, itself, is massless.

[2] The physical pendulum is referred to as a compound pendulum or a dual mass system.

geometry with a sliding or auxiliary mass. Then, the governing differential equations are compared with those of the mathematical pendulum. Similar to the mathematical pendulum, the sliding mass can either attenuate or amplify the oscillations of the physical pendulum.

As the sliding mass traverses the structure, not only may the mass cause vibrational damping or amplification, but also the mass continuously changes the system's dynamic stiffness[3]. With certain assumptions the governing differential equation, associated with the oscillating motion of the sliding mass, can be approximated by the Mathieu-Hill equations[4] [McLachlan, 1951] which are used to analyze parametric vibrations. Although a complete mathematical analysis of these equations is complicated, stable and unstable regions are known for sets of the characteristic parameters of Mathieu's equation. The oscillations in the unstable region progressively increase in time and are called parametric resonance[5]. In general, the cyclic change in the parameters, such as stiffness or inertia, can destabilize the entire system.

Surprisingly, the damping effect, due to the Coriolis forces as explained in Chapter 2, must compete with the destabilizing effects caused by the change in the stiffness parameter. Therefore, prudent planning is necessary to develop a strategy for mass reconfiguration to attenuate oscillations. The interaction caused by the motion profiles for the mass results in either damped or unstable structural vibrations as can be explained by the general features of the Mathieu-Hill equations.

---

[3]The dynamic stiffness of the system is part of the restoring force term from the equation of motion.

[4] Mathieu-Hill equations are linear differential equations with periodic coefficients. The Mathieu equation is a specific form containing sinusoidal coefficients as presented in Section 3.3.2.

[5]Parametric resonance is also termed parametric excitations which are vibrations characterized by monotonically increasing oscillations.

In addition, the effects that the position of the auxiliary mass has on the dynamic stiffness or natural frequency of the system are presented for both the mathematical and a physical pendulum systems.

3.2 Reconfigurable Mass-Pendulum Systems

As discussed in Section 2.2, the mathematical pendulum system intrinsically possesses the attenuation properties. Vibration attenuation can be achieved by properly adjusting the length of the pendulum. The physical pendulum has its own fixed rotational inertia and the damping mechanism becomes an addendum to the structure. The physical system has two distinct masses and therefore can be referred to as a dual mass system. Vibration attenuation is achieved as the auxiliary mass is strategically slid along the structure.

This section describes various structures that can be modeled as pendulum systems. Following the modeling assumptions, the equations of motion are derived. Mathematically, the governing differential equations for the physical pendulum systems can be derived using either Newtonian (force/equilibrium) or Lagrangian (energy) dynamics. Finally, the similarities between the mathematical and physical pendulum structures are presented.

3.2.1 Examples of Pendulum-Slider Systems

Pendulum systems accurately model several existing structures, the most familiar being children on playground swings. Pendulums have been studied seemingly since antiquity [Sanmartin, 1984], yet the pendulum continues to be an active subject of investigation [Yagasaki, 1998 and 1999; Pinsky and Zevin, 1999; Dai and Singh, 1998 and 1994; Nguyen and Ginsberg, 1999; Yoshida and Sato, 1998]. Pendulum motion dating back to the 13th Century describes the use of a censer during liturgical services; this was four centuries prior to any formal, reported studies into pendulum motion [Sanmartin, 1984]. Children playing on swings dates back even further.

Structures where an object is suspended (bridge cranes, payload devices, wrecking balls and various fixtures) can be modeled and rationally analyzed as simple pendulums. Another application where pendulums were critical was in the timing mechanisms of early clocks. In 1656-57, C. Huygen invented the first pendulum clock incorporating the nearly isochronous movement of small amplitude oscillations of a pendulum augmented by adjusting its length using a variable suspension point [Blackwell, 1986]. Other systems readily modeled as a variable length pendulum are cable-suspended objects which include the action of a payload on a crane, the motion of giant censers [Sanmartin, 1984], athletic performances, such as, gymnasts performing "giant circles" or "iron cross" on the ring apparatus [Stilling and Watson, 1993] or a child swinging [Tea and Falk, 1968; Gore, 1970; Burns, 1970; Curry, 1976; Walker, 1990]. Furthermore, investigators often idealize complex structures as single degree of freedom structures.

Often the secondary mass may be significantly less than the main structural mass. This is the case for many examples in the transportation industry where vehicles traverse causeways (vehicles crossing bridges, trains traveling on tracks and passenger cars moving along light rapid transit systems). A more realistic model of a physical pendulum should be used for these cases. The system can be viewed as a dual mass system, the dominant structural mass and an auxiliary mass which traverses the main structure.

Other fields offer additional examples; for instance, from fluid dynamics there are pneumatic transfer systems, biphasic effluent flow through hinged pipeline units and various pipeline network pigging. The motion of the auxiliary mass and the structure may be integral to the system's operation. As shown by these examples, there are several applications which can be accurately modeled as pendulums with moving mass. As well, the potential applications through augmenting systems are numerous.

3.2.2 Assumptions and Simplifications

For this research, the structural vibrations of the pendulum are assumed to be planar. Vibrations may ensue from disturbances where the equilibrium state of the structure is perturbed either externally or internally. Vibrations for the pendulum-mass systems are assumed to be initiated by an initial displacement from the equilibrium position, unless stated otherwise.

For the simple or mathematical pendulum, as previously presented in Section 2.2, the assumptions include the connecting structure (cable or rod) being inextensible and having negligible mass. The concentrated end mass has negligible mass moment about its center. The attenuation mechanism of mass reconfiguration is achieved by changing the pendulum length.

In modeling the physical pendulum systems, the attenuation device is assumed to be small enough to neglect its mass moment of inertia about its centroid in comparison to the mass moment of inertia about the pivot. Various motion profiles for the auxiliary/sliding mass can be prescribed assuming a compatible and equilibrium interface is maintained with the structure. The continual contact between the sliding mass and the structure allows the auxiliary mass to acquire the same kinematics of the structure at the point of contact. Separation between the vibrating structure and the auxiliary mass has not been considered. For most applications, this simplification is inherent in the construction of the system. For example, the mass may be confined to move within a guide or the velocity of the mass is sufficiently small as to prevent separation.

To focus on the mass reconfiguration phenomena, the material damping and structural damping due to internal friction and external drag have been neglected. As structural damping reduces the overall system energy, the affects of the proposed active damping attenuation system would only be enhanced. By neglecting structural damping, the effects of mass reconfiguration for attenuating vibrations are more apparent for a freely oscillating structure.

3.2.3 Governing Equations for Physical Pendulum Systems

The simple pendulum model, as discussed in Section 2.2, is extended to take into account its structural mass. For the physical pendulum system, both the fixed mass of the pendulum and the sliding mass that constitutes the attenuation device are considered. These two masses are commensal and essentially form a coupled oscillating system.

For the physical pendulum system, a guide may exist to allow sliding the auxiliary mass within the structure, as shown in Figure 3.1(a). As the internal and external forces are easily identified, Newtonian dynamics are adopted for analyzing the pendulum-mass system. The free body diagram for the pendulum and the auxiliary mass are shown in Figure 3.1(b) and (c), respectively. The physical pendulum parameters are its mass, m_p, its moment of inertia, I_o, about the pivot (O) and the location of its center of mass from the pivot, l_p. The auxiliary mass is free to slide within a guide towards or away from the pivot as the pendulum oscillates. The auxiliary mass parameters include its mass, m_s, and its location as measured from the pivot, r. The friction between the guide and the slider is assumed to be negligible.

The forces acting on the sliding mass and the pendulum have been identified in Figure 3.1. The internal force between the pendulum and the slider is represented by a contact force, N that is normal to the guide. The force associated with moving the auxiliary mass is denoted by F. The reaction forces at the pivot are represented by R_x and R_y. The gravitational forces acting on the structure and the slider are given by $m_p g$ and $m_s g$, respectively.

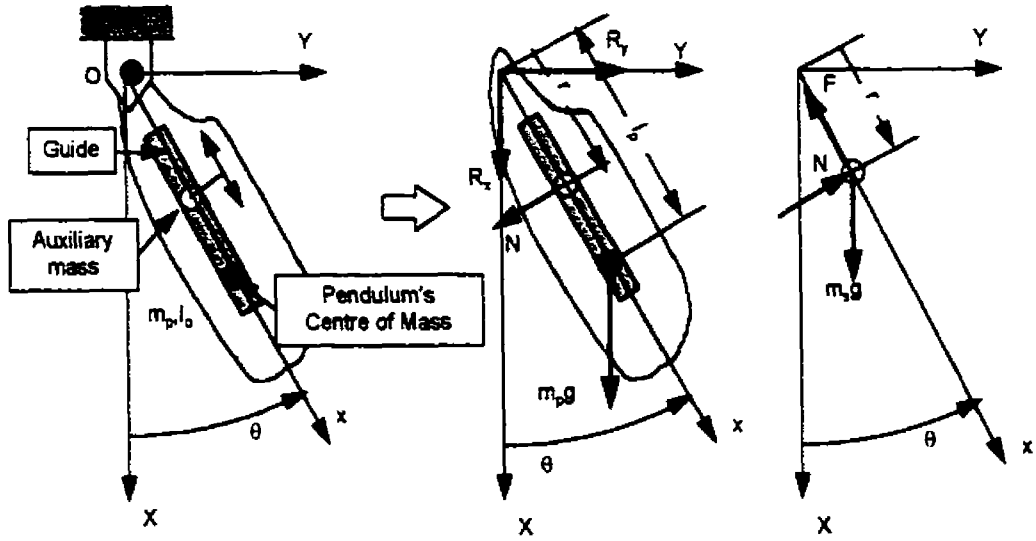

Figure 3.1 Physical pendulum system and the free body diagrams of (b) the pendulum and (c) the auxiliary mass components.

Applying Newtonian equilibrium principles, moments of force can be taken about the pivot and upon incorporating the motion of the slider, the governing differential equations can be stated as

$$\left(I_o + m_s r^2\right)\ddot{\theta} + 2m_s r\dot{r}\dot{\theta} + \left(m_p l_p + m_s r\right)g\sin\theta = 0. \tag{3.1}$$

and

$$F = m_s\left(\dot{\theta}^2 r - \ddot{r} + g\cos\theta\right). \tag{3.2}$$

Details of the derivation are included in Appendix B. Also, Lagrangian dynamics, an energy formulation, can be used to derive the equations of motion producing the same results, as shown in Appendix C.

Various configurations can be considered for the pendulum. Two examples are illustrated in Figure 3.2. One consists of a massless rod with a concentrated mass, m_p, located at a fixed distance, l_p, from the pivot. The second is a uniform rod of mass, m_r, and of length, l_r, that pivots about one

end. For both examples, the damping mechanism is an auxiliary mass that slides along the structure; one is represented as a mass that slides internally within the pendulum strut; the other is represented as a bushing that slides over the pendulum strut.

The governing differential equations describing the angular oscillations are given by:

$$\text{(a) } \ddot{\theta} + \left(\frac{2m_s r}{m_p l_p^2 + m_s r^2} \right) r\dot{\theta} + g \left(\frac{m_p l_p + m_s r}{m_p l_p^2 + m_s r^2} \right) \sin\theta = 0 \qquad \text{(3.3a)}$$

and

$$\text{(b) } \ddot{\theta} + \left(\frac{2m_s r}{\frac{1}{3} m_r l_r^2 + m_s r^2} \right) r\dot{\theta} + g \left(\frac{\frac{1}{2} m_r l_r + m_s r}{\frac{1}{3} m_r l_r^2 + m_s r^2} \right) \sin\theta = 0 \qquad \text{(3.3b)}$$

with the force required to move the auxiliary mass still being described by Equation 3.2.

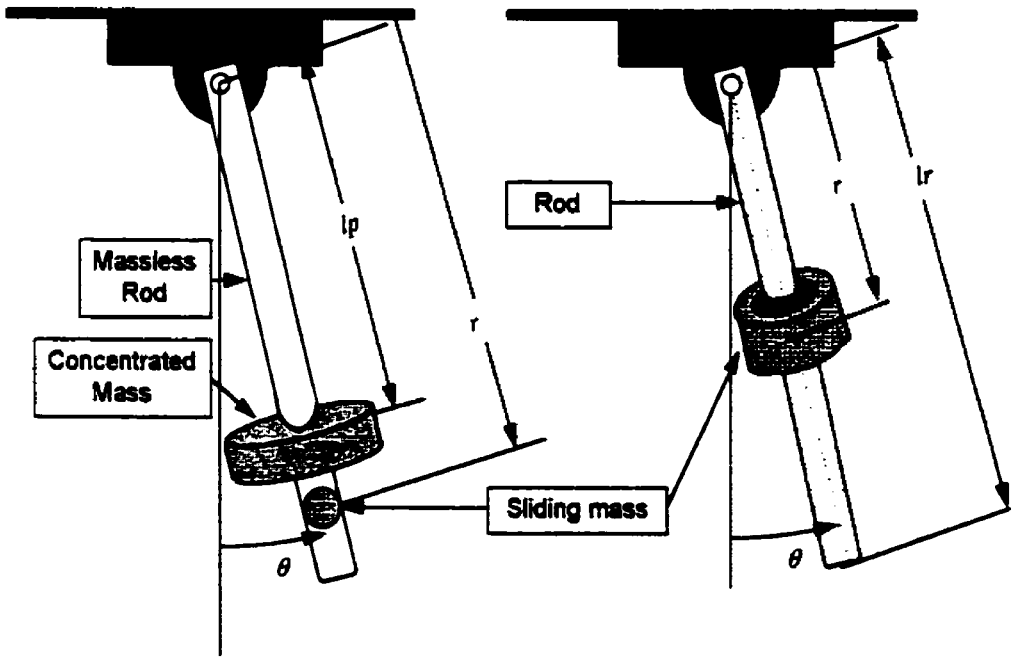

Figure 3.2 Pendulum structures with an auxiliary mass or slider: (a) a massless rod with concentrated mass and (b) an uniform rod with rotational inertia.

Various physical pendulum systems, where the attenuation device is a sliding mass, can be mathematically modeled by the general differential equations of motion, Equations 3.1 and 3.2. The equations describe a nonlinear coupling between the system's two degrees of freedom: the angular motion of the system and the translational motion of the auxiliary mass (or slider). If the sliding mass remained stationary, the system would be conservative and for small oscillations, the angular oscillations would be harmonic. However, the system with a moving auxiliary mass is not conservative and will exhibit the phenomena similar to those described in Section 2.2.2. The translational motion of the auxiliary mass affects the rotational motion of the structure via the second term of Equation 3.1. This second term represents either the addition or loss of energy to the angular motion depending on its sign.

3.2.4 Comparing the Mathematical and Physical Pendulum Models

The physical pendulum has two distinct masses while the mathematical pendulum has only one mass; hence the two systems will be referred to as dual or single mass systems, respectively. The governing differential equations of motion for both systems are given in Table 3.1. The configuration of the pendulum of the dual mass system is a concentrated mass located at a fixed distance from the pivot as shown in Figure 3.2(a). The physical pendulum system provides more accurate modeling of systems where the moving mass is significantly less than the structural mass. However, as the ratio of the structural pendulum mass to the auxiliary, moving mass decreases $\left(\frac{m_p}{m_s} \to 0\right)$, then the differential equations (Equations 3.3a and b) reduce to the mathematical pendulum equation (Equation 2.10).

Note that entries 1 and 3 in Table 3.1 represent the coupled, nonlinear differential equations describing the angular oscillations of the system and the translational motion of the mass along the structure, respectively. The actual

or physical force required to move the mass is the third entry. Entry 2 is a reorganization of the first entry; it merely groups the terms related to the slider to describe a "pseudo-force", $p(m_s,\theta,r,t)$, generated by the moving mass. This "pseudo-force" couples the translational motion of the slider with the angular oscillations of the pendulum to either increase or decrease the energy of the system.

Table 3.1 Governing equations of motion for the pendulum systems.

	Single Mass System	Dual Mass System
1	$\ddot{\theta}+2\frac{\dot{r}\dot{\theta}}{r}+\frac{g}{r}\sin\theta=0$ (2.9)	$\ddot{\theta}+\left(\frac{2m_s r}{m_p l_p^2+m_s r^2}\right)\dot{r}\dot{\theta}+g\left(\frac{m_p l_p+m_s r}{m_p l_p^2+m_s r^2}\right)\sin\theta=0$ (3.1)
2	$m_s\ddot{\theta}+m_s\frac{g}{r}\sin\theta=p(m_s,\theta,r,t)$ (3.4) where $p(m_s,\theta,r,t)=-2m_s\frac{\dot{r}\dot{\theta}}{r}$ (3.4a)	$m_p l_p^2\ddot{\theta}+m_p g l_p\sin\theta=p(m_s,\theta,r,t)$ (3.5) where $p(m_s,\theta,r,t)=-m_s\left(r^2\ddot{\theta}+2r\dot{r}\dot{\theta}+rg\sin\theta\right)$ (3.5a)
3	$F=m_s\left(\dot{\theta}^2 r-\ddot{r}+g\cos\theta\right)$ (2.8)	$F=m_s\left(\dot{\theta}^2 r-\ddot{r}+g\cos\theta\right)$ (3.2)

For the simple pendulum system, the oscillations are independent of the magnitude of the mass being moved or reconfigured within the pendulum structure; vibration attenuation is affected only by how the mass traverses the structure. However, for the physical pendulum system, the magnitude of the pendulum mass and its distribution (mass moment of inertia) along with the magnitude of the reconfigurable mass (the slider) and its position and translation profile affect the vibrations of the system. With the physical

pendulum, the equations of motion can be rearranged to isolate the effects of the auxiliary mass, which includes the rotational inertia, Coriolis effect and the gravitational restoring force. As the governing equations of the single and dual mass systems are similar, the strategy to attenuate the rotational vibrations of the physical pendulum should parallel those of the mathematical pendulum, as previously given in Section 2.2.2.

3.3 Dynamics of the Reconfigurable Mass-Pendulum Systems

The differential equations governing the dynamics of the reconfigurable mass-pendulum systems appear in Table 3.1. Despite the apparent simplicity, the dynamics of the systems considered can display a wide variety of interesting oscillatory and nonlinear behaviors. These unique dynamics arise from competing phenomena, such as parametric resonance and damped vibrations. In addition, the behavior associated with the nonlinearity of the system may interfere to affect the system further, by producing limit cycles. Through simplifying the governing differential equation to a linear equation with variable coefficients, various phenomena can be explained and predicted. However, for a more comprehensive understanding the complete nonlinear equations can be solved numerically with the simulated resultant motion. This is discussed in Chapter 4.

3.3.1 Simplifying the Equation of Motion -- Parametric Vibrations

For small amplitude oscillations, the governing differential equations for both single and dual mass systems, as presented in Table 3.1, can be reduced to linear differential equations with variable coefficients. The focus will be on the mathematical pendulum and the governing differential equation which can be reformulated to parallel the Mathieu-Hill's Equation which models the phenomenon of parametric vibrations.

For the single mass system, the assumption that the angular oscillations of the structure are small, effectively linearizes the governing differential equation (Equation 2.10) to the form,

$$\ddot{\theta}+2\frac{\dot{r}\dot{\theta}}{r}+\frac{g}{r}\theta=0 \tag{3.6}$$

Next, the motion of the sliding mass, m_s, is assumed to be harmonic and given by,

$$r(t)=R_o-\Delta r\ sin\ \varpi t \tag{3.7}$$

where R_o is the average radial distance of the mass from the pivot;

Δr, the constant amplitude or limits of the motion of the slider; and

ϖ, the frequency of the motion.

Note that the frequency of this translational motion is assumed constant.

Upon substituting this slider motion (Equation 3.7) into Equation 3.6, the governing differential equation becomes

$$\ddot{\theta}+2\frac{\left(-\Delta r\varpi\ cos\ \varpi t\right)}{R_o\left(1-\frac{\Delta r}{R_o}sin\ \varpi t\right)}\dot{\theta}+\frac{g}{R_o\left(1-\frac{\Delta r}{R_o}sin\ \varpi t\right)}\theta=0. \tag{3.8}$$

The normalized amplitude of the auxiliary mass motion will be defined as

$$\varepsilon=\frac{\Delta r}{R_o} \tag{3.9}$$

and the natural frequency of the system is given by

$$\omega_n = \sqrt{\frac{g}{R_o}}. \tag{3.10}$$

Using this notation, Equation 3.8 can then be rewritten as

$$\ddot{\theta} + 2\frac{(-\varepsilon\varpi \cos \varpi t)}{(1-\varepsilon \sin \varpi t)}\dot{\theta} + \frac{\omega_n^2}{1-\varepsilon \sin \varpi t}\theta = 0. \tag{3.11}$$

If the amplitude of motion for the auxiliary mass, Δr, is small in comparison to the average location of the mass, R_o, then $\varepsilon \langle\langle 1$ and Equation 3.11 can be approximated as

$$\begin{aligned} \ddot{\theta} - 2(\varepsilon\varpi \cos \varpi t)\left(1 + \varepsilon \sin \varpi t + \varepsilon^2 \sin^2 \varpi t + \cdots\right)\dot{\theta} \\ + \omega_n^2\left(1 + \varepsilon \sin \varpi t + \varepsilon^2 \sin^2 \varpi t + \cdots\right)\theta = 0 \end{aligned} \tag{3.12}$$

With the variable transformation of

$$\varpi t = 2\tau - \frac{\pi}{2}, \tag{3.13}$$

and neglecting the higher order terms of ε, the governing differential equation becomes

$$\frac{d^2\theta}{d\tau^2} - 4(\varepsilon \sin 2\tau)\frac{d\theta}{d\tau} + \frac{\omega_n^2}{\varpi^2}4(1 - \varepsilon \cos 2\tau)\theta = 0. \tag{3.14}$$

This simplified equation is similar to Mathieu's Equation. This equation has some very relevant and known characteristics which are pertinent to this study and are briefly introduced in the next section.

3.3.2 Introduction to Mathieu-Hill Equations

Mathieu-Hill equations are linear differential equations with periodic coefficients. The canonical form of the first order Mathieu Equation is given by

$$\frac{d^2y}{dz^2}+(a-2q\cos 2z)y=0 \tag{3.15}$$

where the parameters a and q are limited to real numbers and z is unrestricted.

The significance and incorporation of the damping terms as evident in Equation 3.14 will be discussed later. One generalized form of the Mathieu equation is Hill's equation where the periodicity of the stiffness parameter does not need to be harmonic [McLachlan, 1951]. In other words, if a relay action for mass reconfiguration is assumed; the governing differential equation will parallel the Hill's equation. The extended form of Mathieu's equation is expressed as,

$$\frac{d^2y}{dz^2}+\left[a-2q\psi(2z)\right]y=0 \tag{3.16}$$

where $\psi(2z)$ is a periodic function.

For the particular case of Hill's equation, the parameters are given as,

$$a=\theta_o \tag{3.16a}$$

and

$$-2q\psi(2z) = 2[\theta_2 \cos 2z + \theta_4 \cos 4z + \ldots]. \qquad (3.16b)$$

The theory of Mathieu equation can be applied to Hill's equation with similar stability and instability characteristics existing [Hayashi, 1964].

By applying Floquet's theory, a particular solution of Mathieu's equation (Equation 3.15) is given as

$$y = exp(\mu\tau)\phi(\tau) \qquad (3.17)$$

where μ is the characteristic index which depends in a very decisive way on the parameters, a and q, and $\phi(\tau)$ is a periodic function of τ with periodicity of π or 2π [Hayashi, 1953].

Since Mathieu's equation (Equation 3.15) is unchanged for a sign change of the dependent parameter, $-\tau$, another independent solution is $y = exp(-\mu\tau)\phi(-\tau)$; hence, the general solution may be expressed as

$$y = c_1 exp(\mu\tau)\phi(\tau) + c_2 exp(-\mu\tau)\phi(-\tau) \qquad (3.18)$$

where c_1 and c_2 are arbitrary constants.

The solution may be of decreasing amplitude or bound amplitude (stable motion) or of increasing amplitude (unstable motion) depending on the values of a and q.

The stable, neutral solution is characterized as periodic and by definition, called Mathieu functions. These functions are elliptic cosine or sine series that define the characteristic curves that divide the a-q plane into stable and unstable regions as mapped in the Haines-Strett diagrams illustrated in Figure 3.3 [McLachlan, 1951].

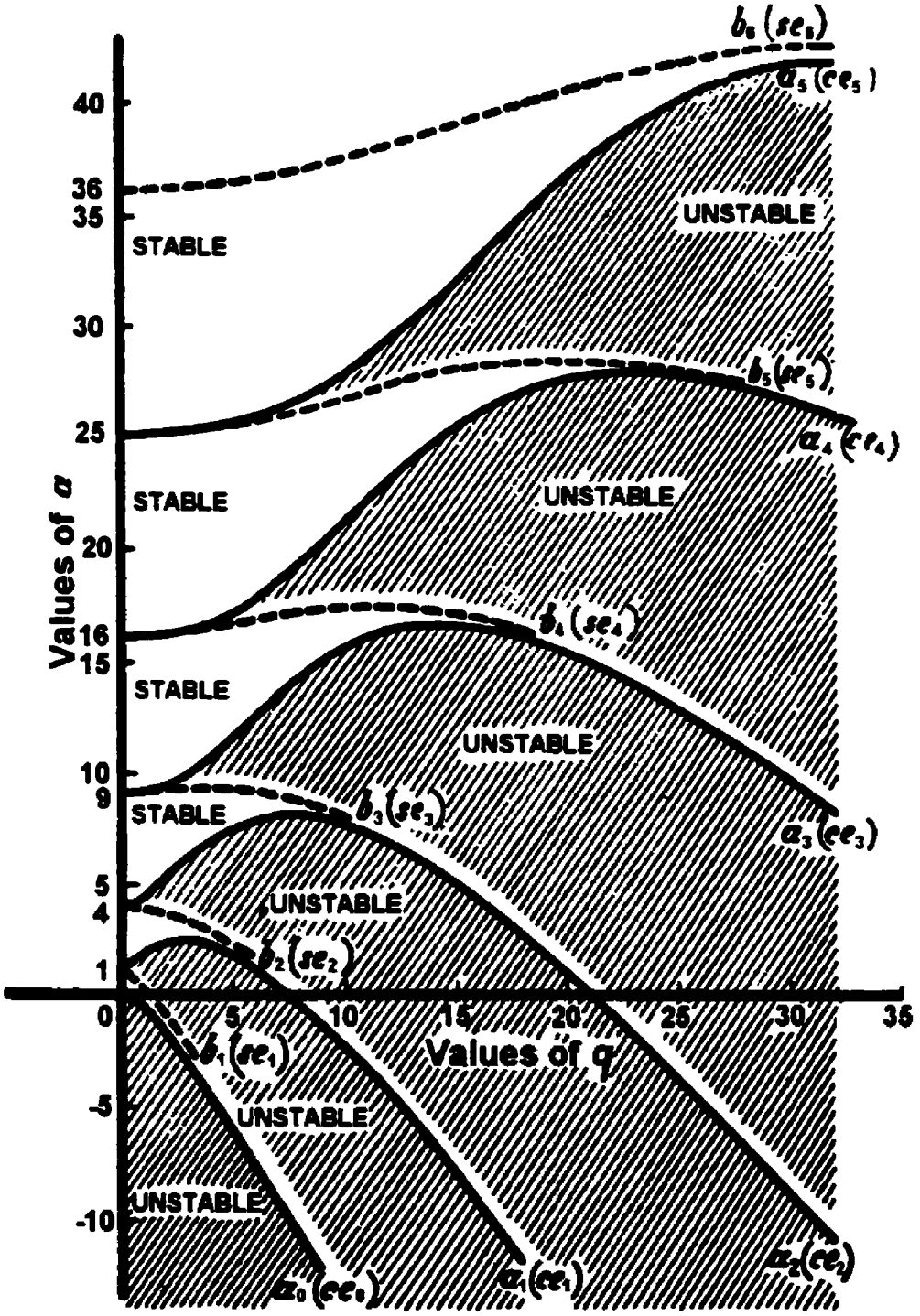

Figure 3.3 Zones of stability and instability (shaded area) for Mathieu's equations.[6]

[6] Note this diagram has been reproduced from Theory and Applications of Mathieu Functions by N. W. McLachlan (1951) p. 40.

With reference to the complete, general solution (Equation 3.18), stability exists if μ is purely imaginary and instability occurs when μ is real.

As shown in Figure 3.3, the ranges of stability alternate with regions of instability. Essentially, Mathieu's equation and the Haines-Strett diagram eliminates the need to solve the differential equation when assessing the stability of the system. The governing differential equation needs to be transformed to the standard Mathieu's Equation 3.15 with the parameters, a and q, being evaluated.

As presented in Section 2.2, one method to attenuate the oscillations of the pendulum is cycling the end mass at twice the pendulum frequency. However, when the end mass cycles at this frequency, then $a = 1$ and the system lies in the broadest instability zone between the characteristic curves, a_1 and b_1[7]. For any mass motion, $q \neq 0$, parametric resonance occurs and oscillations would tend to amplify. To understand how oscillation attenuation can occur for this same scenario, damping effects must be analyzed.

The differential equation for a similar system with viscous damping can be derived in the following form,

$$\frac{d^2y}{dz^2} + 2\kappa\frac{dy}{dz} + (\bar{a} - 2q\cos 2z)y = 0 \qquad (3.19)$$

where the parameter κ represents the viscous damping coefficient. All the parameters of Equation 3.19 are real with both κ and q being positive values. Damped Mathieu functions of fractional order are solutions to this equation. Also, this equation parallels the differential for the reconfigurable mass-pendulum system (Equation 3.14) with the exception being the damping term.

---

[7] The characteristic number corresponding to each Mathieu function which defines the characteristic curves as shown in Figure 3.3. The characteristic number can be expanded as a power series in q (from Equation 3.15).

The pendulum system has a time-varying damping; whereas, Mathieu's equation has a positive and constant damping coefficient.

By assuming a solution in the form

$$y = exp(-\kappa z) \cdot u(z) \tag{3.20}$$

and substituting into Equation 3.19, the differential is converted into Mathieu equation,

$$\frac{d^2u}{dz^2} + (a - 2q\cos 2z)u = 0 \tag{3.21}$$

where $a = (\bar{a} - \kappa^2)$.

If the parameters, a and q, are located in a stable region of Figure 3.3, the solution has the form of exponentially decaying damped oscillations. However, if the parameters are located in an unstable region, then the solution may be stable and converging to zero, unstable and diverging or neutral and periodic depending on the relation between the damping constant, κ, and the characteristic index, μ. The relations can be summarized as follows:

(1) if the defining parameters $(\bar{a}, q)$ lie on the characteristic curve, then $\kappa = \mu$ and the condition is neutral and the motion is periodic. Theoretically, oscillations once initiated would continue unchanged. In practice, natural limitations, either decay the oscillations or allow increased growth to a limit.

(2) if $(\bar{a},q)$ occurs in a stable region then $\kappa > \mu$ and oscillations decay as time progresses.

(3) if $(\bar{a},q)$ occurs in an unstable region then $\kappa < \mu$ and the amplitude increases with time.

The regions of stability are adjusted as shown by the iso-μ curves which lie within the unstable region as shown in Figure 3.4 [McLachlan, 1951]. As seen, the effects of damping have increased the region of stability.

The characteristic index which controls the decay of the solution for the functions of fractional order, is dependent upon the equation parameters, a and q. From Figure 3.4, for small values of q the minimum of the iso-μ curves occurs approximately midway between the bounding curves of the unstable region; therefore to approximate the characteristic index

$$\mu \cong \pm\frac{q}{2}. \tag{3.22}$$

When $a = 1$ and $q \leq 2\mu$, stable motion will occur.

When the solution is quasi-periodic as exists for degenerate cases, the function, $\phi(\tau)$, of Equation 3.17 is defined in terms of a phase shift variable, σ, that varies between 0 and $-\frac{\pi}{2}$. This variable is also interrelated to the other parameters a,q and μ. Iso-μ curves and iso-σ curves are shown in Figure 3.5 for the first instability zone which has been reproduced [Hayashi, 1964][8].

[8] This reference [Hayashi, 1964] employs Mathieu's equation of the following form $\frac{d^2x}{d\tau^2} + (a + 16q\cos 2\tau)x = 0$. Correspondingly, the scaling of the q-axis changes from the previous plots, Figure 3.3 and 3.4 [McLachlan, 1951].

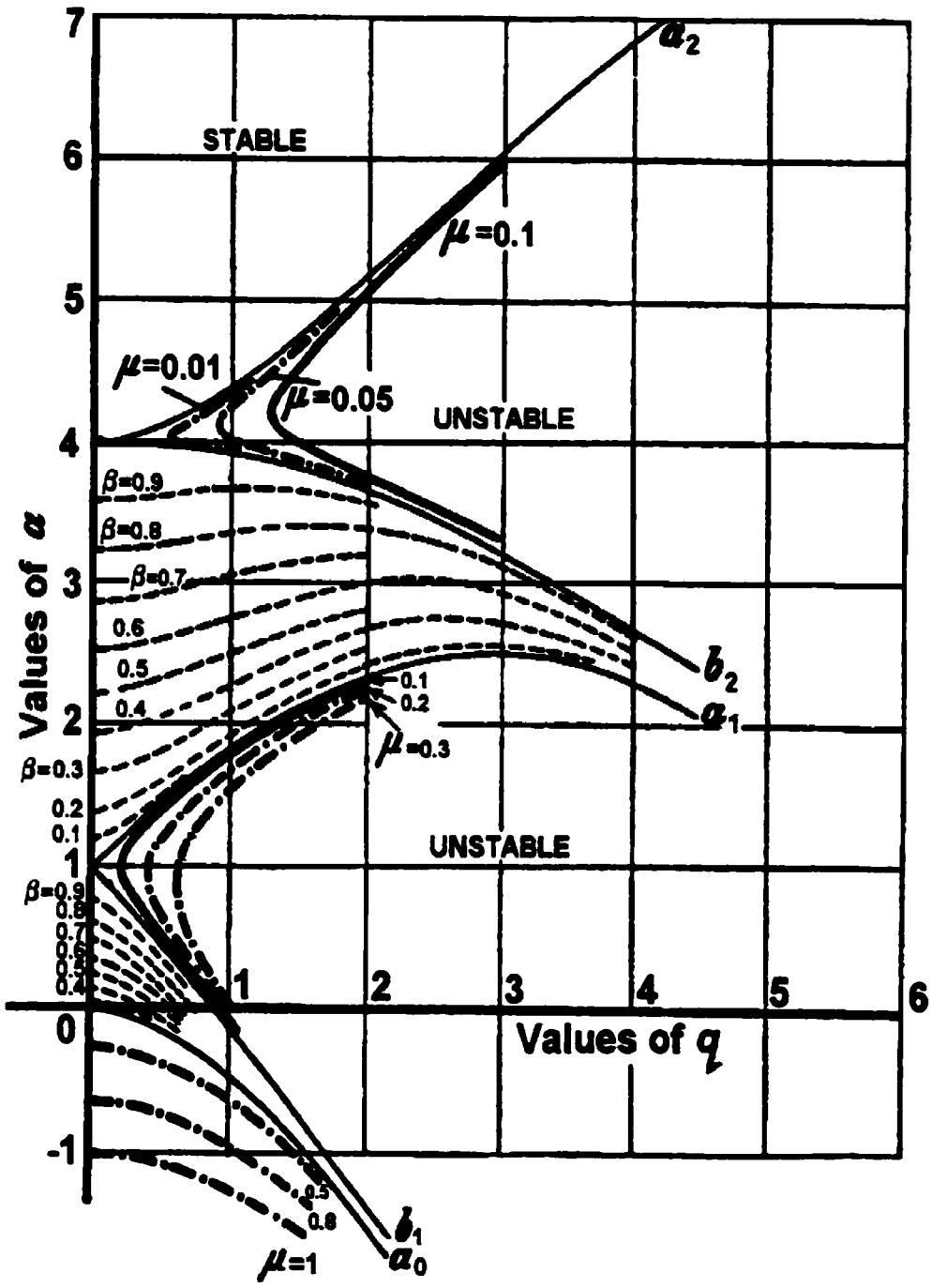

Figure 3.4 Iso-μ stability chart for Mathieu's equations of fractional order.[9]

[9] Note this figure has been reproduced from Theory and Applications of Mathieu Functions by N. W. McLachlan (1951) p.98.

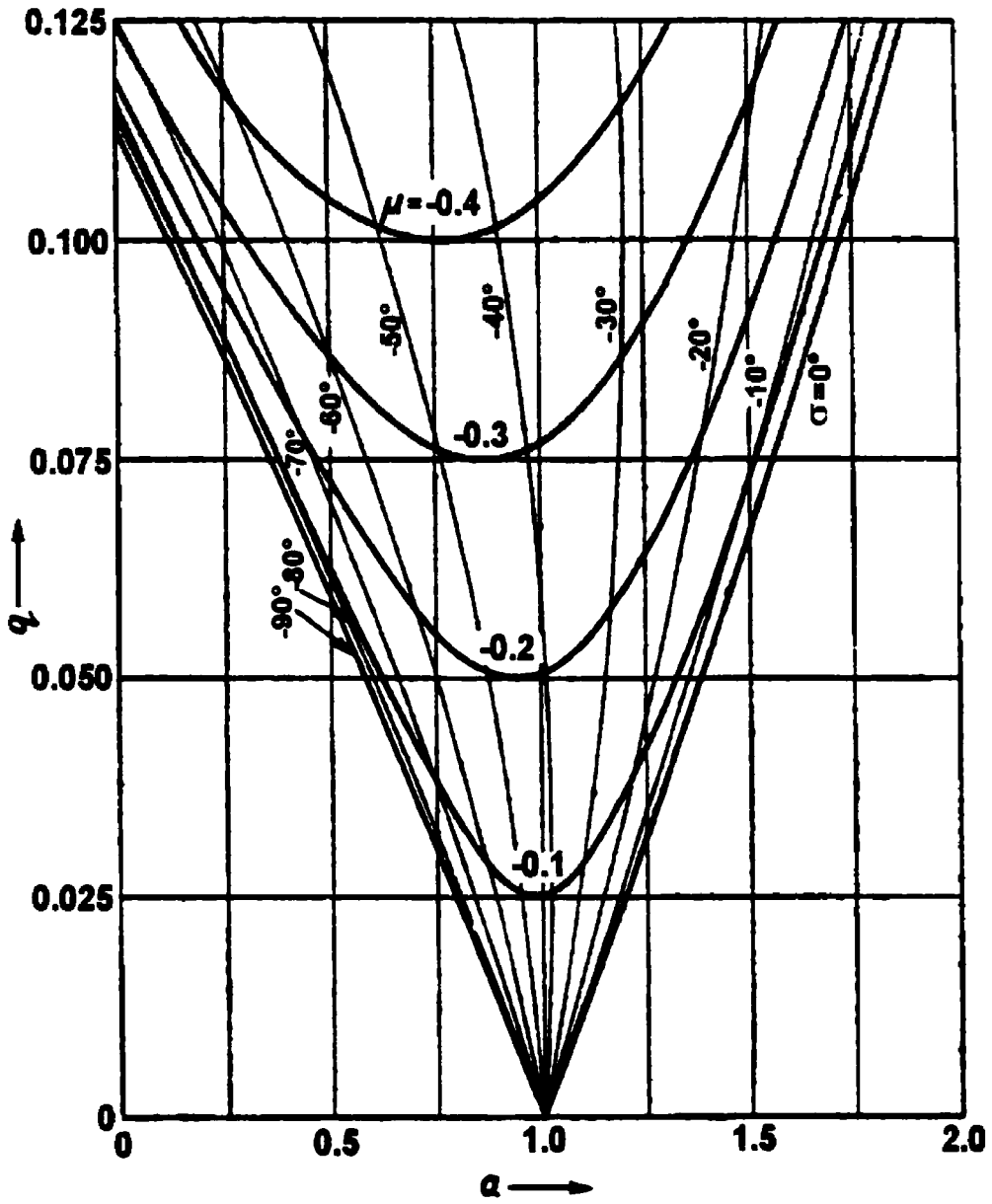

Figure 3.5 First zone of stability for fractional order Mathieu Equation[6] with phase shifts.[10]

As with Figure 3.4, the value of μ determines the stability characteristics, but its value is based on that of σ [Hayashi, 1964]. These iso-σ and iso-μ curves are symmetric about the α-axis. The iso-μ curve

[10] This figure has been reproduced from Nonlinear Oscillations in Physical Systems by C. Hayashi (1964) p.90.

becomes the boundary curve separating stable and unstable regions and these curves are asymptotic to the characteristic curves that bound the unstable region where they lie. Similar charts for the second and third instability region can be found in *Nonlinear Oscillations in Physical Systems* [Hayashi, 1964].

3.3.3 Equivalent Damping Coefficients for Periodic End Mass Motion

The simplified governing differential equation for the pendulum system (Equation 3.14) is very similar to Mathieu's Equation of fractional order (Equation 3.19); the difference lies with the second damping term. Equation 3.14 contains variable damping that may be positive or negative depending on the mass motion; whereas, Mathieu's equation assumes a constant, viscous type of damping. The variable damping in the pendulum system is capable of attenuating the angular oscillations as shown in Section 2.2.2; the function is similar to a viscous damper. To compare the viscous type of damping of Equation 3.19 with the attenuation in the pendulum system, the energy dissipation over an oscillation cycle is calculated and equated for these two types of damping. This allows an equivalent viscous damping coefficient to be defined for the mass reconfiguration system. Then, this equivalent viscous damping coefficient can be used in Mathieu's equation to predict stable and/or unstable motion.

As previously stated, depending on the auxiliary mass motion, the attenuation or amplification of the pendulum's oscillations occurs over a cycle of angular displacement, as discussed in Chapter 2. For attenuation, the net effect over a complete vibration cycle is energy loss, although instantaneously, variable damping may be either positive or negative. In contrast, a viscous damping mechanism dissipates energy whenever there is motion. To quantify these damping effects, the energy dissipation for a given period in these two systems is calculated. A simple "averaging" of the

coefficient for the angular velocity in Equation 3.6 over a cycle is ineffective, as this value is zero.

Consider the motion of a one degree of freedom system, mass-spring-damper system. The governing differential equation for an elastically suspended mass that is free to oscillate has the form,

$$m\ddot{y} + c\dot{y} + ky = 0 \quad \text{or} \quad \ddot{y} + 2\xi\omega_n\dot{y} + \omega_n^2 y = 0 \tag{3.23}$$

where $m\ddot{y}$ represents the inertia force;

ky, the elastic resistance force;

$c\dot{y}$, the viscous resistance force;

$\xi = \dfrac{c}{2m\omega_n}$, the damping ratio; and

$\omega_n^2 = \dfrac{k}{m}$, the natural frequency.

The damping ratio can be related to the energy dissipated in a cycle. First, Equation 3.23 is converted into a work-energy relation consisting of incremental work done or energy change by multiplying each term by an incremental displacement, dy, to obtain

$$m\ddot{y}dy + c\dot{y}dy + kydy = 0. \tag{3.24}$$

Equation 3.24 can be interpreted as the energy balance for the mass-spring-damper system over an infinitesimal displacement. For motion from y_1 to y_2, this balance can be written in the integral form,

$$-\int_{y_1}^{y_2}(c\dot{y})dy = \int_{y_1}^{y_2}(m\ddot{y} + ky)dy. \tag{3.25}$$

The left hand side of the equation represents the energy dissipated, while the right hand side can be explicitly integrated to give the kinetic and potential energy of the system. Integrating by parts over a cycle of vibration defined by the period from $t = 0$ to $t = \tau$ gives

$$\Delta E = -\int_0^{\tau} \left(c\dot{y}^2\right)dt = \frac{1}{2}\left(m\dot{y}^2 + ky^2\right) - E(0) \tag{3.26}$$

where ΔE is the energy dissipated in a cycle and $E(0)$ is the initial energy state.

For small values of the damping ratio ($\xi << 1$), the motion during a cycle can be approximated as simple harmonic motion,

$$y(t) = A\,exp\left(-\xi\omega_n t\right)cos\left(\omega_n\sqrt{1-\xi^2}\right)t \equiv A\cos\omega_n t \tag{3.27}$$

where A is an amplitude at the beginning of the cycle. For a complete cycle of motion, the energy dissipated is evaluated as,

$$\Delta E = -\int_0^{\tau} c\dot{y}^2 dt = -\frac{c}{\omega_n}\int_0^{2\pi} A^2\omega_n^2 sin^2\left(\omega_n t\right)d\left(\omega_n t\right) = -A^2\omega_n c\pi\,. \tag{3.28}$$

The initial energy of the system associated with the energy stored in the spring is given by

$$E(0) = \frac{1}{2}kA^2\,. \tag{3.29}$$

The energy dissipated is normalized with respect to the above initial energy to give

$$\frac{\Delta E}{E(0)} = \frac{2c\pi}{m\omega_n}. \tag{3.30}$$

Using the damping ratio, ξ, as previously defined, the normalized energy dissipation by a viscous damper for a cycle becomes

$$\frac{\Delta E}{E(0)} = -\frac{A^2 c\omega_n \pi}{\frac{1}{2}kA^2} = -4\pi\xi. \tag{3.31}$$

The energy dissipated in a cycle for a variable length pendulum can be calculated in a similar way. The linearized, governing differential equation of motion is multiplied by an incremental displacement, $d\theta$, to obtain an energy balance given by

$$\ddot{\theta}d\theta + 2\frac{\dot{r}}{r}\dot{\theta}d\theta + \frac{g}{r}\theta d\theta = 0. \tag{3.32}$$

This equation can be rewritten as

$$d\left(\frac{1}{2}\dot{\theta}^2\right) + d\left(\frac{1}{2}\frac{g}{r}\theta^2\right) + 2\frac{\dot{r}}{r}\left(\dot{\theta}^2 + \frac{g}{4r}\theta^2\right)dt = 0. \tag{3.33}$$

Then, the energy dissipated, ΔE, per cycle is determined as,

$$\Delta E = -2\int_0^{\tau}\frac{\dot{r}}{r}\left(\dot{\theta}^2 + \frac{g}{4r}\theta^2\right)dt = \frac{1}{2}\dot{\theta}^2 + \frac{g}{2r}\theta^2 - E(0) \tag{3.34}$$

where τ is the period of angular vibration. Again, the right hand side of the equation represents the kinetic and potential energy of the system at any instance of time, and $E(0)$ is the initial energy state. Note that the energy dissipation as given in Equation 3.28 was always negative while that in Equation 3.34 depends on the velocity of the mass as represented by $\dot{r}$.

The attenuation of the angular oscillations for the pendulum system by reconfiguring the system mass follows the strategy as shown in Figure 2.7(a). The translational motion of the end mass, $r(t)$, is assumed to fluctuate by a small amplitude, Δr, about a set position, R_o, with the frequency being twice the pendulum's average natural frequency, $2\varpi = 2\sqrt{\frac{g}{R_o}} = 2\omega_n^2$. The mass motion is given as

$$r(t) = R_o - \Delta r \sin 2\varpi t, \tag{3.35}$$

and the harmonic angular motion of the system for a cycle is approximated as

$$\theta(t) \cong \theta_o \cos \omega_n t. \tag{3.36}$$

These profiles are shown in Figure 3.6.

The corresponding energy dissipated per cycle is then calculated as

$$\Delta E = -2\int_0^{\tau} \frac{\dot{r}}{r}\left(\dot{\theta}^2 + \frac{g}{4r}\theta^2\right)dt = -\frac{3\pi}{2}\frac{\Delta r}{R_o}\theta_o^2\varpi^2 . \tag{3.37}$$

The change in energy over a cycle of angular oscillation is normalized with respect to the initial energy of the system,

$$E(0) = \frac{1}{2}\frac{g}{R_o}\theta_o^2 = \frac{1}{2}\varpi^2\theta_o^2 \tag{3.38}$$

to give,

$$\frac{\Delta E}{E(0)} = \frac{-\frac{3\pi}{2}\frac{\Delta r}{R_o}\theta_o^2\varpi^2}{\frac{1}{2}\varpi^2\theta_o^2} = -3\pi\frac{\Delta r}{R_o}. \tag{3.39}$$

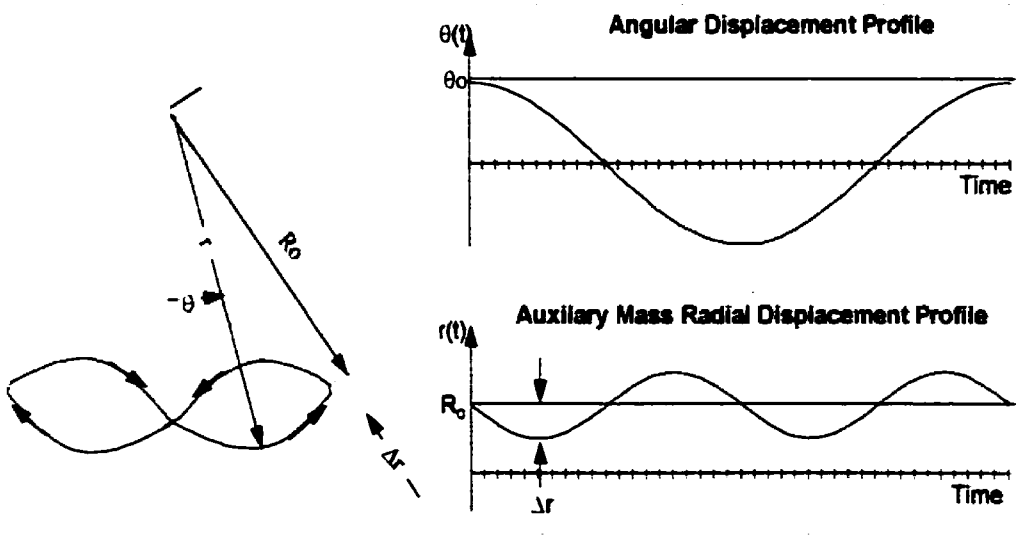

Figure 3.6 Profile of the moving mass and oscillating pendulum system for attenuation.

Equating the normalized energy dissipation for the two systems over a cycle of oscillations (as given by Equations 3.31 and 3.39), an equivalent, viscous damping ratio, ξ_{EQ}, for the sinusoidal mass reconfiguration system is defined as:

$$\xi_{EQ} = \frac{3}{4}\frac{\Delta r}{R_o}. \tag{3.40}$$

As can be seen, when mass reconfiguration within the structure is assumed to be harmonic and at twice the natural frequency of the system (Figure 3.6), the damping ratio depends on the location and amount of translational motion of the end mass.

Note that ξ_{EQ} is negative, if $\Delta r < 0$ which corresponds to the pattern shown in Figure 2.8a. For this case, the mass moves away from the pivot as the pendulum nears its maximum angular displacement and towards the pivot as the pendulum nears its vertical or equilibrium position. Such a pattern causes amplification of the angular oscillations.

If the mass moves towards the pivot once the pendulum reaches its maximum angular displacement and away from the pivot as the pendulum nears its vertical position, then both Δr and ξ_{EQ} are positive, as shown in Figure 2.7. The governing equation for parametric vibrations with viscous damping similar to Equation 3.19 can be written in the form

$$\ddot{\theta} + 2\xi_{EQ}\omega_n\dot{\theta} + \omega_n^2(1+\varepsilon \sin \varpi t)\theta = 0 \qquad (3.41)$$

where the notation is as introduced in Section 3.3.1. Upon substituting the equivalent ratio (Equation 3.40), this equation replaces Equation 3.12 and with the substitution of Equation 3.13, the approximate governing differential equation (Equation 3.14) for the pendulum system with equivalent viscous attenuation properties takes the form,

$$\frac{d^2\theta}{d\tau^2} + 3\varepsilon\frac{\omega_n}{\varpi}\frac{d\theta}{d\tau} + 4\frac{\omega_n^2}{\varpi^2}(1-\varepsilon\cos 2\tau)\theta = 0. \qquad (3.42)$$

This equation, in terms of damping, can be considered equivalent to Equation 3.14 and is of the same form as Mathieu's equation of fractional order (Equation 3.19) whose features were briefly presented in Section 3.3.2.

As the displacement profiles and/or coordination of the moving mass with the angular oscillations of the pendulum vary, different equivalent damping values will be generated. For the motion pattern illustrated in Figure 2.7(b), the relay action consists of moving the mass towards the pivot when the angular velocity of the system is near zero and the motion of the mass is away from the pivot when the mass passes directly beneath the pivot. The range, Δr, of translational motion at the radial distance, R_o, from the pivot and at twice the natural rotational frequency of the pendulum system is assumed. The energy change over an oscillation can then be calculated to be

$$\Delta E = 12g\Delta r(cos\theta_o - 1). \tag{3.43}$$

Normalizing this change of energy with respect to the initial energy of the system (Equation 3.36) gives

$$\frac{\Delta E}{E(0)} = \frac{12g\Delta r(cos\theta_o - 1)}{g(R_o + \Delta r)(1 - cos\theta_o)} = -12\frac{\Delta r}{R_o + \Delta r} \approx -12\frac{\Delta r}{R_o}. \tag{3.44}$$

Upon equating this energy dissipation with that of the viscous damped system (Equation 3.31), the equivalent, viscous damping ratio of the relay profile for mass reconfiguration is given as

$$\xi_{EQ} = \frac{3\Delta r}{\pi R_o}. \tag{3.45}$$

This strategy provides more effective damping than the harmonic motion which is consistent with the discussion presented in Section 2.2.2 and

illustrated in Figure 2.7. In general, the equivalent damping ratio depends on the location and amount of translational motion of the moving mass.

3.3.4 Some Properties of Mathieu's Equation Applied to the Reconfigurable Mass-Pendulum System

The simplified governing differential equation (Equation 3.14) assumes the translational motion of the end mass is sinusoidal and at twice the mean frequency of the angular oscillations of the simple pendulum. Furthermore, the amplitude of motion of the auxiliary mass is significantly less than its mean radial position as measured from the pivot. The magnitude of the angular oscillations are assumed to be small allowing the governing differential equation to be linearized.

For the described mass reconfiguration, the simplified governing differential equation is given by Equation 3.14 or 3.42 for the mathematical pendulum system, the corresponding parameters of the classic Mathieu's Equation 3.15 when the damping effects are neglected are

$$a = 4\frac{\omega_n^2}{\varpi^2} = 1 \tag{3.46}$$

and

$$q = 4\frac{\omega_n^2}{\varpi^2}\frac{\varepsilon}{2} = \frac{\varepsilon}{2}. \tag{3.47}$$

As predicted by Figure 3.3, any mass motion, $q \neq 0$, at this resonant frequency, $\varpi = 2\omega_n$ (that is, $a = 1$), would yield unstable behavior. When various normalized displacement modulations, ε, are plotted on a Haines-Strett stability chart, the interceptions in the unstable regions increase as the modulation value increases. In other words, the frequency range associated with unstable motion increases.

When plotting these displacement modulations on the stability chart for Mathieu's Equation of Fractional Order as done in Figure 3.7, it is apparent that the required characteristic index, μ, for stable dynamic behavior is small. For small values of mass motion, q, the value of the characteristic index is also very small, as given by Equation 3.22.

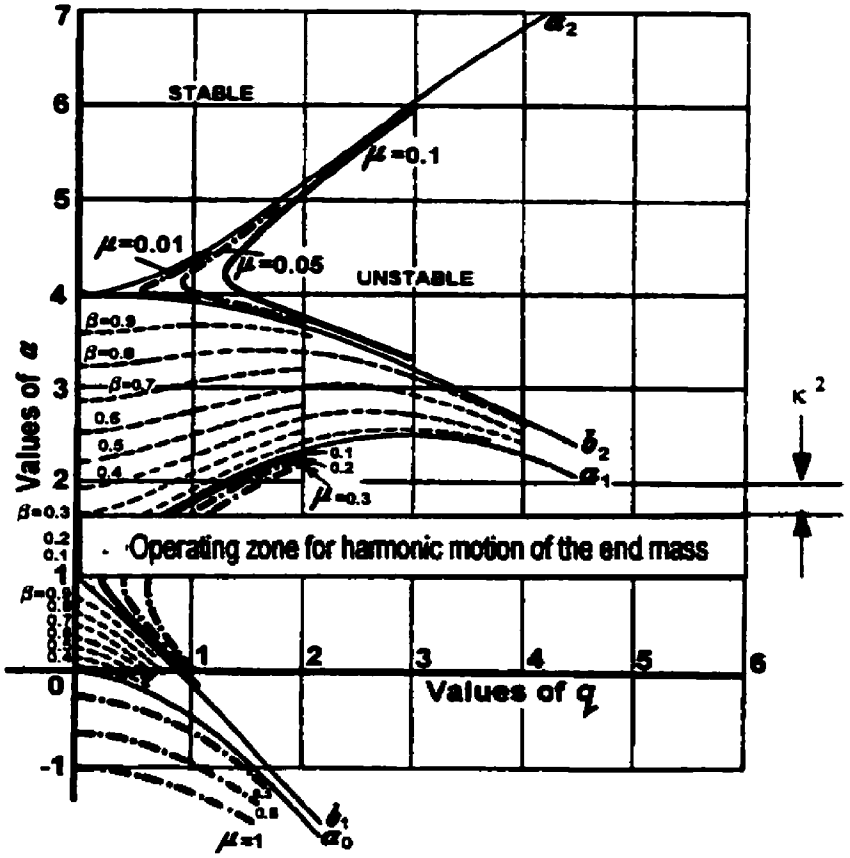

Figure 3.7 Stability chart[11] for constant displacement modulations for a reconfigurable mass-pendulum system.

When damping is considered, an equivalent damping coefficient can be evaluated. The governing differential equation can then be approximated by Equation 3.42 with the defining Mathieu's Equation parameters being

[11] The background figure has been reproduced from Theory and Applications of Mathieu Functions by N. W. McLachlan (1951) p.98.

$$\kappa = \xi_{EQ}\omega_n = \frac{3}{2}\varepsilon\frac{\omega_n}{\varpi} = \frac{3}{4}\varepsilon \tag{3.48}$$

$$a = \bar{a} - \kappa^2 = 4\frac{\omega_n^2}{\varpi^2} - \kappa^2 = 1 - \frac{9}{16}\varepsilon^2 \tag{3.49}$$

$$q = \frac{\varepsilon}{2} \tag{3.50}$$

and

$$\mu = \frac{q}{2} = \frac{\varepsilon}{4} \tag{3.51}$$

Damping extends the stability zone and for the above parameters, the stability criteria of $\kappa \geq \mu$ is satisfied both for the trivial case of no auxiliary mass motion, $\varepsilon = 0$, and for all displacement modulations when $\varepsilon > 0$.

Consider the mathematical pendulum where the average position of the end mass is $R_o = 1.0\,\text{m}$. The frequency of vibration of the end mass is twice the average angular oscillations of the system of $\omega_n \cong 3.1321\,\text{rad/s}$. As shown, this pendulum system will exhibit stable behavior if the amplitude of the translational motion of the end mass is positive, $\Delta r > 0$.

As a specific example, if the translational amplitude of the sinusoidal displacement is selected where $\Delta r = 0.25\,\text{m}$, the equivalent damping coefficient as evaluated from Equation 3.40 is $\xi_{EQ} = 0.1875$. The corresponding Mathieu parameters are $a = 0.9648$, $q = 0.125$ and $\kappa = 0.1875$, and this point, (a,q) lies in a stable region of the Haines-Strett diagram[12]. Furthermore, $\mu \cong \pm\frac{1}{2}q = \pm 0.0625$ which satisfies the stability criteria of $\mu < \kappa$.

For the reconfigurable mass-pendulum system (Equation 2.10), the coefficients of the governing equation are actually time varying. The dynamic stiffness and the damping values are continually changing as a result of the

[12]Note for Figure 3.5, $q = 0.015625$ and hence the operating point is in an extended zone of stability.

mass reconfiguration (Equation 3.7 or 3.35). Instantaneously, the corresponding Mathieu's Equation parameters may lie in either the stable or unstable zone. Based on the simplified governing equation (3.14), where the mass reconfiguration occurs at twice the system's natural frequency the corresponding Mathieu's equation parameters are

$$\kappa = -2\varepsilon \sin 2\tau \tag{3.52}$$

$$a = 4\frac{\omega_n^2}{\varpi^2} - \kappa^2 = 1 - 4\varepsilon^2 \sin^2 2\tau \tag{3.53}$$

and q and μ are as previously defined by Equations 3.50 and 3.51, respectively.

As presented in Section 3.3.2, for stability, $\mu \le \kappa$ and the corresponding displacement modulation limits is expressed as the following inequality,

$$\varepsilon \le -8\varepsilon \sin 2\tau . \tag{3.54}$$

or when using the former transformation (Equation 3.14) of $2\tau = \varpi t + \frac{\pi}{2}$

$$\varepsilon \le 8\varepsilon \cos 2\omega_n t \tag{3.55}$$

Stability is predicted when either

(1) there is no auxiliary motion: $\varepsilon = 0$ or

(2) for $\varepsilon > 0$, $\cos 2\omega_n t \ge \frac{1}{8}$ (3.56)

For the second condition, this inequality is only satisfied for a portion of each oscillation cycle of the pendulum. Instantaneously, the system behavior may lie outside the stable zone. Alternately, this fluctuation between stable and

unstable zones can be seen by plotting the range of (a,q) on Figure 3.5 or 3.6[13] where $a \in \left[1-\kappa^2, 1\right]$.

In general, variations in the system parameters, such as the range of motion of the auxiliary mass, its frequency of motion and/or the phase with respect to the structural angular oscillations will affect the system dynamics. Predicting the dynamic behavior for a pendulum with reconfigurable mass is quite involved, even though a similar system – a child swinging – is seemingly intuitively solved as the child learns how to control the oscillations of the swing. Based on numerical simulations, the dynamic behaviors of the pendulum with reconfigurable mass for various paradigms, are explored in Chapter 4 with reference to the discussion herein.

3.4 Parameterization of Systems for the Computer Simulations

The technique of reconfiguring the structural mass is used to control the dynamics of the system. As the mass moves along the structure, it alters the system's characteristics; such as the damping and the dynamic stiffness.

The effects of the moving mass are indicated in the governing differential equations of Table 3.1. For the mathematical pendulum, only the position of the moving mass alters the system's parameters. For the physical pendulum, both the magnitude and position of the moving mass affect the parameters.

The "instantaneous" frequency or the dynamic stiffness of the mathematical pendulum changes with the mass position, as given by

$$\omega(t) = \sqrt{\frac{g}{r(t)}}. \tag{3.57}$$

[13] See previous footnote [7].

As the length of the pendulum increases, the natural frequency decreases and vice versa. For a physical pendulum (Figure 3.2a), the position and magnitude of the auxiliary mass and the structural inertia and rigidity both affect the dynamic stiffness and the instantaneous frequency, as given by

$$\omega(t) = \sqrt{g\left(\frac{m_p l_p + m_s r(t)}{m_p l_p^2 + m_s r(t)^2}\right)} = \sqrt{\frac{g}{r(t)}\left(\frac{1+\frac{m_p l_p}{m_s r(t)}}{1+\frac{m_p l_p^2}{m_s r(t)^2}}\right)}. \qquad (3.58)$$

As the ratio of the pendulum or structural mass to the sliding mass approaches zero $\left(\frac{m_p}{m_s} \to 0\right)$, the dynamics of the system can be effectively modeled as a mathematical pendulum; Equation 3.58 reduces to Equation 3.57. This is shown in Figure 3.8, where the pendulum is of length, 1 m. To approximate the dual mass system as a simple pendulum, the structural mass should be chosen to be ~10% or less than the magnitude of the sliding mass, and the sliding mass motion should be limited to $0.75 < r(t) < 1.25$ m.

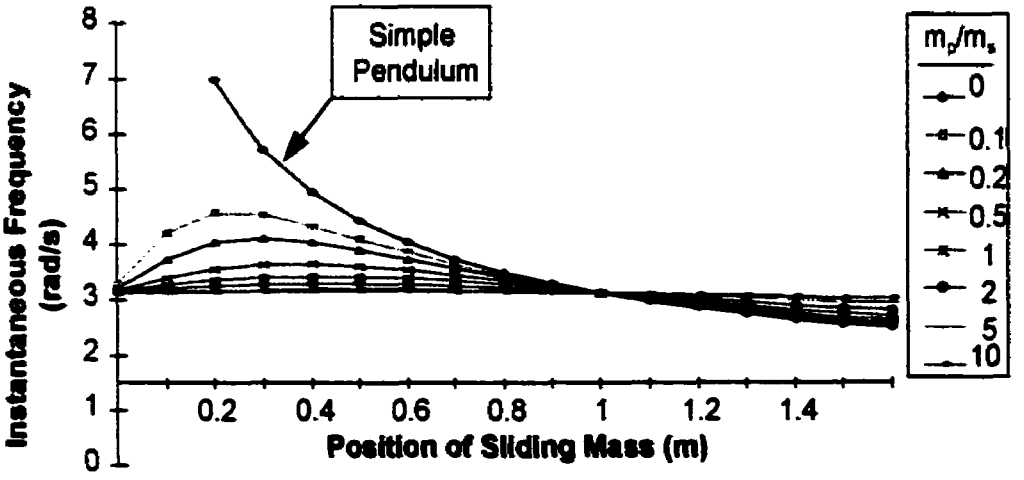

Figure 3.8 Effects of magnitudes of the structural mass, sliding mass and slider position on dynamic stiffness.

The damping coefficient is a time-varying parameter. The corresponding damping force is a function of the position of the sliding mass and its first time derivative, its magnitude and the angular motion of the pendulum. The nature of the damping is described through examining various temporal displacement profiles for the sliding mass in Chapter 4.

For investigating the dynamics of the reconfigurable mass-pendulum system the following parameterizations were made. For the simple pendulum system, a length of 1.0 m was chosen with a range of motion for the end mass being restricted to 0.25 m about this point. The corresponding natural frequency, as calculated from Equation 3.57, ranges between 2.80 to 3.58 rad/s (with the corresponding period being 1.74 to 2.24 s). Selecting a shorter pendulum would increase the natural frequency and decrease the available time to implement control. Hence a faster control system would be required.

For the physical pendulum system, the pendulum mass was selected as a concentrated mass of 7.5 kg located at a distance of 1.0 m from the pivot. The natural frequency of the system is 3.1321 rad/s and the period of oscillations is about 2 seconds which is comparable with the characteristics of the mathematical pendulum. The auxiliary mass was selected to be 0.75 kg with its motion bound between 0.75 to 1.25 m away from the pivot. The range of the undamped natural frequency as calculated using Equation 3.58 varies between 3.08948 to 3.15977 rad/s. Note also that when examining only the slider, its motion and characteristics are equivalent to the mathematical pendulum system.

In the next chapter numerical simulations of the dynamics for the above parameterized systems for various temporal profiles of the auxiliary mass are presented. Through reconfiguring the system mass, a mechanism for active damping is achieved.

3.5 Summary

Mass reconfiguration within the system by either internally or externally moving an auxiliary mass within or along the structure can be used to achieve active vibration attenuation. Pendulum structures are accurate models for many physical systems which exist in numerous and diverse applications. Many of these systems require a mechanism to prevent and/or alleviate vibrations.

In developing a mathematical model of the system, other damping factors, such as drag or material damping, are neglected to accentuate the effects that the moving mass has on attenuating the structural vibrations. These other forms of damping will further enhance the stability and damping of the systems.

Accounting for the structural mass enables segregating the auxiliary mass and further extends the modeling accuracy. In addition, the moving mass attenuation device can be viewed as a separate mechanism that can be retrofitted to existing structures. As shown, the physical pendulum or dual mass system can be reduced to the mathematical or single mass system where the effects of moving the end mass are more apparent.

To provide insight into the dynamics of the variable length pendulum model, the describing equation for the angular oscillations was simplified and reduced to linear equations with variable coefficients. These equations which resemble Mathieu-Hill's equations are valid for small, structural angular oscillations and small translational motion of the end mass which has a frequency twice the structural angular oscillation frequency. Mathieu's Equations are oscillatory with defined regions of stability and instability. The unstable physical phenomenon associated with periodically varying parameters is called parametric excitation. For the pendulum with reconfigurable mass, such excitations or amplifications arise from the harmonic motion of the mass which creates variable stiffness, particularly when the frequency is twice that of the system.

Next, an equivalent viscous damping value was determined based on energy dissipation over a single cycle of oscillations for two proposed modes of mass motion. Using the equivalent viscous damping value, the governing differential equation was reformulated into Mathieu's Equation of fractional order. For the harmonic motion profile for the slider, parameterization was completed to illustrate the expected stability features both over a cycle and instantaneously. As the mass moves, the parameters vary and the operating behavior switches between stable and unstable zones. Hence, determining a strategy for effectively attenuating angular oscillations no longer appears to be intuitive.

4. Dynamics Associated With Mass Reconfiguration

4.1 Introduction

The effects of the active damping mechanism on structural vibration energy are investigated for various scenarios. The active damping mechanism can be visualized as a redistribution of structural mass; either the mass slides along/within the structure or the structure is reconfigured with a different mass distribution. The interaction of redistributing the mass is studied using numerical simulation techniques. Typical results are represented graphically throughout this chapter as displacement, force and energy history curves or phase plots.

The governing differential equation has been solved numerically for various displacement profiles of the moving mass. Since simulation packages were developed for this investigation rather than employing commercial packages, several accuracy tests or benchmarks were established. These included assessing the local truncation error, evaluating convergence associated with the discretization of the integration routine and establishing stability using a conservative system. Additional evaluations of the simulated package were performed for various damping strategies.

In predicting the dynamics of the reconfigurable mass-pendulum system, simplifications were made as discussed in Chapters 2 and 3. One involved linearizing the governing differential equation; the effects associated with this simplification are given for various conditions. Also, Mathieu's equation for the first three instability zone have been simulated.

To appreciate the significance of a moving mass rather than approximating the dynamics by a moving force, simulations were conducted

for a mass and a force of equivalent weight with the same movement pattern. The physical pendulum or dual mass system was modeled when conducting this analysis. The comparison examines the energy profiles and kinematic histories for the two systems.

The primary profiles for translating the mass along the structure that were investigated included continuous, harmonic motion and discontinuous, relay motion. In each case, parameters were selected to enable comparison to be easily made. For the simulations, the parameterization of the systems was as given in Section 3.4 (and tabulated in Appendix D), where the frequency of free vibration was approximately 3.1321 rad/s.

Preliminary optimization to generate temporal translational patterns for redistributing the mass to minimize the structural energy for a given time period was also conducted. The objective function was to minimize the structural energy over a previously defined interval. Both continuous and relay-type displacement profiles were considered.

4.2 Simulation Procedure for Investigating the Dynamics of the Reconfigurable Mass-Pendulum Systems

The governing equations of motion for the pendulum-mass reconfiguration systems contain nonlinear relations (Table 3.1). Simplifications can be made to reduce the analysis to a linear treatment; however, for a complete analysis the nonlinearities and the associated phenomena were included.

The closed form solution for reconfiguring the mass of a pendulum structure has only been completed for a few specific cases. For example, if the pendulum changes its length at a constant rate, the solution can be defined in terms of Bessel Functions [Relton, 1965; Whittaker, 1927; Farrell and Ross, 1971]. For harmonic motion of the sliding mass, the dynamics were reduced to Mathieu's Equation as shown in Section 3.3. However, for general motion, an explicit solution may not exist. Hence, the dynamics of the

reconfigurable mass-pendulum systems were studied through numerical simulations.

The simulation procedure assumes a displacement profile for the sliding mass, $r(t)$. Then, the governing, second order differential equation describing the pendulum and its mass reconfiguration, either Equations 2.9 or 3.1, was solved using an initial value problem solver. In this manner, for a particular $r(t)$, the corresponding structural angular displacement profile, $\theta(t)$, can be determined. The force required to implement the motion can then be calculated from Equations 2.8 or 3.2. Details of the software development follow.

4.2.1 Integration Algorithms

Depending on the algorithm and discretization used, a variety of numerical methods exist for approximating solutions for ordinary differential equations. Usually, the procedure for solving the equation(s) of motion requires transforming the higher order governing differential equation into a set of first order differential equations. Then, the solution for this set of coupled, ordinary differential equations can be numerically determined for discrete instances using various initial value solvers.

Initial value solvers essentially time step through the problem, with the solution based on the initial conditions of the system. The three types of initial value solvers include:

1) one step, direct methods (e.g. Runge-Kutta algorithms),

2) extrapolation methods (e.g. Richardson and Bulirsch-Stoer algorithms), and

3) multi-step, predictor-corrector or iterative methods (e.g. Adams Predictor-Corrector method).

Runge-Kutta methods are general purpose techniques that provide moderate accuracy. These methods propagate a solution over an interval by

combining the information from several Euler-style steps (each involving one evaluation of the right hand functions). Then, by using the information obtained, a match to a Taylor series expansion up to some higher order is done. Runge-Kutta methods approximate the solution for the next time interval solely on the previous time.

Extrapolation uses the concept of extrapolating a computed result to the value that would have been obtained if the step size had been very much smaller than it actually was. The first practical methods of this concept were Bulirsch-Stoer methods. These routines are difficult to initiate and direct methods are often used to establish the dynamics for the first few time steps.

Predictor-Corrector methods store the solution and use these results to extrapolate the solution for the next step and correct the extrapolation using derivative information at the new point. Typically, they require one step methods to initiate the process. These techniques tend to be computationally more efficient than direct methods and are well suited for very smooth functions [Press, et. al., 1992a&b, Burden and Faires, 1985].

The initial value routines are described in detail and their algorithms are outlined in Appendix E.

4.2.2 Software Development

Customized, dynamic simulation packages were chosen to investigate vibration attenuation using mass redistribution. In the process of creating these packages various support software tools were also programmed; these tools were developed to be reusable and extensible. The software was initially developed in Forth, a language claimed to be pure and elegant, yet, it lacks in fundamental support tools. As a scientific programming environment, Forth was very limited. Linear algebra software [Stilling and Watson, 1994a; Watson and Stilling, 1991b], numerical integration routines for solving ordinary differential equations and controllers were developed with good interfacing capabilities [Stilling, 1990b and 1993b] being explored. The

extensibility of this language was very tractable, especially, when the entire scope of the project was considered.[1] Later in the doctorate program, procedural languages were deemed acceptable and much reprogramming was completed for the simulation and dynamic investigations of this research was repeated and extended in the procedural language, C.

Originally, the linear algebra package, MATMATH [Stilling and Watson, 1994a and Watson and Stilling, 1991b] was developed in Forth as a tool for all phases of the thesis research. The package was very tractable for integrating the dynamic simulation and implementing the controller. The entire package was developed as a general purpose environment that would conserve memory, yet be easily extended. The coding style was modular with operations being succinct units that could be loaded independently; only the pertinent routines which need to be accessed are loaded. Details of this tool appear in Appendix F.

All of the simulation software was programmed in a modular style. Investigating various movement profiles for the auxiliary mass along the structure and examining mathematical or physical pendulum systems was easily accommodated, since the code was confined to a few statements or case statement routines. The basic simulation was adapted to incorporate the various initial value solvers. Output routines were tailored to provide graphic displays of the pendulum operation with the moving mass and/or numerical output for further analysis and processing. The dynamic simulation software was a part of the completed control systems which varied from a user-interactive forum to a fully automated control system simulation.

4.2.2.1 Implementation for Dynamic Simulation

The numeric simulation for the dynamics of the mass traversing the pendulum structure required solving the appropriate governing differential

[1] "Extensible languages provide a good impedance match between how we think and how they represent knowledge." [Forsley, 1993].

equations (Equation 2.10 for the mathematical system and Equation 3.1 for the physical pendulum system). The procedure requires expressing the governing differential equation as a set of first order differential equations in terms of the time dependent variable. Using $y_1 = \theta$ and $y_2 = \dot{\theta}$, the set of governing first order differential equations for the mathematical pendulum can be written as

$$\dot{y}_1 = y_2 \tag{4.1}$$

and

$$\dot{y}_2 = -2\frac{\dot{r}}{r}y_2 - \frac{g}{r}\sin y_1. \tag{4.2}$$

Initially, the set of first order differential equation was solved using a direct method, a fourth order[2] Runge-Kutta algorithm (See Appendix E). Then, various evaluations of the software programs were conducted (Section 4.2.3). The dynamic interaction for the reconfiguration of mass for a pendulum-based system were then simulated for various profiles (Section 4.4). To ensure the simulated dynamics were representative of the actual physical phenomena and not artifacts of the computation methods, various initial value solver algorithms were implemented. A variable, self-adjusting step-size algorithm was incorporated. The Adams Fourth Order Predictor-Corrector Algorithm and an extrapolation algorithm were programmed as the initial value solver.

4.2.3 Verification of Software Simulation Packages

Elementary evaluations of the simulation process involved comparing the simulated results with an exact solution to assess the local error, adjusting the time discretization as a further test on convergence and performing

[2]A method is conventionally called nth order, if its error term is $O(h^{n+1})$ where h is the step size.

extended program runs to assess stability. Initially, these evaluations were performed using the Runge-Kutta direct method algorithm. After investigating various mass reconfiguration profiles (Section 4.4), the algorithms were changed to incorporate those with decreasing local truncation errors to ensure the simulated results were representative of the actual physical phenomena. A further evaluation of the simulation was deemed necessary. This method involved an assessment which incorporates the physics of the problem: a work-energy balance for the dissipate system was performed for each time step of the simulation period to account for energy loss, gain or exchange. (See Appendix G.)

All results, as reported herein, are based on the parameterization as discussed in Section 3.4 (or tabulated in Appendix D), unless otherwise stated. The verifications were completed in both software development languages, Forth and C on various platforms.

Firstly, the local error was evaluated using a similar second order differential equation. A conservative system, a constant length pendulum, was selected; its governing differential equation is given by:

$$\ddot{\theta} + \frac{g}{l_p} sin\theta = 0. \tag{4.3}$$

and when linearized for small oscillations, it becomes:

$$\ddot{\theta} + \frac{g}{l_p}\theta = 0. \tag{4.4}$$

The closed form solution of Equation (4.4) is expressed as,

$$\theta(t) = \theta_o cos\omega_n t + \frac{\dot{\theta}_o}{\omega_n} sin\omega_n t. \tag{4.5}$$

where $\omega_n = \sqrt{\frac{g}{l_p}}$ is the natural frequency;

θ_o, the initial angular displacement; and

$\dot{\theta}_o$, the initial angular velocity of the pendulum.

All other notation and selected parameter values are tabulated in Appendix D.

The governing differential equation (Equation 4.4) was solved using the fourth order Runge-Kutta algorithm using various time increments (Δt = 0.1, 0.05, and 0.01 second). The local truncation error[3] for the angular displacement history is variable as illustrated in Figure 4.1 and reported in Table 4.1. For the various time discretizations, the error decreases with smaller time steps. The magnitude of the error for the time step of 0.01s after approximately five (5) time constants was of order, 10^{-6}. Note that the local truncation error associated with this initial value solver is divergent.

Table 4.1 Accuracy of the Runge-Kutta algorithm

Time	Exact Solution	Runge-Kutta Simulated Solution		
		Δt=0.1	Δt=0.05	Δt=0.01
0	0.5236	0.5236	0.5236	0.5236
T/4	0.002487	0.002551	0.002491	0.002487
T/2	-0.52358	-0.52358	-0.52357	-0.52358
3T/4	-0.00746	-0.00746	-0.00747	-0.00746
T	0.523552	0.50111	0.523502	0.523552
~4T	0.52355	0.521739	0.522074	0.52355

[3] The difference or amount that the exact solution to the differential equation fails to satisfy the difference equation used in the numerical approximation is called the local truncation error.

For the variable length pendulum (Equation 2.10) with harmonic, radial end mass motion, an exact solution is not readily attainable. A convergence test was performed, whereby the solution was compared at various instances between simulations which were conducted with decreasing time steps. The results appear in Figure 4.2 when the motion is in phase and at the same frequency as the angular displacement.

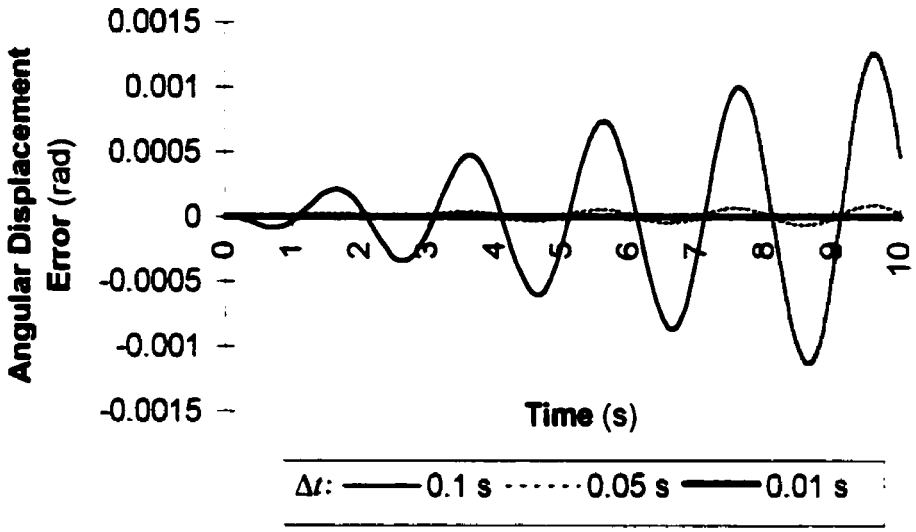

Figure 4.1 Local truncation error for various time steps for a constant length pendulum solved using a Runge-Kutta algorithm.

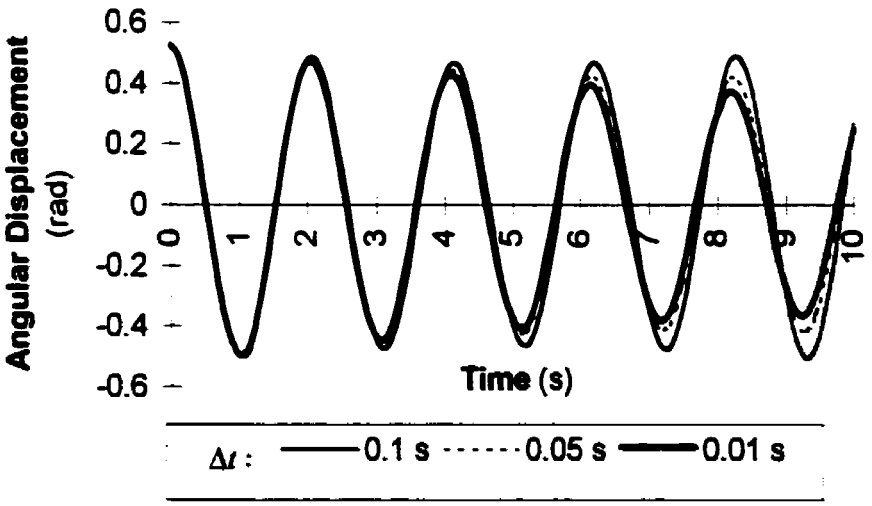

Figure 4.2 Angular displacement profiles for a simple pendulum with harmonic end mass motion.

When the time step was decreased by an additional order of magnitude ($\Delta t = 0.001$ second), the angular displacement profile for the first four time periods was not significantly different.

Lastly, to ensure numerical stability[4] in the program, the conservative, constant length pendulum system (Equation 4.3) was simulated for an extended time period, over 200 time constants. For this system, the potential (U) and kinetic energy (T) should continually transform as the pendulum oscillates with no loss or gain of energy. This did occur. The energy profiles of the system indicated the algorithm and its coding did not suffer from any appreciable round off error or overflow problems, as conservation of total energy prevailed. Figure 4.3 illustrates the energy profiles for the initial 25 seconds for the case where $\theta_o = 30^o$ and $\Delta t = 0.01s$.

Subsequent to obtaining the nonlinear results as presented in Section 4.4, incorporating higher order local truncation error algorithms was deemed necessary. A discussion of the simulation algorithms, the Runge-Kutta, Adams 4th Order Predictor-Corrector algorithm and an extrapolation algorithm which were used, appears in Appendix E. A comparison for the conservative system using a time interval of 0.01s showed no appreciable difference in the solution.

For the nonconservative case, an assessment of work and energy during the angular motion of the pendulum as the mass is being continually reconfigured was performed. A work-energy balance was performed over a given integration period. The energy loss or gain associated with moving an auxiliary mass along the structure was tracked in a cumulative manner. This balance gave an indication of the numerical accuracy of the simulation. (See Appendix G.) Again, better convergence was obtained by refining the time discretization for the simulation.

---

[4] For the purpose of simulation evaluation, stability refers to the system's ability to maintain an equilibrium form for the given state.

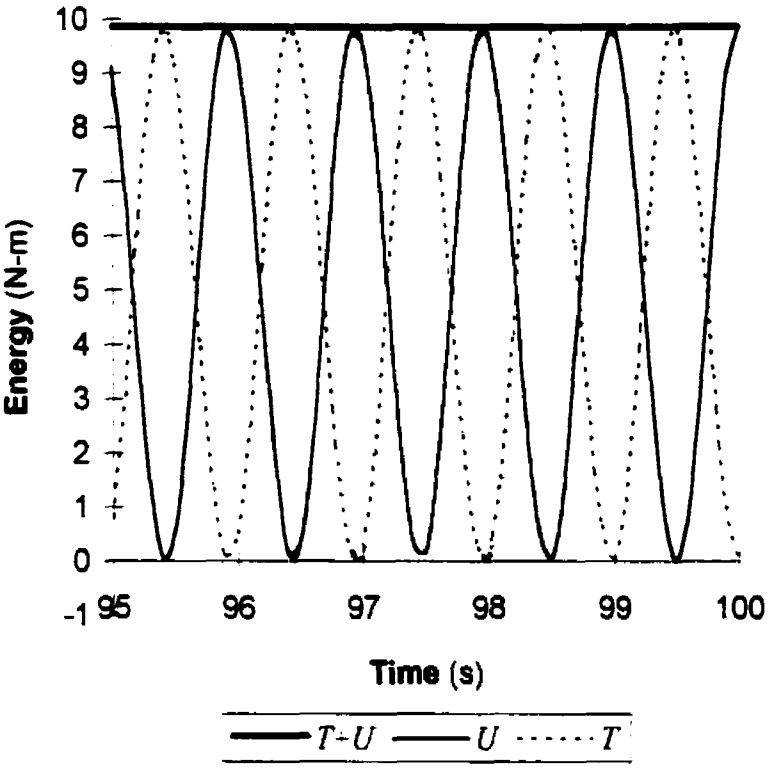

Figure 4.3 Assessing stability of the integration routine on a conservative system.

4.2.4 Effects of Various Simplifications on the Results

To explain the effects of mass reconfiguration of pendulum structures various approximate solutions were assumed. The assumptions or simplifications and ensuing dynamics are compared for a few discrete cases.

Firstly, the assumption of small vibration which was made in Section 3.3.1 eliminates the nonlinearities associated with the gravitational restoring force. For the constant length pendulum, the governing differential Equation 4.3 is reduced to Equation 4.4. The time history profiles of the angular displacement was simulated for the initial conditions of $\theta_o = 15°$, 30°, 60° and 90° and $\dot{\theta}_o = 0$ for four consecutive periods for this conservative system using the Runge-Kutta algorithm with a time step of 0.01s. A comparison between the angular displacement time history for the linearized $(\theta_l(t))$ differential equation to that without linearization $(\theta(t))$ is made in Figure 4.4. As shown,

the linearized models deviation from the nonlinear representation increases as the angular oscillations increase. Note the linearized model has a shorter period than the nonlinear system.

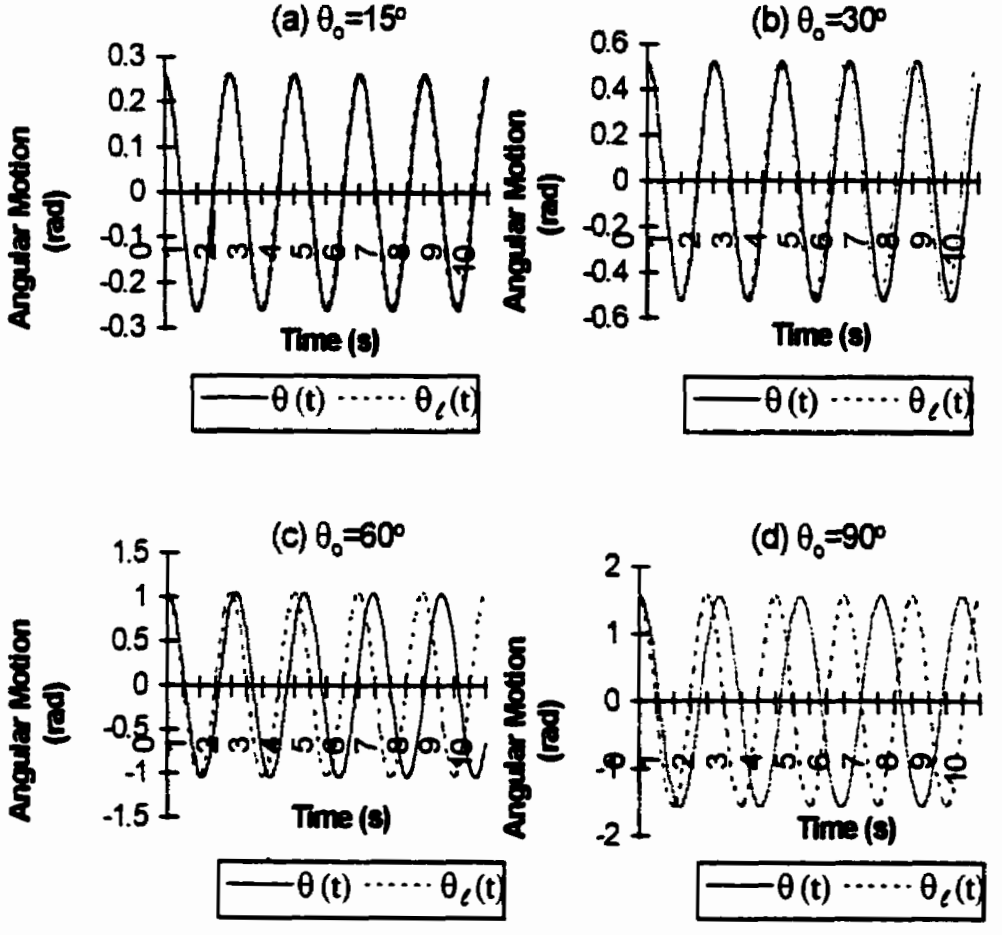

Figure 4.4 Effects of linearizing the governing equation of motion for various initial conditions.

Next, the Mathieu's Equations were evaluated. The governing differential equation for the reconfigurable mass, pendulum system (Equation 2.10) was reformulated. First the assumptions of small angular oscillations and small amplitude harmonic, slider motion were made and the resulting equations were the Mathieu's Equation (3.15) and the fractional order

Mathieu's Equation (3.19). The parameters were evaluated based on those chosen to model the simple pendulum system as given in Appendix D.

The reconfigurable mass was assumed to cycle at twice (2), nine (9) times and sixteen (16) times the frequency of the angular oscillations of the pendulum. These correspond to the first three instability zones shown in the Haines-Strett diagrams (as shown in Figure 3.3 and 3.4). The angular displacement histories for the first few cycles are illustrated in Appendix H. Unstable behavior that is characterized as unbounded (divergent) growth was expected for the undamped cases and did occur for the case when the mass motion was at twice the angular oscillation frequency. However, for the other two cases the motion was constant amplitude, oscillatory motion; this indicates that the given parameterization results lie along the characteristic curves (shown in Figures 3.3 or 3.4). For the damped cases where the governing differential equation was reduced to Mathieu's Equation of Fractional Order (Equation 3.19) the motion was stable with the angular oscillations being bounded (a decaying, oscillatory motion).

4.2.5 Software Development Environments

The programming environment for the simulation package was Forth with software developed on the following major platforms: Motorola 68000 based machines (Atari™ ST520, ST1040 and Mega ST), Motorola HC6811 (New Micros 68HC11F), Intel 8088-based machines (IBM/PC compatibles) and Sun Workstations. Later code was developed using the procedural language C for all platforms except Motorola HC6811. Initial value solvers included Runge-Kutta, Adams Predictor-Corrector and an extrapolation algorithms. The simulated response of the system was expected to provide good accuracy for time steps of 0.01 seconds or smaller with stable responses expected for runs of ~150 time periods when the initial angular displacement was 30°. Satisfactory results were anticipated regardless of the computational environment.

4.3 Attenuation Mechanism:

Comparison of Moving Mass and Moving Force Concept

Often researchers approximate moving masses as loads [Zheng, et al., 1998]. This representation neglects the inertia forces associated with the mass [Xu et al., 1997]. For the physical pendulum system, the mass could be represented by a gravitational force with magnitude equal to the weight of the sliding auxiliary mass as modeled in Figure 4.5.

To compare the dynamics of the moving mass with the moving force model, identical translational excursion patterns for each were assumed.

The governing differential equations for a moving mass and a moving force along the pendulum system are tabulated in Table 4.2.

Table 4.2 Modeling attenuation device as a moving mass or force[5]

	Governing Differential Equations for Moving Mass Model	Governing Differential Equations for Moving Force Model
1	$\ddot{\theta}+\left(\frac{2m_s r}{m_p l_p^2+m_s r^2}\right)\dot{r}\dot{\theta}+g\left(\frac{m_p l_p+m_s r}{m_p l_p^2+m_s r^2}\right)\sin\theta=0$ (3.1)	$m_p l_p^2\ddot{\theta}+Wr\sin\theta+m_p l_{pg}\sin\theta=0$ (4.6)
2	$m_p l_p^2\ddot{\theta}+m_p g l_p \sin\theta=p(m_s,\theta,r,t)$ (3.5) where $p(m_s,\theta,r,t)=-m_s\left(r^2\ddot{\theta}+2r\dot{r}\dot{\theta}+rg\sin\theta\right)$ (3.5a)	$m_p l_p^2\ddot{\theta}+m_p l_{pg}\sin\theta=f(W,r)$ (4.7) where $f(W,r)=-Wr\sin\theta$ (4.7a) and $W=m_p g$ (4.7b)
3	$F=m_s\left(\dot{\theta}^2 r-\ddot{r}+g\cos\theta\right)$ (3.2)	$F=W\cos\theta$ (4.8)

[5] The structure is assumed to be a physical pendulum; that is, the pendulum possesses mass itself.

The magnitude of the load was equated to be the weight of the moving mass (Equation 4.7b). For the moving load, the force acts at a given location as described by its motion and for the moving mass, it interacts at the point described by its motion (Equation 4.9).

The radial motion of either the mass or the force may be sinusoidal as given by

$$r(t) = R_o - \Delta r \sin(n\omega t) \tag{4.9}$$

where R_o is the position about which the attenuation device oscillates;

Δr is the amplitude of oscillation; and

$n\omega$ is the driving frequency of the attenuation device.

The moving force model can be approximated by Mathieu's equation, and when $n = 2$ unstable motion of the first zone of instability is predicted. As there is no damping, the moving load forces the system to oscillate.

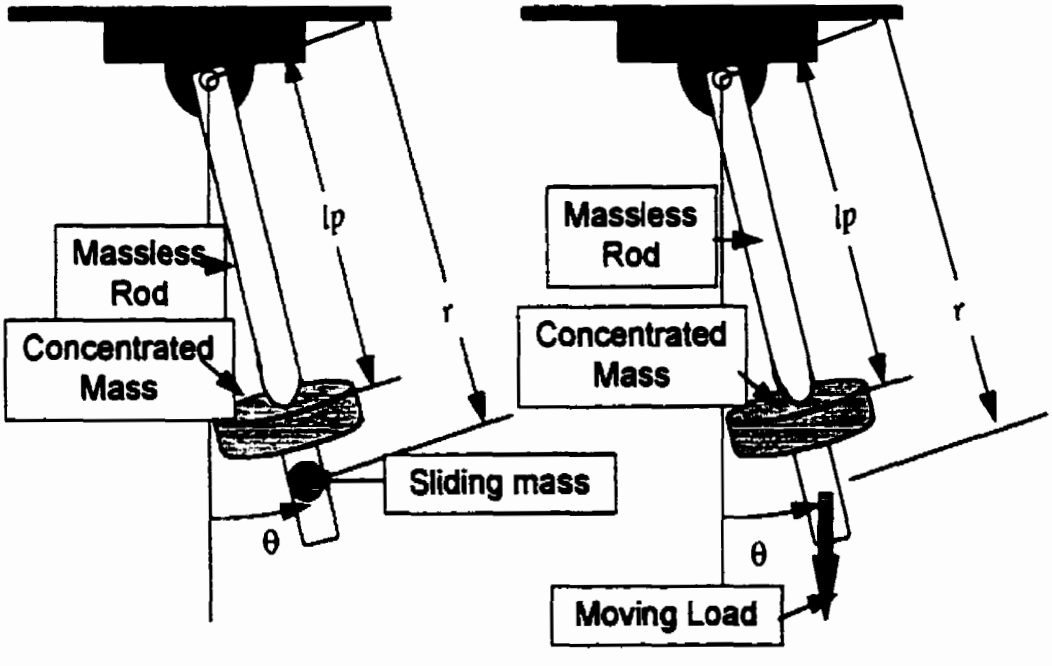

(a) Moving Mass (b) Moving Load

Figure 4.5 Two attenuation devices for the physical pendulum system.

The primary difference in the magnitude of the "driving function" (Equations 3.5 and 4.7) is that the moving mass contains terms related to the Coriolis and inertia force in addition to the gravitational restoring force. The contribution that the mass makes to the structural characteristics of the system (Equation 3.1) is unique to the moving mass case. The moving force continually acts with a constant magnitude (Equation 4.8) on the structure with its applied torque about the pivot changing as a function of its temporal displacement pattern (Equation 4.7a).

Dynamic behavior results were obtained using the Runge-Kutta initial value solver using a time step of 0.01 seconds for the governing differential equations. The attenuation mechanism has an assumed mass of only 10% of the original pendulum mass. The motion for the attenuation device was sinusoidal with $R_o = 1.0\,\text{m}$, $\Delta r = 0.25\,\text{m}$ and $n = 2.0$. The natural frequency for pendulum was 1.321 rad/s. The displacement profile is shown in Figure 4.6.

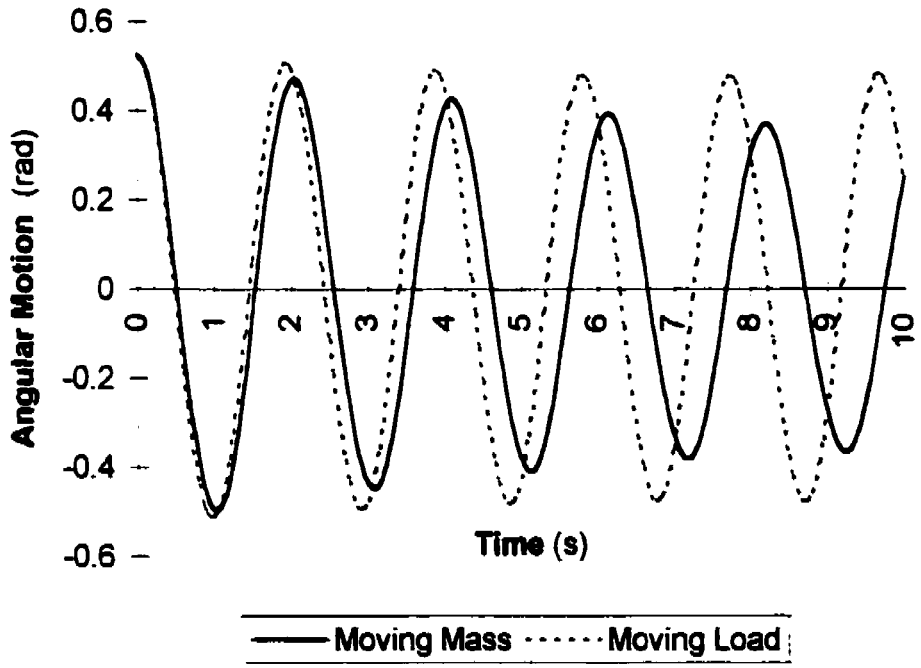

Figure 4.6 Angular displacement profiles when a mass or a load traverses the pendulum sinusoidally at twice its natural frequency.

As shown in the angular displacement history the moving mass for these conditions provides more damping effects than the moving load. This is evident in the amplitude of the angular oscillations and in the changed period of oscillations.

The corresponding force to move the mass or load (row 3 of Table 4.2) is shown in Figure 4.7.

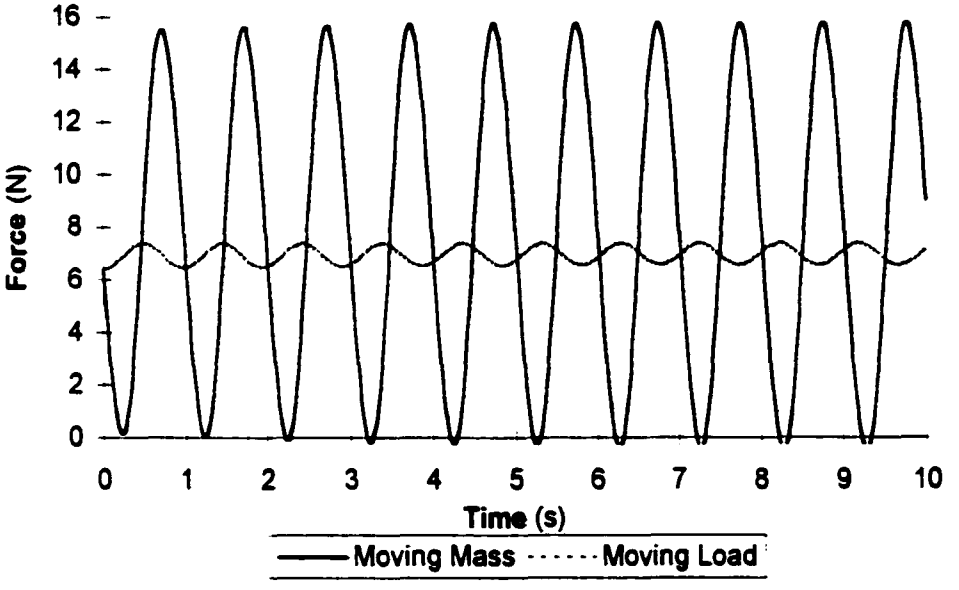

Figure 4.7 Comparing forces required to move mass or load sinusoidally.

Despite the magnitude of the sliding mass being significantly less than that of the structure, for the prescribed motion, the slider increases the system inertia by 5.6 to 15% and increases the stiffness by 7.5 to 12.5% for its indicated range of motion. A significant difference in the driving force being modeled as either a mass or a force also exists. The force to move the mass is sinusoidal with an average value that is greater than the moving load, since inertia effects have been taken into account. Peak values for the force to cause motion of the mass are approximately twice those associated with the applied load for this assumed motion profile.

Although the governing differential equation can be reformulated whereby the terms relating to mass reconfiguration are grouped together as a "pseudo-force" (Entry 2 of Table 4.2), examining the differential equation (Entry 1 of Table 4.2) shows that the mass redistribution provides time-varying modification to the system parameters. In contrast, the moving force is a forced vibration problem. For both systems, a resonance condition may be anticipated when the natural frequency is related by an integer or fractional multiple of the system's natural frequency. For both cases, the oscillations were parametric where the system periodically amplifies and attenuates the angular displacement. This will be discussed further in Sections 4.4 and 4.5.

The damping provided by using the concept of a moving force may be improved by using a variable magnitude force. The force may be formulated as an exponentially decaying sinusoidal function.

To conclude, for the physical pendulum structure, a significant difference between the two modeling techniques has been illustrated. Despite this difference, several researchers continue to represent a moving mass as a moving load. Often, the physical examples cited for a moving mass along a structure are made in the transportation field; such as a vehicle traversing a bridge. The modeling is simplified so that the vehicle is approximated as a load rather than a mass. However, applications that require "ultra"-precision such as cutting tools traversing its guideway/pathway for medical applications or manufacturing may benefit if the moving masses are modeled as masses rather than loads.

4.4 Investigating Various Mass Reconfiguration Profiles

The results reported in this section will focus on both the mathematical and physical pendulum models. The mathematical pendulum system closely approximates the dynamics of many actual systems. For cases, where the

auxiliary mass is of significant magnitude with respect to the structure, the mathematical pendulum is a very good approximation.

The key mass reconfiguration profiles that were considered included a continuous, harmonic motion and a discontinuous relay profile.

4.4.1 Interaction of the Attenuation Mechanism

The mass of the attenuation device is restricted to move along or within a structure. The moving mass remains in contact and acquires the dynamics of the point of contact of the vibrating structure. As previously presented in Section 2.2, the interaction of moving a mass along a rotating and vibrating structure can result in

(1) an increase in the system energy,

(2) a decrease in the system energy, or

(3) no change in the system energy.

For understanding the interaction of the reconfiguration of mass along a structure, the ensuing dynamics are presented as time history profiles and phase plots. The dynamics are examined over complete periods of angular oscillations for the structure. The effects of the active damping mechanism can be viewed either as a damping term or as a fictitious forcing function that drives the oscillations of the system as given in Table 3.1.

4.4.2 Sinusoidal Motion for Mass Reconfiguration

Sinusoidal translational motion for an auxiliary mass along the pendulum structure provides a continuously differentiable mode for mass reconfiguration. This profile can be mathematically described by the following equation

$$r(t) = R_o - \Delta r \sin(n\varpi t + \phi) \tag{4.10}$$

where R_o is the average radial position of the end or auxiliary mass measured with respect to the pivot (1.0 m);

Δr , the amplitude of the translational motion of the end or auxiliary mass (0.25 m);

ϖ, the average structural frequency (1.1321 rad/s);

n, an integer or fractional multiple (1, 2, 9 or 16); and

ϕ, the phase shift (0 or $\pi/2$).

The chosen parameters for the mathematical pendulum system maintained a period of oscillation between 1.74 to 2.24 seconds. Also, note that the average radial position of the end mass was constrained between $0.75 \leq r(t) \leq 1.25$ m.

The selected radial, translational frequencies correspond to the zones of instability as predicted by Mathieu's Equations (and shown in the Haines-Strett diagrams of Figures 3.3 and 3.4). Details of the ensuing dynamics when the mass was reconfigured at frequencies that were the same, nine (9) times and sixteen (16) times the structural, natural frequency appear in Appendix I and are summarized in Section 4.4.2.2. The results associated with the mass being cycled at twice the structural, natural frequency follow in Section 4.4.2.1.

The phase shift was chosen so that the transitional motion of the moving mass (slider) was initially either "in phase" or "out of phase" with the angular oscillation to illustrate the extremes in altering the energy state of the system. Note that "in phase" will refer to the coordination between the translating mass and the angular oscillations shown in Figure 2.7 and "out of phase" refers to the coordination shown in Figure 2.8. The "in phase" coordination for an initial angular displacement has $\phi = 0$; initially, the radial distance between the pivot and the auxiliary mass decreases as the angular oscillations decrease.

4.4.2.1 Mass Reconfiguration at Twice the Structural, Natural Frequency

When the translational frequency of the auxiliary mass is twice the average angular frequency of the system, a significant change in the structural energy occurs. The temporal displacement profiles (angular system oscillations and the translational vibration of the auxiliary mass) are shown in Figures 4.8 and 4.9 for the extreme cases of the auxiliary mass motion being initially in phase ($\phi = 0$) and out of phase ($\phi = \pi/2$) with the angular vibrations (when $\theta_o \neq 0$ and $\dot{\theta}_o = 0$), respectively. The parameterization are as given in each figure. For the simple or mathematical pendulum, a simulated instability occurred when the end mass motion was set to twice the average structural frequency ($n\varpi = 6.2642$ rad/s) as predicted by Mathieu's Equation for the first zone of instability (Figure 4.5). The corresponding energy profiles for the cases indicated in Figures 4.8 and 4.9 are shown in Figure 4.10.

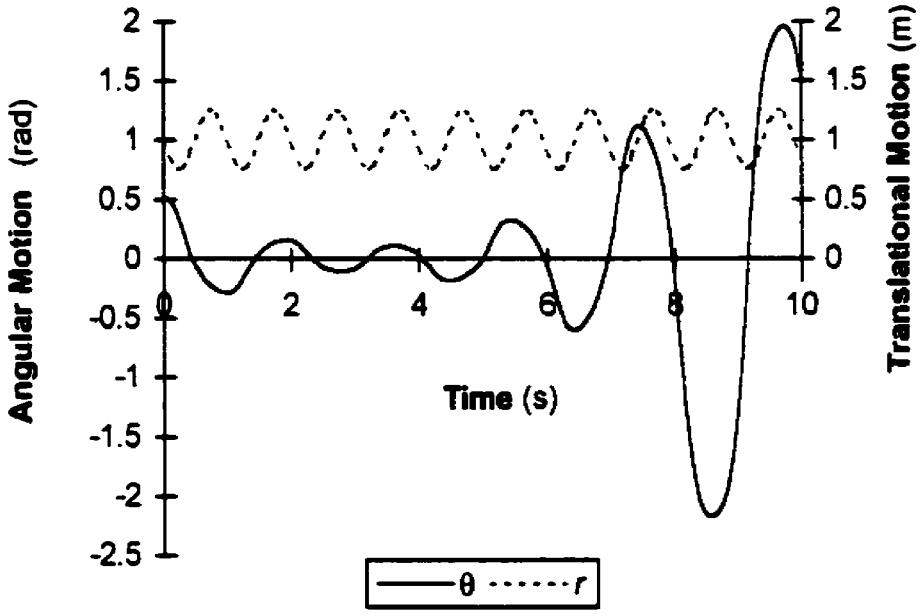

Figure 4.8 Coordinated displacement profiles for the simple pendulum when slider motion is $r(t) = R_o - \Delta r \sin(n\varpi t + \phi)$ where $n\varpi = 6.354797$ and $\phi = 0$.

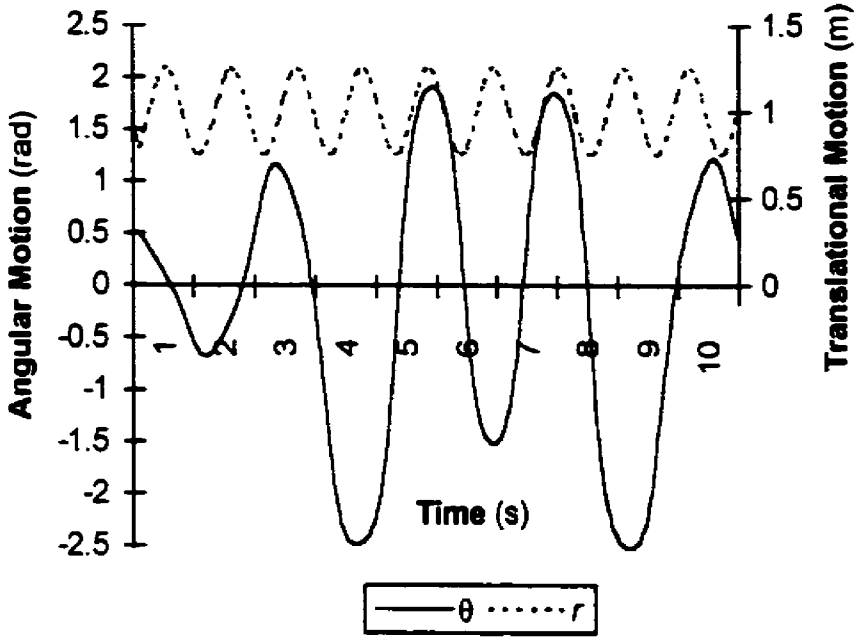

Figure 4.9 Coordinated displacement profiles for the simple pendulum when slider motion is $r(t) = R_o - \Delta r \sin(n\varpi t + \phi)$ where $n\varpi = 5.810217$ and $\phi = \pi/2$.

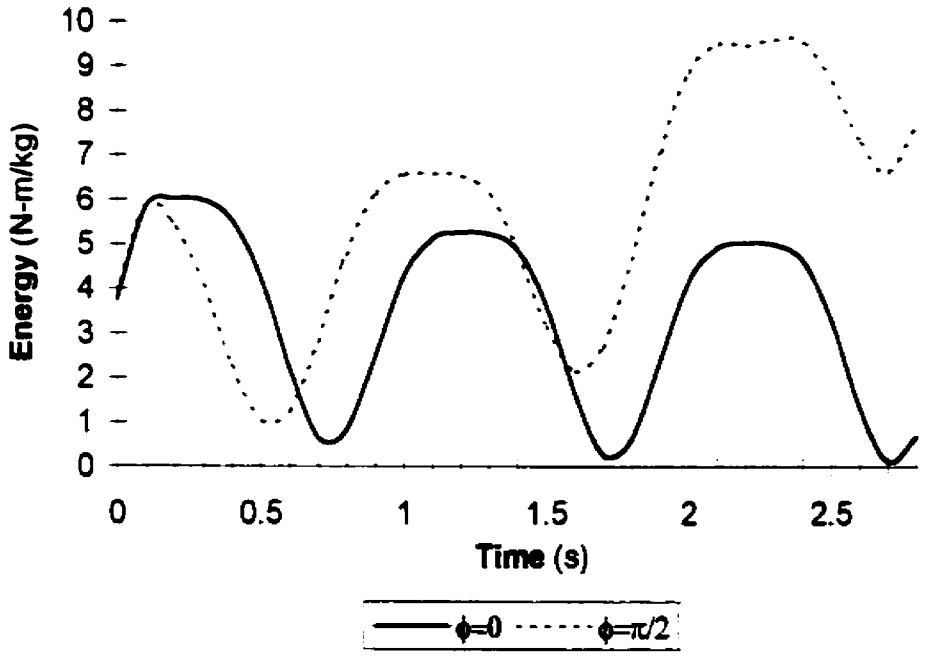

Figure 4.10 Energy profiles for the end mass motion at approximately twice the frequency of the pendulum.

For the physical pendulum (Figure 3.2), the transient response for the first four (4) time constants shows either parametric amplification or parametric attenuation. When the sliding mass initially is in phase ($\phi = 0$) with the angular oscillations of the pendulum, the oscillations are attenuated as shown in Figure 4.11. In contrast, when the sliding mass initially is out of phase ($\phi = \pi/2$), the pendulum oscillations are amplified as shown in Figure 4.12. To investigate whether or not the former action would arrest the angular oscillations, the simulation period was extended. For both cases, the steady state response consists of a regular pattern of bounded, parametric attenuation and amplification; this beating phenomena is illustrated in Figure 4.13.

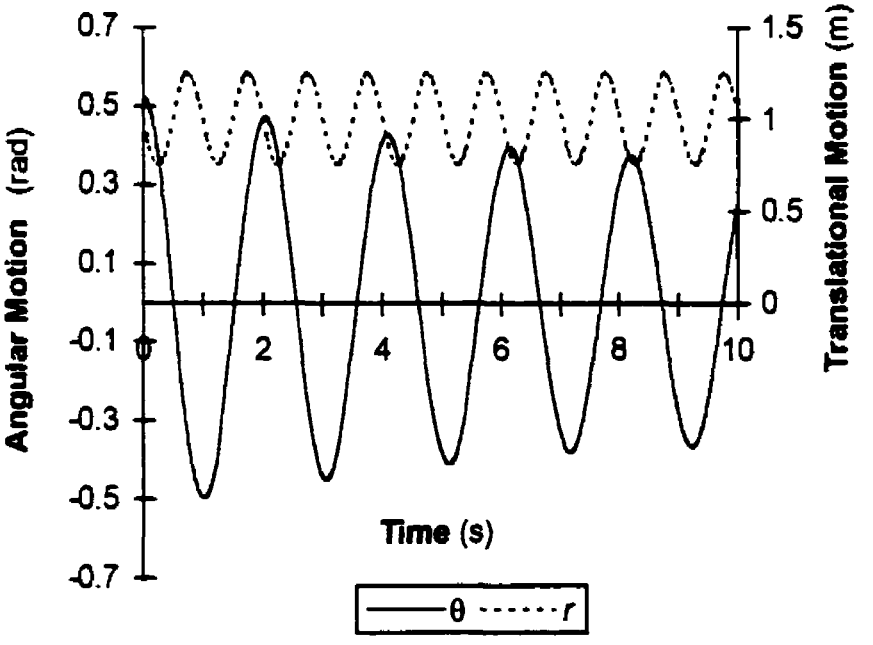

Figure 4.11 Coordinated displacement profiles for the physical pendulum when slider motion is $r(t) = R_o - \Delta r \sin(n\varpi t + \phi)$ where $n = 2$ and $\phi = 0$.

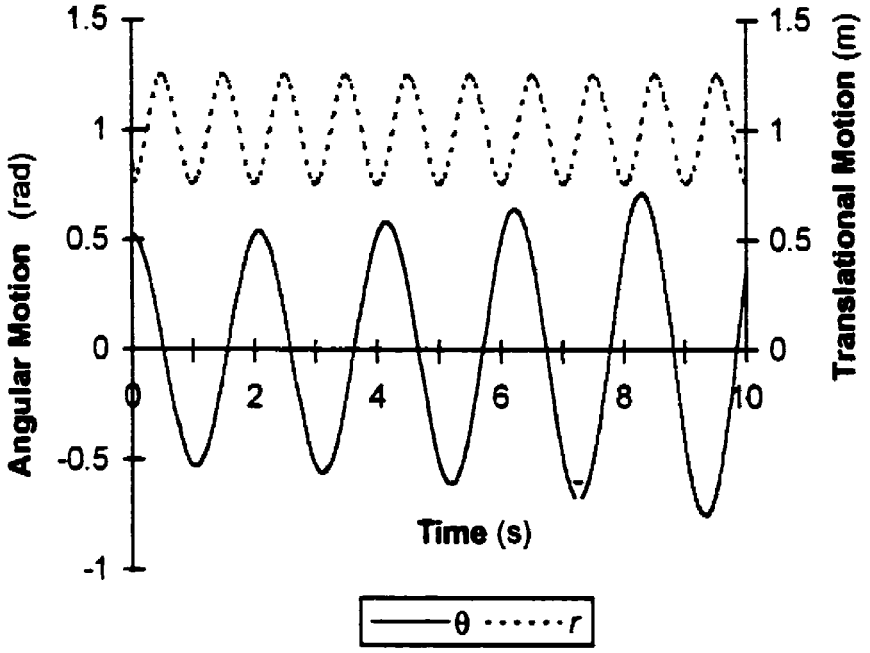

Figure 4.12 Coordinated displacement profiles for the physical pendulum when the slider motion is $r(t) = R_o - \Delta r \sin(n\varpi t + \phi)$ where $n = 2$ and $\phi = \frac{\pi}{2}$.

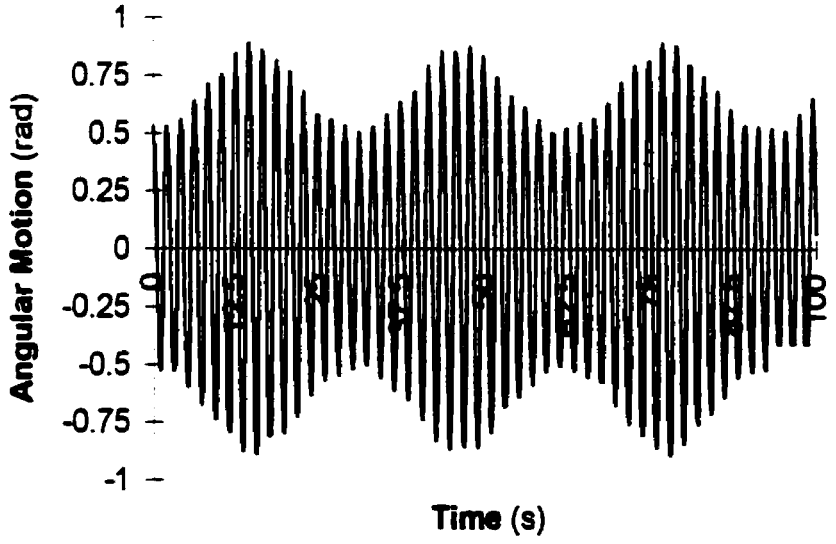

Figure 4.13 The angular displacement profiles for the physical pendulum when the slider motion is $r(t) = R_o - \Delta r \sin(n\varpi t + \phi)$ where $n = 2$ and $\phi = \frac{\pi}{2}$.

The corresponding force to cause this type of reconfiguration is shown in Figure 4.14.

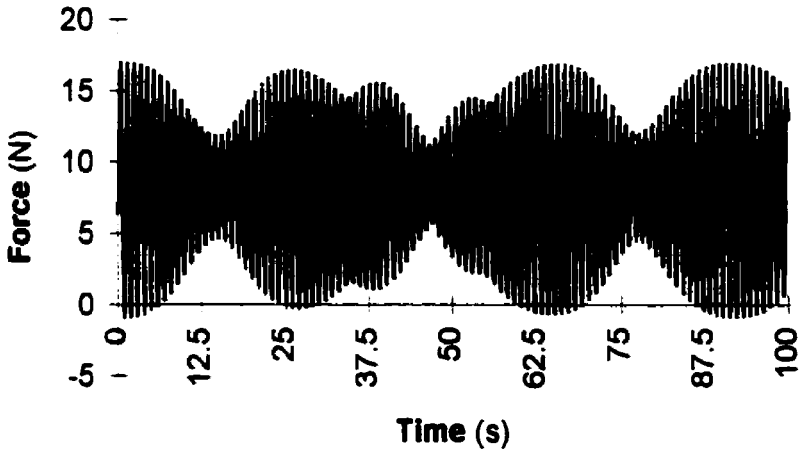

Figure 4.14 The driving force required to reconfigure the mass at $r(t) = R_o - \Delta r \sin(n\omega t)$ where $n = 2$.

The energy profile is shown in Figure 4.15.

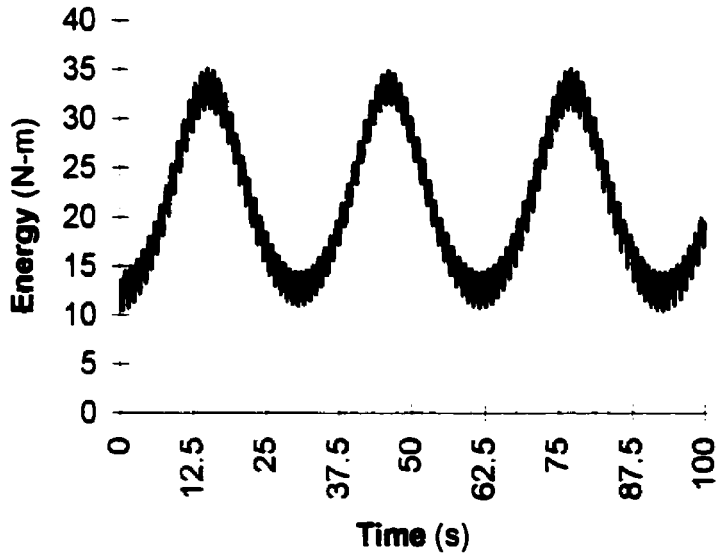

Figure 4.15 The energy profile of the physical pendulum for 100 seconds.

Details for alleviating this condition of beating were created by properly coordinating the mass reconfiguration with the angular oscillations as presented in Section 4.5.

4.4.2.2 Summary of Dynamics for Sinusoidal Slider Motion

The details for various sinusoidal mass reconfiguration profiles appear in Section 4.4.2.1 and Appendix I. This type of motion requires a continuous, time-varying force (Equations 2.9 or 3.2) as shown in Figure 4.14. The structural, angular displacement profiles for the presented cases were continuous without any discontinuities or singularities. However, the beating behavior can occur (Section 4.4.1.2).

The simulated dynamic profiles were dependent on the selected frequency of mass motion along the structure and its coordination with the structural angular oscillations. When the mass motion was at the same frequency as the structure, the moving mass and the pendulum oscillations were nearly synchronized. Due to the motion of the mass, the frequency was not exactly the same as the sliding mass. The coupling between rotational and translational motion resulted in a transfer of the oscillations or energy between the two degrees of freedom. The sliding mass transfers its translational energy to rotational motion. These results appear in Appendix I.

The conditions studied in Section 4.4.2.1 (mass reconfiguration at twice the structural frequency) showed that the excitation for in phase coordination initially attenuated the angular oscillation and for out of phase coordination amplified the angular oscillations. The potential for a good attenuating reconfiguration strategy seemed apparent; namely sinusoidal mass reconfiguration that is coordinated in phase with the angular oscillations should produce parametric oscillations. However, when several time periods were examined the ensuing dynamics exhibited a beating effect where the oscillations or energy periodically grew and decayed. The competing effects of damping stabilized the dynamics of the structure but the parametric

structural parameters destabilized the system. When a sinusoidal profile for mass reconfiguration was not perfectly coordinated or tuned with the structural vibrations, the strategy appeared ineffective. Determining a strategy to attenuate vibrations no longer seemed to be an intuitive exercise.

Mass reconfiguration at the higher frequencies of nine (9) and sixteen (16) times the structural frequency did not produce the same phenomena as those at twice the natural frequency. Initially, the systems appear to be oscillating at a constant amplitude. Examination of the change in energy also suggested that parametric amplification or attenuation will not occur. This observation of constant amplitude, structural, angular oscillation suggests that the chosen parameterization lies along a characteristic curve of the Haines-Strett diagrams (Figures 3.3 and 3.4).

4.4.3 Relay Motion for Mass Reconfiguration

The next option considered for mass reconfiguration was a discontinuous profile, a relay action. The motion as previously described (Sections 2.2.1 and 2.2.2) can be formulated as the following control logic and algorithm

$$\text{if } |\theta(t)| > \theta_a \text{ then } r(t) = r(t-\Delta t) - \dot{r}\Delta t \tag{4.11a}$$

$$\text{if } |\theta(t)| < \theta_a \text{ then } r(t) = r(t-\Delta t) + \dot{r}\Delta t \tag{4.11b}$$

$$\text{otherwise } r(t) = r(t-\Delta t) \tag{4.11c}$$

$$\text{and } r_{min} \le r \le r_{max} \tag{4.11d}$$

where Equation 4.11a represents moving the end mass towards the pivot, Equation 4.11b represents moving the mass away from the pivot at a constant velocity, $\dot{r}$ and Equation 4.11c represents a dwell phase (mass remains at the same distance from the pivot). Furthermore, displacement limits for the end mass, Equation 4.11d, were imposed.

The bounds (θ_a and θ_b) for triggering the motion are set so that the mass is raised near maximum angular excursion and lowered near vertical angular displacement. For comparative purposes to the sinusoidal profiles of Section 4.4.2, the maximum radial, translational velocity was selected to be a 1.0 m/s [6] and the range of displacement was bound by $0.75 \le r(t) \le 1.25$ m for the auxiliary mass. Because the mass reconfiguration motion is tied directly with the angular position, its frequency remains twice the natural frequency of the angular oscillation and stable, parametric motion is expected.

The temporal displacement profiles are shown in Figure 4.16 where $\theta_a = 0.3295$ rad and $\theta_b = 0.2884$ rad.

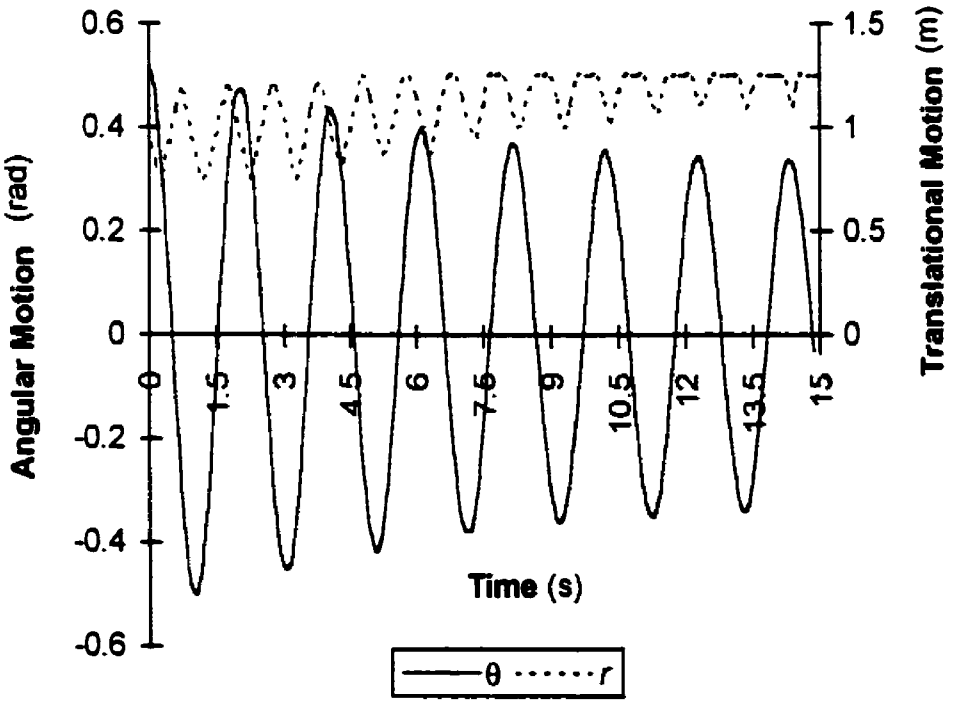

Figure 4.16 Coordinated displacement patterns of the structure and moving mass for the simple relay reconfiguration scheme.

[6] The constant velocity value of 1 m/s was selected for the relay motion since this approximates the corresponding root mean square average velocity for the sinusoidal motion given by, $r(t) = 1.0 - 0.25\sin(2 \cdot 1.321 \cdot t + \phi)$

For the chosen limits of the governing logic for the relay action continual amplitude attenuation over the shown period is produced, without requiring the auxiliary mass to traverse its available range. The logic has been implemented so that the auxiliary mass returns to its lowest potential energy position.

The corresponding energy profile for the system is shown in Figure 4.17.

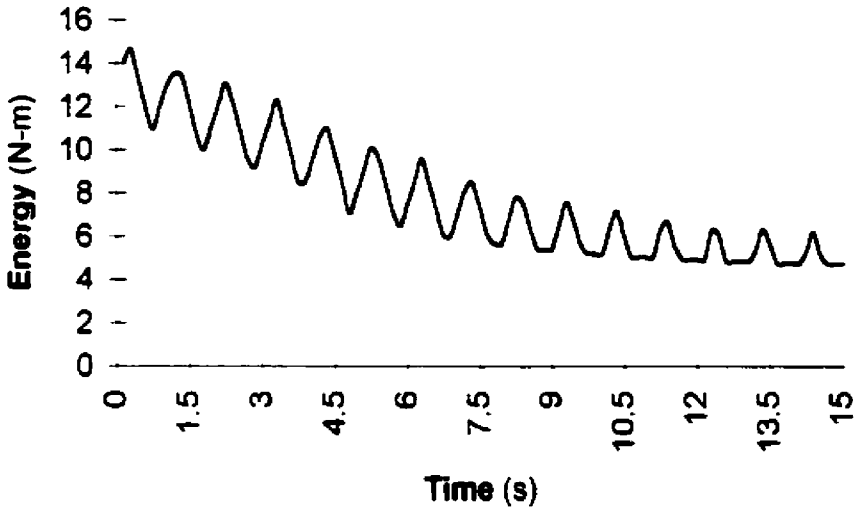

Figure 4.17 Energy profile when the auxiliary mass moves in a relay pattern along the pendulum structure.

As seen, this technique was very effective in attenuation the angular vibrations of the pendulum system. However, the acceleration profiles imposed on the reconfigurable mass produced discontinuous forces which may become prohibitive and unachievable when the velocity values are increased (i.e. a change in the auxiliary mass profile). The step size of the integration step was the controlling limit for these simulations.[7] This is

[7] When using a time step of 0.01 s, the acceleration value is bound by +/- 200 m/s^2 which is prohibitively high. However, this value assumes a velocity magnitude that was comparable to the sinusoidal displacement patterns.

evident by examining the force required to effect this motion pattern as shown in Figure 4.18. Therefore, the profile for raising the mass and lowering the mass may need to be cycloidal or otherwise, to achieve a smooth transition between points of rest and motion for the translation of the reconfigurable mass.

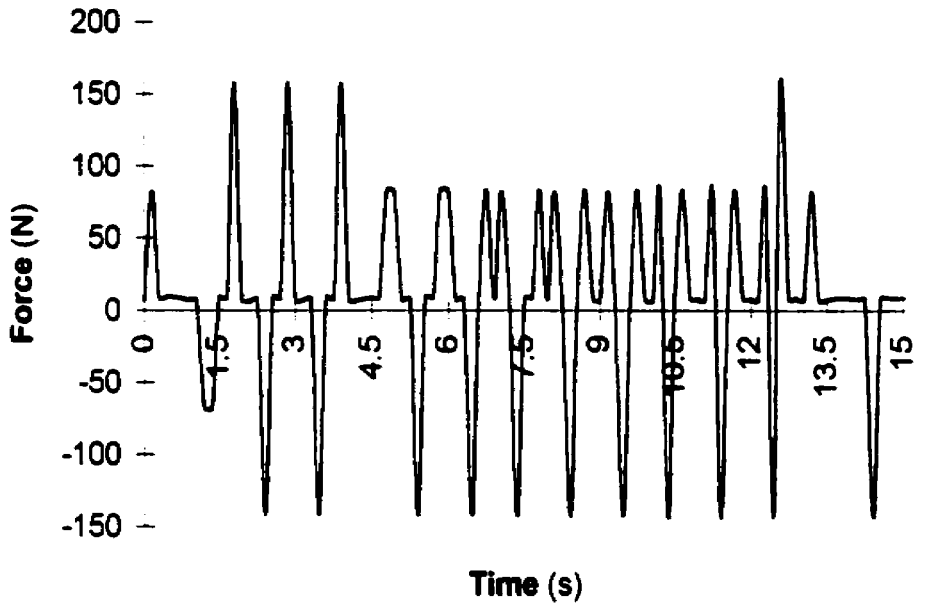

Figure 4.18 Force required to move the mass with this relay action. [8]

Improved damping was achieved for this mass reconfiguration profile when the range of the auxiliary mass was increased, when the rate of motion was increased and/or the mass motion was more proximal to the pivot.

The long term stability of this assumed reconfiguration pattern is evident in Figures 4.16 and 4.17, as the mass no longer traverses its entire range, yet the amplitude of oscillations continues to attenuate. For a constant value of the determined limits (θ_a and θ_b), residual energy remains. When another disturbance occurs additional energy is introduced to the system and the attenuation process would be re-initiated. To advance this system, the

[8] The negative force values assumes the connecting structure (rod) that the mass slides along can carry a compressive force.

energy of the system must be monitored and self-adjusting limits of operation or optimizing the velocity rates at which the mass moves towards or away from the pivot is required. This is investigated further in Chapter 8. However, the beating phenomena that plagues sinusoidal motion of the auxiliary mass at near resonance did not occur. This algorithm (Equations 4.11) also incorporates a self-imposed stop so the auxiliary mass motion is automatically arrested.

4.4.4 Summary of Assumed Mass Reconfiguration Profiles

The two basic strategies for moving the auxiliary mass were based on the previously discussed heuristic of cycling motion within a cycle of structure oscillations (Section 2.2.2). One strategy was to move the mass in a continuous motion; the profile was assumed to be sinusoidal. Various strategies were presented for this sinusoidal motion of the end/auxiliary mass; those presented included adjusting the frequency and the phase of the translational vibrations of the mass. The second strategy employed a nonlinear relay displacement profile for the mass. The motion was coordinated based on the angular displacement of the structure. For each of the above patterns the behavior of the system arising from the various movement patterns of the attenuation device were characterized by the angular displacement of the system and translational displacement of the auxiliary mass, the structural energy profiles and the required external force to cause the motion of the mass for a short and extended time period.

For the sinusoidal motion of the auxiliary mass, the following dynamics were observed. When the two motions were initially at the same frequency, the angular displacement output was symmetric when the motion was in phase with angular displacement and antisymmetric when the motion was out of phase with the angular displacement. When the radial motion was at twice the system's natural frequency, parametric attenuation resulted for out of phase coordination and amplification when in phase coordination existed.

The sinusoidal motion has the benefits of smooth displacement and force profiles and appeared as though continued motion would arrest the angular vibrations. However, for extended runs the deviation between the actual dynamic stiffness and the assumed constant frequency of the moving mass produced a time varying phase which transpired as a beating effect. Instability regions as predicted by Mathieu's Equation (Section 3.3.2) occurred only when the motion of the mass was at twice the natural frequency.

For the relay motion, both the force to generate the motion of the mass and the resulting translational motion of the mass were discontinuous. However, the algorithm did effectively attenuate the vibrational energy of the system and incorporated a self-initiated arrest feature and did not suffer from any beating behavior. The rate of change between the constant velocity states of moving the mass towards or away from the pivot is a limiting factor, as the force to produce this change may be unrealistic with respect to implementation.

4.5 Sinusoidal Mass Reconfiguration and Stability: Beating Phenomena

The phenomena of beating occurs when the assumed mass reconfiguration is harmonic at a constant frequency that is approximately double the structural natural frequency. An extended run of 50 time constants was illustrated in Figure 4.13 for this case.

Initially, the motion appears to be attenuating parametrically, then this behavior goes awry as the amplitude of oscillation increases. Similarly, parametric amplification is stabilized by the same phenomena; the system dynamics does not permit continual, unbounded growth in the amplitude of angular oscillations. With time, the phase between the translational motion of the auxiliary mass and the angular oscillations varies as shown in Figures 4.19 and 4.20. The phase shifts to create periods of negative and positive damping. Note that the "angular peak ordinal" is referenced to the peak

angular displacement as shown in Figure 4.19; the phase difference has been determined with respect to the angular displacement.

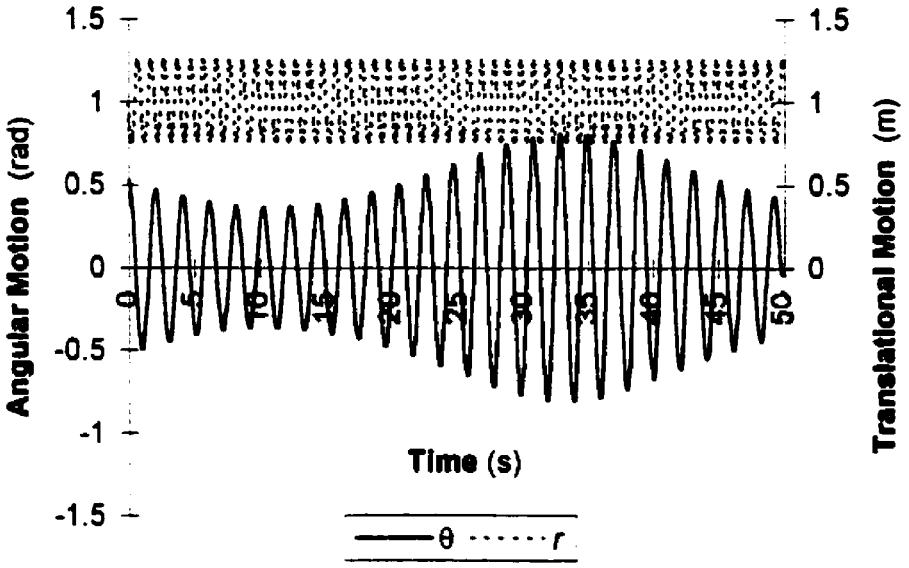

Figure 4.19 Relation between angular oscillations and translational motion of the auxiliary mass for the physical pendulum.

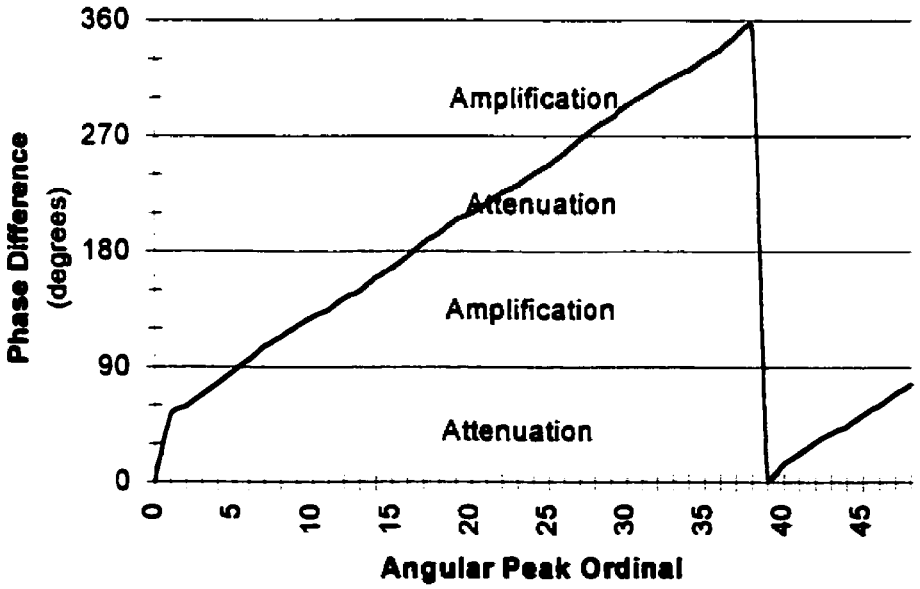

Figure 4.20 The phase between peak excursion values of the angular and translational motion of the moving mass for the physical pendulum.

To avoid this beating behavior the following process was devised. Rather than assuming a constant frequency for the radial vibration of the auxiliary mass, its motion was tuned to the time-varying or dynamic stiffness of the system. A "variable frequency", harmonic motion for the auxiliary mass was proposed whereby the motion is described by

$$r(t) = R_o - \Delta r \cos\left(2\omega_n(t)\cdot t + \phi\right) \tag{4.12}$$

where

$$\omega_n(t) = \sqrt{\frac{g}{r(t)}} \tag{4.12a}$$

To simulate this motion, a recursive or iterative program was required as the parameters describing the motion of the end/auxiliary mass itself depends on its current position. To provide efficient convergence an algorithm based on bisection was used; employing techniques using higher order derivative failed due to the nature of the imposed motion.

Prescribing sinusoidal motion where the frequency is tuned to the system parameters enables the damping mechanism to operate continuously, without the beating phenomena as shown in Figure 4.21. Note that this simulation was completed using an extrapolation algorithm.

The desirable control of vibration attenuation is achievable and potential damage resulting from starting or stopping the control process as exists with the relay profile are eliminated. This may be of particular importance when the moving mass attenuation mechanism is integral in the system's design.

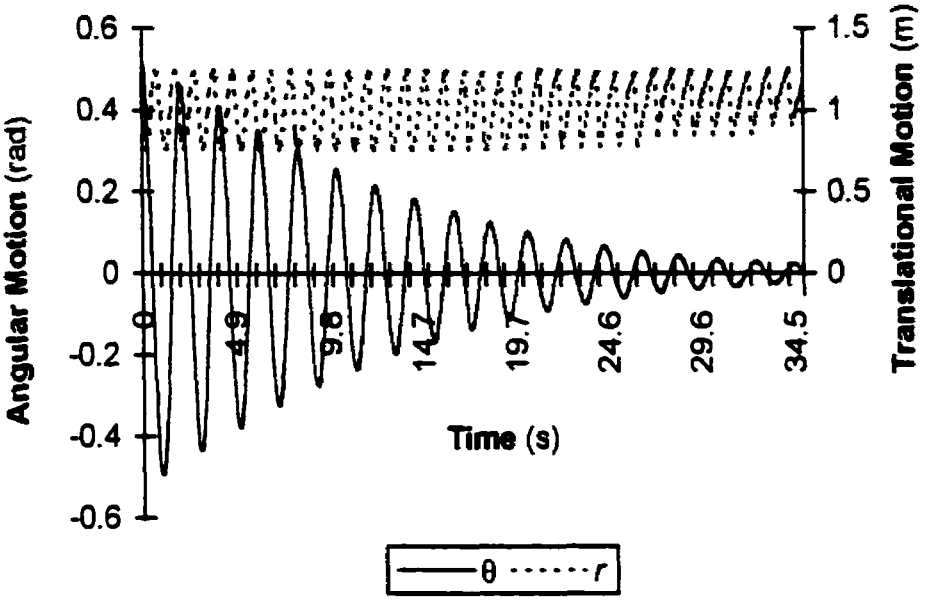

Figure 4.21 Coordinated dynamics when using a variable frequency sinusoidal mass reconfiguration profile for the physical pendulum system.

The method of self-tuning the coordination of the translational vibrations of the auxiliary mass with the system rather than at a fixed, frequency avoids the beating phenomena. This strategy can produce an autonomous vibration attenuation mechanism.

4.6 Optimizing the Mass Reconfiguration Profile to Attenuate Vibrations

Often engineering or industrial applications require the prudent use of resources or efficiency in their operation, so optimization is incorporated into the design and/or operation processes. For this research, auxiliary or end mass motion that characterizes the mass reconfiguration was optimized to attenuate the structural vibrational energy for various time periods. The focus was on parameterizing the sinusoidal and relay motion of the auxiliary mass. Also, to generate a general pattern, the auxiliary mass displacement profile was expressed as a Fourier series where the amplitude, frequency and phase coefficients were adjusted.

4.6.1 The Optimization Process

The basic concept of optimization is to find the extrema of an objective or cost function. This function quantifies a performance criteria. For this research, the objective function was to minimize the vibrational energy of the structure by varying the design parameters that define the mass reconfiguration profiles. The complexity of the optimization problem increases as limitations are placed on the performance criteria and/or the design variables. For the pendulum, these limitations include ensuring system stability and providing consistency amongst the various attenuation schemes was imposed.

Typically, algorithms for the direct method of optimization require an initial set of the design parameters, then the space is searched to find the "best" solution (maximum or minimum) for the objective function. The search process, its direction and distance, is based on the objective function. The degree or order of the optimization method is determined by the information used in the objective function. Zero order methods (such as: bisection methods, random searches, evolutionary programs and genetic algorithms) require only an evaluation of the function when searching the design space. First order methods (such as, steepest descent or conjugate gradient) use the first derivative of the objective function to find its extrema; second order methods use second derivative information and so on.

In searching for a "best" solution when using an iterative algorithm process, a convergence criteria for terminating the process is required. Often the criteria may be based on executing a set number of iterations and/or the change in evaluating the objective function or its derivatives meets a specified tolerance limit.

4.6.2 Applying the Optimization Process

Optimizing the reduction of the vibrational energy via mass reconfiguration is essentially a dynamic control problem. However, the

problem can be converted into an iterative, parametric optimization. The reconfiguration profile was parameterized using the equation of motion for the end/auxiliary mass, $r(t, \mathbf{A})$ where $\mathbf{A}$ represents a vector of design variables. For a given set of design variables, $\mathbf{A}$, the system dynamics can be simulated to evaluate the effectiveness for vibration attenuation. In accordance with the search algorithm, the design parameters are adjusted to improve performance. This process is represented as a flowchart in Figure 4.22.

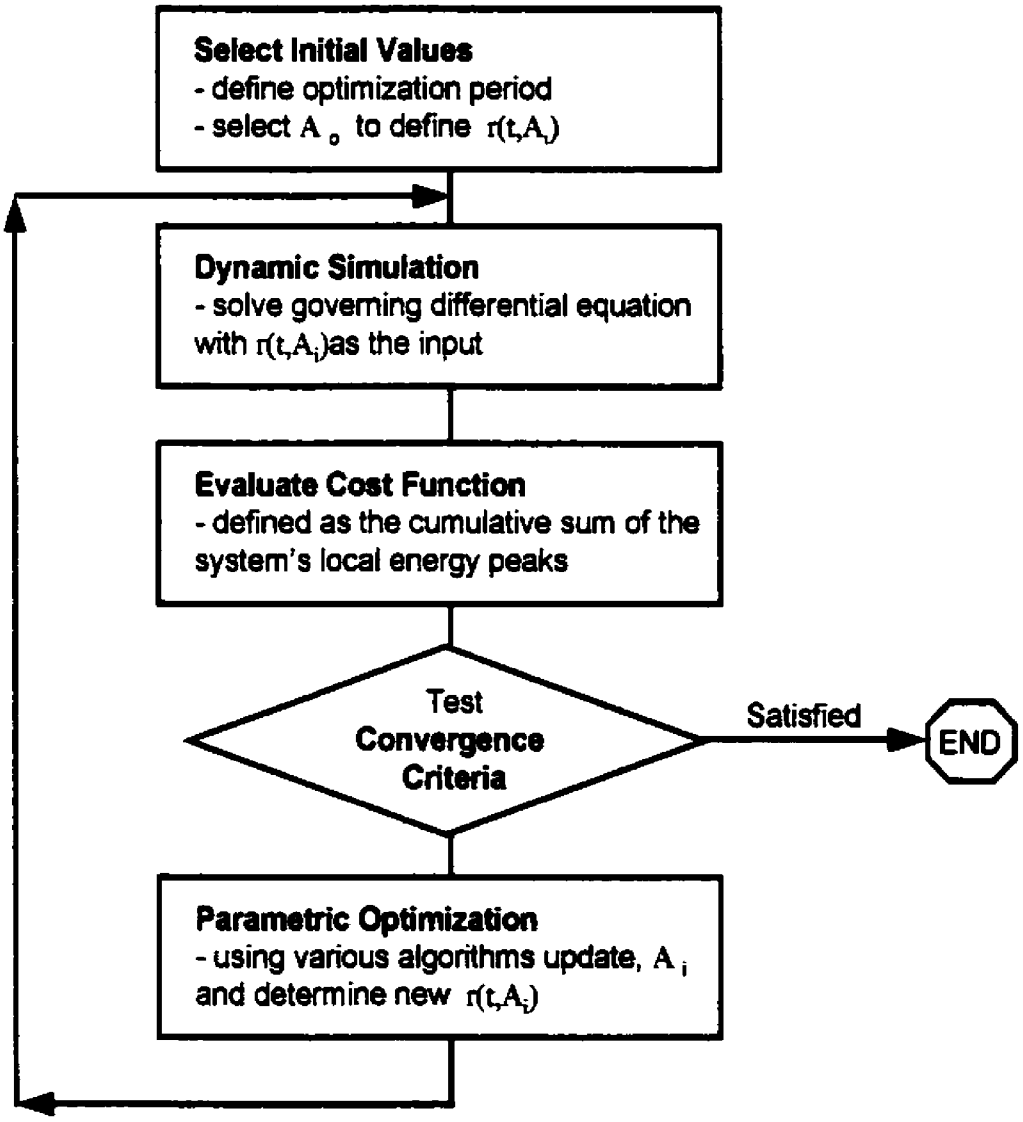

Figure 4.22 Flowchart of the optimization process.

The objective function was defined in terms of a cumulative sum of local structural energy peaks. Two equations were used; one examined the initial portion of the energy profile (J_{ip})

$$J_{ip} = \sum_{i=0}^{n} e_{MAX_i} \,. \tag{4.13a}$$

the other examined the final portion of the energy profile

$$J_{fp} = \sum_{i=N-n}^{N} e_{MAX_i} \tag{4.13b}$$

where e_{MAX} is the local maximum (peak) energy of the system,

N is the total number of peak energy values occurring during the simulation period, and

n is the number of peaks considered for the optimization as shown in Figure 4.23.

The optimization based on Equation 4.13a provides good initial attenuation, whereas the optimization based on Equation 4.13b provides attenuation at the end of the period under examination.

The system energy value is comprised of the potential energies of the structure (pendulum) and the attenuating device (sliding auxiliary mass) and the kinetic energy of the structure. By considering the peak energy values, the problem was discretized and the optimization could be considered for a given period of operation. When n is small, only part of the simulation is considered; when $n \to N$ as $N \to \infty$, the optimization becomes more encompassing. As shown in Figure 4.23, the energy profile may be harmonic of the angular displacement profile and for the attenuation profiles, as previously presented in Section 4.4, extrema in energy occurs near maximum and minimum values in the angular excursion pattern.

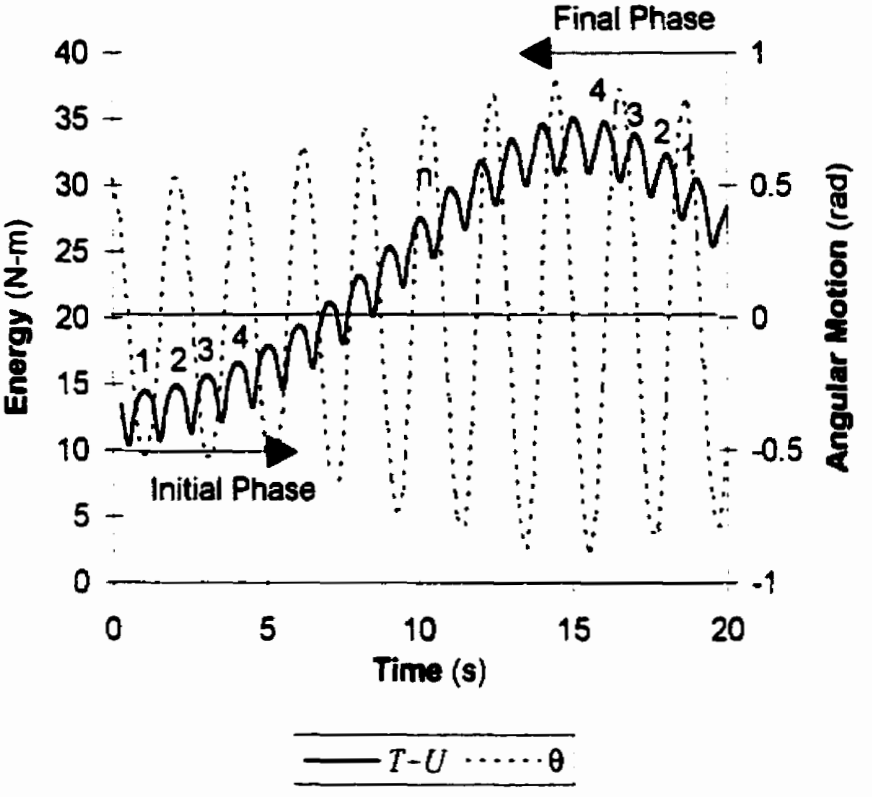

Figure 4.23 Typical temporal energy and angular displacement profile for sinusoidal auxiliary mass motion.

The following profiles were used to define the translational motion of the auxiliary mass along the pendulum structure, $r(t, A)$:

a) sinusoidal based motion

$$r(t, A) = R_o - \Delta r \sin(a_1 \varpi t + a_2), \tag{4.14a}$$

b) relay motion

$$\text{if } |\theta(t)| > a_3, \text{ then } r(t) = r(t - \Delta t) - \dot{r}\Delta t \tag{4.14.b.1}$$

$$\text{or if } |\dot{\theta}(t)| < a_4, \text{ then } r(t) = r(t - \Delta t) + \dot{r}\Delta t \tag{4.14.b.2}$$

c) generalized motion

$$r(t,A) = a_o + \sum_{j=1}^{4} a_{5_j} \sin\left(a_{6_j}\varpi t + a_{7_j}\right), \tag{4.14.c}$$

d) proportional and derivative control motion

$$r(t,A) = a_8\left|\theta(t)\right| + a_9\left|\dot{\theta}(t)\right|. \tag{4.14.d}$$

where a_k for $k = 1$ to 9 indicate the design parameters. The parameters were restricted so that the translational motion was restricted to $0.75 \le r \le 1.25$ m, as measured radially from the pivot. All variables representing angles were unconstrained.

Optimization was primarily performed for the physical pendulum system. The pendulum, as shown in Figure 3.2, had a concentrated mass of 7.5 kg and an effective length of 1.0 m. The auxiliary or sliding mass was selected to be 10% of the pendulum/structural mass. For each optimization case, the set point or operating state of the pendulum system was based on the pendulum having an initial energy state due to an angular displacement of 30° from the vertical equilibrium position. The dynamic simulation software used either the fourth order Runge-Kutta or an extrapolation algorithm as the initial value solver for Equation 3.3a. The time period for which the optimization was conducted was varied.

The optimization algorithm that were employed included both zero order and first order methods. Primarily, evolutionary programming was used with start positions based on Powell method, variable metric methods or an understanding of the control action. (A description of each method appears in Appendix J.) The convergence criteria when employing nondeterministic techniques of evolutionary programming was based on completing 400 to 4000 iterations of the optimization loop due to the stochastic nature of the algorithm. Otherwise, no significant change (10^{-4}) in the cumulative energy value (Equation 4.13) was used.

Results for the various displacement profiles, as given by Equations 4.14.a to 4.14.d, follow.

4.6.3 Optimization Results

Optimization for the displacement profiles were limited to set time intervals. For each of the time periods, the results included the final value of the objective criteria (Equation 4.13) and the final design parameters. Although several runs were completed using stochastic search routines, only the "best" results are reported. Note that this optimization problem featured several local minima.

A typical convergence of the parameters given in Equation 4.14a when using the evolutionary algorithm technique for objective function 4.13a is shown in Figure 4.24. A good initial guess had been selected to initiate the process.

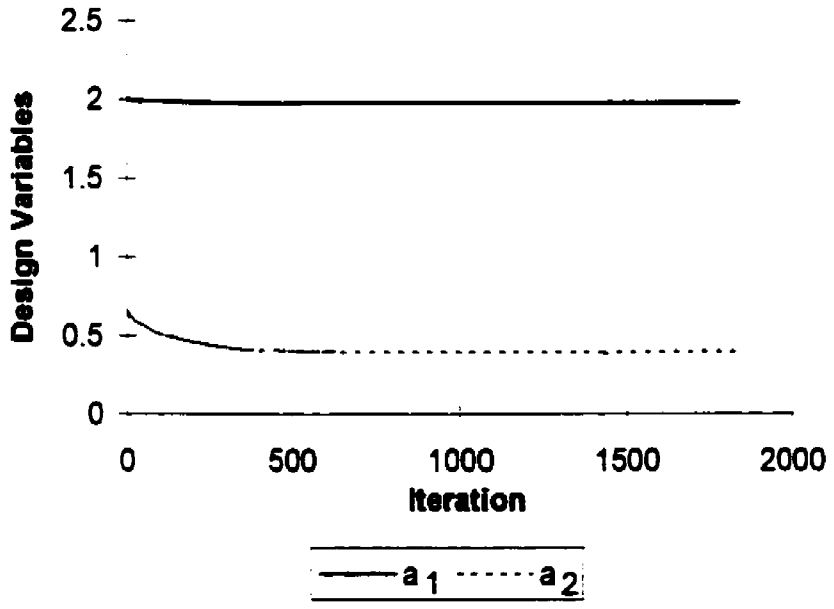

Figure 4.24 Convergence of the design variables for $R_o - \Delta r \sin(a_1 \varpi t + a_2)$.

4.6.3.1 Sinusoidal Mass Reconfiguration Profile

When the end or auxiliary mass displacement profile is sinusoidal (Equation 4.14a), various phenomena may arise as discussed in Section 4.4.2. Based on Equation 4.14a, the frequency ($a_1\varpi$) and the phase (a_2) were chosen as the design variables. The other parameters were set as $R_o = 1.0\,\text{m}$, $\Delta r = 0.25\,\text{m}$ and $\varpi = 3.1321\,\text{rad/s}$. The optimization for reducing the vibrational energy of the simple pendulum was completed using Equation 4.13b where the last five (5) peak energy values for various time intervals were used.

Regardless of the initial parameterization for the reconfiguration profile and the optimization interval, the sinusoidal motion that reduced the structural energy converged to nearly twice the average natural frequency of the system (Table 4.3, column 2). This agrees with the underlying physics as discussed in Section 2.2.2.

Table 4.3 Optimization of $R_o - \Delta r \sin(a_1\varpi t + a_2)$

Optimization Interval (seconds)	Frequency $a_1\varpi$ (radians/s)	Phase shift a_2 (radians)	Cost Function $\sum_{i=N-n}^{N} e_{MAX_i}$ where $n = 5$ (J)
5	5.940	0.4836	44.7957
10	6.122	0.2564	19.5293
20	6.260	0.5958	8.8198
40	6.255	0.4998	2.610

The phase shift varied depending on the length of the simulation (Table 4.3, column 3). A variation in the phase angle accounts for coordinating the energy minimization with the chosen optimization period. This was shown in Figure 4.15 where the energy profile varied periodically and was entrained with a higher harmonic. As shown in Figure 4.15, the total structural energy at $t = 5$, 20 or 40 seconds were similar; this may account for attaining similar phase shifts.

The optimization examines only a small portion of the energy profile. Ideally, the mass reconfiguration should be properly coordinated with the angular oscillations to produce energy attenuation. Thus, the initial energy of the system through repeated cycling of the slider would be reduced parametrically. Hence, the cumulative energy value (Table 4.3, column 4) should decrease with longer time intervals, as was shown.

The results in Table 4.4 were obtained optimizing Equation 4.13a for the physical pendulum system. Various time periods were considered as indicated in Table 4.4, columns 1 and 2. Note the initial value of the objective function (column 3) when compared to the final optimized value (column 6) indicates the starting parameterization was well chosen for the problem.

Table 4.4 Optimization of $R_o - \Delta r \sin(a_1 \varpi t + a_2)$ for physical pendulum

Simulation Length (s)	n	J_{ip} (initial) (N-m)	Frequency $a_1\omega$ (rad/s)	Phase shift a_2 (rad)	J_{ip} (final) (N-m)
5	5	76.9392	6.038105	0.253559	73.7337
	7	88.8764	6.038112	0.253554	83.3628
10	5	76.9392	6.038110	0.253563	83.4717
	7	100.6743	6.107198	0.195438	90.0640
	9	124.2942	6.134335	0.957718	106.0382
	11	148.1438	6.125754	0.179486	126.2281
	15	197.9203	6.126433	0.178906	170.2469
	21	210.8743	6.126421	0.178918	180.8739
30	7	100.6743	6.107182	0.195443	90.0640
	9	124.2942	6.137197	0.124463	106.0330
	11	148.1438	6.145833	0.117086	120.4586
	21	283.2215	6.167618	0.113882	177.5810
	41	756.6214	6.173288	0.131348	380.9746
50	9	124.2942	6.124569	0.182365	106.1628
	11	148.1438	6.147330	0.115797	120.4573
	15	197.9203	6.158987	0.105826	145.6359
	21	283.2215	6.178183	0.044040	177.0017
	41	756.6214	6.176631	0.450911	443.7935
	61	1068.3294	6.321721	0.360554	991.8176

For the chosen mass reconfiguration displacement profile, energy is initially added prior to any attenuation. To appreciate the optimization effectiveness of the attenuation process, a percentage difference was calculated with respect to the system energy without continued mass reconfiguration. The reference energy can be either the first peak energy of the system with the chosen mass reconfiguration displacement profile or the initial energy of the system. The percent difference is given as follows:

$$\frac{|J_o - J|}{J_o} x100\% \tag{4.15}$$

where $J = J_{ip}$ or J_{fp} is the final optimized cumulative energy sum, and

$J_o = (n+1)e_{max\,o}$ is the reference cumulative energy sum with

$e_{max\,o}$ = 14.30 N-m or 13.25 N-m, the initial peak energy for this system or the initial energy of the system[9].

The optimization results given in Table 4.4 also indicated the desirable frequency for attenuation should be nearly double the natural structural frequency. The phase shift appears to be very dependent on the number of peaks in the optimization interval with less consistent convergence resulting as the optimization interval was increased.

The optimized solution was effective for the time interval defined by the number of peaks considered. Regardless of the optimized parameters, this mass reconfiguration profile for extended time runs generated the beating phenomena. Nonetheless, significant attenuation occurred for the optimization period. Generally, as the time period was extended the improvement achieved by the optimization process also improved.

[9] For the simple pendulum system, the initial energy value is 9.55 N-m and for the physical pendulum system, the initial energy value is 13.25 N-m.

The significance of performing this optimization lies with a possible implementation. As constant frequency, mass reconfiguration is easier to achieve, the implementation could consist of operating this control action for only a given time period. The control action could be initiated once the structural, vibrational energy reaches a set value. The optimization results provide the recommended frequency for various attenuation rates and/or steady state energy values. Having the attenuation device operate as required also has the advantage that the structure is not continually subjected to the radial vibrations of the sliding mass.

4.6.3.2 Relay Action for Mass Reconfiguration

The optimization of the relay motion examined not only changing the intervals where the slider moved either towards or away from the pivot but also the stating of conditional logic in terms of its parameters and governance. These intervals were delineates by structural angular displacement or angular velocity states; these limits or switching values, a_3 and a_4 were the selected design parameters. The velocity, $\dot{r}$, of the auxiliary mass was held constant at 1.0 m/s. This velocity is not only physically feasible, but also is comparable to the root mean square velocity for the previous sinusoidal motion. The results were tabulated over various time intervals using the objective function described by Equation 4.13a.

The parameterization achieved during optimization for the various rules as indicated appear in Tables 4.5, 4.6 and 4.7. The optimization was completed by examining the peaks of the first portion of the energy profile.

For the relay action based on angular displacement limits (Table 4.5), the optimization effectiveness can be calculated using Equation 4.15 where this mass reconfiguration has an initial peak energy value of $e_{max_0} = 14.76\,\text{N-m}$.

Table 4.5 Optimization for Relay action,

RULE: if $|\theta(t)| < a_3$, then $r(t) = r(t-\Delta t) + \dot{r}\Delta t$

else if $|\theta(t)| > a_4$, then $r(t) = r(t-\Delta t) - \dot{r}\Delta t$

Simulation Length (s)	n	J_{ip} (initial)	a_3 (rad)	a_4 (rad)	J_{ip} (final)
5	5	87.3908	0.219699	0.527839	68.43058
	11	158.0495	0.288389	0.329530	145.19608
10	9	144.0662	0.295850	0.305973	132.00449
	11	171.9686	0.324446	0.432622	136.25458
	15	226.8085	0.295924	0.434288	169.25932
30	9	144.0662	0.321032	0.478952	112.91154
	11	171.9686	0.311054	0.455049	133.31333
	15	226.8085	0.341271	0.297213	165.00674
	21	306.7916	0.296427	0.386322	222.03186
	41	552.9481	0.275943	0.332988	344.45600
50	9	144.0662	0.288261	0.270128	133.03961
	11	171.9686	0.345607	0.416392	138.81834
	15	226.8085	0.294457	0.428416	169.65215
	21	306.7916	0.299502	0.412360	215.65916
	61	767.2641	0.195729	0.195956	507.40849
	99	1080.7786	0.15263	0.225519	774.95712

This optimization reflects the previously discussed logic that the mass should be raised when the oscillations are away from the vertical and lowered when the pendulum passes beneath the pivot; that is, $a_3 < a_4$. Note that exceptions may be due to the nature of the optimization technique. The variation in the optimized design parameters indicates the time dependent nature of this problem.

The next results employ control logic based on angular displacement and velocity limits. The control logic varies; Table 4.6 used a "if...else" structure and Table 4.7 employs a series of "if ..." statements. Again, the optimization effectiveness can be calculated using Equation 4.15 where this mass reconfiguration has an initial peak energy value of $e_{max_o} = 13.25$ N-m.

Table 4.6 Optimization for Relay action,

RULE: if $|\theta(t)| < a_3$, then $r(t) = r(t-\Delta t) + \dot{r}\Delta t$

else if $|\dot{\theta}(t)| < a_4$, then $r(t) = r(t-\Delta t) - \dot{r}\Delta t$

Simulation Length (s)	n	J_{ip} (initial)	a_3 (rad/s)	a_4 (rad)	J_{ip} (final)
3	3	50.09114	0.219279	0.094472	48.04105
5	11	114.41989	0.204742	0.118691	112.7111
7	3	50.09114	0.227700	0.068406	47.89143
10	9	114.4199	0.194721	0.117999	112.7454
	11	135.3023	0.125243	0.135414	135.0475
	15	176.5470	0.124327	0.141216	175.1296
	21	216.6305	0.124436	0.138792	214.1480
30	11	135.3023	0.194896	0.120133	133.6307
	15	176.5470	0.176122	0.166963	174.3708
	21	236.2482	0.154877	0.174943	231.8839
	41	416.4584	0.126061	0.265844	380.8840
50	11	135.3023	0.198795	0.100658	133.7181
	15	176.5470	0.162591	0.121420	174.8444
	21	236.2482	0.186871	0.172462	231.9784
	41	416.4584	0.156483	0.326833	370.6925
	61	569.7094	0.157813	0.289592	487.8780
	99	787.6889	0.110486	0.258885	648.6624

Table 4.7 Optimization for Relay action,

RULE: if $|\dot{\theta}(t)| < a_3$, then $r(t) = r(t-\Delta t) - \dot{r}\Delta t$

if $|\dot{\theta}(t)| > a_4$, then $r(t) = r(t-\Delta t) + \dot{r}\Delta t$

Simulation Length (s)	n	J_{ip} (initial) (N-m)	a_3 (rad/s)	a_4 (rad)	J_{ip} (final) (N-m)
5	9	114.4199	0.070508	0.227908	112.3845
10	9	114.4199	0.163295	0.204169	112.9137
	11	135.3023	0.177447	0.176329	134.3922
	15	176.5470	0.172184	0.190425	173.9518
	21	236.6305	0.172128	0.172377	213.1989
30	9	114.4199	0.135145	0.162559	113.5587
	11	135.3023	0.166531	0.204416	133.5282
	15	176.5470	0.189711	0.138709	174.9121
	21	236.6305	0.143724	0.124261	233.3368
	41	416.4584	0.280887	0.14125	377.6087
50	9	114.4199	0.077165	0.151851	113.2230
	11	135.3023	0.120872	0.163752	134.1168
	15	176.5470	0.140772	0.194692	174.5706
	21	236.6305	0.228133	0.127645	231.4356
	61	569.7094	0.309712	0.136023	480.3219
	99	787.6889	0.255174	0.111024	649.6805

This relay action, as indicated in Section 4.4.3, provides autonomous control without self-exciting vibrations as had occurred with the constant frequency sinusoidal mass reconfiguration profiles.

The optimization attained could be applied to other time periods without devastating effects; that is, the system behavior remained stable. However, residual structural energy did exist and varied with the parameterization. The residual energy is the system energy which remains once the structural vibrations are sufficiently attenuated so that triggering the relay action of mass reconfiguration no longer occurred. These values are presented in Chapter 8. Generally, when the time intervals over which the optimization was conducted were increased, the magnitude of the residual energy decreased. Correspondingly, a change in the response time also occurred. Furthermore, these optimization results also serve to set limits for

the self-adjusting parameters of the knowledge base controller presented in Chapter 8.

4.6.3.3 General Profile for Mass Reconfiguration

To describe a general reconfiguration pattern for the auxiliary mass, the first four terms of a Fourier sine series were considered, as given by Equation 4.14c. The only constraint placed on the reconfiguration was that the motion remained bound between (0.75,1.25). The design variables included the amplitude coefficients, a_0 and a_5, frequency scaling factor of a_6 and a phase shift of a_7. The natural frequency was assumed to be 3.1321 rad/s. Initial expectations were that this general motion would provide better performance than either the sine or relay patterns as previously selected.

The results of various optimizations was a convergence to the sinusoidal motion whereby the slider moved at twice the natural frequency of the pendulum. The attenuation process was dominated by the "fundamental frequency" of the mass reconfiguration profile which was at twice the structural, natural frequency. The results as with the sinusoidal motion of Section 4.6.3.1 were dependent on the period for which the optimization was performed.

4.6.3.4 Mass Reconfiguration Using Modified Proportional and Derivative Action

The radial motion of the end mass was based on a modified proportional and derivative controller. The error signals were based on the angular displacement and velocity of the system with respect to the desired operating state of zero angular displacement and velocity. Due to the oscillatory nature of the problem the absolute value of these signals were used as given by Equation 4.14d. The design parameters were the proportional gain, a_8, and the derivative gain, a_9. Again, the translational displacement trajectory of the end mass was restricted.

Similar to the sinusoidal motion with tuned frequency as presented in Section 4.5, this reconfiguration profile will remain coordinated with the angular displacement. This following optimization results were based on the simulation of a simple pendulum where the end mass position was confined between $0.75 \le r \le 1.25$. Optimization was completed for various time intervals as indicated in Table 4.8.

Table 4.8 Optimization Results for $r(t, A) = a_8|\theta(t)| + a_9|\dot{\theta}(t)|$

Simulation Length (s)	n	J_{ip} (initial) (N-m)	a_8 (k_p)	a_9 (k_d)	J_{ip} (final) (N-m)
5	11	62.525635	-2.665191	1.078098	57.949268
10	9	110.90562	-3.122069	1.090214	100.175625
	11	110.90562	-3.122074	1.090216	100.175625
	15	110.90562	-3.089274	1.092528	100.16623
	21	110.90562	-3.122064	1.090213	100.175625
30	9	110.90562	-3.122076	1.090217	100.175625
	11	127.685742	-3.188820	1.112100	113.448700
	15	158.049673	-3.358870	1.147632	135.556020
	21	197.618443	-3.592639	1.203158	160.688751
	41	258.855962	-3.580447	1.199175	200.661549
50	9	110.90562	-3.083492	1.091123	100.165764
	11	127.685742	-3.249181	1.121573	113.387570
	15	158.049673	-3.335123	1.151067	135.613518
	21	197.618443	-3.536795	1.190637	160.927906

Note the optimization performed over 10 second interval had only 10 peak energy values; hence, optimizations considering higher number of peak than 10 had the same design variable convergence.

The results reflect the characteristics of the system with the relation between the design parameters or gains satisfying the following relation

$$\omega_n > -\frac{a_8}{a_9}. \tag{4.16}$$

This ratio of gains is less than the natural frequency as the mass reconfiguration profile provides damping and as expected the damped natural frequency (ω_d) is less than the natural frequency (ω_n) of the system ($\omega_d = \omega_n\sqrt{1-\xi^2}$) with the damping ratio (ξ) ranging between 0.3 to 0.6 .

4.7 Summary

The dynamic interaction of the proposed active damping device were studied using numerical simulations. After programming the initial value simulation software, the local truncation error, nature of convergence and stability of the program were reviewed. Based on the known solution for the conservative system of a constant length pendulum, the software was assumed to produce reliable results.

Initial simulations examined the assumptions and simplification made in previous sections to explain the expected dynamics associated with mass reconfiguration for pendulum structures. Also investigated was the difference in modeling the attenuation device as a moving mass compared to a moving force.

The effects of reconfiguring the mass within the pendulum system were studied for the single and dual mass pendulum systems based on various patterns for the radial motion of the auxiliary mass. As shown, the motion of the slider can excite various system responses.

When harmonic motion is assumed for the slider, the frequency and phase of the motion greatly affect the ensuing dynamics. When the radial, translational frequency is twice the natural structural frequency and the radial vibrations are in phase with the angular oscillations then parametric amplification initially ensue and if the coordination is out of phase, parametric attenuation initially results. For extended runs, the beating phenomena was observed where periodic, bounded amplification and attenuation occurred.

To ensure continued attenuation, proper coordination between the attenuation device and the angular oscillations was necessary. The position of the sliding mass affects the system's parameters; that is the natural frequency of the system changes with the slider position. One proposal to achieve continual parametric attenuation when harmonic mass reconfiguration is assumed was tuning the frequency of the slider to the structural frequency. The frequency of the sliding mass was variable and a temporal function of its position.

Various displacement patterns for the auxiliary mass were analyzed and optimized to achieve improved energy reduction for set periods. The optimization involved parameterization of the displacement profile of the auxiliary mass. Four modes of motion were studied; namely, sinusoidal motion at a constant frequency and phase shift, relay action based on either current angular displacement and/or velocity, general profile defined using a Fourier series and a modified proportional and derivative based displacement profile. For each displacement profile, the optimized design parameters were dependent on the time period being analyzed. The following trends were observed:

1. For a cycle of pendulum motion where the mass reconfiguration is also cyclic, energy is initially added to the system before being removed. The auxiliary mass motion was initially raised at maximum angular displacement (thereby, adding energy to the system) prior to being lowered (thereby decreasing energy);

2. the "best" attenuation for the auxiliary mass motion defined using sinusoidal functions was observed to be nearly twice the structural natural frequency;

3. for the relay based profiles, the design parameter for raising the mass corresponded to a larger displacement from the vertical than the angular displacement limit for lowering the mass; and

4. the relation between the proportional and derivative gains is negative and their ratio is slightly less than the structural natural frequency which indicates the system frequency is being damped.

Based on the interaction between the radially vibrating mass and the angular oscillating pendulum structure, several seemingly viable approaches for training and operating the controller exist. Sinusoidal motion for the auxiliary mass is appropriate if its motion remains at twice the natural frequency of the system and properly coordinated with the angular vibrations. The tuned or time varying frequency sinusoidal motion provided continual parametric attenuation. A perturbation between the natural frequency and that of the mass may result in beating phenomena. When employing a constant frequency, sinusoidal mass reconfiguration profile, the auxiliary mass motion must be coordinated and operates for only a set time period to avoid the beating effect. The nonlinear relay action was effective at reducing the system's energy without any beating effects observed. By virtue of the conditional logic, this technique provided automatic initiation and cessation of slider motion. To conclude, the proposed technique of strategically moving a mass along a structure can be used to regulated the vibrational energy of the structure.

5. Controllers

5.1 Introduction

Through a computer simulation approach, various controllers were used to integrate the plant (a pendulum structure) with the vibration attenuation device (a mass redistribution mechanism). This chapter provides a brief introduction to the controllers employed in this research. For each controller, the basic concepts, properties, potential and related terminology are given. Implementation and performance details of each controller when integrated with the structure are presented in subsequent chapters.

The controllers can be categorized as a human operator that interacts with the system, a nonconventional controller that has similarities to a proportional and derivative action, a rule-based or knowledge based system that is based on heuristics from the human operator and an artificial neural network that imitates an appropriately controlled system. For this application, each controller was expected to operate using multiple, time-varying, nonlinear input parameters. In addition, the controller should be extendable, adaptive and ultimately autonomous (Sections 2.2.3 and 2.2.4). The performance of each controller was evaluated on its ability to attenuate structural vibrations. Since the design focus was initially on innovation, applications of artificial intelligence techniques were examined.

In constructing the complete control system, various tools for both the simulation and artificial intelligence controllers were developed and customized accordingly. As application software and/or hardware for artificial neural networks was in its infancy at the time of initiation of this research and was commercially unavailable, original simulation software had to be

developed [Stilling and Watson, 1994; Stilling, 1993; Stilling and Watson, 1992; Watson and Stilling, 1992; Stilling and Watson, 1991; Watson and Stilling, 1991; Stilling, 1990]. Furthermore, the philosophical premises of some of the artificial intelligence technology were just being established and applications, as reported in the literature, were limited.

5.2 Human Operator Controller

The process of redistributing the mass to attenuate energy is akin to a "playground swing" situation where through mass redistribution angular oscillations are amplified [Walker, 1990; Curry, 1976; Gore, 1970; Burns, 1970; Tea and Falk, 1968]. Through trial and error, children can effectively learn to "pump" the swing to generate motion. Foreseeably, the inverse problem of arresting the oscillations can be learned heuristically.

The physics of the interaction of moving an end mass towards and/or away from the pivot for the simple pendulum (Section 2.2.2) suggests a solution can be developed and generalized as a conditional rule. In this study, applying this generalization to the variable length pendulum became an exercise in hand-eye coordination. As the operator pulls or releases the pendulum cable to adjust its length, its angular vibrations can be attenuated. The operator processes various pendulum dynamic information and applies it to attenuate the system's vibrational energy.

Despite the inherent inexactness of a human controller, one can become skilled at the task and acquire sufficient expertise to outperform many conventional, linear or nonlinear control systems. In implementing a human controlled system, the dynamic process of reconfiguring the mass were simulated and animated on a computer. The results for the interactive sessions had direct implications for implementing rule-based controllers and will be considered in detail in Chapter 6.

5.3 Controller with Modified Proportional and Derivative Action

An initial proposal was a controller that uses proportional and derivative action to implement the two phase control strategy as given in Section 2.2.2,

(1) lengthen the pendulum as it passes beneath the pivot (its 'neutral'[1] position) when the angular velocity is maximum, and

(2) shorten the pendulum at points of maximum angular excursion (its extrema positions[2]) when the angular velocity is minimum.

Although the control strategy is stated in a discrete manner with respect to the extrema of the time-dependent vibration displacement profile, developing a linear-based controller should be possible; this controller would provide a continuous control signal. The control strategy was relaxed by identifying the point where the pendulum changes its length as a region; that is, the pendulum was lengthened as it approaches the neutral position and shortened as it nears its maximum angular displacement. This continuous motion for the attenuation device had desirable, physical implementation characteristics.

One possible two phase control strategy is illustrated in Figure 5.1 where a single period of simple harmonic vibrations for the undamped pendulum system is being considered. The desired control action at example points is also illustrated in this figure. The first phase of the control law as illustrated (1) applies near the extrema in the angular velocity and the second

[1] For the pendulum system, the neutral position refers to the case when the pendulum is vertical beneath the pivot.

[2] Extrema positions are measured with respect to the 'neutral' or vertical position of the pendulum.

phase (2) applies near the extrema in the angular displacement profile. Both axes have been normalized (the abscissa, with respect to the period of an oscillation and the ordinate, with respect to its corresponding maximum value). The strategy of moving the mass at approximately twice the natural frequency appears to indicate that the control action could be based on angular displacement (proportional control action) and angular velocity (derivative control action).

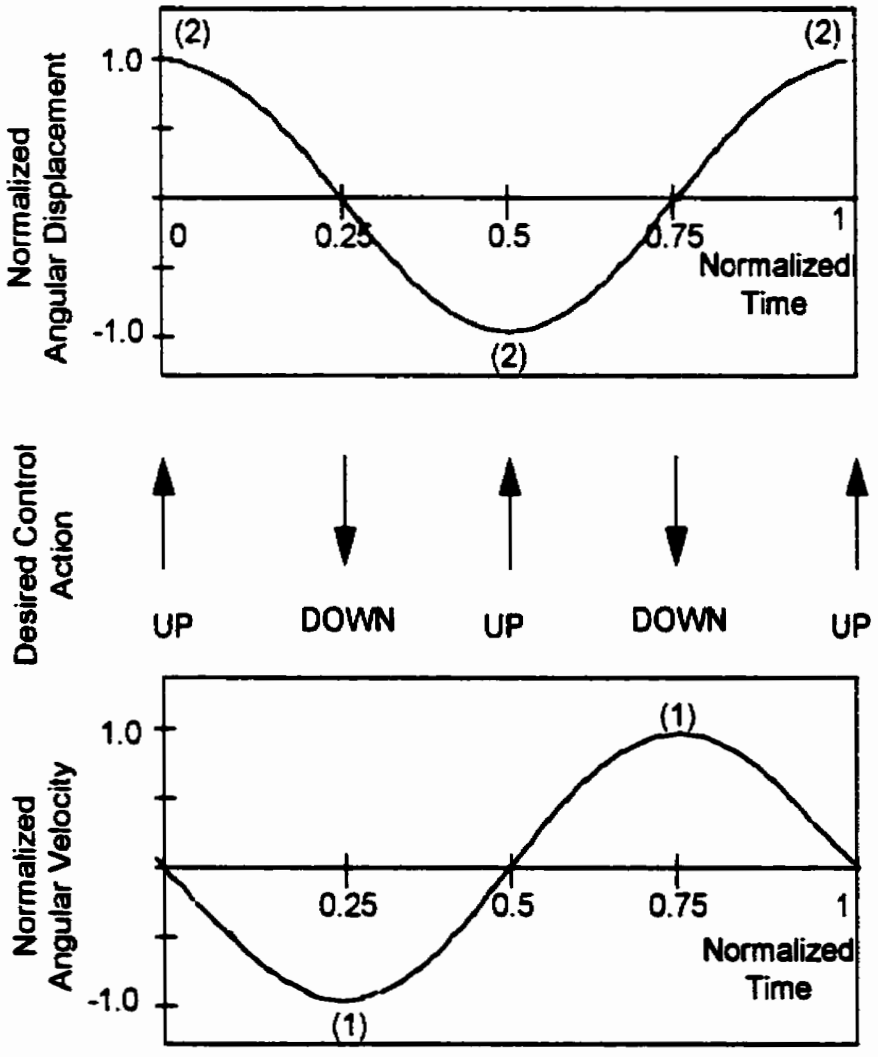

Figure 5.1 Applying the control law of (1) lengthening and (2) shortening the pendulum for simple harmonic vibrations.

The operation of linear controllers have been well studied and provide good control for linear systems [Ogata, 1970]. Proportional and derivative controllers provide anticipatory action as the derivative control action responds to the rate of change of the error which can give significant correction prior to the actual error becoming too large. Also, the proportional-derivative controller tends to increase the system stability by adding damping to the system, but has the drawback of amplifying noise that can lead to saturation effects.

A controller with proportional and derivative action was considered first. Mathematically, the control signal fed to the plant or pendulum structure can be expressed as :

$$m(t) = k_p e(t) + k_d \dot{e}(t) \text{ or } m(t) = K_o \hat{e}(t) + K_d \dot{\hat{e}}(t) \tag{5.1}$$

where $m(t)$ represents the control signal;

k_p or K_p, proportional gain;

k_d or K_d, derivative gain;

$e(t)$, the error signal that corresponds to the difference in angular displacement measured with respect to the zero, equilibrium position ($e(t) = \theta_{REF} - \theta(t) = 0 - \theta(t) = -\theta(t)$);

$\dot{e}(t)$, the first time derivative of the error signal which corresponds to the angular velocity as measured with respect to the desired, equilibrium state ($\dot{e}(t) = 0 - \dot{\theta}(t) = -\dot{\theta}(t)$); and

$\hat{e}(t)$ and $\dot{\hat{e}}(t)$, normalized error signals where $|\hat{e}(t)| \leq 1$ and $|\dot{\hat{e}}(t)| \leq 1$.

Physically, the control signal ($m(t)$) would drive a mechanism to move the attenuation device, an auxiliary mass. For example, the mass could be lowered when the control signal, $m(t)$, was positive and raised when the signal was negative. Hence, the control signal produced by Equation (5.1) would not be capable of efficiently attenuating the pendulum vibrations. For the case where both the proportional and derivative gains are positive with $K_d = K_p = 1$, the control signal represents the desired control law for only part of the period. As shown in Figure 5.3, this signal has the same frequency as the oscillations of the system, rather than the desired control action which should be at twice the frequency of the pendulum. Therefore, the sign of the control signal cannot be consistently related to the desired control action. Note that the axes have been normalized, with the control signal being the sum of the two normalized error signals as given by Equation 5.1.

This analysis was completed for only one period with the natural frequency of the system assumed to be constant. Subsequently, the phase shift between the control signal and the dynamics of the system would remain constant. However, the physical application of reconfiguring the mass within the pendulum system to effect damping does result in changes to the natural frequency during a period of oscillation, as discussed in Sections 3.4, 4.4.2 and 4.5. Implementing a linear controller, based on Equation 5.1, with the actual system would produce nonoptimal control as the control action would not be properly coordinated with the dynamics of the plant over the entire period. Also, other effects, such as beating phenomena, may be encountered as described in Sections 4.42 and 4.5 or some bifurcations as recently reported [Yagaski, 1999].

The control logic based on extrema, as illustrated in Figure 5.1, required the control action to be at twice the natural frequency. Unfortunately, a proportional and derivative controller provides control action at the same frequency as the structural oscillations, as shown in Figure 5.2.

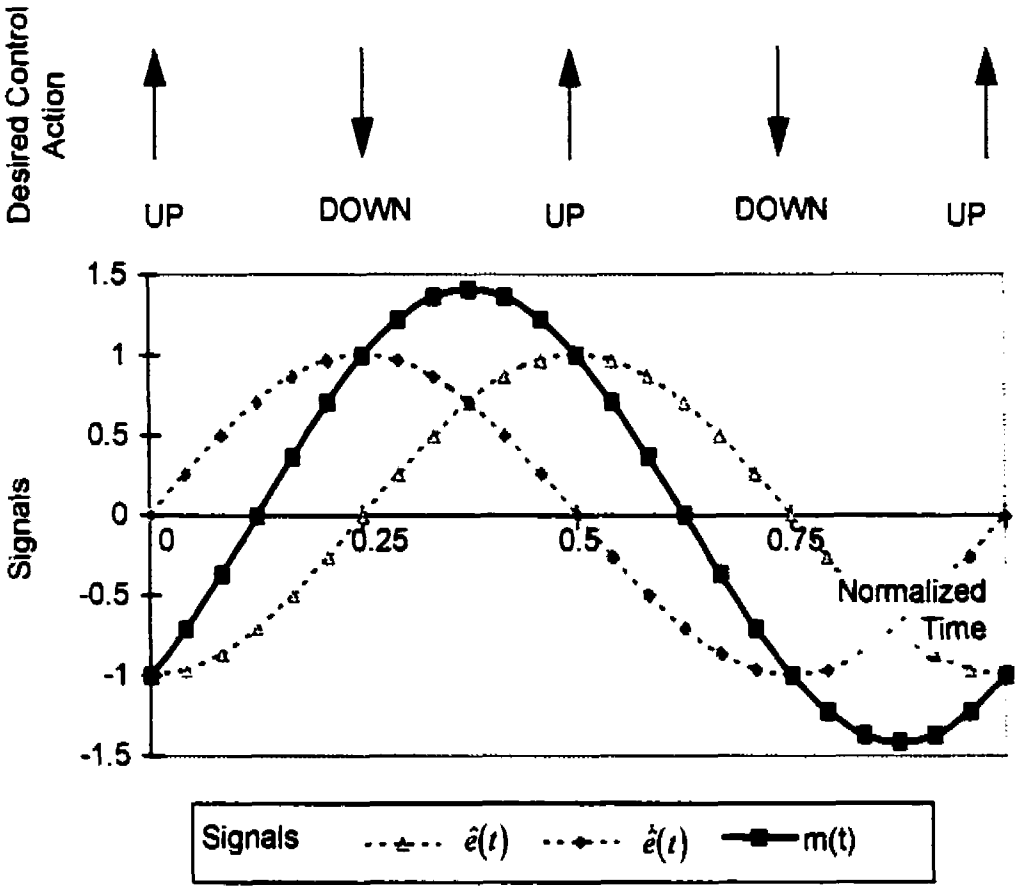

Figure 5.2 Comparison of linear proportional and derivative control signal with the desired control strategy at each extrema.

A control strategy that satisfied the desired control action, yet retained the desirable characteristics of a proportional and derivative action was possible, if the error signal and its derivative were rectified. The control signal would then be defined as

$$m(t) = K_p|\hat{e}(t)| + K_d|\dot{\hat{e}}(t)| \tag{5.2}$$

with the notation being the same as previously given in Equation 5.1. This type of action will be referred to as a "modified, proportional and derivative control action".

When the gains were both positive, then the control signal oscillated at twice the frequency of the plant and remained positive throughout the cycle of angular oscillation. Generating this action to physically represent the displacement profile of the attenuation device satisfied the frequency relation; however, the coordination between the translational motion of the attenuation device and the angular oscillations would not alter the system energy. However, if the gains were chosen so that $K_p < 0$ and $K_d = -K_p$, then the control signal would be a "saw-tooth" pattern as shown in Figure 5.3 when $K_p = -1$ and $K_d = 1$. This profile satisfied the control logic for each extremum and would be appropriately mapped to the velocity profile of the auxiliary mass. Desirably, this control action would require the "proportional" and "derivative" gains to be adaptable to eliminate the structural, vibrational energy.

Other control signals would also satisfy the control logic, such as a control signal based on the rectified error with a given offset. Mathematically, this can be stated as,

$$m(t) = K_p|\hat{e}(t)| + \Theta \tag{5.3}$$

where Θ represents some bias and $K_p < 0$.

This type of control action can be considered as a biased, rectified proportional controller and is illustrated in Figure 5.4 for $K_p = -1$ and $\Theta = 0.5$. This control action would be used to drive the attenuation device and would be representative of its velocity profile. With this control signal, achieving

'complete' vibrational attenuation would also require an adjustable bias[3]; otherwise, some residual energy would remain. Although this control signal was not implemented, it illustrates that a variety of control signals exist and may be implemented to satisfy the desired control logic.

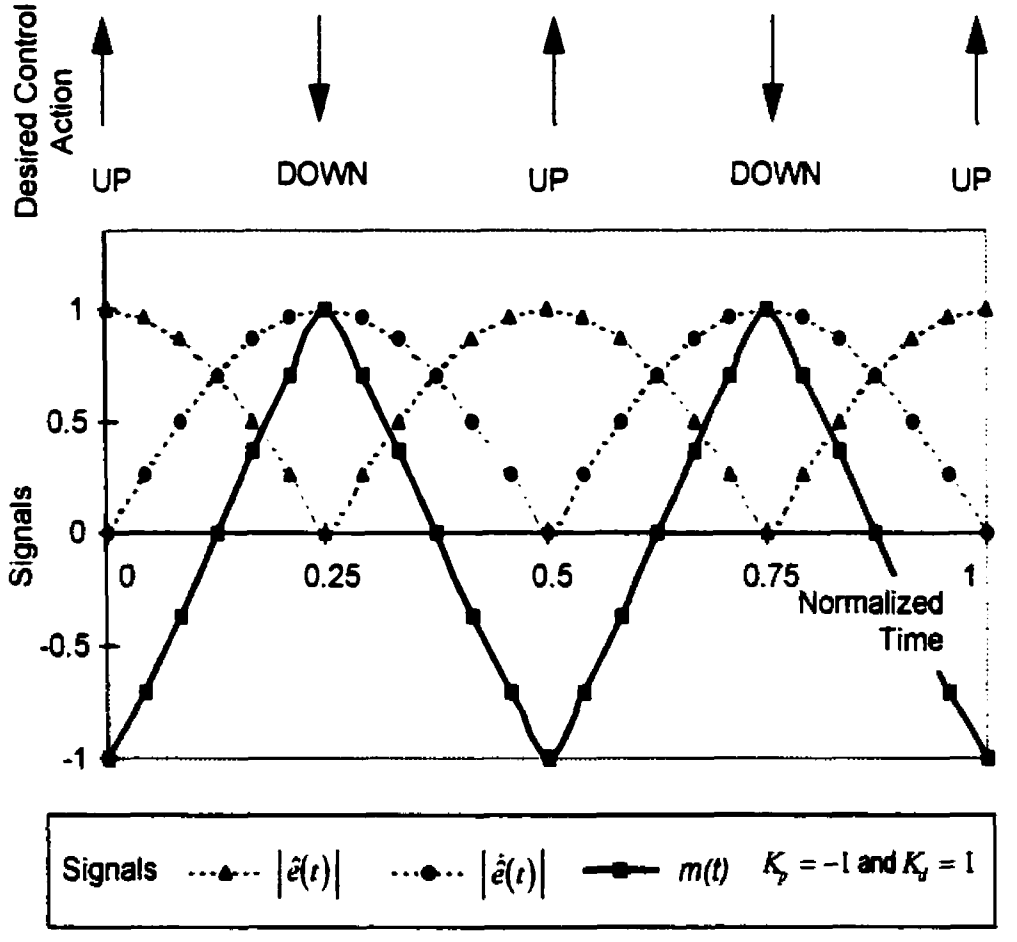

Figure 5.3 Control signal with modified, proportional and derivative action satisfies the control law.

[3] An adjustable bias may be based on the normalized error function and may be defined as $\Theta = k\frac{|e(t)|}{e(t)_{MAXIMUM}}$ where k is an optimized constant and $e(t)_{MAXIMUM}$ is the maximum value of the error function for a period.

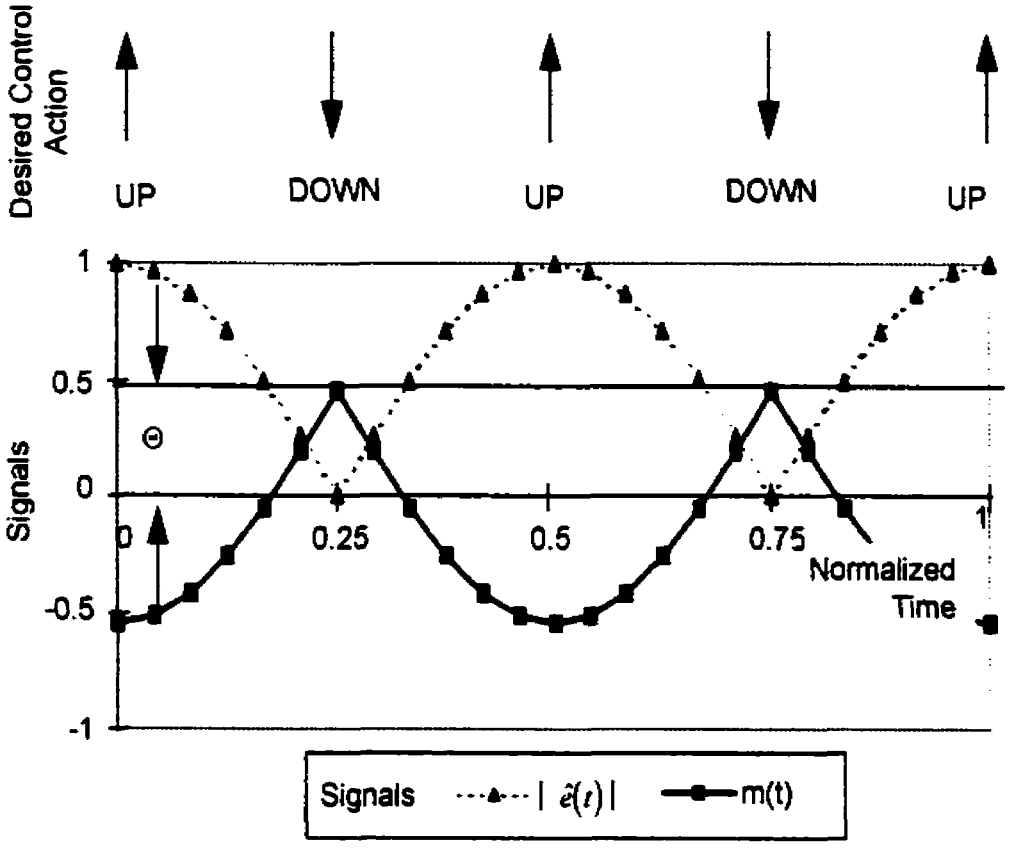

Figure 5.4 A biased, rectified proportional control action also satisfies the control logic.

The controller with the modified, proportional and derivative action is represented as a block diagram in Figure 5.5. This controller with appropriately chosen gains was expected to be effective for a given set point.

A similar control action where the auxiliary mass translated radially in a continuous, sinusoidal pattern along the pendulum has been simulated in Sections 4.4.2 and 4.6.2. When the frequency of motion of the auxiliary mass was fixed, the dynamics of the system exhibited beating phenomena (as shown in Figure 4.24). This phenomena was avoided by using a "tuned" frequency for the auxiliary mass motion, as described in Section 4.5. Since the control signal in Figure 5.5 was based on the actual angular position and velocity as feedback parameters to calculate the error signal and generate the

control signal, this phenomena was not expected. The feedback parameters, themselves, would provide the necessary tuning and the control action would remain coordinated with the error signal.

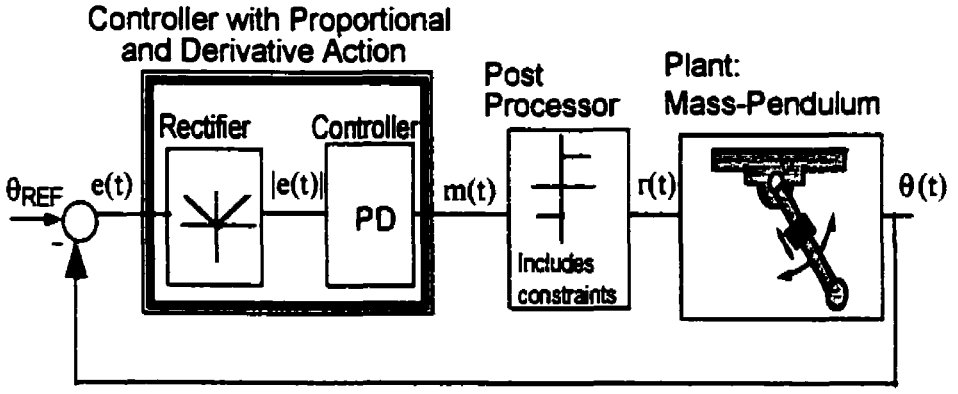

Figure 5.5 Block diagram implementation of the controller with modified, proportional and derivative action.

Details of the operation of this controller are given in Chapter 7.

5.4 Artificial Intelligence Technology

Artificial intelligence is a unique blend of biological processes with technology. In emulating various human or biological processes, several techniques and/or tools have evolved which include knowledge based expert systems, artificial neural networks, genetic algorithms and evolutionary programming. Research in the field of artificial intelligence is truly interdisciplinary as contributions or applications have included psychology, physiology, biology, neuroanatomy, social sciences, mathematics, physics, engineering, applied mathematics and computational sciences, to name but a few [Miller, 1990]. The advances made in these areas during this portion of the thesis research have been immense [Sànchez-Sinecio and Lau, 1992].

Typically, artificial intelligence technology provides a method of handling knowledge, where knowledge refers to information or models that are used to interpret, predict and appropriately respond to actual systems

[Haykin, 1994]. Often the representation of knowledge is redundant, incomplete and error prone; artificial intelligence technology can handle these problems in an effective manner. Despite industrial applications being limited [Miller, 1990], this field was considered very tractable to the thesis research. The next two sections provides a brief introduction and describes the potential implementation of knowledge based or expert systems and artificial neural networks as control candidates.

5.5 Knowledge Based Systems

Knowledge based systems (KBS) or expert systems are one of the tangible products of artificial intelligent research. KBS essentially attempt to capture human expertise or specialized knowledge for an application area. Several architectures for KBS have been developed. Typically, a knowledge based or expert system controller is comprised of a knowledge base, an inference engine and a working memory or interface system [Wolfgram, 1987; Krishnamoorthy and Rajeev, 1996]. Basically, the knowledge base contains the relevant information regarding the area that the system is to provide expertise and assistance; this may be formulated as facts and/or governing rules. The conditional logic used to control the attenuation device, as previously stated in Section 5.3, could form the knowledge base for attenuating vibrations by mass reconfiguration. The working memory or inference engine accesses this information, appropriately. The interface system is the link between the user/system and the knowledge base. Typically, when KBS are used to assist a human operator, an interactive session consists of the operator providing appropriate data as prompted by the KBS through a computer terminal and keyboard interface. For an automated control system, sensors would provide the necessary input data for the inference engine to act on.

Knowledge based systems are applied where the expertise can be formulated into a hierarchy of heuristics or conditionals. Early applications

were nonnumerical problems that related to areas of assessment, monitoring and diagnosis. The MYCIN project for medical diagnosis was one of the earliest projects in this field [Alty and Coombs, 1984]. Other applications included prediction, identification, speech understanding, design, repair, problem identification, monitoring, planning, debugging, instruction, plant dynamics and control [Stilling, 1989, Walker and Miller, 1990]. For control applications, the input data or information is assessed and processed by the inference engine according to the hierarchy of heuristics or control laws; then the appropriate control action is generated.

The challenge of creating an expert system is in extracting the knowledge base as the human expert appears to operate in an inexact, contradictory and error-prone manner. Often, the human operator cannot articulate the heuristics in a fashion suitable for creating a knowledge base system. Furthermore, expert systems tend to be very domain specific and are not reliable outside the programmed operating environment. If the knowledge based controller were programmed to attenuate vibrations for the pendulum structure based on a disturbance that caused an angular displacement offset of, say, 10°; one would expect less efficient performance for a similar disturbance causing an offset of 90°. Nonetheless, when operating conditions can be defined and processing rules can be arranged logically, knowledge based systems can be developed that provide consistent and efficient performance [Waterman, 1986].

In applying this technology to direct the reconfiguration of mass to attenuate the angular oscillations of a pendulum structure, the heuristic used by the human operator (Sections 2.2.2 and 5.2) must be quantified. A block diagram for the system when using a knowledge based controller is a feedback system with the parameters of the structure and controller being continually monitored as indicated in Figure 5.6.

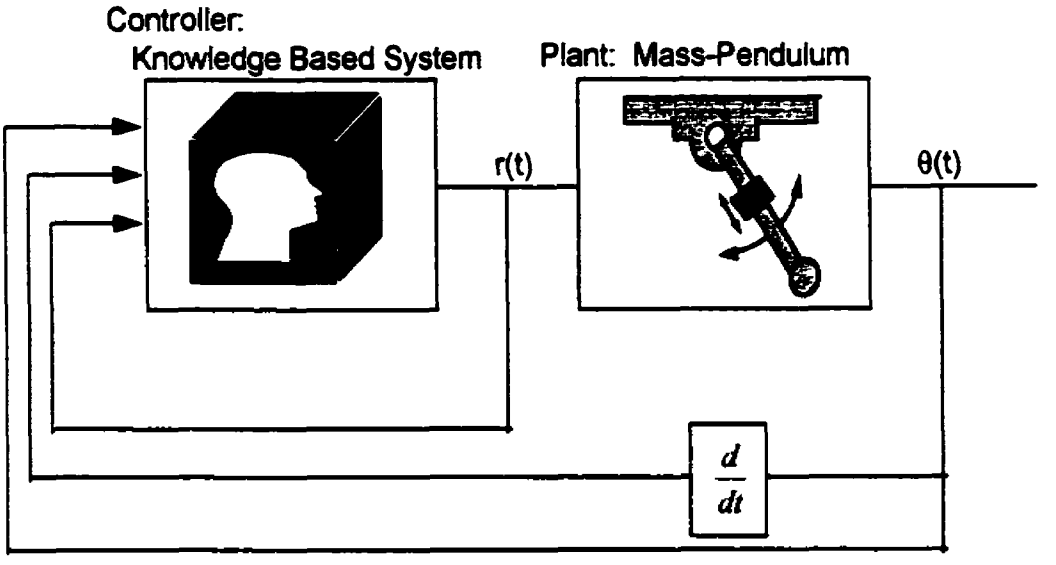

Figure 5.6 Block diagram representation of Knowledge Based System controller.

The traditional control signals, namely reference and error signals, are contained within the knowledge base. The control output signal, $m(t)$, has been post processed by the knowledge based controller to generate, $r(t)$, the displacement of the attenuation device. Also, constraint operating conditions for the mechanism may also be embodied in the knowledge base. The inference engine of the expert system will process this data to direct the mass reconfiguration. To avoid problems of operating outside a given domain or operating condition, the control logic must be as general as possible and preferably self-adapting.

Details of the knowledge based controller and the corresponding results are presented in Chapter 8.

5.6 Artificial Neural Networks

Another development from the field of artificial intelligence is artificial neural networks[4]. These nets originated as symbolic and computational approximates of the biological neural system.

Artificial neural networks were developed based on mathematical modeling of the biological system as introduced in the following brief historical review. The connectionist or parallel distributed processing model of behavioral and cognitive functions can be traced to work by Jackson (1869/1958) and Luria (1966) [Rumelhart et al., 1986]. A mathematical model for the functioning of brain neurons dates back to 1943 in work by McCulloch and Pitts; their model was a binary, time dependent logical neuron. By the 1950's, Rosenblatt presented the concept of a single layer of neurons; this artificial neural net was called a perceptron. Perceptrons had limited computational abilities, but advances by Kohonen, Grossberg and Anderson in the 1980's resulted in more powerful, multi-layer networks [Neelakanta and De Groff, 1994]. Since these developments in the 1980's, neural network research has been continually growing.

With access to powerful computers and advances in training multiple layer nets, the interest and research in the area of artificial neural networks advanced to an implementation level [Warwick, 1995]. Successes employing artificial neural networks began to compete with traditional methods and models in areas of processing and prediction. Implementations included classification of undersea sonar signals, speech analysis, vision recognition, robotic control and others [Lawrence, 1990]. Early prototypes, labeled as "Adeline" and "Madaline", were developed in 1960's [Widrow and Lehr, 1990]; they were constructed using various logic devices (i.e. AND, OR and majority-vote-taker elements) [Haykin, 1994] and were used as control units.

---

[4] Artificial neural networks are also called neural networks, neural nets, nets, parallel distributed processing (PDP) models, connectionist models or neuromorphic systems by various researchers.

Artificial neural nets are viable computational models for a wide variety of problems which include pattern classification, speech synthesis and recognition, adaptive interfaces between humans and complex physical systems, function approximations, image data compression, associated memory, clustering, forecasting and prediction, combinatorial optimization, nonlinear system modeling and control [Hassoun, 1995].

5.6.1 Motivation for Selecting Artificial Neural Networks

At the time of initiation of this research, applications using artificial neural nets for control were very novel; the majority of the reported applications focused on system identification and possible implementations techniques. During the extended research tenure of this project, applications and extensions related to the field of control and engineering have advanced significantly as reported in various academic journals.

Although the control logic for this application can be clearly postulated, extending the concept of vibration attenuation by mass reconfiguration to more complex systems may not be intuitive. In 1989, Tursby et al. reports that "artificial neural nets can be very useful in a large system where the identification of control elements and the determination of algorithms based on mathematical models of the structure may be difficult if not impossible to achieve." These criteria existed at the onset of this research; hence an artificial neural network that can parallel a controlled system for the mass-pendulum application was developed.

5.6.2 Overview of Artificial Neural Networks

A conceptual and mathematical framework for understanding the functionality of neural networks is provided to serve as a foundation for discussing its implementation as a controller in Section 5.6.3. When this research commenced, very little information for net synthesis was available. Since design principles did not exist, this section summarizes the

considerations, development and related advancements for creating the neural network tool for this application with details provided in appendices.

A neural network consists of a dense maze of interconnected nodes that act in parallel [Redger and Aleksander, 1995]. Mathematically, at each node is a simple, computational element called a neuron[5]. Similar to the biological neural cell, a computational neuron processes inputs from connecting nodes to generate a single output that may be passed to several other neurons.

The neural activity can be represented in several ways. The most common processing protocol is a linear combination or a weighted sum of the input signals, as shown in Figure 5.7. The value is then scaled using a logistic or squashing function[6]. The generated output value is passed to subsequent nodes.

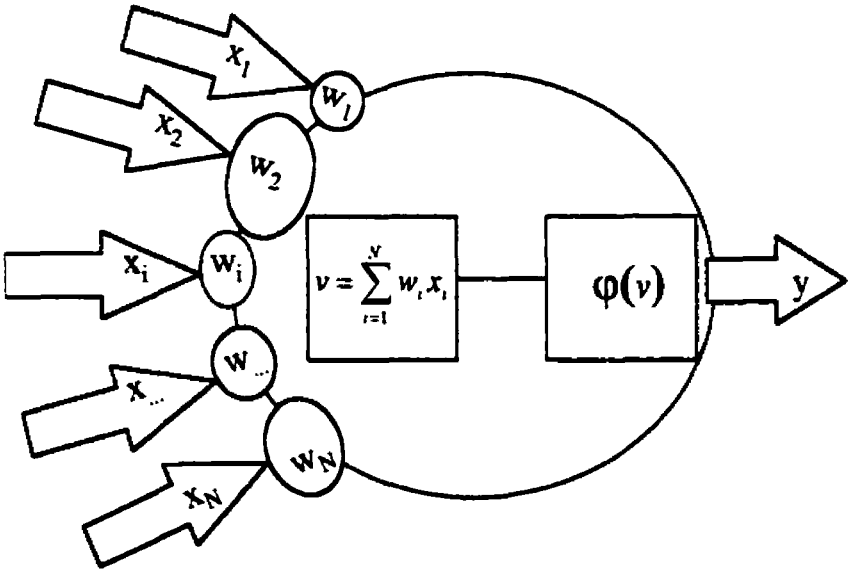

Figure 5.7 A neuron is a fundamental computational unit of artificial neural networks.

[5] The fundamental elements of an artificial neural network are also called processing elements, computation units, neurons or nodes.

[6] Logistic functions are also called activation functions, transfer characteristics or threshold functions; the function depends on the mapping required.

The squashing function is usually a nonlinear function that models the activation levels in biological systems [Lippman, 1987]. Various activation functions exist, including signum threshold functions, piece-wise linear functions or sigmoid[7] functions as shown in Figure 5.8 and mathematically described in Appendix K.

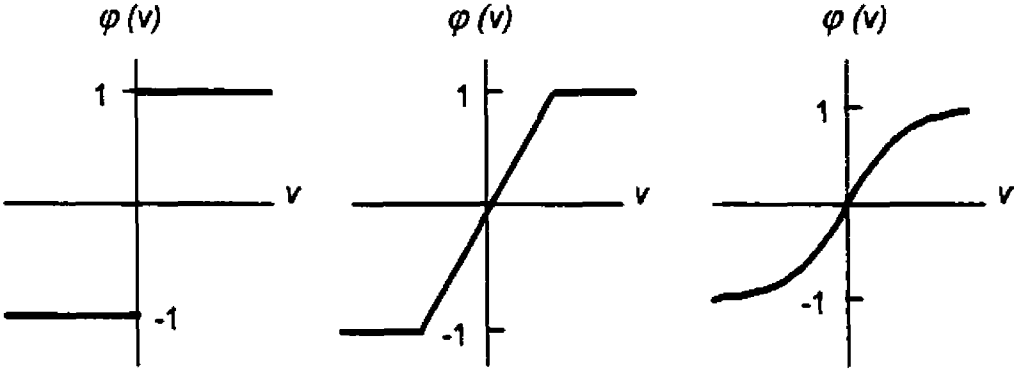

Figure 5.8 Typical squashing functions include: (a) antisymmetric step function, (b) ramp function and (c) sigmoid function.

Mathematically, the computation performed at a node is given as,

$$y = \varphi(v)$$

$$\text{where } v = \sum_{i=1}^{I} w_i x_i \tag{5.2}$$

and y represents the output for the node;

v, the linear combination of inputs or the internal activation level;

w_i, the adjustable weight associated with the ith input;

x_i, the ith input;

I the number of input signals; and

$\varphi(\ )$, the activation function.

[7] The popular sigmoid function is a continuous, differentiable, monotonically increasing function exhibiting asymptotic properties; a hyperbolic tangent function was chosen for the implemented controller.

Another numerical processing feature associated at the neuron level is biasing or threshold setting. Each neuron can have an internal, unique threshold provided by either an adjustable bias input or a threshold value defined by the logistic scaling function. In this research, a bias for each node was included by having an additional fixed input of value 1 with its own synapses[8].

The input-output values can be either binary or continuous. The input-output relations are learned though the weighted connections. By adjusting the weights applied to each input signal, the relevancy of the input is established for generating a desired output. The adjustment of these weights can be accomplished in either a supervised or unsupervised training mode [Hassoun, 1995; Simpson, 1992]. Techniques for training are discussed later.

The architecture of the net or the connection scheme of the neurons to form the network can also vary. The architecture affects the mapping complexity between input-output relations[9]. The most popular format in use is a multiple layer, feed-forward network. The selected network, as illustrated in Figure 5.9, featured no intra-connection of nodes within a layer and nodes of a previous layer all feed to each node of the adjacent layer. This type of net can be labeled as *I-J-K-L* where the indices represent the number of nodes/neurons in each layer. This type of net was used and its mathematical representation of the output can be expressed as,

$$y_i = \varphi\left(\sum_{k=0}^{K} w_{ik} \cdot \varphi\left(\sum_{j=0}^{J} w_{kj} \cdot \varphi\left(\sum_{i=0}^{I} w_{ji} \cdot x_i\right)\right)\right) \tag{5.3}$$

---

[8] Synapses, a biological term for the connection between neurons, refers to the connecting weights between neurons for artificial neural networks.

[9] A single layer net (perceptron) provides direct, linear mapping relations; two layer structures permit mapping of convex, open or closed regions; three layer systems can model arbitrary complexities with inclusions and exclusions as determined by the number of nodes.

where x_i is the ith node of the input layer with I being the total number of nodes of this layer;

w_{ij}, the (i,j) weight connecting the ith input node to the jth node of the first hidden layer where J is the total number of nodes of this layer;

w_{jk}, the (j,k) weight connecting the jth node of the first hidden layer to the kth node of the second hidden layer where K is the total number of nodes of this layer;

w_{kl}, the (k,l) weight connecting the kth node of the second hidden layer to the lth node of the output layer;

$\varphi(\ )$, is the activation function; and

y_l is the lth node of the output layer with L being the total number of nodes of the output layer.

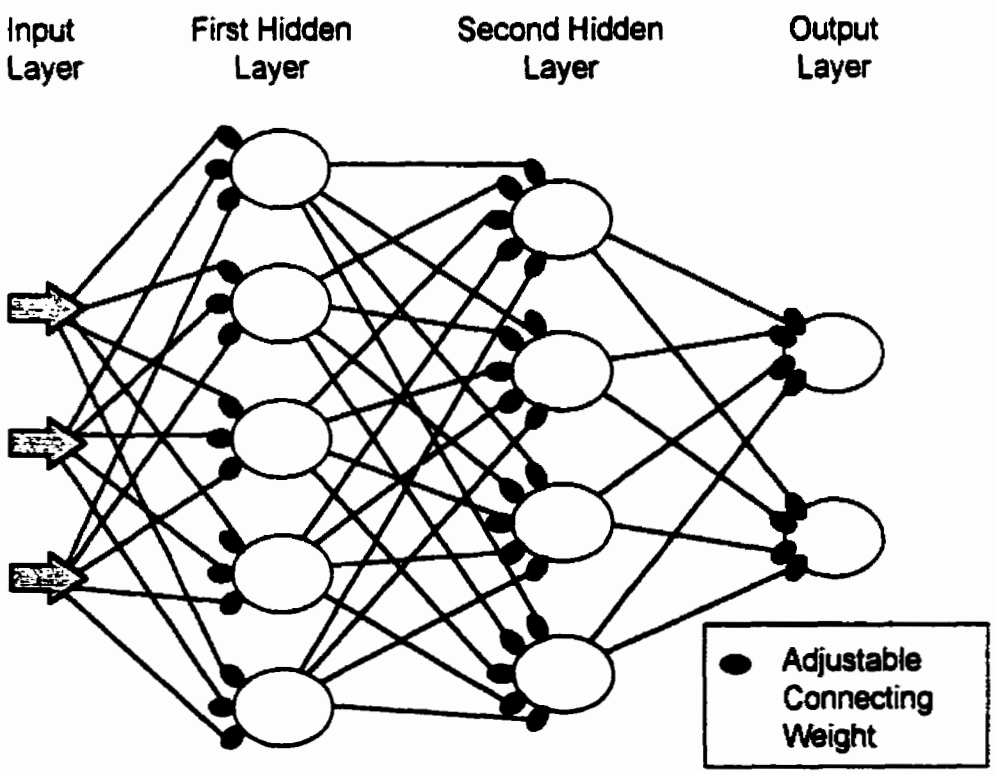

Figure 5.9 Multiple layer feed forward neural network (3-5-4-2)

Another category of networks are recurrent neural nets. Structurally, the nets possess "feed forward" and/or "feed backward" connections and the connections may be within a layer and/or among nonadjacent levels or elements. The "feedback" connections, typically, incorporate derivative or time delay information. These nets have been successfully applied to identify dynamic systems [Pham and Karaboga, 1999]. Unfortunately, these nets require a large number of additional nodes which infers more extensive computations and training requirements. Thus, these networks tend to be more susceptible to noise and their training as an independent simulators are difficult. Real time control applications have successfully incorporated recurrent nets [Ku and Lee, 1995]. Sample architectures are given in Appendix K. However, to achieve dynamic processing ability in an artificial neural network for this research, the input parameters were selected to contain the first time derivative data. When compared to a simple recurrent net that posses nodal time delays, the derivative input data provided good performance and required less computational resources. [See Appendix K].

Learning behavior is intrinsic to both artificial and biological neural nets. Artificial neural nets achieve good performance through associations and generalizations without the use of rules [Brown, 1987]. Learning is achieved by adjusting the connecting or synaptic weights and threshold values. As the complexity of the net increases either in number of nodes or types and number of interconnections, the run-time operation increases and the training becomes increasingly involved.

Various learning algorithms and/or training paradigms have been developed [Rahim, 1994; Masters, 1995]. The training of the net that is relevant to this research is classified as supervised. Supervised training requires external information, often as a set of matched input-output patterns which are called exemplar patterns. For supervised, error-based training, the process consists of repeated presentation of the input patterns with known output performance; the net generated output patterns then are compared to

the desired output and adjustments to the weights and threshold values are made to force the net to generate the desired output. The training is assumed complete for a set of exemplar patterns when the output patterns for the applied input patterns converges, such that the output pattern remains unchanged through successive training iterations or an acceptably small difference between the net generated and the desired output exits.

The training or adjusting of the weights was accomplished by applying various optimization methods which included steepest descent or back propagation, coordinate search, conjugate gradient, Powell method, evolutionary algorithms and others. The algorithms are presented in Appendix J. Each training algorithm was evaluated on a benchmark training suite with the results being as summarized in Table 5.1.

Table 5.1 Evaluation of Training Methods

Training Method	Computational Steps Ranking	Convergence Ranking	Minimum
Back Propagation	3	4	local
Coordinate Search	2	3	local
Conjugate Gradient	4	1	local
Powell	5	2	local
Genetic Algorithms	6	5	global
Evolutionary Programs	1	6	global

Note that each ranking is from 1 to 6, the computational steps per training iteration are ranked from fewest to most computations; the training convergence is ranked from fewest to most training iterations; and the minimum has been classified as most likely to converge to either a global or local minimum. As comparable results were obtained when Powell and conjugate gradient training algorithms were used, the latter was chosen for the training of the artificial neural networks controllers as it was relatively easy to implement in both languages and apply to the application being studied. The training details are discussed further in Appendices J and K.

To summarize, through parallel processing, nets provide a complex mathematical mapping of input data to output by establishing appropriate links. By adjusting the interconnecting weights, nets can be trained to recognize the important parameters and provide appropriate output. A unique feature of nets is their ability to learn performances through training rather than through programming. For simple nets, associations are learned through adjusting the weights connecting computational elements. With the ability to train, a net provides good performance for a range of operating states. Continued learning using current results enables the net to adapt dynamically and to adjust to minor variations in the input data. Since nets consist of numerous interconnected elements, good performance has been observed under conditions of incomplete or noisy input data. Also the inherent robust nature of nets accommodates modeling uncertainties and undefined dynamics of the system.

For this research the neural net framework was a feed forward, multi-layer, static net[10]. The processing capabilities of each neuron was described as the summation of continuous, unbounded inputs to generate an output bounded by the domain [-1,1] and expressed in Equation 5.2. Bias or threshold attribute was achieved by adding another node to input layers. The output of the net was expressed by Equation 5.3. Inputs were chosen to contain derivative information and recurrent network architecture was not incorporated. Training the network was supervisory using optimization techniques. The selection of input-output parameters and the number of nodes and layers are discussed in the next section.

[10] A static network is defined as one that has only feed forward connections; there is no recurrence. In contrast a dynamic net has both feed forward and feed backward connections. [Zbikowksi and Gawtrhop, 1995].

5.6.3 Artificial Neural Networks as the Controller

This section presents the neural network as the control unit. Since design and function are closely linked; the control philosophy and neural network characteristics and operation are discussed concurrently. The network implementation depends on the required operating philosophy and its corresponding training protocol.

Often a neural network as a controller is viewed as a "black box" that accepts inputs to produce outputs. The function of the input-output relations is to provide control action so as to approximate an appropriately controlled system, as shown in Figure 5.10. The net was trained to learn the relation between system dynamics and the necessary control action to effect vibration attenuation. This type of control action for the neural net will henceforth be referred to as a "proxy" controller.

When the neural net functions as a "proxy" of one of the previously described controlled systems, the trained neural net operates as a feed forward controller in a closed loop, as shown in the bottom portion of Figure 5.10. Although the neural network and its post processor were to operate similar to other controllers, it was a proxy; the neural net cannot be viewed as a direct substitute. The neural network performs more than a traditional controller. The control system incorporating the neural network is neither a traditional open or closed loop controller. Despite providing multiple input, feed forward control, the network using feedback in a nontraditional way.

The controller was to process multiple inputs as given by the input vector, $\vec{X}(t)$, to generate a multiple output vector, $\vec{Y}(t)$. The output signal from the net would then be post processed to generate the control signal, $m(t)$ used to drive the control mechanism that would change the mass configuration as defined by $r(t)$ to attenuate the vibrations ($\theta(t) \rightarrow 0$).

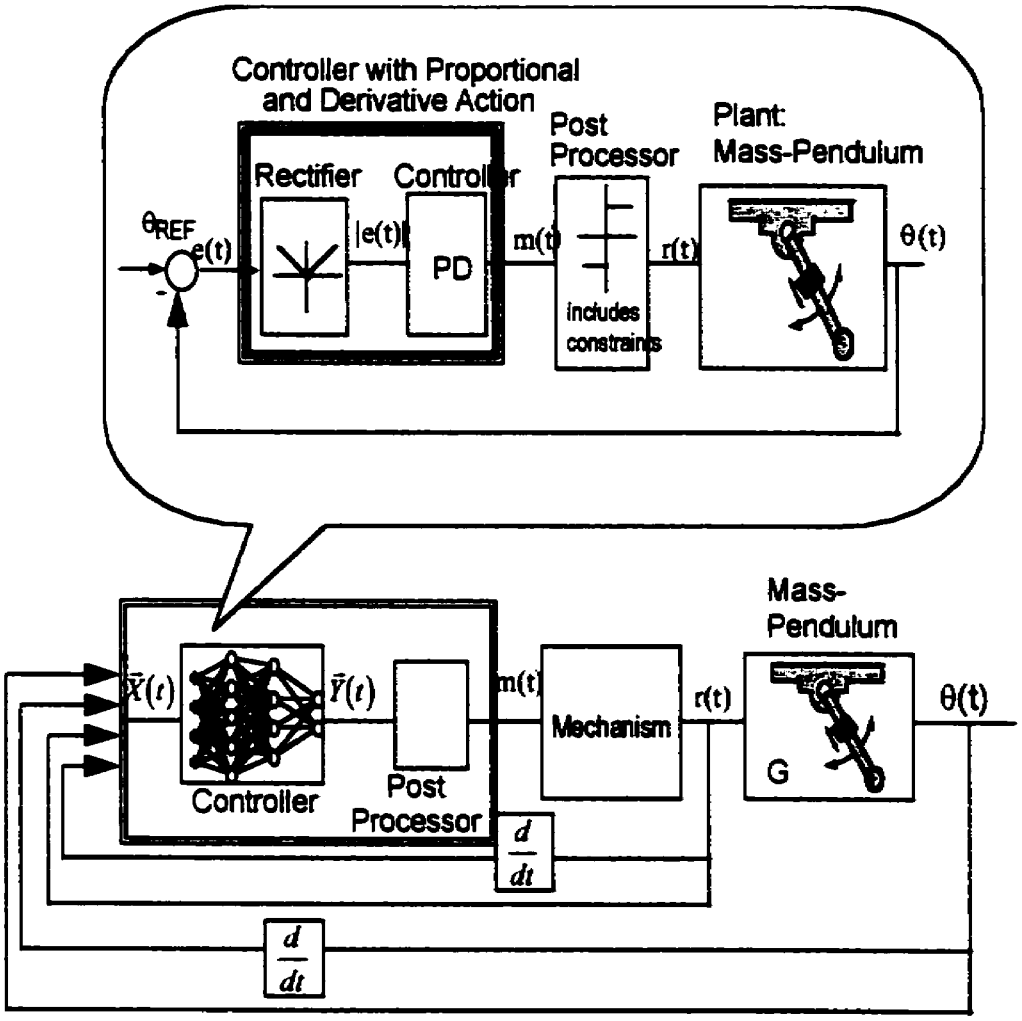

Figure 5.10 "Proxy", neural net controller trained to imitate other controlled systems.

As shown, the operation deviates significantly from a classical closed loop control block diagram, as was previously shown in Figure 5.4 for the control system using proportional and derivative action. Firstly, a reference signal and the corresponding error signal that typically drives the controller is not explicitly generated. Secondly, the selection of inputs and outputs from the controller have not been identified in a classic approach to reflect the desired control objective. Consequently, post processing from the controller to drive the mechanism is required. Lastly, the dynamics of the system have

been incorporated by selecting time derivative input information rather than introducing time delay elements. Each of these aspects is discussed next.

The neural net controller internally processes the error signal with respect to a reference signal. This was achieved by training the net with patterns that represent an appropriately controlled system; thus, the error signal is embedded within the trained connections. Hence, the desired or reference input, $\theta_{REF} \rightarrow 0$, does not appear explicitly in the control diagrams, rather it is inferred and embedded through training.

The control objective can be stated as attenuating angular oscillations, $\theta(t)$, by mass reconfiguration, $r(t)$. The classic control approach would be to identify the control input signal as $\theta(t)$ and control output signal as $r(t)$. However, for the neural net controller the input signal was selected to represent the state dynamics of the mass-pendulum system. The inputs were chosen to be easily measured, dynamic parameters, namely, the angular displacement, angular velocity, translational displacement and translational velocity, $\vec{X}(t) = \left[\theta(t), \dot{\theta}(t), r(t), \dot{r}(t)\right]$. The selection of both the angular and translational displacement time profiles were chosen since the governing differential equations are coupled (Table 3.1) and as discussed in Section 2.2.2, the control strategy depends on proper coordination between the angular oscillations and the mass reconfiguration profile. Furthermore, the attenuation device's translational kinematics for an input parameter enables constraint information for mass reconfiguration to be incorporated into the net. Note that dynamic information was automatically included as time derivative data was part of the input vector[11], as discussed in Section 5.6.2.

[11] When the net morphology was developed [Stilling, 1991 and 1990a; Stilling and Watson, 1991 and 1990], providing appropriate dynamic input parameters was novel. The net was freed from storing time dependent operations internally; this technique has since been practiced by others [Qian et al., 1998].

The neural net controller processes parameters that characterize the dynamics of the system to generate control output signal(s). Two unique sets of outputs were considered for the neural network to provide the control action; one set had four output parameters and the other, three. Since, the control action can be expressed as either discrete or continuous signal as shown in Figure 5.11 which maps the control output action over a cycle of simple harmonic motion, the neural net output was mapped as either continuous or discrete values. Each network would require post processing prior to being fed to the mechanism to effect mass reconfiguration, $r(t)$.

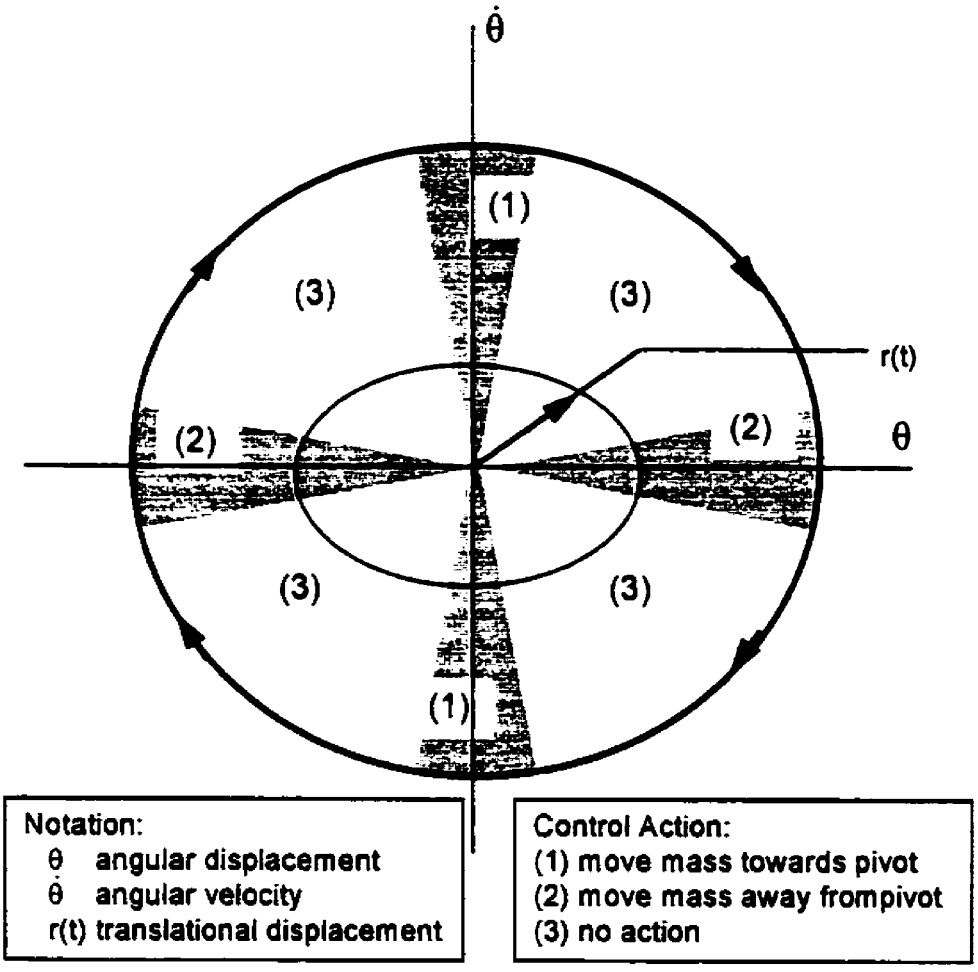

Figure 5.11 Mapping of neural net input-output patterns for typical control action of the mass-pendulum system over one period.

For the four node output network, the output parameters were assumed continuous and chosen to be the angular displacement and translational displacement of the auxiliary mass and their time derivatives; that is $\bar{Y}(t_1) = \left[\theta(t_1), \dot{\theta}(t_1), r(t_1), \dot{r}(t_1)\right]$. These were the same parameters identified as viable input parameters. When the output data was continuousand unbounded (not normalized), the sigmoid processing operation of the final output layer was removed.[12] This net mapped current dynamics with appropriate control action that represented the dynamics at a future time step. The neural net controller was trained to have predictive capabilities.

By considering the training protocol, the development and operation can be better illustrated as explained in Appendix K. The training protocol for a supervised, error-driven trained net is shown in Figure 5.12.

The supporting rationale for selecting this set of input-output parameters was as follows:

(1) these variables could be measured from an actual structure;

(2) the process could be extended to more complex structures; such as: continuous structures;

(3) supervised, error-based training was easy to implement; and

(4) prototype development for training and implementing the controller was conceptually plausible.

[12] When input and output data were normalized or bounded between -1 and 1, each layer of the net had sigmoid functions.

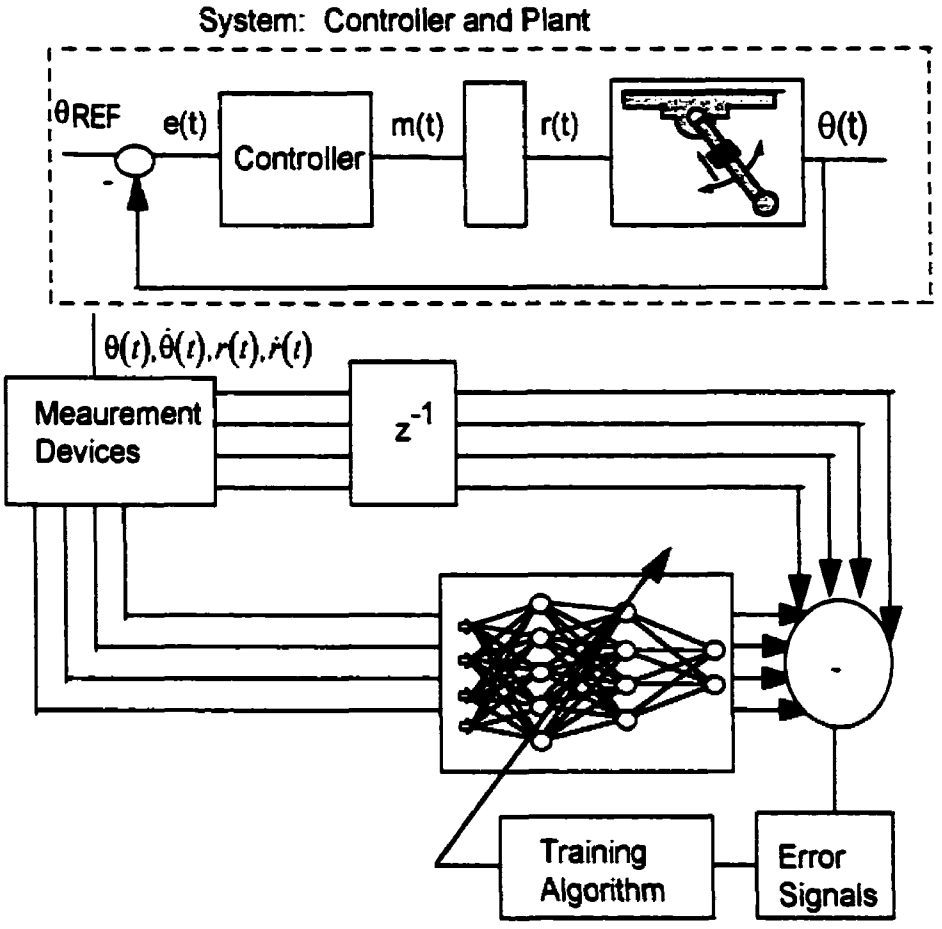

Figure 5.12 Training of the "proxy" neural network controller.

To appreciate the predictive nature of the operating mode provided through training the neural net controller, the time sequence operation is illustrated in Figure 5.13. Beginning at Point A, a set of measured parameters that represent the dynamics of the system $\vec{X}(t_o)=\left[\theta(t_o),\dot{\theta}(t_o),r(t_o),\dot{r}(t_o)\right]$, are processed by the neural net controller. The neural net maps this behavior to a corresponding controlled performance at Point B. The control output at Point B, approximates the controlled plant performance for time, $t=t_o+\Delta t$ given the initial conditions at $t=t_o$. Then, the system operates using this control action to generate its response at Point C which corresponds to $t=t_o+2\Delta t$ for the controlled system. The neural net controller uses this plant

behavior that is denoted by Point C as its new condition which become the new Point A and the time-dependent sequence is repeated.

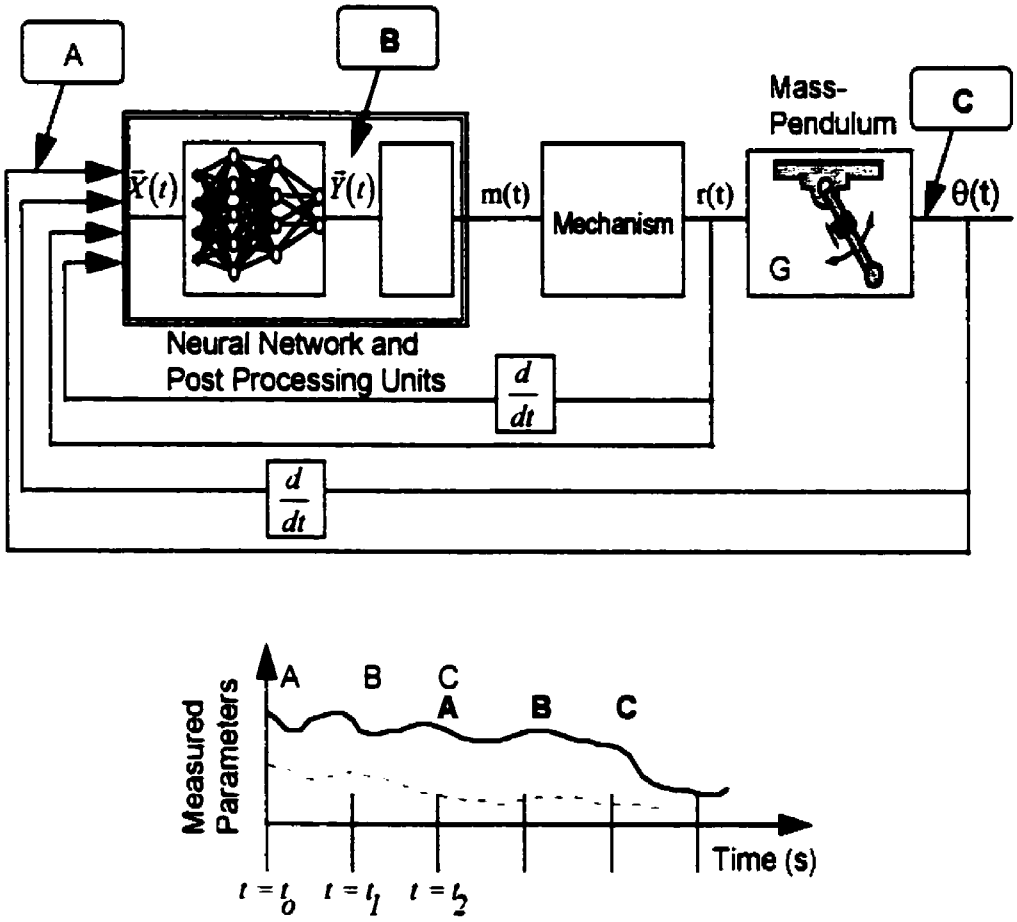

Figure 5.13 Time sequential operation of the "proxy" neural net controller.

For the three node output net, the control action was encoded by all three nodes. A tri-state, three element vector represented the neural net output; $\vec{Y}(t) \in \{[-1\,-1\,-1],\ [0\,0\,0]\ \text{or}\ [1\,1\,1]\}$ with the vector sets corresponding to motion of the attenuation towards the pivot, no motion or motion away from the pivot, respectively. Other numerical combinations were not part of the training regime. The rationale for selecting these values was multifaceted. Using three values instead of a single value added redundancy which is associated with increased reliability Through a post processor, the control action can be based on the majority from the combined output signals.

Various reconfiguration profiles for the auxiliary mass[13] can be readily mapped to discrete output patterns. This net architecture focused on the control action with the net performing the majority of the processing rather than on generating state parameter data to be using in the control process. Furthermore, the output format could easily be implemented with digital control. The exemplar patterns used to train the three node output were generated similarly to the four nodal output network; an additional step required that the measured control action from the plant be mapped to the appropriate output patterns to form the exemplar output or target patterns.

To summarize, the neural network was trained to approximate an appropriately controlled system. By sampling at time, t and $t+\Delta t$, the controlled system dynamics would be incorporated into the trained weights of the net. This eliminated the need to compute error signals as the network would intrinsically have processed such signals. Parameters as identified in the governing equations of motion were chosen as the input parameters. The trained network results in creating a predictive controller. Further details of the morphology, operation and training for the neural network and its implementation as the control unit for vibration attenuation as used during this research appears in Appendix K or in Chapter 8.

5.7 The Control Tool: Software Developments

During the thesis, much software was developed, as commercial neural network software/hardware was not accessible [Stilling and Watson, 1991]. Also, tools in the area tended to be protected by proprietary rights and implementation details were usually withheld. Hence, a code accessible, readable and computationally efficient software package was developed. Originally, a linear algebra package was created; it was called MATMATH [Stilling and Watson, 1994a; Watson and Stilling, 1991b]. The software was

[13] For values associated with the mass reconfiguration kinematics, refer to Chapters 6, 7 and 8.

designed to be highly portable, serviceable, extensible and reusable. Later in the research, as new training algorithms were being explored, source code was developed in both Forth and "C" languages. Programming in these two environments necessitated the development of communication/translation utilities so results could be easily accessed by either system and platforms.

5.7.1 MATMATH

The linear algebra package, MATMATH, was developed in FORTH (Appendix F). As previously mentioned early simulations of the dynamics were coded with this package. The operation and training algorithms for the neural networks were also coded using this utility package.

Forth is fast, compact and easy to program, debug and maintain [Noble, 1988; Noble 1989]. In addition, Forth efficiently exploits available resources. Several unique coding techniques were developed, such as, operator overloading, vector execution to create generic operators, internal operand adjustment, mnemonic kludges for loop indices, dynamic memory allocation, access to host hardware (when necessary) and others. The modular style of programming enabled the code to be extensible, reusable and tailored for an application.

As a comprehensive utility package, the matrix operators span those that would be required in most engineering design and analysis. Also, unique element operators for data manipulation were designed. Although the set of operators is not exhaustive, supplemental functions can be derived by combining operators or by modifying the source code. Basically, the operators included data structure defining routines, initialization commands, input and output utilities, matrix operations of addition, subtraction, multiplication, determinants, inverses, eigenvalues/eigenvectors, norm computations and element arithmetic operators. The computations can be performed as single/double precision integer arithmetic and as short/long IEEE floating point arithmetic.

The attractiveness of Forth for the thesis research was its small kernel with the ability to access platform hardware. The transfer of the research to a prototype using highly portable microcontrollers/chips; such as Motorola 68HC11 or RTX-2000A was tractable. Since Forth provides easy access to platform hardware, prototype development where the structure and related sensors and actuators could be easily interfaced was deemed feasible. Appropriate utilities were developed in Forth for interfacing with a microcontroller/processor [Stilling, 1993b and 1990b; Watson and Stilling, 1992; Stilling and Watson, 1992].

5.8 Summary

The control action for mass reconfiguration to attenuate vibration for the mass-pendulum system may be implemented in several ways. The control logic may be postulated in several ways as either discrete or continuous action. The controllers as presented included human operator, proportional and derivative action, knowledge based systems and neural networks.

A human operator either through a priori knowledge of the physics governing the interaction between the mass-pendulum or through heuristics should be capable of effecting vibration attenuation. Also proportional and derivative action was analyzed. Although standard linear control action appears inappropriate, when using a rectified error signal, the control signal parallels the desired control action. Based on the heuristics from the human operator or the specialized domain knowledge from the physics of this problem, a knowledge based system can be created to generate appropriate control action. Artificial neural networks, a relatively untested controller for this application was proposed to generate control action by approximating appropriately controlled systems. This novel application was examined to assess the feasibility of using a network for this type of control application.

The following chapters examine the performance of each of the aforementioned controllers.

6. Human Operator as the Controller

6.1 Introduction

One option for implementing the control system involves a human operator. For this scenario, the operator assesses the plant dynamics and generates appropriate control action to attenuate its vibrations. The plausibility of this method is established by the fact that the inverse problem to vibration attenuation can be modeled by interpreting a child learning to swing as vibration amplification by mass reconfiguration. Through trial and error and, indeed, in a very short time, a child can coordinate squatting and standing to initiate swinging [Walker, 1990] and then can increase the amplitude of oscillations of the swing. The inverse problem of attenuating oscillations is not as easily learned. However, by observing the cause and effects of moving a mass radially along an oscillating pendulum system, a human operator should be capable of deducing a strategy to attenuate the vibrations.

Implementing a human controller had a two-fold purpose. Firstly, the understanding of the dynamics of the proposed system was furthered in a more tangible environment. Through interactive simulations of the human operator-controlled process, additional analysis was possible. Secondly, benchmarks or measures for evaluating the control systems were established. In establishing these benchmarks necessary data to implement other controllers were also acquired.

To evaluate the practicality of establishing a human operator controlled system for attenuating vibrations by moving a mass along the structure, several control experiments [Stilling, 1993a; Stilling and Watson, 1993] were

conducted with subjects of whom the majority had some post-secondary education. The participants constructed a simple pendulum and adjusted its length to control the vibrations. Also, some procedures for vibration control were made available to the participants on instructional cards. For these cases, the participants were able to learn heuristics to minimize the vibrations. Thus, operator-defined heuristics were considered as a feasible control approach for attenuating the structural vibrations.

An interactive computer simulation was later developed to permit human operator control. Various user-generated control strategies for coordinating the translational motion of the auxiliary mass with the oscillating pendulum structure could be studied. Data representing the structural kinematics and energy profiles revealed characteristics associated with energy attenuation for the pendulum structure. The temporal angular and translational displacement profiles, along with their derivatives, illustrated effective, coordinated control action. From this data, force histories and damping coefficient graphs characterizing the type of human control were also generated.

6.2 Software Considerations and Developments

To investigate human control, the computer simulation for the variable length pendulum was customized to be interactive as indicated in the flowchart of Figure 6.1. A visual (or graphic) interface was created to represent the dynamics of the system. The vibrations of the pendulum and the translational motion of the mass (attenuation mechanism) were animated. For each program iteration[1], the screen was refreshed[2] with updated positions of the pendulum and the auxiliary mass displayed. Keyboard input was used to control the motion of the end mass. The input was limited to two functional

[1] A program iteration refers to the outer loop of Figure 7.1 where the dynamics were solved for one time step.

[2] Although the term, refreshed, infers the screen is cleared, the graphics were updated using XOR line draw routines.

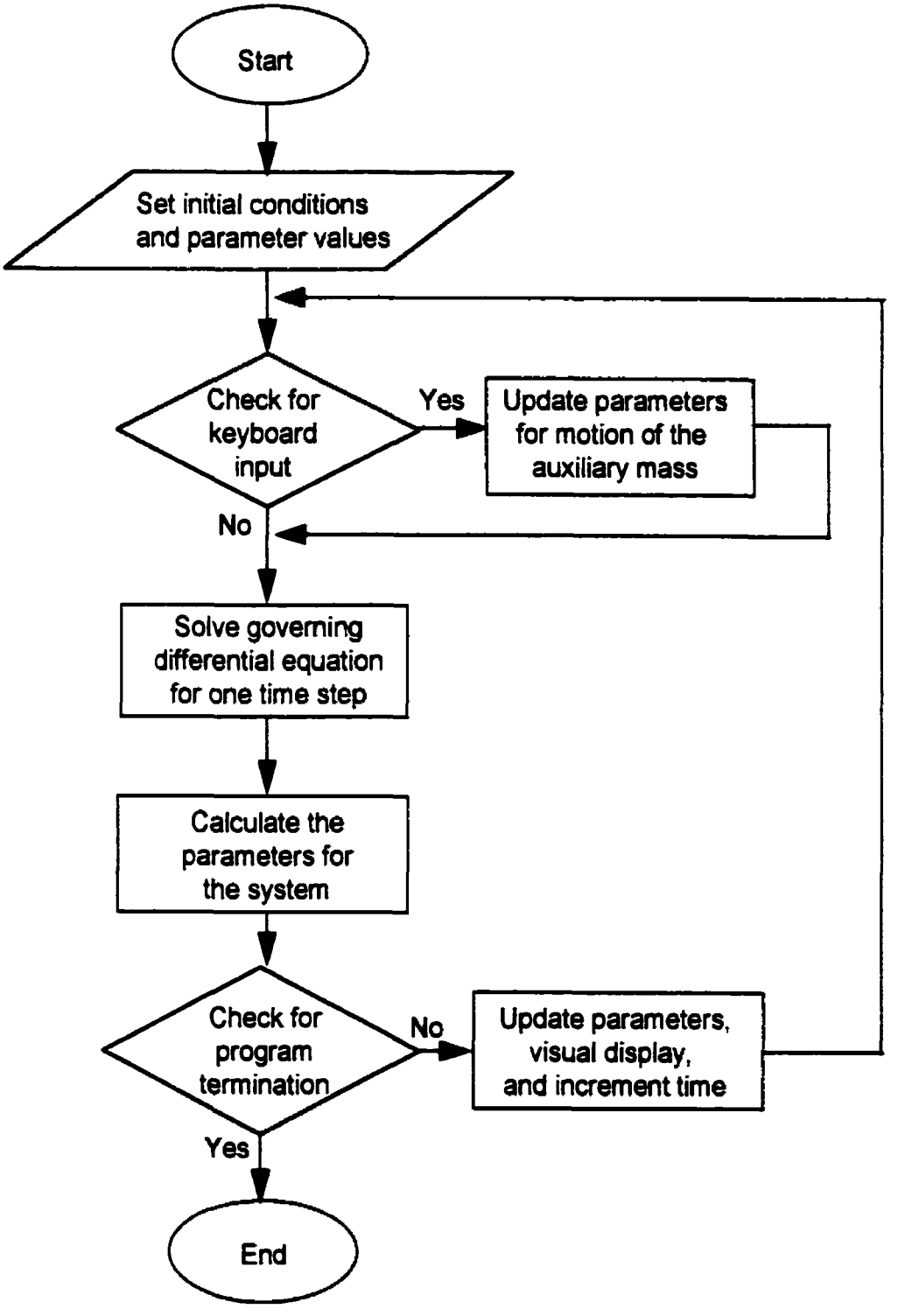

Figure 6.1 Flowchart for the interactive computer program to simulate a human operator controller.

keystrokes; one corresponded to moving the mass towards the pivot and the other, to moving the mass away from the pivot. Through software the keyboard buffer was continually updated and accessed to control the motion of the auxiliary mass along the pendulum.

Delay routines were added to allow adequate time for human interaction. These routines either accessed the internal computer clock or executed a series of null operations. This feature approximated real-time computing and control.

Program operation began with an introductory screen; then the user selected the speed of operation for the simulation. Program termination was based on achieving 99.99% reduction in the initial system energy or on executing a user-defined number of iterations.

6.2.1 Pendulum Parameterization for Numerical Simulation

A fourth order Runge-Kutta algorithm was used as the initial value solver[3] for the differential equation describing the variable length pendulum motion, as given by:

$$mr^2\ddot{\theta} + 2mr\dot{r}\dot{\theta} + mgr\sin\theta = 0 \qquad (6.1)$$

where m represents the pendulum mass[4] (1.0 kg);

g, an acceleration due to gravity of 9.81m/s^2; and

r, the pendulum length.

---

[3] For consistency, results are reported to at least the third decimal place. Note that the numerical simulations employed algorithms of order h^4 or higher where h represents the time step.

[4] Selecting the auxiliary mass magnitude was arbitrary as the governing differential equation (Equation 7.1) was independent of mass; however, the mass value was used to calculate energy magnitudes.

An initial length for the pendulum was selected as 1.0 m and the motion of the mass was restricted to a range of 0.75m to 1.25 m from the pivot. Thus, the natural frequency (ω_n) of the system could vary between 3.616 to 2.801 rad/s which corresponds to a period of oscillation (T) ranging from 1.737 to 2.243 seconds.

The time step (Δt) for the initial value solver was chosen to be 0.05 seconds, which is approximately $1/35$ to $1/45$ of the oscillation period depending on the location of the auxiliary mass. Based on user input, the incremental motion for the mass (Δr) was set to be ±0.05 m; hence limits for the instantaneous translational velocity were bounded between ±1.0 m/s which corresponded to acceleration limits of ±40.0 m/s^2. For the preliminary trials, the initial position of the pendulum was 30° from the vertical with a corresponding initial energy of 1.314 N-m. All of these parameters could be changed to permit several scenarios to be investigated.

6.2.2 Additional Display Features for Interactive Computer Simulation

To assist the operator in monitoring performance, the number of iterations were tracked on-screen. Also, the intangible parameter of the current total structural energy and its components were displayed. The total structural energy consist of the potential energy, U and the kinetic energy, T, as defined as

$$U = mgr(1 - cos\theta) \tag{6.2}$$[5]

$$T = \frac{1}{2} mr^2 \dot{\theta}^2 . \tag{6.3}$$

[5] Note that the potential energy is minimized when the mass is at its lowest possible position which occurs when the pendulum is beneath the pivot.

The energy of the system is an essential parameter to determine the effectiveness of the chosen strategy for moving the mass. In Chapter 4, the structural energy was integral in defining the objective function to optimize the displacement profiles for mass reconfiguration.

6.2.3 Implementation Platforms

The platforms that the interactive control system software was developed for included the Atari™ ST520, ST1040, MegaST and TT using Forthmacs©[6]. Forth enabled access to low level graphics, timing registers and BIOS[7] routines. Floating point mathematics[8] was available through software and/or hardware. The software, MATMATH[9] [Stilling and Watson, 1994a; Watson and Stilling, 1991a; Appendix F] was developed as a generic tool and was used when programming the initial value solver.

6.3 Results from Human Operator Performance

The operator gained experience in attenuating vibrations for a pendulum via moving a mass along the structure by executing the interactive program several times. For a fixed length of the pendulum, the simulation produced constant amplitude oscillations about the vertical position. However, for some of the end mass displacement profiles (as implemented by the user), the simulation did emulate various unstable and nonlinear phenomena. For instance, unstable behavior, such as a state of "infinite" energy, occurred when the mass was allowed to approach the pivot ($r \rightarrow 0$). To prevent this from occurring the mass motion was constrained. Also, the user could increase the energy of the pendulum to cause the pendulum to

---

[6] Copyright by Bradley Forthware, 1986.

[7] BIOS refers to the basic input and output systems, such as keyboard, disk and memory access.

[8] The floating point mathematics as programmed by Bradley Forthware uses Motorola Fast Floating point format and is IEEE double precision.

[9] MATMATH is a linear algebra package developed in Forthmacs.

circle the pivot. Eventually, these simulations would fail as the energy increased sufficiently so that the computer registers associated with calculating and monitoring system parameters overflowed.

Preliminary testing showed that a human operator could learn how to attenuate the vibrations when the mode for free vibrations was about the stable equilibrium position. Operators generated several trajectories for moving the end mass which resulted in vibration attenuation. Improved performance was noted as the operator gained experience and/or was informed of the following heuristic:

a) move the mass away from the pivot as the pendulum passes beneath the pivot, and

b) move the mass towards the pivot, as the pendulum reaches points of maximum angular displacement.

Typically, the user generated control action employed the above control logic in a relay fashion.

6.3.1 Detailed Trial Analysis for Human Controller

A sample, as taken from one operator's experience, is presented by examining the time relationships among the state variables of the system, the temporal energy profiles, the force histories and characterizing the dynamic parameter profiles. For this case, the initial structural energy of 1.314 N-m was reduced to 0.0087 N-m (99.3% reduction) in approximately four cycles of the angular displacement motion. The motion of the attenuation device, the auxiliary or end mass, was restricted to $0.75 \leq r \leq 1.25$ m.

As illustrated in Figure 6.2, the phase portrait of the angular motion indicates vibration attenuation as the magnitude of oscillations are continually decreasing. The motion appears to be converging to the stable position of zero angular displacement and velocity.

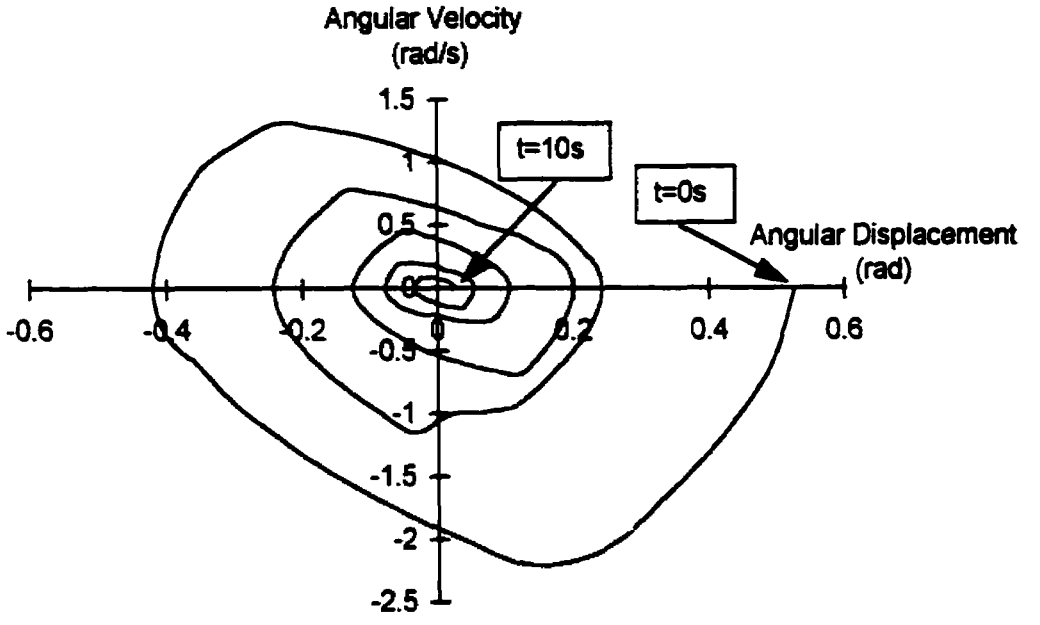

Figure 6.2 Phase plane diagram for a trial of the human controlled simple pendulum system.

The angular displacement and its first time derivative profiles are shown in Figure 6.3. The motion shows a decrease in the amplitude of oscillations and is characteristic of damped vibrations. The angular velocity lags the angular displacement and their profiles remain reasonably periodic and asymmetric. Also, superimposed on this figure is the translational velocity ($\dot{r}$-curve) of the auxiliary mass to illustrate the coordination of the control action with the angular oscillation profiles. The control strategy for attenuating vibrational energy as used for this trial can be deduced by examining the $\dot{r}$-curve. The motion of raising, lowering or holding the auxiliary mass stationary was coordinated with the oscillations of the pendulum. Achieving precision in the mass motion was difficult due to the inherent inefficiencies of the human operator; nonetheless, the mass appears to be moved at extrema in the angular displacement/velocity profiles.

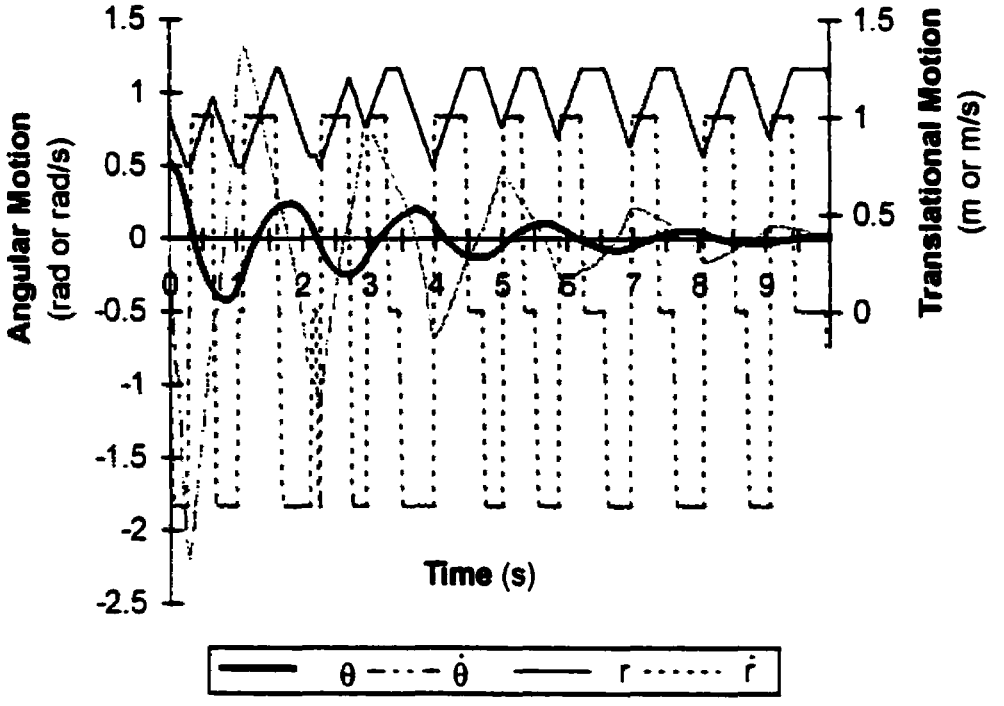

Figure 6.3 Coordinated control action of translational motion of the auxiliary mass with angular oscillations of the pendulum.

For this case, the trend for the total structural energy history followed an exponential decay as shown in Figure 6.4. A characteristic increase in system energy occurred during the attenuation process as highlighted in the insert. The human operator appears to be anticipating the moment at which the mass should be moved towards the pivot. The early raising of the mass increases the total system energy. Based on the first three time periods of the kinetic energy profile, the logarithmic decrement is approximately 0.55.

Based on the first three time periods, the average damping ratio was calculated to be ~0.0411 with a natural frequency of 1.079 rad/s.

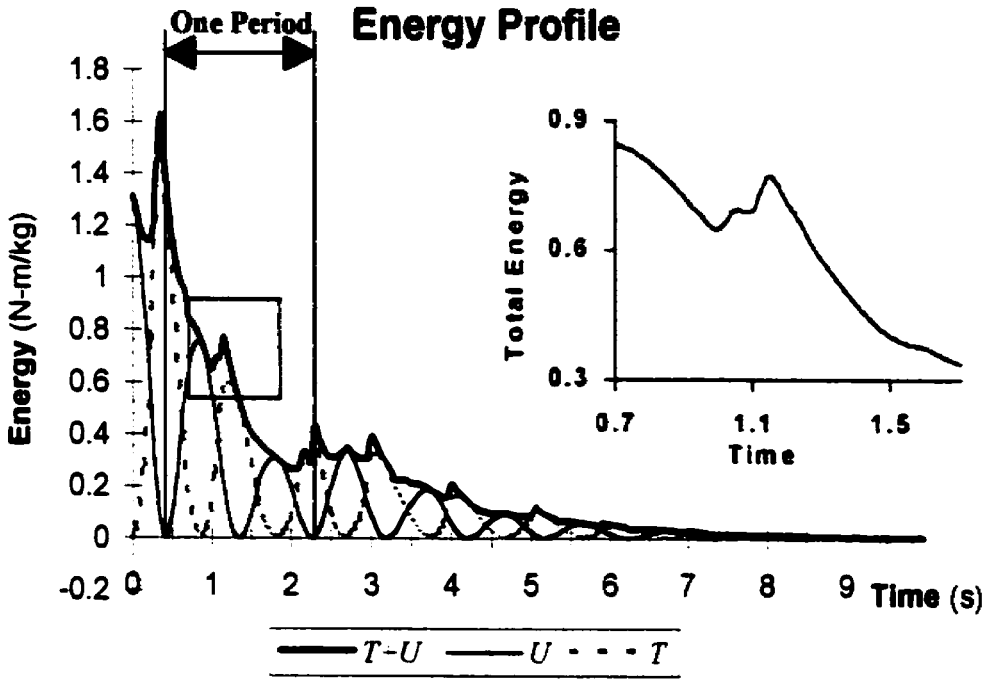

Figure 6.4 Structural energy profile and its components for this human operator control trial .

The influence of the fundamental frequency on the Coriolis inertia force is evident as a net positive and net negative value as coordinated with the gravitational force profile, shown in Figure 6.5 The inertia forces that drive the system are based on the position profiles of the pendulum and the sliding mass. As illustrated, the frequency of the Coriolis inertia force varies continuously and apparently at a higher harmonic of the frequency of the restoring gravitational force. The influence of the fundamental frequency in the Coriolis inertia force is evident as net positive or negative values are synchronized with the gravitational restoring force profile as derived in Appendices B and C.

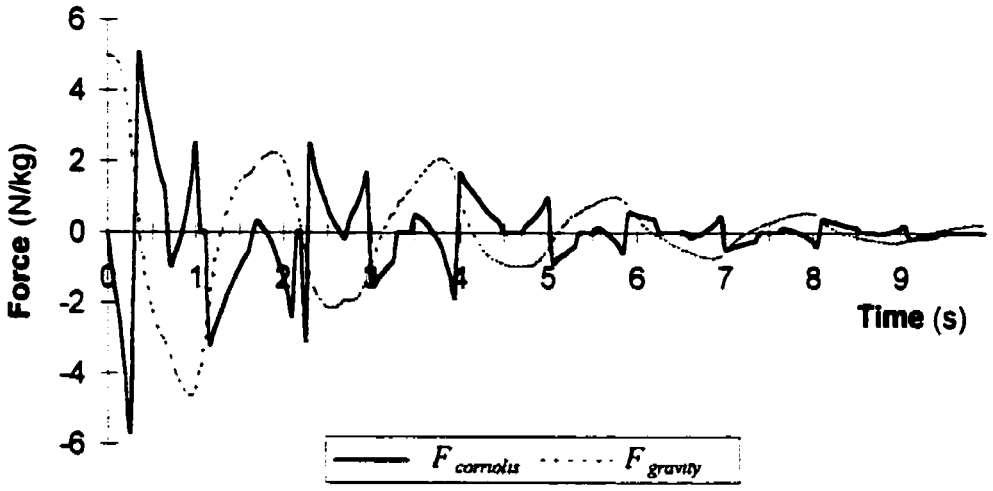

Figure 6.5 Forces driving the angular acceleration of the pendulum under human operator control.

The "instantaneous" damping coefficient, as defined by $2\frac{\dot{r}}{r}$, varies discontinuously producing both positive and negative damping values as illustrated in Figure 6.6. The coefficient has a small mean value.

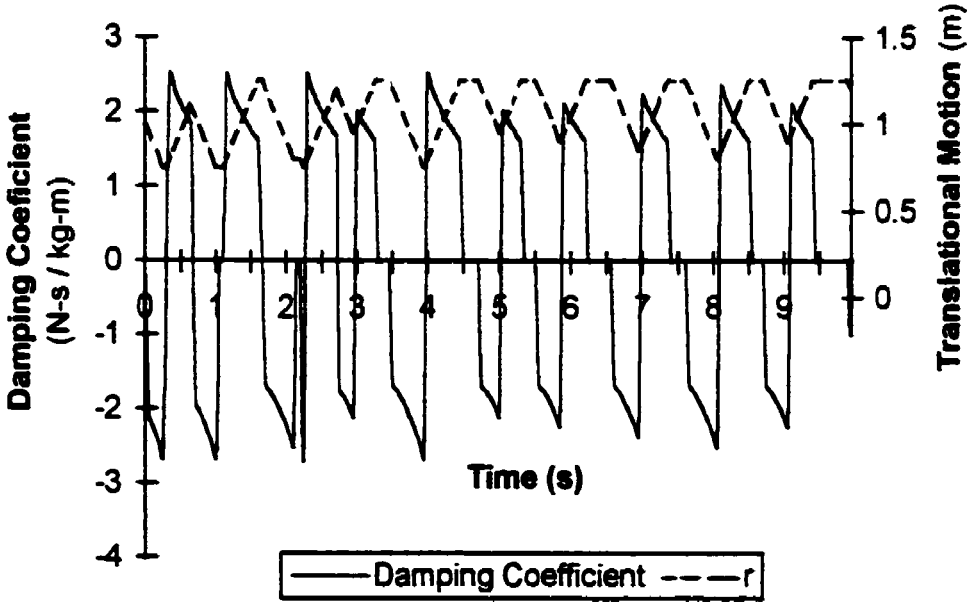

Figure 6.6 Instantaneous damping coefficient produced by the control action from a human operator.

The force in the cable to cause the temporal displacement of the auxiliary mass was also calculated from Equation 2.9. This force along with the translational displacement profile appears in Figure 6.7. The force is periodic with a frequency that is approximately *twice* the frequency of the angular displacement profiles that were previously shown in Figure 6.3. Also, as predicted in Section 2.2, the force is larger when the mass is being lowered than when the mass is being raised.

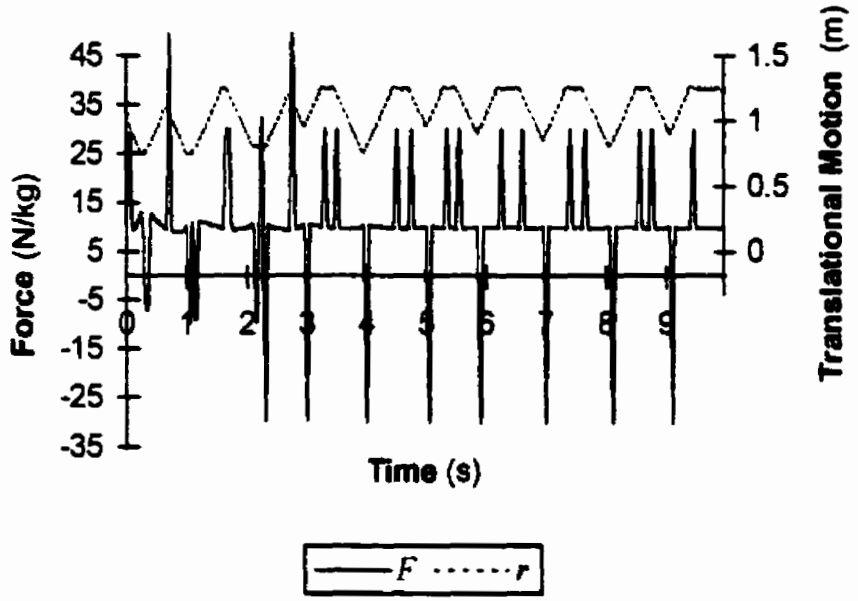

Figure 6.7 Force required to effect motion of the auxiliary mass for vibration attenuation as generated by a human operator.

6.3.2 Analysis and Generalization from Other Trials

Other strategies were also employed to reduce the total structural energy. For instance, when the restriction on mass motion was eliminated, the mass moved towards the pivot until the system gained sufficient energy to circle the pivot. Then, the mass was strategically moved away from the pivot at maximum velocity.

Other observations were made from the various human operator trials. For instance, when the mass motion oscillated closer to the pivot point an increase in the magnitude of damping occurred.

In addition, simulations were altered by selecting different initial conditions and introducing random disturbances during operation. Also, constraints on the motion of the end mass were imposed. Regardless of the changes to these values, with most trials, the human operator was capable of adapting and effecting vibration attenuation.

Under human operation, the system stability was maintained. Despite the imprecision of the control generated by the human operator, stable, energy attenuation of the system was accomplished by moving the mass along the pendulum structure.

6.4 Data Sampling for Future Implementation

The characterizing state parameters of translational and angular displacements and velocities were saved for implementing other control systems, as will be discussed in Chapter 8. These data sets were generated and saved at a frequency of 12.5 Hz.[10]

The data sets characterized control action for attenuating pendulum vibrations. Two data formats were kept. The first data set paired the current state parameters with those at a time increment ($\Delta t = 0.08$ seconds) later; that is, $\theta(t), \dot{\theta}(t), r(t)$ and $\dot{r}(t)$ and $\theta(t+\Delta t), \dot{\theta}(t+\Delta t), r(t+\Delta t)$ and $\dot{r}(t+\Delta t)$ values were incrementally saved. The second data set matched the current state data, $\theta(t), \dot{\theta}(t), r(t)$ and $\dot{r}(t)$ with a corresponding trinomial output that corresponded to raising, lowering or not moving the end mass.

[10] The average period of oscillation for the simple pendulum is 2.006 seconds, or its frequency is 0.499 Hz (see Appendix D)).

6.5 Summary

Through an interactive program, a tool to investigate human control for vibration attenuation through mass reconfiguration of a simple pendulum was developed. A human operator with minimal training demonstrated sufficient hand-eye coordination and reasoning to effectively attenuate the vibrations. The ability to attenuate energy by moving a mass along the pendulum improved with practice and/or the knowledge of the given heuristic of Sections 2.2 and 6.2.

Some very important observations were noted from these trials. The human operator appeared to process position and derivative data of the oscillating system when controlling the system. Also, measures of the structural energy values were available for the user when executing a control strategy for attenuating vibrations. The dynamics as generated from the human controller showed that attenuation could be achieved when the translational mass motion was at twice the frequency of the oscillating pendulum structure. An increased rate of attenuation results when the slider motion was closer to the pivot.

Data characterizing the interaction of motion of the auxiliary mass along the pendulum and data representing appropriate control action were gathered for analysis and future control implementation. This data was to serve as a measure for performance evaluation and as a basis for implementing other controllers.

Despite the inherent inexactness that a human operator possesses, this controller was extremely effective in attenuating the angular vibrational energy of a pendulum structure through mass reconfiguration. The operator demonstrated adeptness in adapting to several trial scenarios.

7. Modified Proportional and Derivative Action Controller

7.1 Introduction

The performance of a continuous signal controller for mass reconfiguration that is based on proportional and derivative action is considered in this chapter. A proportional and derivative control action uses error signals that are measured with respect to the static equilibrium position of zero angular displacement and zero angular velocity. To generate a control signal that fits the control strategy of Section 2.2.2, the proportional and derivative controller was modified by using rectified error signals.

The operation mode of the control system is a feed forward controller that operates in a closed loop as previously shown in Figure 5.5. The current angular displacement and velocity are fed into the controller to generate an error signal for producing the control signal. The control signal is then post processed to effect motion of the auxiliary mass that is used to attenuate the structural vibrations of the pendulum system. Details of the processing are presented in Section 7.2

As with the previous chapter, the purpose of this chapter is to present the dynamic interaction and the attenuation characteristics of this controller with a pendulum structure. The results include structural kinematic and energy temporal profiles, force history curves and damping coefficient graphs. Unless otherwise stated, parameter definitions are as defined in the previous chapters.

7.2 Implementation Considerations

As defined in Section 5.3, the control signal for the modified proportional and derivative action controller was expressed as

$$m(t) = k_p|e(t)| + k_d|\dot{e}(t)|. \tag{7.1}$$

To achieve a control signal that has twice the frequency of the oscillations of the pendulum, the normalized error functions can be used, as defined as

$$m(t) = K\left(-|\tilde{e}(t)| + |\tilde{\dot{e}}(t)|\right) \tag{7.2}$$

where K represents the gain;

$\tilde{e}(t)$, the normalized error function which may be defined as $\dfrac{\theta(t)-\theta_{REF}}{|\theta_{MAX}|}$;

and $\tilde{\dot{e}}(t)$, the normalized error function which may be defined as $\dfrac{\dot{\theta}(t)-\dot{\theta}_{REF}}{|\dot{\theta}_{MAX}|}$.

For the case where the angular motion is sinusoidal at a frequency of ω_n, then $|\dot{\theta}_{MAX}| = |\omega_n \theta_{MAX}|$ and the relation between the "proportional" and "derivative" gains may be given as

$$k_p = -\omega_n k_d. \tag{7.3}$$

Then, the control signal can be processed to drive the attenuation mechanism, the motion of an auxiliary mass. As previously shown in Figure 5.3, the magnitude and sign of the gains alter the control signal. Gains can be appropriately selected so that the control signal is proportional to the velocity of the attenuation device.

7.3 Software Considerations

7.3.1 Simulation Procedure

The control action may be represented by defining the translational velocity of the auxiliary mass, $\dot{r}(t)$, as

$$\dot{r}(t) = k_p|e(t)| + k_d|\dot{e}(t)| \tag{7.4}$$

When calculating the translational displacement for the auxiliary mass, updates were based on assuming constant velocity over the time step, as given by the following equation:

$$r(t) = r(t - \Delta t) + \dot{r}(t)\Delta t \tag{7.5}$$

Next, the displacement constraint of $0.75 \le r \le 1.25\,\text{m}$ was imposed and translational derivatives were calculated using standard backward difference equations.

As given by Equations 7.4 and 7.5, the translational motion of the auxiliary mass is not only time dependent, but also a function of the current angular displacement and velocity. When applying multi-time step initial value solvers, the translational displacement values were updated accordingly. The simulation procedure for the modified proportional and derivative controller is summarized by the flowchart of Figure 7.1. These simulations did not feature a visual interface. The program was typically terminated by defining a set computation period.

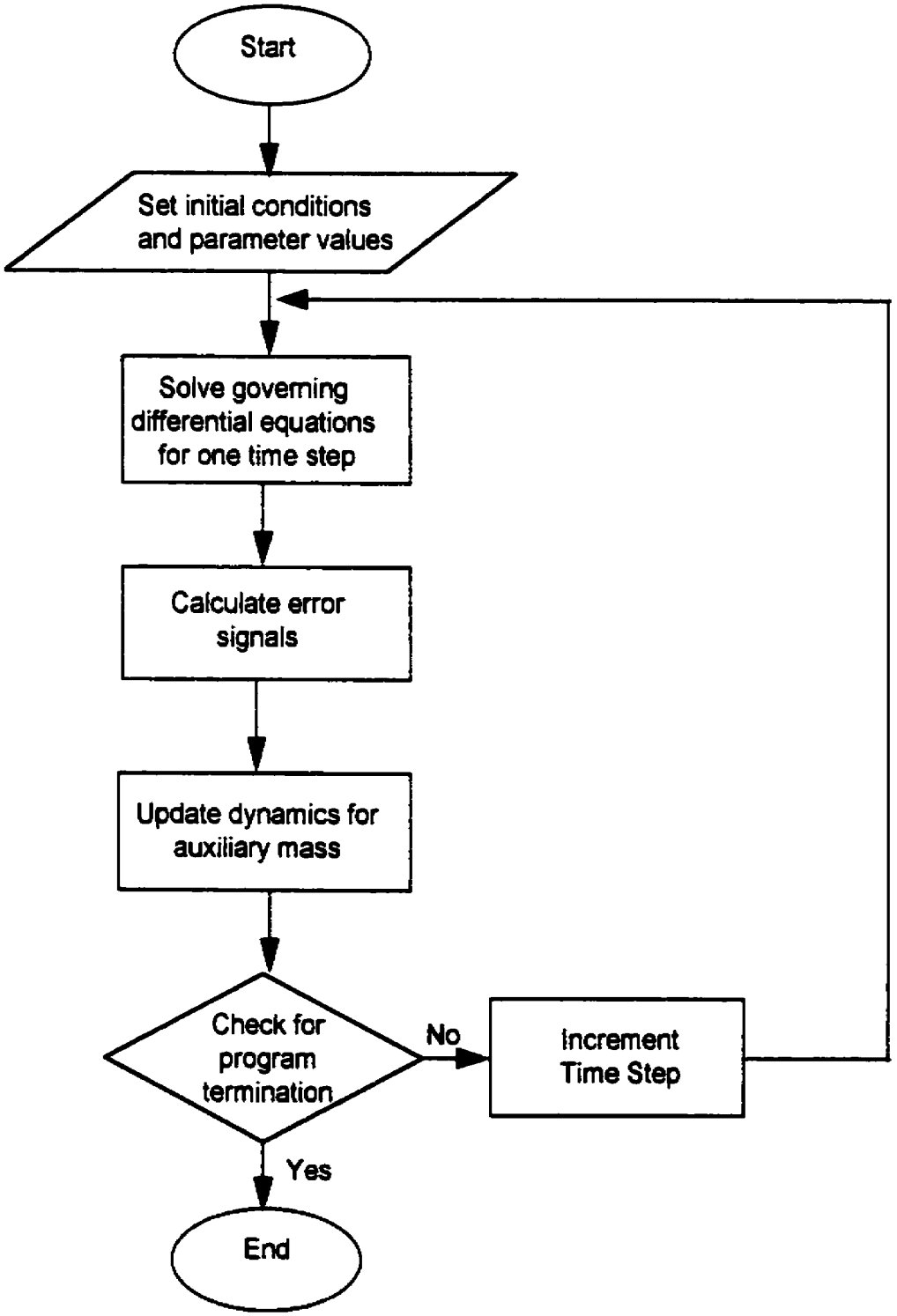

Figure 7.1 Modified proportional and derivative controller flowchart.

7.3.2 Parameterization of Pendulum System for Numerical Simulation

The system being investigated was a physical pendulum whose dynamics were defined by Equations 3.1 and 3.2. The selected parameters included a concentrated mass of 7.5 kg located 1.0m from the pivot and an auxiliary mass of 0.75 kg with a permissible translational range of $0.75 \le r \le 1.25\,\text{m}$. The acceleration due to gravity is 9.81 m/s^2. The simulations were based on an initial angular displacement of 30°. The controller gains were selected to be $k_p = -3.0$ and $k_d = 1.0$. Note that the average natural frequency for this system is approximately 3.1321 rad/s.

The initial value problem solver used a fourth order Runge-Kutta with the time step interval being 0.01s. Simulations were also completed with higher order solvers.

7.3.3. Software Implementation

The simulation software was developed in the C language (namely, Zortech C++[1] and was also compiled using Lattice[2] and GCC[3]). This software had access to floating point utilities. The simulations were performed on a 486 based personal computer.

7.4 Results and Discussions

The analysis of the performance of this modified proportional and derivative controller are made with comparisons drawn to the human control action of Chapter 6. Although maximum energy attenuation may not have occurred for the chosen parameterization, only the first four or five cycles of the pendulum motion are presented in reviewing the dynamic performance of the modified proportional and derivative controller. However, energy profiles

---

[1] Zortech C++ is copyrighted from 1986-89- by Zortech Limited.
[2] Lattice C is copyrighted from 1990-3 by HiSoft and Lattice, Inc.
[3] GCC is GNU FreeSoftware Foundation that is "copyleft".

are presented for longer time intervals to illustrate the controllers performance for an extended period of time.

The first four cycles of motion are represented in the phase portrait of Figure 7.2. In comparison to Figure 6.2, a stable focus also occurs over the shown time interval. This portrait has improved symmetry over the dynamics ensuing from the human operator controller. However the rate of attenuation of the angular oscillations is significantly lower as evident from the temporal angular and translational displacement profiles of the auxiliary mass shown in Figure 7.3. As with the human controller, the coordinated control action of the auxiliary mass has a translational displacement frequency that is twice the frequency of the angular displacement trajectory. Also note that the control action is continuous in comparison to the discontinuous pattern produced by the human operator.

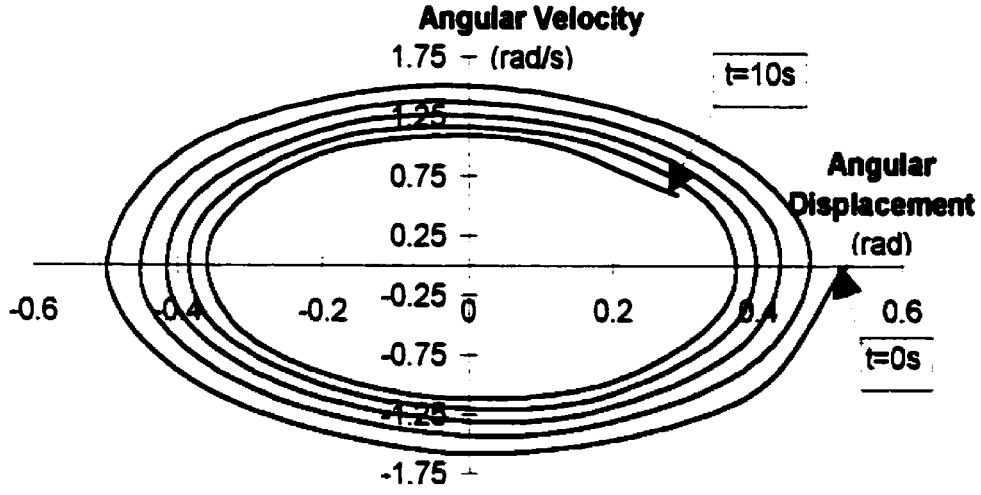

Figure 7.2 Phase portrait of the angular displacement profile with modified proportional and derivative control action.

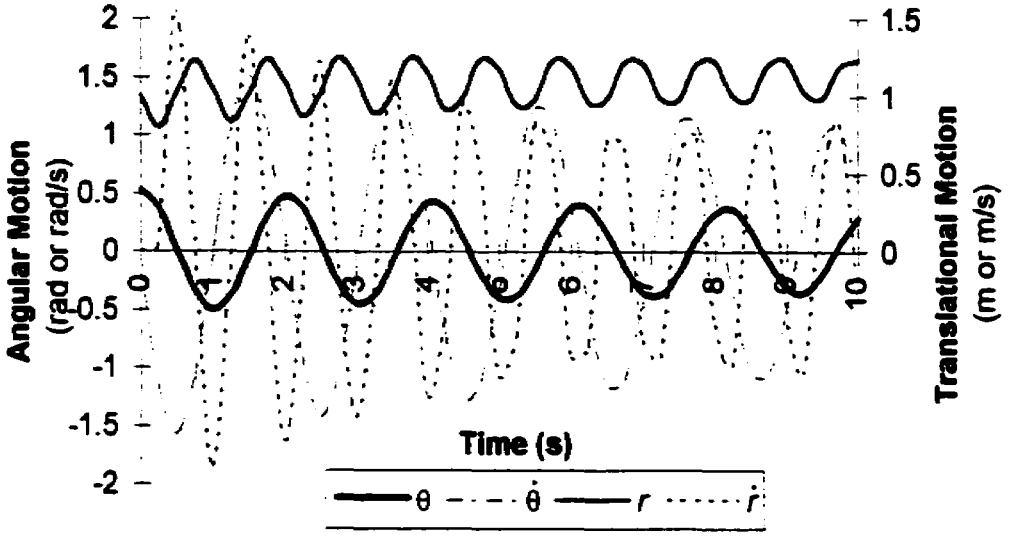

Figure 7.3 Coordinated displacement profiles when using modified proportional and derivative control action.

The energy for the physical pendulum includes both contributions from the structural mass (i.e. the pendulum) and the auxiliary mass (i.e. the slider); the potential energy and kinetic energy have been defined as:

$$U = m_p g l_p (1 - cos\theta) + m_s g(1.25 - r\, cos\theta) \tag{7.6}$$

and

$$T = \frac{1}{2} m_p l_p^2 \dot{\theta}^2 + \frac{1}{2} m_s r^2 \dot{\theta}^2 + \frac{1}{2} m_s \dot{r}^2 \tag{7.7}$$

respectively.

The energy history of Figure 7.4 indicates a logarithmic decrement of 0.114 based on the first three time periods of the kinetic energy profile.

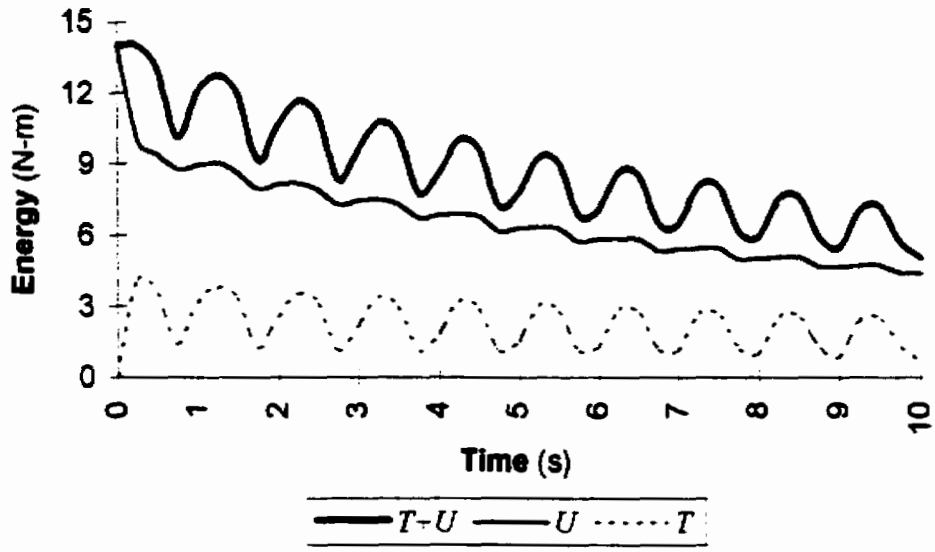

Figure 7.4 Structural energy profiles for modified proportional and derivative control action.

Shown in Figure 7.5 is an extended run using the same control action to illustrate the stability of this control action. The control action remains tuned to the dynamics of the structural vibration as it processes the current structural angular motion to generate the control action. However, due to the variation in frequency between the control action and the vibrations of the pendulum a "beating effect" is observed at periodic intervals. At these instances the motion of the slider is not oscillating at twice the frequency of the pendulum.

Both the damping ratio and the natural frequency vary slightly. Based on the first three time periods of the angular displacement profile, the average damping ratio was calculated to be ~0.0142 with a natural frequency of ~3.090 rad/s.

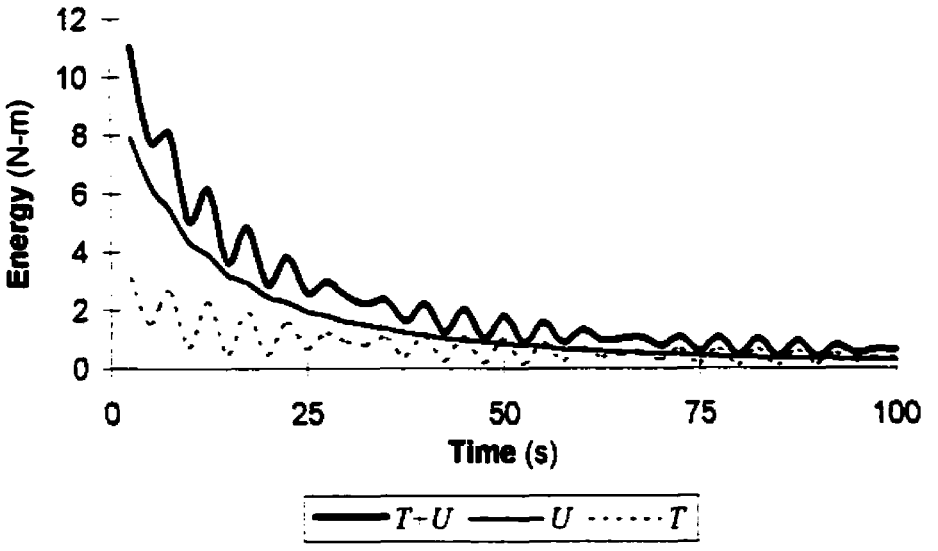

Figure 7.5 Structural energy profiles for an extended period of operation.

The inertia force associated with the motion of the auxiliary mass or slider (Equation 3.5a) and its components are shown in Figure 7.6. The gravitational restoring force and the angular inertia component retain their conservative nature and essentially cancel one another. Thus, the "pseudo-force" generated by the slider consists primarily of the Coriolis inertia force. As with the human operator, the force associated with the slider $p(m_s,\theta,r,t)$ is harmonic and coordinated with the gravitational restoring force of the pendulum, as shown in Figure 7.7. These forces are continuous with the slider force being a higher harmonic of the gravitational force.

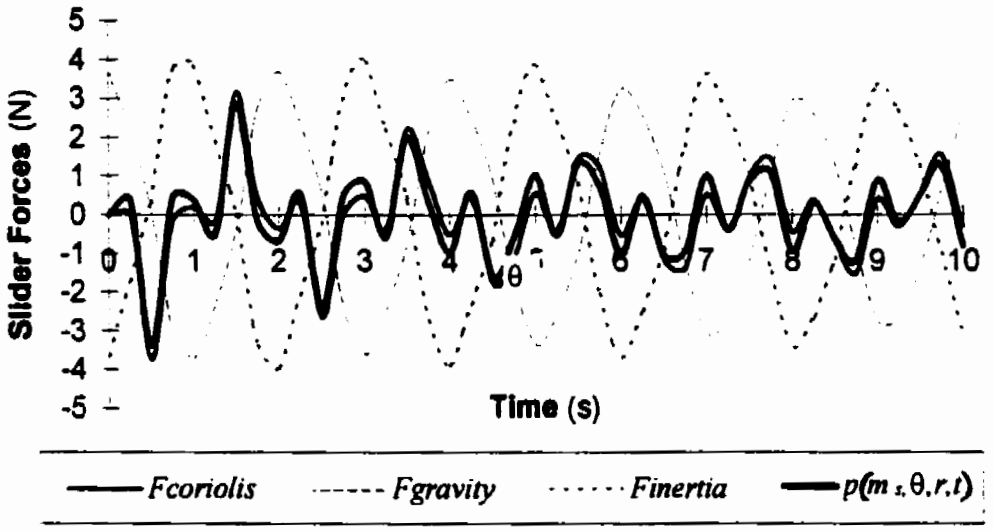

Figure 7.6 Forces associated with the slider when its motion is controlled by modified proportional and derivative action.

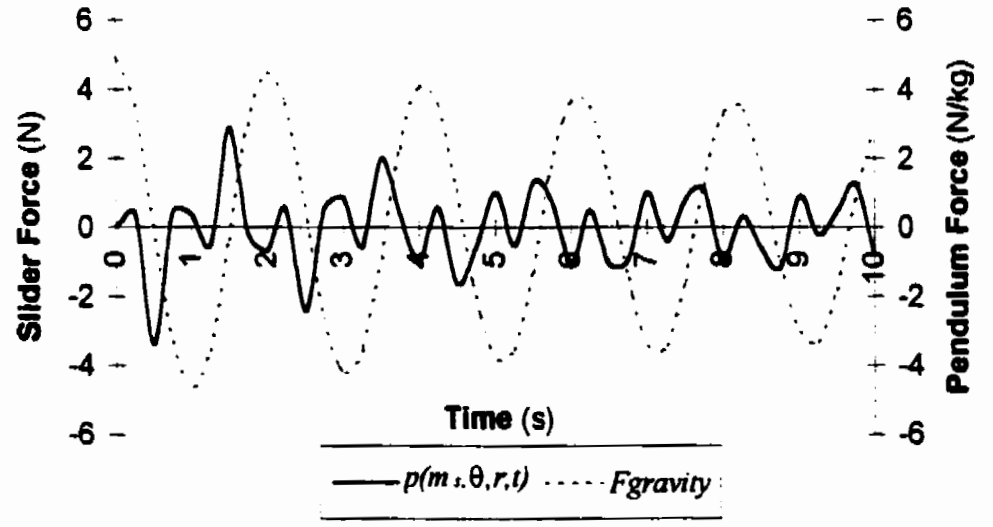

Figure 7.7 Forces driving the angular motion of the pendulum under proportional and derivative control action.

The "instantaneous" damping coefficient varies continuously producing both positive and negative damping values as illustrated in Figure 7.8. Since the motion of the slider is proportional to the rectified value of the error and its derivative, the coefficient is nearly sinusoidal rather than the discontinuous profile produced by the human operator. Since the translational excursion of

the slider attenuates proportionally with the angular oscillations, the damping coefficient is also attenuated.

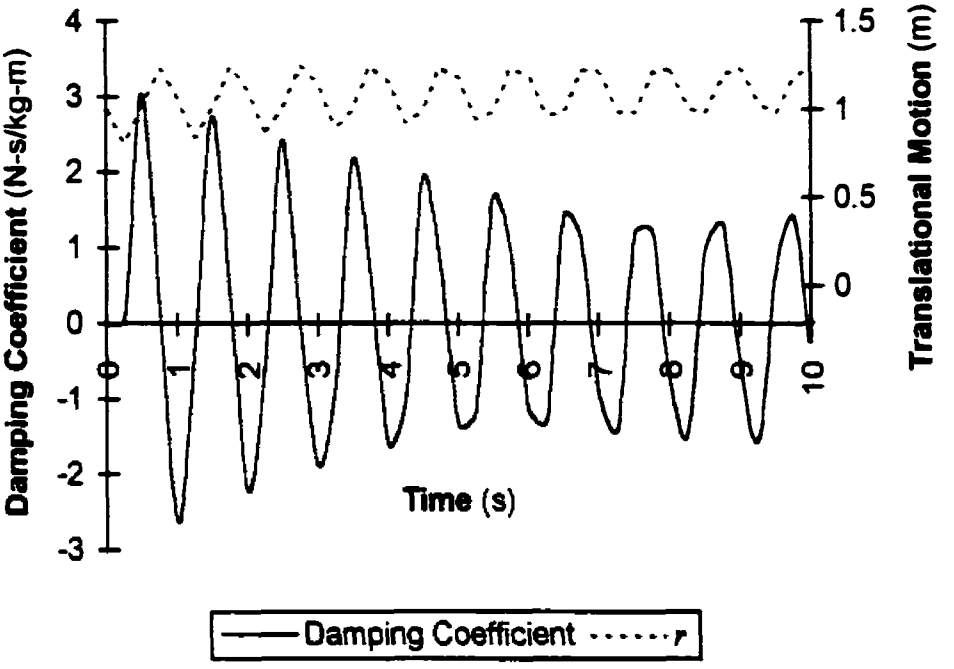

Figure 7.8 Instantaneous damping coefficient produced by modified proportional and derivative control action.

The force in the cable to cause the temporal displacement of the auxiliary mass was also calculated and is plotted in Figure 7.9. The translational displacement profile of the slider has also been superimposed on this graph. Again, the force is continuous and periodic at twice the frequency of the previously shown angular displacement. As shown the force remains negative regardless if the slider is being lowered or raised.

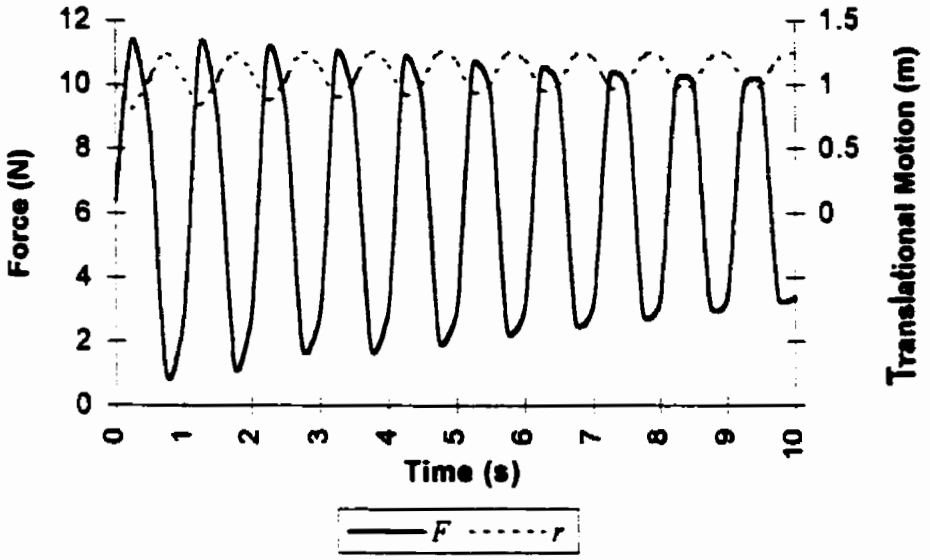

Figure 7.9 Force required to effect motion of the auxiliary mass for vibration attenuation as generated by the modified proportional and derivative action.

To assess the generality of this control action, the simulations were also conducted using various initial conditions. The energy profiles when the initial angular displacement was 60° are shown in Figure 7.10. As expected, good attenuation prevails since the control action is tuned to error signal. Note the chosen gain values may not be optimal for these conditions.

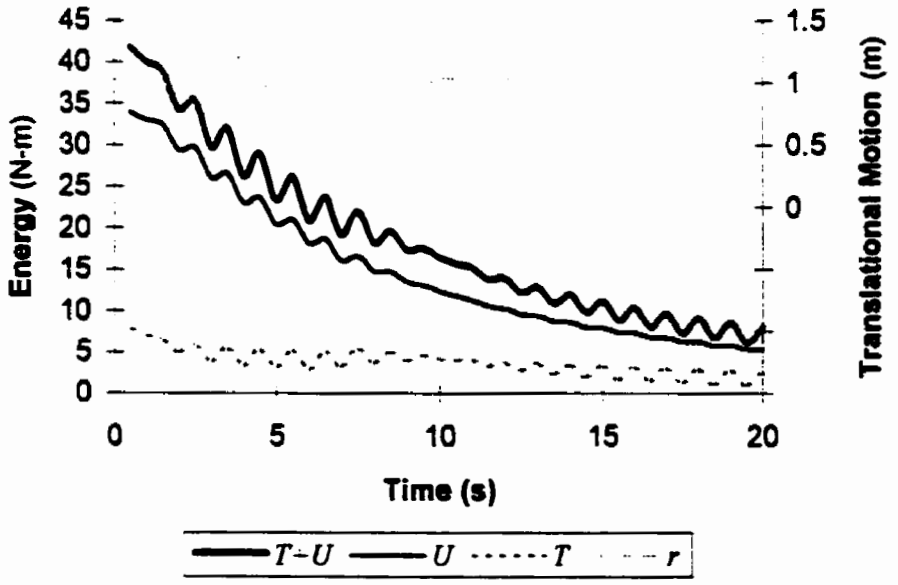

Figure 7.10 Energy profiles when the initial displacement is 60° .

7.5 Summary

The continuous signal provided by the modified proportional and derivative action controller proved effective in attenuating the vibration energy. However, the technique was not as efficient at reducing the structural energy as the relay type of control action provided by the human operator. Again, the effectiveness of the energy attenuation was noted to occur when the translational motion of the auxiliary mass was at twice the frequency of the oscillating pendulum.

8. Artificial Intelligence Techniques as the Controllers

8.1 Introduction

Since artificial intelligence technology seeks to represent human knowledge or expertise, the control strategy for reconfiguring the mass to attenuate vibrations was programmed using artificial intelligence techniques. The techniques used as the control units were knowledge based systems and artificial neural networks.

As shown in Chapter 6, a human operator could effect vibration attenuation for this problem, and the strategy for attenuating vibrations could be postulated as heuristics or rules. A logical advancement was to automate this control by programming these heuristics as the controller; thus, knowledge based systems were applied to automated human control. Essentially, the knowledge based consisted of conditional logic rules that were postulated in various ways. The details are discussed in Section 8.2

An artificial neural network was also implemented as the controller. At the time of its implementation, this was a very novel application of this artificial intelligence technique. The ANN processed input data that represented the kinematic state of the system to generate control action for reconfiguring the mass. Initially, the training process was based on "trial and error" where the system energy was assessed for possible mass reconfigurations. Later, the network was trained to imitate a properly controlled system; that is the network controlled system was a "proxy" of a properly controlled system. Details follow in Section 8.3.

8.2 Knowledge Base Systems as the Controllers

The proposed knowledge based system controller would operate in a closed loop mode (Sections 2.3 and 5.5). The controller would monitor and assess state parameters, then determine the direction for the required auxiliary mass motion for attenuating the vibrations. The upwards and downwards motion for the slider was assumed to be at a constant velocity; this paralleled the action used for the human operator controller. As shown in Chapter 7, the parameters of interest could be based on angular displacement and/or velocity of the pendulum structure.

The knowledge based system quantified the rules associated with moving the mass into conditional logic statements. Initially, these rules contained fixed, predetermined limits for operation based on the angular displacement. The next generation for the knowledge based system was to incorporate a level of variability in the limits. Rather than using preset angular displacement values, one of the conditionals for the auxiliary mass motion was based on angular velocity. To add greater adaptability, the values for the limits defining the conditional statements were matched to the current maximum excursion values. The latter approach required monitoring and updating the maximum angular displacement (and/or velocity) parameters. Hence, the rule base was reposed to be self-adjusting; that is, it possessed a degree of intelligence.

A computer program was developed that integrated the knowledge based controller (the set of conditional logic statements for determining motion of the auxiliary mass) with the dynamic simulations of the governing differential equation for the physical pendulum and slider system. The details of implementing the controller are presented in Section 8.2.1. The results are presented in terms of the angular phase portrait, temporal kinematic profiles, energy histories, force profiles and parameter graphs. The dynamics behavior of the controller is presented for the initial ten seconds. These curves are compared to the results from the human operator controller of

Chapter 6. Also, extended simulation runs illustrating the energy profiles are shown.

The control for the motion of the sliding mass which regulates the interaction between the mass and the pendulum structure was based on current angular kinematics. The data from this rule based controlled simulations was also saved for further analysis and to support implementation of the artificial neural network controller.

8.2.1 Considerations in Developing the Knowledge Base Controller

The controller was to implement the heuristic developed in Section 2.2 and proven to be effective in Section 6.3. The control action can be categorized as:

(a) moving the mass towards the pivot,

(b) moving the mass away from the pivot and

(c) stationary position of the mass with respect to the pivot.

Motion for the mass was arbitrarily selected to be a relay action (see Figure 6.3) which employed constant velocity per time increment as was previously used in the human operator controller. Based on a priori knowledge of the interaction between the auxiliary mass and the vibrating structure, zones for each movement category can be mapped as shown in Figure 8.1. The control logic can be expressed as conditional statements based on the current pendulum dynamics as angular displacement limits, angular velocity limits or a combination of angular displacement and velocity limits.

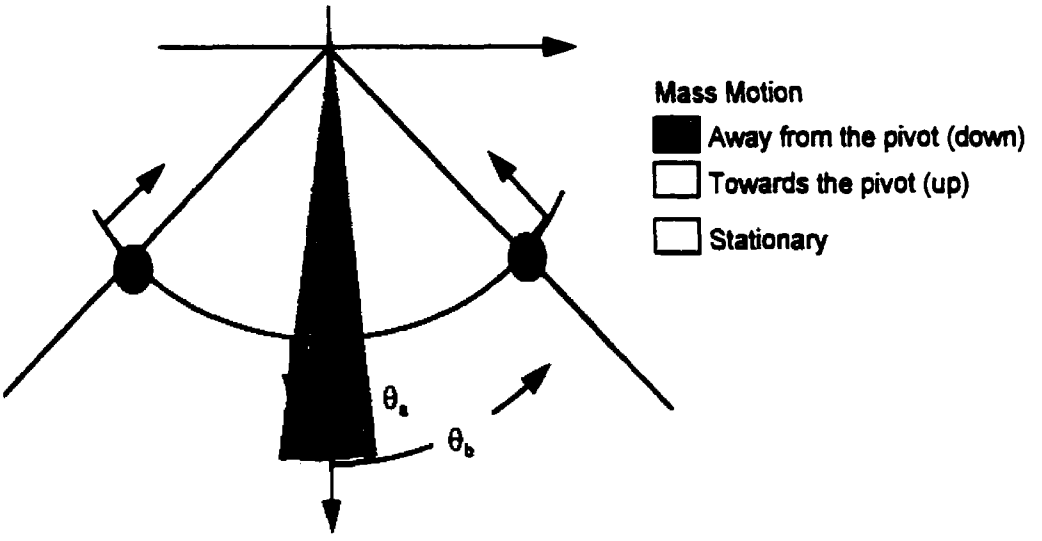

Figure 8.1 Visual representation of heuristic governing the mass motion for attenuating vibrations.

8.2.1.1 Angular Displacement Limits

Initially, quantifying the zones for controlling the mass movement was completed using angular displacement limits, θ_a and θ_b, as indicated graphically in Figure 8.1 and in the algorithm of Figure 8.2. Next, displacement constraints were applied. Afterwards the corresponding translational derivatives were calculated.

Let $\dot{r} = constant$,

If $|\theta(t)| < \theta_a$, then mass is moved away from the pivot;

Else if $|\theta(t)| > \theta_b$, then mass is moved towards the pivot;

Else mass remains stationary.

Figure 8.2 Algorithm for the rule based controller using fixed angular displacement limits.

This algorithm assumes that θ_b is sufficiently less than the maximum angular displacement for the oscillating pendulum. Also, this control

algorithm may possess residual energy. The maximum residual energy of the system can be related to the limit associated with moving the mass towards the pivot, θ_b. The potential energy may be as great as $mgr(1-cos\theta_b)$. Therefore, if the absolute maximum angular displacement of the structure is smaller than the limit, θ_b and this limit is nonzero then the structural vibrations may not be completely eliminated. However, selecting smaller values for θ_b reduces the final energy state of the system, but the rate of energy attenuation will be decreased as shown in Section 8.4.

When implementing this control logic, as stated, downward motion of the auxiliary mass ensues. This feature forces the mass to return to its lowest position and provides additional attenuation in the structural energy, as suggested in Section 2.2.2. Once the pendulum oscillations cease to exceed an amplitude of θ_b; the mass remains stationary until the oscillations are less than θ_a, then the mass moves away from the pivot. Generally, the implementation of the algorithm assumes the zones for upward and downward motion of the auxiliary mass are not coincidental and that $\theta_a < \theta_b$. However, if this condition of overlapping regions do exist, the downward motion will predominated. This ensures the mass returns to its position of lowest potential energy to attenuate the system's energy.

8.2.1.2 Angular Displacement and Angular Velocity Limits

To advance the knowledge based controller, an angular velocity limit was used to determine when the auxiliary mass motion was to be towards the pivot. The value for this limit was based on selecting either a maximum, tolerable, residual kinetic energy level, E_R, for the structure or a permissible angular displacement. Thus, the angular velocity limit could be calculated for the physical pendulum as:

$$\dot{\theta}_{Limit} = \sqrt{2\frac{E_R}{m_p l_p^2}} \text{ or } \sqrt{2\frac{g}{l_p}(1-cos\theta)} \qquad (8.1)$$

As the energy of the system changes, the location where this limit occurs also changes. When initial excess energy exists, the location for mass motion will be away from the vertical, but as the energy is attenuated, the location for mass motion nears the vertical. In other words, the corresponding angular displacement for the limit to determine when motion is towards the pivot will decrease as the system energy is attenuated.

The conditional logic can be formulated as the algorithm given in Figure 8.3.

This knowledge base controller features improved attenuation as the system energy decreases. It may be viewed as approximating nonlinear, proportional and derivative control action and appears to be the *modus operandi* of the human operator as shown in Figure 8.3.

Let $\dot{r} = constant$,

If $|\theta(t)| < \theta_a$, then mass is moved away from the pivot;

Else If $|\dot{\theta}(t)| < \dot{\theta}_b$, then mass is moved towards the pivot;

Else mass remains stationary.

Figure 8.3 Algorithm for the rule based controller using angular displacement and velocity limits.

8.2.1.3 Adjustable Angular Limits

Adaptive parameters/limits that are based on the current state of vibrations creates a continually self-adjusting system. With this controller the residual energy level could be significantly reduced from the former implementations. The updating of limits for the rule base was completed by tracking the maximum angular displacement over a set number of cycles. After each given set of cycles this maximum value was reset so that the current maximum value could be found. The flowchart that incorporates adjusting limits to the changing dynamics is shown in Figure 8.4.

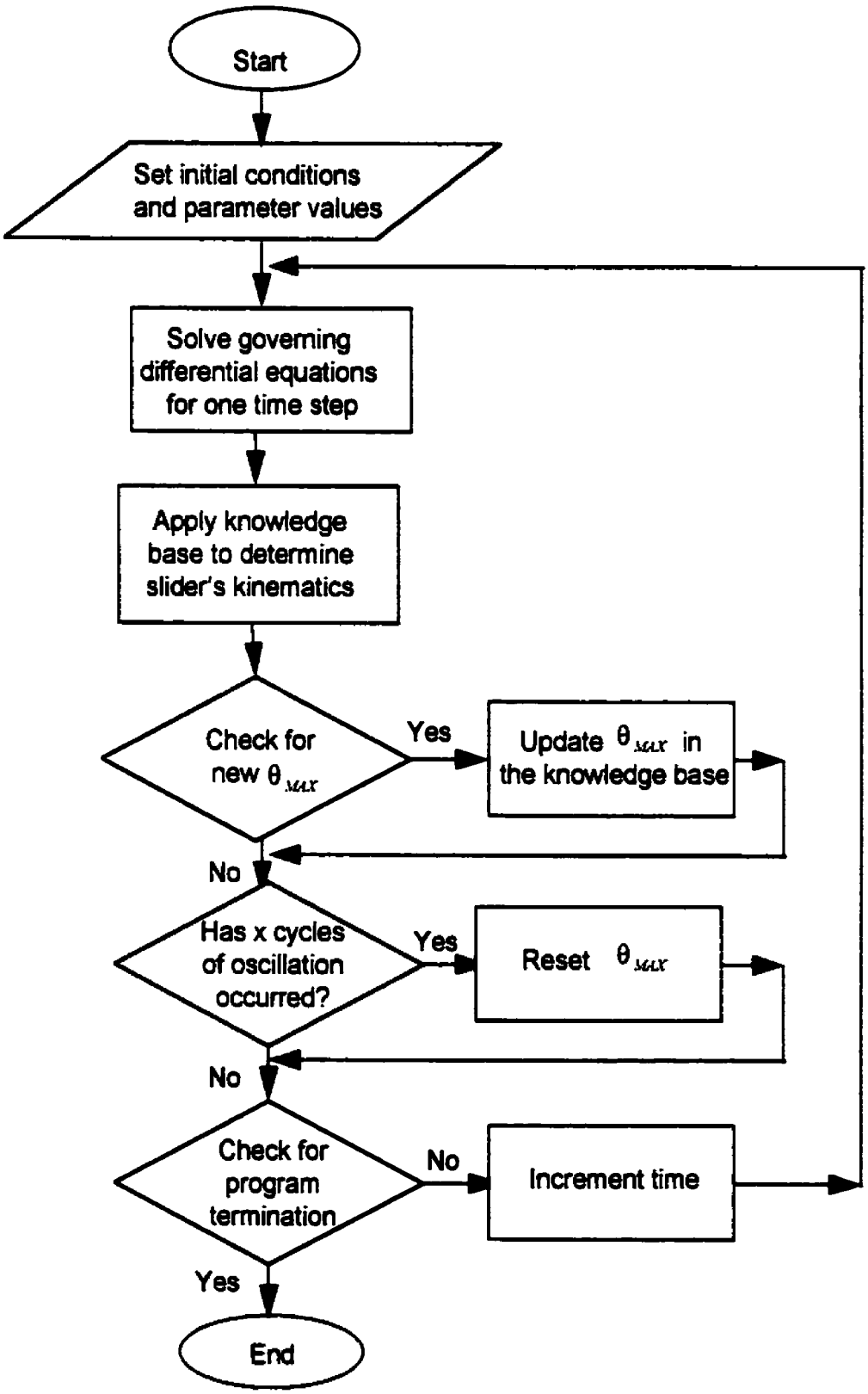

Figure 8.4 Flowchart of the adaptive knowledge based control system.

8.2.2 Simulation Considerations

The physical pendulum system was the selected model for the knowledge base controlled simulations. The parameters were selected the same as those used for the proportional and derivative action controller. Namely, the concentrated mass of 7.5 kg was located 1.0 m from the pivot; the acceleration due to gravity was 9.81 m/s^2; and an auxiliary mass of 0.75 kg with a permissible translational range of $0.75 \leq r \leq 1.25\,m$ was chosen. The simulations were based on an initial angular displacement disturbance of 30°.

The constant velocity for the motion of the auxiliary mass was chosen to match the value previously assumed in the human operator simulation; that is $\pm 1\,m/s$. When the iteration time step was chosen to be $0.01\,s$, this velocity corresponds to maximum acceleration limits of $\pm 200\,m/s^2$. This value has been noted as being unrealistic; however, a comparison among the various displacement profiles can be readily made.

The initial value problem solver was a fourth order Runge-Kutta. Simulations were also completed with higher order solvers. As with the proportional and derivative action controller simulation, when multi-step initial value solvers were used, the translational data for the moving mass were updated for the current angular kinematic data for the intermediate steps.

8.2.2.1 Software Implementation

This particular control system was programmed both in Forth and in C languages. The commercial software used include Forthmacs and Zortech C++, Lattice C and GCC. The hardware platforms were the Atari systems (Section 6.2.1) and personal IBM-compatible computers.

8.2.3 Results and Discussion

The displacement based limits were conducted for a physical pendulum with the results for various limits based on an initial energy of 14.243 N-m being tabulated in Table 8.1. As the limit for motion away from

the pivot decreases the residual system energy is attenuated; however the rate of attenuation decreases. The kinematic results follow for the algorithm of Figure 8.2 where $\dot{r} = 1\,m/s, \theta_a = 0.3060 rad$ and $\theta_b = 0.2959 rad$. These values were obtained using the optimization as discussed in Chapter 4. Next, results when the auxiliary mass motion was based on angular displacement and angular velocity limits are given. These results follow the conditional logic of Figure 8.3 where the optimized limits were 0.1582 rad/s and 0.2442 rad. Lastly, the physical pendulum performance when the limits were adjusted based on the current maximum, angular excursion values where displacement limits for motion towards or away from the pivot were based on 60% and 40% of this value, respectively. These simulations were completed in C. Comparisons are primarily drawn to the human operator control system as this system was intended to be its automated counterpart. Note each technique does provide vibration attenuation.

Table 8.1 System Energy for Various Angular Displacement Limits

Limit for Motion Towards the Pivot		Limit for Motion Away from the Pivot		System Energy (N-m)	
$\%\theta_a$	θ_a (rad)	$\%\theta_a$	θ_b (rad)	$E(t=10s)$	E_{ss} or $E(t=50s)$
0.75	0.3927	0.70	0.3665	6.2922	6.2922
0.75	0.3927	0.50	0.2618	6.2922	6.2922
0.75	0.3927	0.40	0.2094	6.2967	6.2922
0.75	0.3927	0.30	0.1571	8.5009	5.9568
0.55	0.2880	0.50	0.2618	5.7422	3.4084
0.55	0.2880	0.40	0.2094	8.2656	3.4052
0.55	0.2880	0.30	0.1571	10.8261	3.4057
0.35	0.1833	0.30	0.1571	12.2194	1.3860**
0.35	0.1833	0.20	0.1047	13.1790	**
0.35	0.1833	0.10	0.0524	13.8105	**

** Steady state value has not been reached at t=50s.

8.2.3.1 Results based on Angular Displacement Limits

As shown in the phase plane portrait of Figure 8.5, when compared to the human operator dynamics, this knowledge based controller provides more consistent attenuation. However, the attenuation rate is significantly lower than the sample shown in Chapter 6. The attenuation rate is more comparable to that provided by the proportional and derivative controller shown in Figure 8.3.

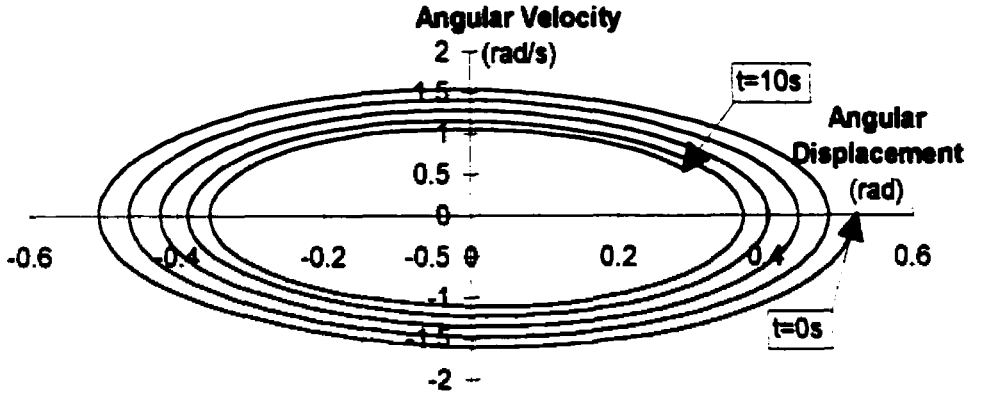

Figure 8.5 Phase plane portrait for the knowledge based control system.

The coordinated angular kinematics and translational motion of the slider are shown in Figure 8.6. The auxiliary mass motion remains coordinated with the angular displacement so that the mass moves towards the pivot near maximum displacement and away from the pivot as the pendulum passes near its vertical. The motion for the slider is discontinuous and the slider reaches its excursion limits.

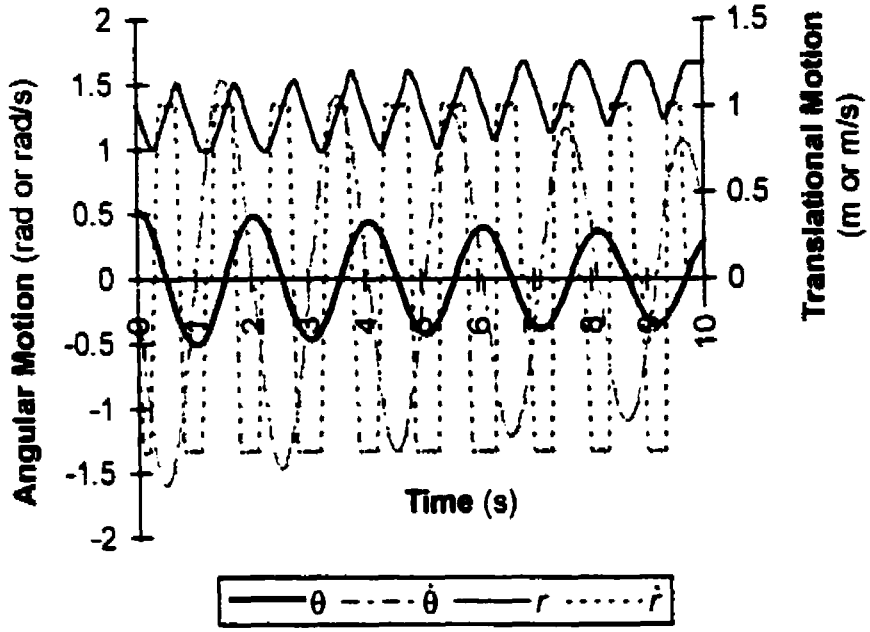

Figure 8.6 The temporal kinematic profiles for the knowledge based controller with angular displacement limits.

As shown by the energy profile of the system in Figure 8.7, the attenuation in total energy is comparable to the proportional and derivative control action and is significantly less than the human operator controller. This controller, unlike the constant frequency, sinusoidal motion described in Section 4.4.2, is stable over an extended period, as shown in Figure 8.8. For this case, the structural energy was attenuated to a residual value.

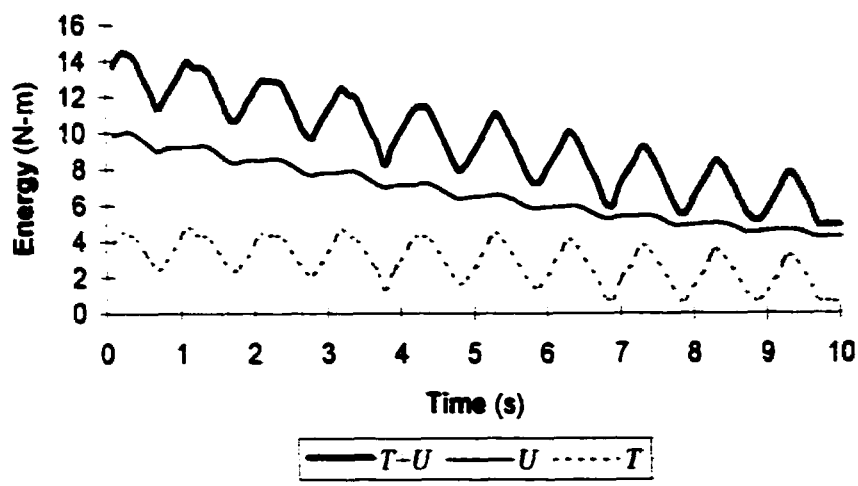

Figure 8.7 Energy profiles with fixed angular displacement limits in the rule base controller.

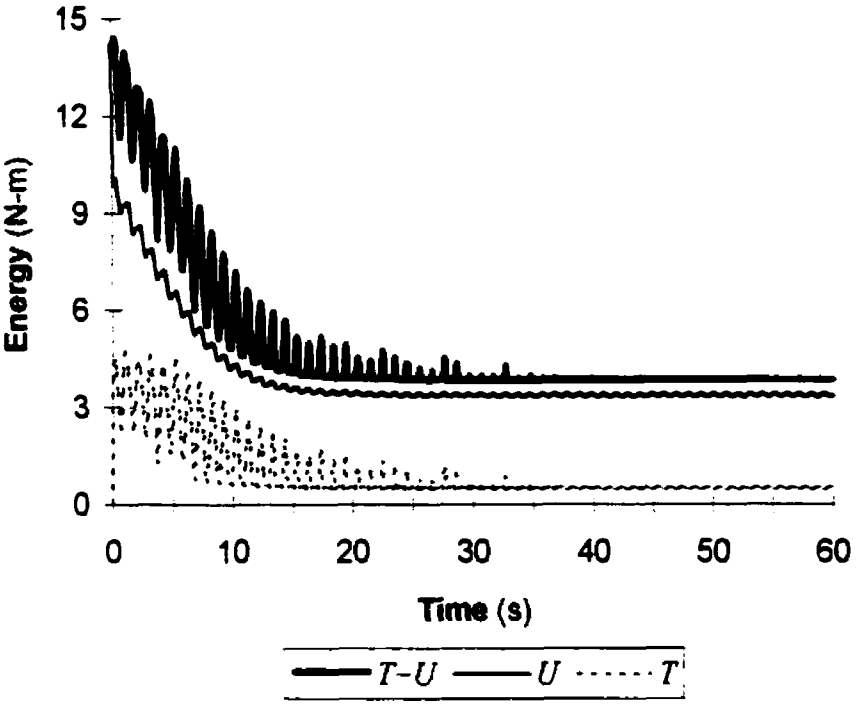

Figure 8.8 Energy profile with the coordinated auxiliary mass motion for an extended simulation period.

8.2.3.2 Angular Displacement and Velocity Limits

The dynamics when the limits for the rule base are based on angular velocity for motion towards the pivot and angular displacement to determine motion away from the pivot are similar to those using angular displacement limits. As shown in Figure 8.9, the phase portrait for the oscillations remains symmetrical.

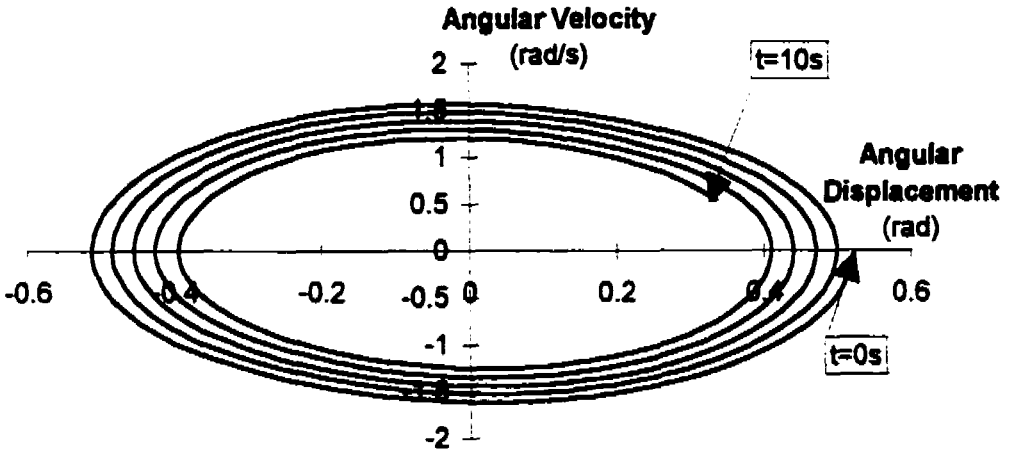

Figure 8.9 Phase portrait for angular motion when the rule base controller has angular displacement and velocity limits.

The coordinated temporal profile is shown in Figure 8.10. The generalization that translational motion of the attenuation device is at twice the frequency of the angular oscillations still holds. The governing rule that auxiliary mass motion away form the pivot occurs when angular oscillations nears the vertical is evident. The primary difference with the previous knowledge based controller is that the angular displacement limit used to determine the auxiliary mass motion towards the pivot varies with the total energy of the system.

The energy profiles are shown in Figure 8.11. Based on the kinetic energy, the logarithmic decrement over the first three cycles of angular motion is 0.03 with this rule base (Figure 8.3).

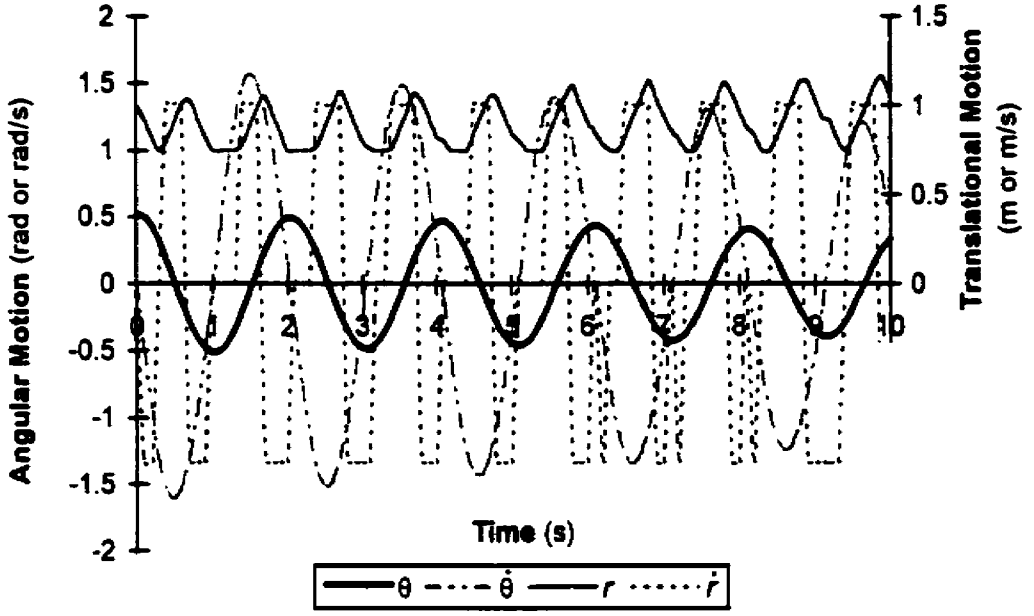

Figure 8.10 The kinematic profiles for the knowledge based controller with angular displacement and velocity limits.

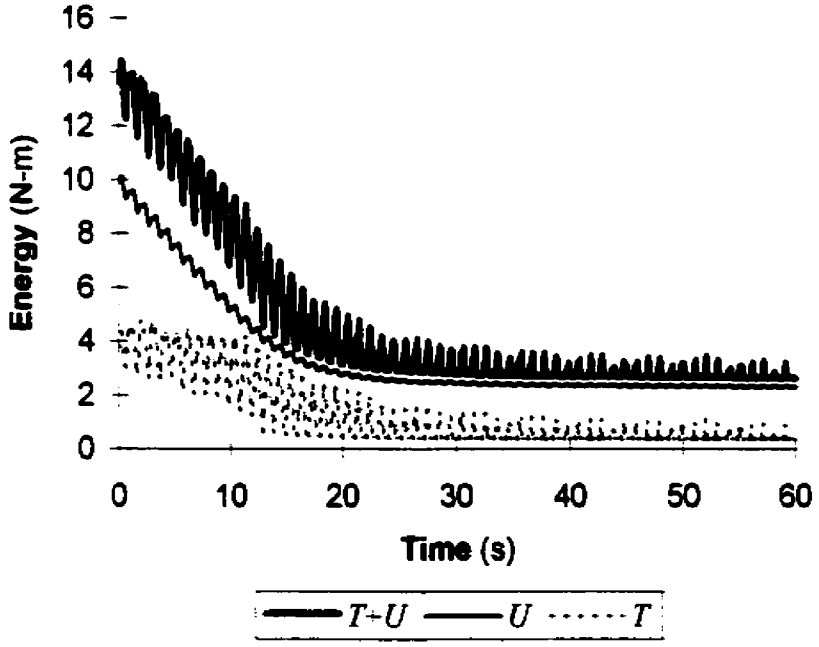

Figure 8.11 Energy profile for the knowledge based controller using angular displacement and velocity limits.

8.2.3.3 Adjustable Limits

The rule base formulated using adjustable limits also produced stable attenuation for extended runs as evident in the phase portrait of Figure 8.12 and temporal energy profiles shown in Figure 8.13.

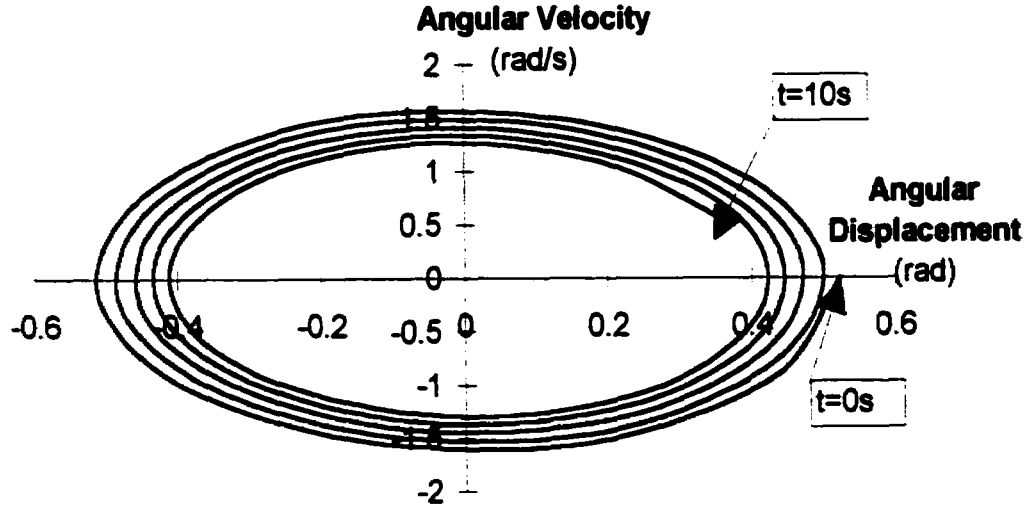

Figure 8.12 Phase portrait for adjustable limit controller.

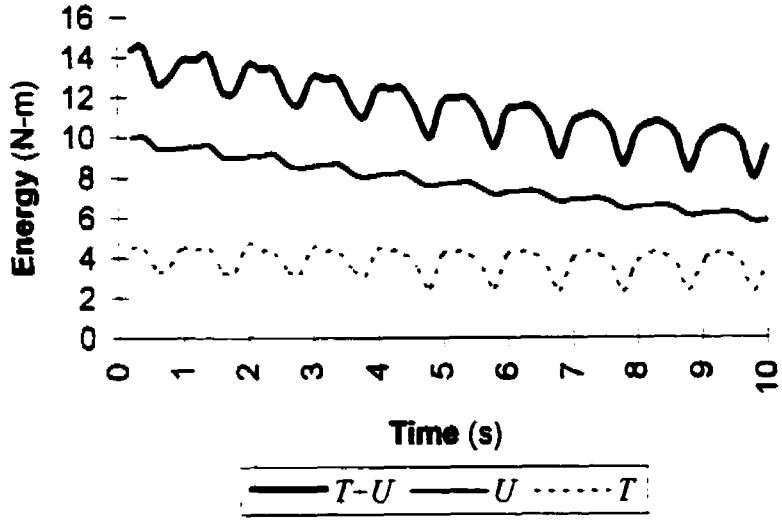

Figure 8.13 Temporal energy profile for adjustable limit controller.

The limits were adjusted every second cycle with limits set at 60% and 40% of the current maximum angular excursion values. The temporal kinematic profiles are illustrated in Figure 8.14, and the dynamics of the limits are illustrated in Figure 8.15. The energy profile has been superimposed on the time-varying, absolute values of the limits that control the auxiliary mass motion.

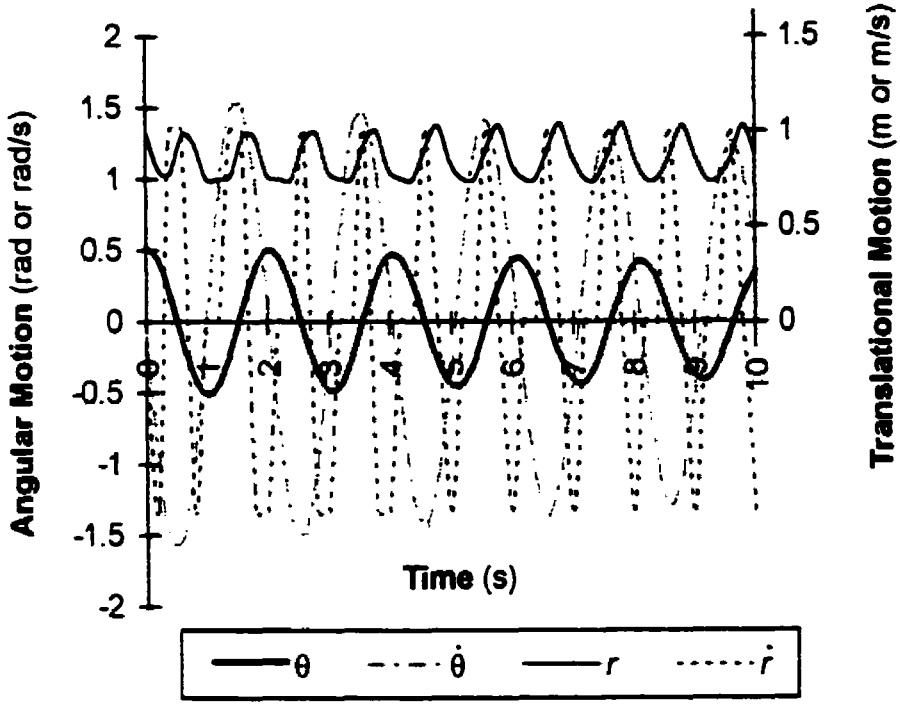

Figure 8.14 The kinematic profiles for the knowledge based controller with adjustable limits.

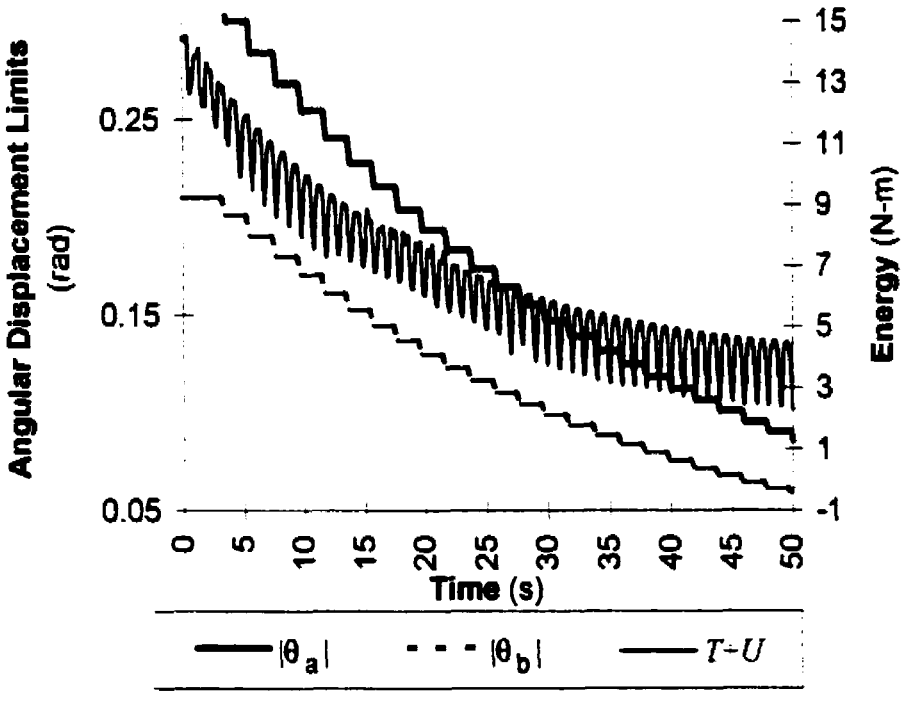

Figure 8.15 Monitoring the limits as the energy is attenuated.

8.2.3.4 Safety Concerns

As the knowledge based system, an application of artificial intelligent technology, was deemed to be an acceptable, autonomous controller, safety concerns related to self-excited parametric oscillations exist. Specifically, the system should not gain excessive energy as had occurred when the auxiliary mass moved sinusoidally at a constant frequency. As shown in Figures 8.7, 8.11 and 8.13 for the case where oscillations ensue from initial displacement of 30°, the rule base controller attenuates the system energy to an acceptable residual value. As shown in Figure 8.16 for various initial angular displacement values of 10°, 60°, 90° and 120°, the adjustable limits rule base appears to respond in a consistent and "stable" manner.

Furthermore, the adjustable limit rule base provides the ability to adjust to disturbances or operating situations in comparison to controllers where the control signal has fixed limits or gains.

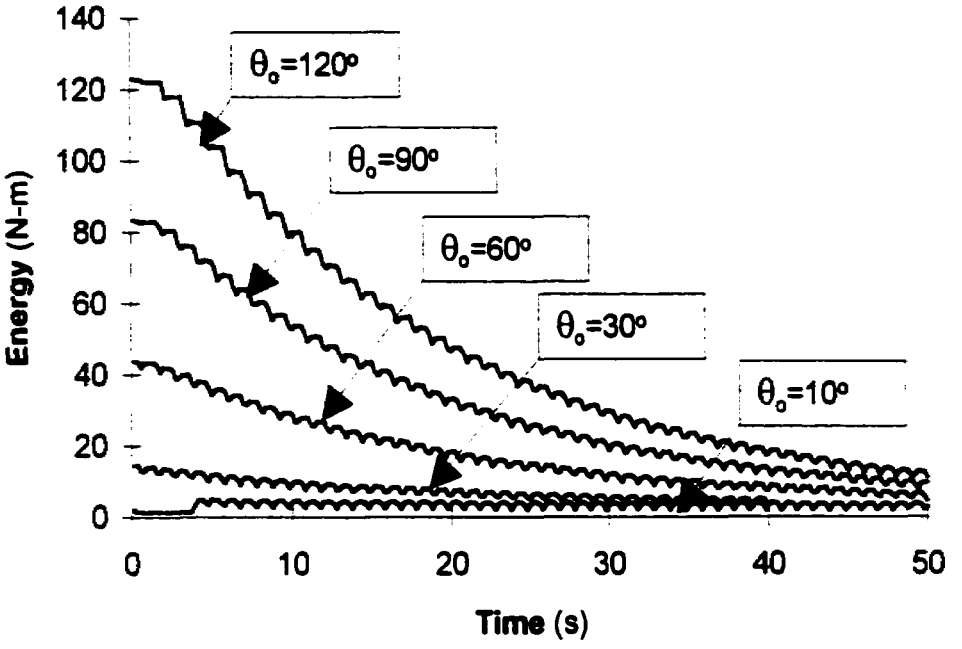

Figure 8.16 Energy attenuation using adjustable angular displacement limits under various initial conditions.

8.2.4 Summary

To summarize, the conditional logic used as the knowledge base controller was based on the current state parameter values of angular displacement and/or velocity. By continually assessing the structural angular dynamics, motion for the auxiliary mass was determined. The slider motion was based on using displacement values corresponding to step increments using velocity values of either 1, 0 or -1 m/s.

Adaptive limits were next incorporated into the logic. By redefining the limits using the current dynamics of the system, an internally self-adjusting controlled system resulted. The controller appears capable of attenuating vibrations for various initial disturbances. Hence by providing the controller with a degree of intelligence through being capable of internally monitoring its state to establish limits proved to be quite effacious for this control problem.

These knowledge based or conditional logic driven controllers operate on the same premise as employed by the human operator; namely, the frequency of the translational motion of the slider is approximately twice that of the angular oscillations of the system.

8.3 Artificial Neural Networks as the Controller

The proposed artificial neural network controller unit was a multilayer, feed forward, static net. The unit operated in the feed forward loop and processed plant dynamics to generate appropriate control action (Figure 5.10). The operation of the controller presented herein imitates another appropriately controlled system. Although during the research, several architectures and control strategies were explored, this section focuses on the architecture and topography of the network used, its training and implementation, along with the control it provided. The net was trainined in an "off-line" mode using a supervisory training algorithm; the training was validated using data generated under the same control conditions as the training data; then the control system was evalued by its energy attenuation.

8.3.1 The Artifical Neural Network

The artificial neural network selected for the controller was a multilayer, feed forward network. The nodal processing capabilities was defined by Equation 5.2 as a summation of continuous, unbounded inputs that were passed through an activation function. The activation function was a sigmoid function that was defined using a hyperbolic tangent function (as given in Appendix K). The nodal output value was a normalized, continuous signal.

The net consisted of fully interconnected neurons between adjacent layers with no interconnections within a layer. The data processing was contiguous as data was processed and passed through consecutive layers and defined by Equation 5.3. The input data consisted of kinematic state

parameters $(\theta(t),\dot{\theta}(t),r(t),\dot{r}(t))$ and each input layer had a bias node with its own set of interconnecting weights.

Two sets of networks were considered with each having two hidden levels of processing nodes.[1] The nets were distinguished by the output parameters used to provide control action. One set had four output nodes *(I-J-K-4)* and the other had three output nodes *(I-J-K-3)*. The first network output was mapped to continuous functions[2] representing the kinematic state parameters $(\theta(t),\dot{\theta}(t),r(t),\dot{r}(t))$ and the latter was mapped to discrete output values ([111], [000] or [-1-1-1]).

The size of the neural net affects its "learning abilities" [Huang and Huang, 1991; Chakraborty and Nuguchi, 1997] and its computational ability [Holler et al., 1988], in other words, its ability to learn patterns, to generalize and to operate efficaciously. When this part of the research was completed very little work had been completed with regards to tailoring and parsimony of networks [Mirchandani and Cao, 1989; Hirose, et al., 1991]; thus, once the net structure was chosen it remained fixed.

To establish the net size, the net was trained using a set of exemplar patterns[3], that modeled the dynamics of a translating mass along the rotating pendulum system. This exemplar data patterns were sampled one simulation time step apart as shown in Figure 8.17. The simulation used random translational motion, $r(t)$ and achieving convergence or reduction in the training error was used as a measure of the success for training this net. This net was trained to represent the system dynamics and was believed to be a superset of the desired control action for vibration attenuation; thus, using the

---

[1] This net was assumed capable of solving complex mapping and had been reportedly applied to decision regions of arbitrary shapes [Lippman, 1987].

[2] To achieve convergence for continuous output either the sigmoid function of the final output layer was omitted or the output data was normalized.

[3] Exemplar patterns refer to paired input-output patterns for neural net training.

same architecture was deemed sufficiently capable of modeling the control problem.

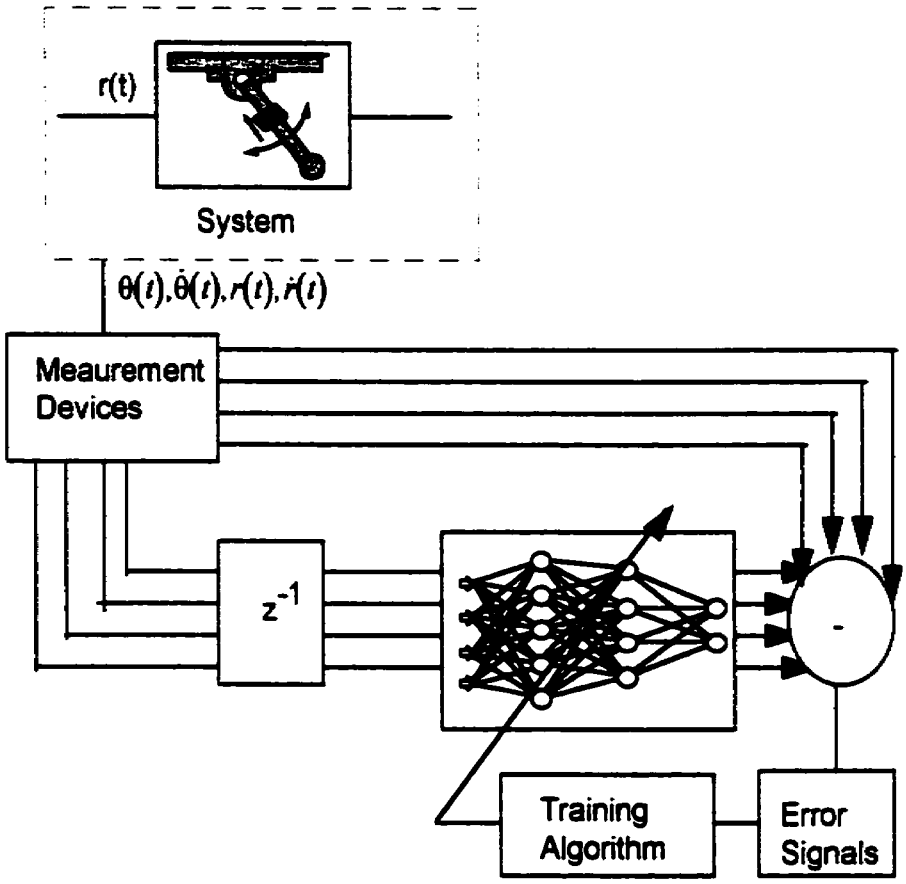

Figure 8.17 Training of the neural network to establish net size.

The selected net had an input layer, first and second hidden layers and an output layer. This structure provided three sets of adjustable weights. The number of nodes in each layer were chosen as follows:

a) input or source layer had 4 nodes (angular displacement and velocity of the structure and the translational position and velocity of the reconfigurable mass);

b) first hidden layer, 13 nodes;

c) second hidden layer, 11 nodes; and

d) output layer, 4 nodes or 3 nodes.

When the neuron or processing nodes of a layer contained a bias or threshold, the number of nodes of the previously layer was effectively increased by one. This representation of the bias/threshold created an internal input node with a preset value of 1; these net architectures can be referred to as either a 5-13-11-4 or a 5-13-11-3 net. (The number of connecting weights were 252 and 241, respectively.)

8.3.2 Training of the Artificial Neural Network

A very important feature of artificial networks is their adaptive nature; they "learn by example" rather than by traditional programming. This process is called "training" of the neural network and is explained in Appendix K. In this thesis, the training paradigm was "supervised"; that is, the net output was compared to a target[4] to generate an error value, and then the weights were adjusted to reduce this difference using optimization techniques as described in Appendix J. By repeated and persistent presentation of exemplar patterns, the net can be trained to respond more efficiently.

Once the neural network was trained using the training suite -- a set of input-output patterns as generated from a controlled system -- the training was validated. The validation process used a set of input-output patterns that had also been generated from the controlled system but was not identical to the training suite. The cumulative error from this validation suite provided an indication of how well the net had "learned" the controlled system of input-output relations. Sample training and validation data suites appear in Appendix L. The final assessment of the neural network was evaluating its performance when implemented as the controller for generating the mass reconfiguration for the system.

Exemplar patterns were sampled while a controlled system operated properly; the data was generated from simulations and were not entrained with artifacts or noise. Regardless of the control system employed (human,

[4] Target values are the ideal or desired output.

knowledge based, proportional and derivative action or otherwise), the training process was illustrated in Figure 5.12. Essentially, the net behaves as a "smart" function generator whereby the state parameters of $\theta(t), \dot{\theta}(t), r(t)$ and $\dot{r}(t)$ served as input and the net generated an appropriate control signal ($m(t)$) based on an output signal that sampled one time iteration, later. The dynamic nature of the problem was incorporated by the selection and sampling process of input-output parameters. By selecting the input-output parameters as state variables of the system, the neural net controller had the standard control signals embedded within the net. To provide time-dependent sensitivity, the parameters included derivative data.

For the tri-state output pattern neural network, additional processing was required. When generating the exemplar patterns the control action was mapped to the target signal. The state data from the system no longer served as output parameters for the network. Also, when operating the net, the output from the neural net controller had to be post processed. The training process is represented in Figure 8.18. This neural net was particularly useful when generic or other control action were to be investigated.

Training was completed for two types of exemplar patterns. One set of exemplar patterns consisting of approximately 80 - 100 patterns that matched temporal kinematic or state parameter data for input and output patterns; the other set matched input kinematic, state parameter data to the tri-state, three value output vector. Typical data as sampled from the human operator controller is provided in Appendix L.

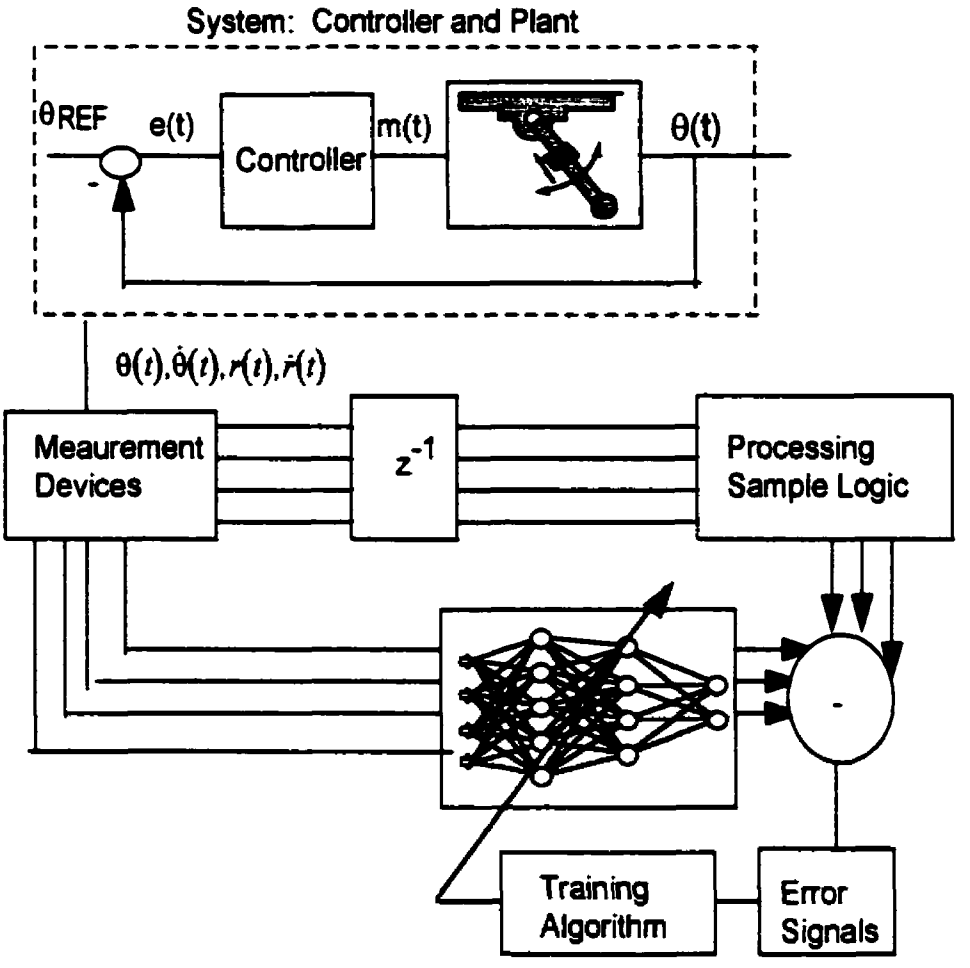

Figure 8.18 Training layout for *I-J-K-3* "proxy", neural network controller.

The training was based on reducing the sum of square of the error between the net generated output vector with the exemplar output pattern over the entire training suite. Figure 8.19 illustrates a typical convergence sequence that was achieved during training using data that was generated for the human operator controlled system. For this particular example, an average error of <1% existed for an exemplar pattern.

The weighting matrices were saved for various training convergence levels. These weights were then accessed to implement the neural net controller for the system.

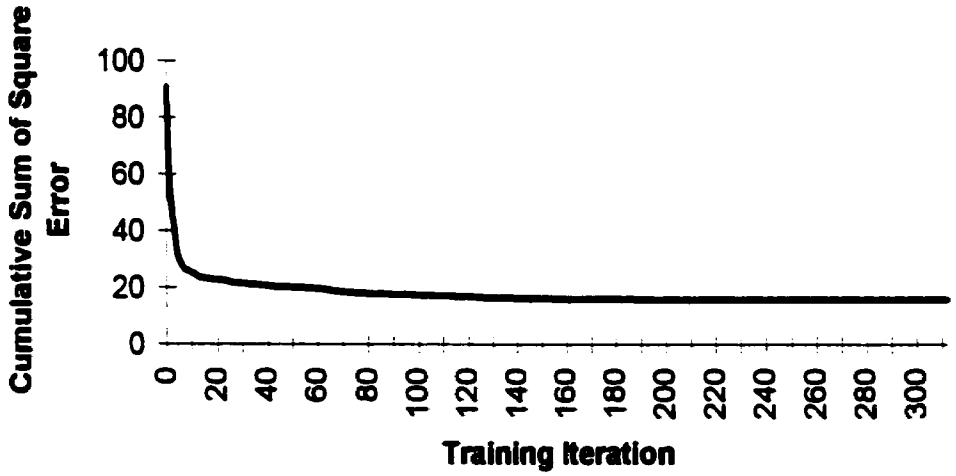

Figure 8.19 Training convergence using a conjugate gradient technique to create a proxy of the human operator controller.

8.3.4 Implementation and Operating Mode

The implementation of the neural network as the control unit involved providing input to the net, calculating the output and post processing the output as a control signal. Assessing the dynamic behavior of the system was necessary to provide input to the network which the net used to generated a corresponding output signal. The output signal was processed and converted to provide the necessary displacement data for the mass reconfiguration. In this manner, the net continually received feed back from the system and processed it to generate control action.

8.3.4.1 Software Considerations and Platform Implementations

Although various optimization routines were developed to train the neural net as discussed in Appendix J, this chapter reports only results trained using the conjugate gradient technique. The software was programmed in the Forth language and run using Forthmacs and GNUForth

compilers. Training was initially completed using the Atari computers and was later redone on IBM based machines.

8.3.4.2 Simulation Considerations

The system being modeled was the simple pendulum with parameters for the system being as previously stated (see Appendix D). As an example, the controlled system was based on imitating the control action of the rule based controller which implemented the conditional logic based on fixed, angular displacement limits, as described earlier in this chapter. Another example was to be a proxy to the human operator controlled system as reported in Chapter 6.

8.3.4.3 Implementation of the Neural Network as the Controller

In implementing the neural net controller for the system, the current kinematic state parameter data was passed to the neural net controller. This data served as input for the neural network. Essentially, the simulation of the neural net controller was a series of matrix computations as given by Equation 5.3. The post processing converted the net output to suitable translational dynamics to be processed by the next iteration of the simulation process for determining the angular oscillations of the pendulum.

Depending on the net architecture, (*I-J-K-3* or *I-J-K-1*) the output values require different processing prior to being fed to the control mechanism (or simulation package that implements the control action). For the *I-J-K-1* network, the output nodes corresponding to the translational velocity of the attenuation mechanism required only a unity gain as the post processor, as the value was readily incorporated into the simulation package of the controlled system. The translational position and acceleration for the auxiliary mass was calculated using finite difference equations; these values were also returned to the simulation program.

For the discrete, three node output network the patterns were matched to the three possible modes of control, namely, moving the mass towards the pivot [-1-1-1], no motion of the mass [000] and moving the mass away from the pivot [111]. The magnitude for the incremental motion, Δr, is based on the mass velocity, $\dot{r}$, and the selected time step, Δt, as discussed in the implementation of the various control systems. The net output was then combined using a "winner-takes-all" principle as defined by

$$z = \frac{1}{L}\sum_{l=1}^{L} y_l$$

$$\begin{aligned} &\text{if } z \le z_a && \text{then move the mass towards the pivot,} \\ &\text{if } z_a < z \le z_b && \text{then no control action is taken, and} \\ &\text{if } z_b < z && \text{then move the mass away from the pivot.} \end{aligned} \tag{8.2}$$

where z represents an averaged output that is compared to the defined limits of z_a and z_b.

This architecture provided improved implementation flexibility as the net generated control output may be matched to a variety of movement profiles for the attenuation device.

The neural net controller was accessed for each time step of the simulation where the angular displacement of the system was then calculated and returned to the controller.

8.3.5 Performance Results for the Neural Network Controller

Good energy attenuation was achieved for various "proxy" neural networks. Regardless if the net was trained using kinematic or tri-state output values, appropriate control action was generated by the neural net controller.

The tri-state output was easily mapped to a relay action for mass reconfiguration and tended to convert other control action to this type of control. A more complex post processing of the neural net output was necessary to generate non-relay action. The tri-state output was a more

flexible system allowing deficiencies in training to be corrected through redefining limits in the post processor.

Despite the net being trained on a subset of the controlled operation, yet accessed more frequently during the controlling of the pendulum system, the neural net controller provided appropriate control action. The neural net controller appeared able to interpolate control action for system kinematic states for which it had not been explicitly trained.

A sample energy profile for the "proxy", neural net controller of the knowledge based system that used fixed, angular displacement limits in its rule base is shown in Figure 8.20 [Stilling, 1991]. The time axis has been normalized with respect to the average period of the structure and the system energy has been normalized with respect to the moving or end mass. The performance of the neural network exceeded the original rule base system that it was to imitate. For each energy profile, the system was initiated with an identical disturbance that corresponded to 8.50 N-m/kg or an initial angular displacement of 30°.

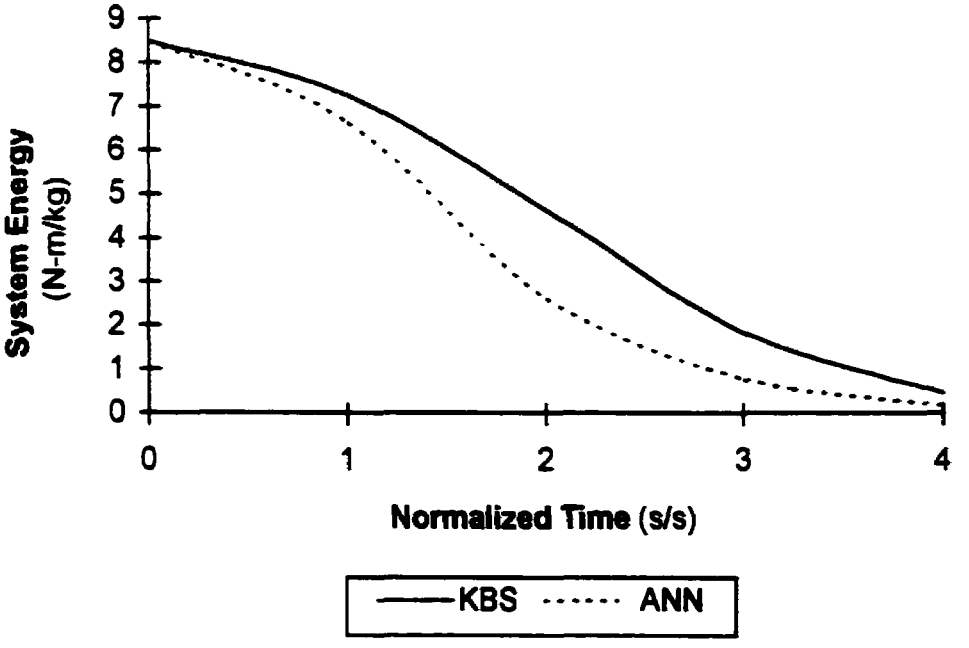

Figure 8.20 Comparison of energy attenuation for the rule based controller and the "proxy", neural network controller.

The extrapolation ability of the neural network was evaluated by presenting the "proxy", neural network controlled system with conditions that were not included in the training suite. Specifically, initial conditions that corresponded to an initial angular displacement of 15°, 45°, 60° and 90° were simulated. Energy attenuation was observed for each case with the most efficient energy attenuation occurring when the disturbance lied within or was near the condition that the net had been trained with.

8.3.6 Summary

The artificial neural network was capable of performing autonomous control for vibration attenuation. Energy attenuation appeared stable for long simulations. Also, the trained net could be applied to other initial conditions. For the example given, the rate of energy attenuation was an improvement over the system being used as the model. Controllers trained using the tri-state output had additional flexibility as the post processing allowed limits to be placed on the norm of the output that would correspond to various mass movements.

9. Summary, Conclusions and Recommendations

9.1 Summary and Discussion

The development of the concept of mass reconfiguration for structural vibration attenuation was investigated. This vibration attenuation concept was applied to pendulum structures whereby mass reconfiguration was achieved by a radially, translating mass along an oscillating pendulum. The control strategy was implemented as mass reconfiguration displacement profiles using various types of controllers. Numerical simulation and optimization techniques were applied to investigate this problem.

First, the physics associated with a moving mass along a rotating system was presented. The rotational and translational motion of the auxiliary mass gives rise to the Coriolis inertia force which affects the angular motion of the pendulum system. This Coriolis effect can be viewed as producing positive or negative damping. Specifically, when the mass is moved away from the pivot, the Coriolis force opposes the oscillatory motion and acts to decrease the oscillation amplitude. In contrast, when the mass is moved towards the pivot, the Coriolis force acts with the oscillation motion and will increase the amplitude.

For the systems as studied, the mass must remain in contact with the structure which leads to assuming a cyclic motion. For cyclic mass motion, the angular displacement is periodically increased and decreased. As the structure vibrates, the magnitude of the Coriolis force varies. To achieve vibration attenuation over a cycle of the structural oscillations, the mass should be moved towards the pivot when the Coriolis force is small, thereby minimizing the increase to the rotational oscillations; then, the mass should

be moved away from the pivot when the Coriolis force is large, thereby maximizing the decrease in the oscillations. In terms of the angular excursion and/or velocity, this control logic is postulated as:

1) the auxiliary mass is moved away from the pivot when the angular velocity and the Coriolis force are maximum which occurs when the pendulum nears the vertical, and

2) the auxiliary mass is moved towards the pivot when the angular velocity and Coriolis force are minimum which occurs when the pendulum nears its maximum angular excursion.

Alternately, the physics associated with mass reconfiguration can be understood by examining the work-energy balance from the interaction. Moving the mass towards the pivot generates positive work since the force to cause this motion is in the same direction as the motion which increases the system energy. Conversely, moving the mass away from the pivot produces negative work as the force to cause this displacement is in the opposite direction as the motion which decreases the system energy. As the system oscillates, the magnitude of the force to cause mass reconfiguration varies. Therefore, a strategy for periodic motion of an auxiliary mass to cause attenuation can be deduced which parallels the above logic; namely, motion of the mass occurs during the turning points in the angular oscillations.

Next, a mathematical model was developed to represent the mass reconfiguration for pendulum structures. Internal and external damping factors were neglected to accentuate the attenuation effects by mass reconfiguration. Then, simplifications to the governing equation enabled parallels to be drawn to the Mathieu-Hill equations, where regions of stability and instability were identified. Specifically, harmonic motion at twice, nine (9) and sixteen (16) times the natural frequency were examined. Predicting the dynamic behavior for the simple structure of a pendulum with reconfigurable mass was shown to be quite involved.

Through extensive computer modeling and simulations, the dynamics of the mass-pendulum system were investigated. The auxiliary mass displacement profiles that were examined were periodic (Equations 4.14a to 4.14d) and the mass motion was restricted (Equation 2.11). The profiles, which satisfied the proposed control strategy for achieving vibration attenuation, included:

1) continuous, harmonic motion using fixed frequency and phase,

2) relay action using piece-wise "constant velocity" motion that was based on the current, structural angular displacement and/or velocity, and

3) motion based on modified proportional and derivative action of the structure.

Based on the sinusoidal motion (Equation 4.10), the optimization of the parameters regardless of the optimization period approached twice the natural frequency of the system ($n = 2$). Attenuation initially occurs when $\phi = 0$. As shown by the optimization results (Table 4.6), the phase shift varies with the period of optimization. Since the mass motion affects the natural frequency of the structure (Figure 3.7) and causes damping, a variation between the frequency of the angular oscillations and the mass motion results. This frequency variation resulted in a "beating phenomena" (Figures 4.13, 4.15 and 4.19). Thus, the displacement profile of the mass must be properly coordinated for the time period of interest.

An improvement to this displacement profile that retained the sinusoidal characteristics was proposed. The frequency of the mass motion was tuned to the frequency of the system. This profile was defined as:

$$r(t) = R_o - \Delta r \sin\left(2\omega(t) \cdot t\right) \text{ where } \omega(t) = \sqrt{\frac{g}{r(t)}}.$$

This tuned displacement profile produced continual, parametric attenuation (Figure 4.21).

The relay action using piece-wise, "constant" velocity also produced good attenuation. The velocity was selected to be -1, 0 or 1 m/s. The structural dynamics did not exhibit beating effects; however, depending on the parameterization of the control logic, residual energy remained. Also, the simulation process defined the transition between velocity states; that is, the acceleration of the translating mass was defined by the time step of the simulation. As the time step was decreased, the acceleration of the translating mass had the potential to become physically unattainable. The control logic to select the mass motion was formulated using various logic paradigms and structural angular displacement and/or velocity limits as presented in Chapter 4. Also, the parameter limits were optimized for various time intervals (see Tables 4.5, 4.6 and 4.7). As the time interval was lengthened, the magnitude of the residual energy was reduced, but the rate of energy attenuation was decreased.

To enhance the attenuation of the structural energy, the conditional limits were made adjustable as was presented in the controlled system (see Section 8.4.3). This technique capitalized on the fast attenuation rate without high residual energy levels remaining.

The displacement profile based on modified proportional and derivative action was considered in Chapters 4 and 7. This profile provided a more continuous action than the relay technique and avoided discontinuities that produce high acceleration values for the auxiliary mass. The parameters (or gains) for the mass displacement profile when optimized accounted for the fact that the damped natural frequency was lower than the natural frequency of the system. Good vibration attenuation was also achieved using this displacement profile.

Several profiles for mass reconfiguration were formulated and proved effective in providing structural vibration attenuation.

Integrating the mass reconfiguration with the pendulum structure produced the control system. The fundamental requirement of the controlled system was to attenuate vibrations. Multiple input, closed loop controllers were considered. Other desirable requirements that were identified included being general purpose, adaptive with learning capabilities and being autonomous. The identified input parameters were the temporal angular displacement of the structure and/or the temporal translation of the reconfigurable mass. Uniquely, the controllers embedded the standard input signals which the controller internally generated to produce the control signal that defined the sliding mass motion. The control systems presented included a human operator controller based on a relay mass reconfiguration profile, a modified proportional and derivative controller using proportional and derivative action, a knowledge or rule based controller using a relay mass reconfiguration profile, and an artificial neural network trained to imitate a proven, effective reconfiguration control strategy. The effectiveness of each control system reflected the mass reconfiguration strategy that was implemented. A summary of the mass reconfiguration strategy and the corresponding controller implementation(s) appears in Table 9.1.

Neural networks were selected as a controller due to their originality and learning capabilities; at the initiation of the project, the nature of the problem was not well defined. The development of artificial neural network was in its infancy at the time of implementing this control system. The selection of the net was a feed forward, multiple layer net. The net was made time-sensitive and time-dependent by selecting input-output parameters that contained time derivative information (angular and translational displacements and velocities). Also, the exemplar patterns matched input states of the system to the time-delayed output action. The development of the artificial neural network controller involved training the net, validating the training of the net and then, implementing the net as the controller. Various

optimization techniques were implemented for training the net, as were tools for creating, training and implementing this controller

Table 9.1 Comparing mass reconfigurations and control implementations

Mass Reconfiguration Strategy	Nature of the Strategy & Its Performance	Controller and Comments
Sinusoidal Motion with constant frequency and phase	- continuous, differentiable motion - time dependent - similar to Mathieu's Equations - energy attenuation can be parametric provided proper phase shift employed - produced "beating" phenomena	Not Implemented - would require logic to select phase magnitude and logic to arrest the control action to avoid amplification from the "beating" effects
Sinusoidal Motion with tuned (variable) frequency	- continuous, differentiable motion - time dependent - when properly coordinated provided parametric energy attenuation	Not Implemented - when initiated the mass motion should be "in phase" with the angular oscillations
Relay Action - piece-wise, constant velocity profile	- discontinuous displacement profile (implementation did not provide for smooth transition between velocity states) requires conditionals to select velocity - provided good rate of energy attenuation with the energy decreased in steps - residual energy existed	Human Operator - with experience operator skills improved. - best energy attenuator Knowledge/Rule Based Controller - good attenuation - improved results obtained when adjustable limits for selecting velocity were used.
Proportional and Derivative Based Action	- continuous displacement motion - gain parameters were selected as constants - the beating phenomena was evident as stalls in the auxiliary mass motion	Modified Proportional and Derivative Control Action - good, nearly parametric attenuation without beating - recommend defining adjustable gains.
Selected from above		Artificial Neural Network - when properly trained led to good energy attenuation - example provided improved attenuation over trained system and accommodated changes to operating conditions

9.2 Conclusions

The objective of the thesis was to investigate mass reconfiguration within or along a structure for attenuating the structural, vibrational energy. Since the approach taken examined the complete controlled system to achieve vibration attenuation, the research, as reported within, encompassed several domains. These included structural dynamics, numerical simulation, optimization, control and artificial intelligence technology. Based on the results from this investigation where mass reconfiguration consisted of a radially, translating mass along a rotating structure (mass-pendulum system), several conclusions can be drawn.

The most important conclusion is that mass reconfiguration can be an effective vibration attenuation mechanism. Mass reconfiguration can alter the characteristics of the system and thereby increase, decrease or cause no change to the structural energy. Therefore, a strategy for mass reconfiguration can be deduced to effectively attenuate the vibrational energy in structures. When studying mass motion along a structure, accounting for the inertia effects of the mass becomes involved and complex.

Based on the mass reconfiguration displacement profiles that were studied by simulating the ensuing dynamics and optimizing the time-dependent displacement profile, several characteristics for the mass reconfiguration strategy for effective attenuation can be made. Namely, for vibration attenuation the profile should be cyclic at approximately twice the angular frequency of the system. To achieve parametric attenuation, a sinusoidal auxiliary mass motion that is tuned to twice the frequency of the angular oscillations of the system can be used. To avoid beating effects, relay action can be employed to synchronize the mass motion with the current frequency of the pendulum motion. Regardless of the auxiliary mass displacement profile, improved attenuation with respect to maximizing the rate of the attenuation and minimizing the residual energy can be achieved by using proper parameters for the reconfiguration profiles and/or by using

adjustable parameters based on the current system dynamics or parameters. Autonomous control required adjustable parameters for defining the mass reconfiguration profile.

The technique of reformulating the complex, dynamic control problem as an iterative, parameter optimization can be beneficial. The effectiveness for this study varied with the improvement depending on the period of optimization and the technique being investigated. Optimization using random search methods showed that several iterations were required to converge to or towards the global solution.

A variety of controllers to implement the mass reconfiguration attenuation control strategy can be developed and employed, as was shown. Controllers based on time-dependent reconfiguration profiles, conditional logic and modified proportional and derivative action were developed and shown to achieve good structural, vibrational energy attenuation for the pendulum systems. Based on the implemented controllers, the human operator performance was best at employing mass reconfiguration to attenuate vibrations followed by controllers based on artificial intelligence technology.

In developing the artificial neural network controller, the following conclusions can be drawn:

1) by providing time dependent parameters, a "dynamic" or time-dependent neural network for control purposes can be developed;

2) by using displacement and velocity parameters, effective control for a nonlinear second order system can be achieved;

3) by generating exemplar patterns from a controlled system, training suite data for creating a "proxy" neural net controller can be accomplished;

4) by implementing parametric optimization techniques (such as, Powell Method, Conjugate Gradient, Coordinate Search, Evolutionary Algorithms and others), supervisory training for neural networks can be enhanced over back propagation methods;

5) by presenting a data suite that is independent, yet similar to the training suite, the training of the neural network can be assessed;

6) by presenting the entire training suite (batch training), the neural net can be trained more expeditiously; and

7) by avoiding "over-training", the neural network provided more general control and responds better to conditions that the net was not explicitly trained for. The phenomena was not investigated in detail and hence a general conclusion cannot be drawn.

All the simulation, optimization and control systems were custom programmed for the thesis research. Based on the programs developed, modular programming was concluded to be effective for developing software tools that can be customized for various languages and programming platforms.

9.3 Contributions

Several original contribution from this research were made. The key contribution was the development and application of the concept of mass reconfiguration using either internal mass redistribution or an addendum system of an auxiliary mass to attenuate vibration in a rotating system. The understanding of the mechanics of this system were presented. Parametric excitations were applied to control vibrations [Stilling and Watson, 1994b and 1993]; the technique for inverse parametric amplification (i.e. attenuation) was achieved using a tuned-frequency, harmonic mass redistribution.

Secondly, artificial intelligence technology methods were successfully applied as controllers for this problem. Both knowledge based systems and artificial neural networks were effective controllers.

Thirdly, extensive tool development for computer simulations were completed. These were done on various platforms in both Forth and C languages. The custom software packages that were developed

encompassed linear algebra packages, initial value solvers, optimization search techniques and neural network programs.

The formulation of the problem in a nontraditional or classic manner provided new insight into the problem and motivated unique solutions. For example, a pseudo-force comprised of the slider related terms transformed the freely vibrating system into a forced vibration problem. The "pseudo-force" was defined by the mass reconfiguration. Also by examining the fluctuations with respect to the natural frequency of the system, the beating phenomena could be explained and circumvented by creating a self-tuning frequency reconfiguration profile. Also, the controller embedded standard control signals, thereby expanding its typical processing capabilities associated with generating appropriate control action.

In addition, the concept of changing the dynamic characteristics (parameters in the governing differential equation) provides new engineering design venues to solve problems. This thesis examined the specific case of mass reconfiguration in a dynamic system. The concept can be extended to adjusting the boundary conditions to change the dynamics of the system to achieve a desired goal; for instance achieving vibration attenuation in a transmission line may involve adjusting the tension and length of the vibrating cable by lengthening and shortening the cable over a large pulley at its attachment point.

9.4 Recommendations for Future Work

Regarding the concept of mass reconfiguration, a continuation of the investigation with the pendulum structure could involve developing a profile that provides the rapid attenuation of the relay action without encountering high acceleration patterns in the auxiliary mass. This "jerk" could be avoided using appropriate transition patterns (such as cycloidal motion). Further optimization and improvements on the adjustable limits would be desirable.

The research reports the effects associated when 10% of the structural mass is employed as an auxiliary mass to traverse 40% of the structure's span. Both of these factors should be investigated further. As well the location of the mass motion (that is the proximity to the pivot) will affect the attenuation characteristics of the mass reconfiguration system. Furthermore, when applied to large structures, multiple control units (i.e. masses) may prove more effective.

Completion of a prototype of the system is recommended. This would permit an investigation into not only the process of training a neural network based on sampling a controlled system, but also the dynamics and/or limitations associated with the sensors and actuators could be investigated.

To better represent more systems, the structure considered should be continuous. Initial investigation with a cantilever beam [Stilling, 1990; Stilling and Watson, 1997] showed that additional inertia/relative acceleration terms need to be considered. Examining the effects of an auxiliary mass along a structure alters its eigenvalues and eigenvectors (modal frequencies and shapes). The general strategy for damping the first mode of vibration involved moving the mass at twice this modal frequency over the length of the structure. But other strategies associated with higher frequency motion may also be appropriate, especially when all modes of vibration are considered.

REFERENCES

Alty, J.L. and M.J. Coombs. (1984) *Expert System Concepts and Examples.* Great Britain: National Computing Center Limited.

Barr, A.D.S. (1993) "Parametric Vibration In Beams". In *CANCAM '93 Proceedings of the 14th Engineering Mechanics Symposium,* Eds. P.H. Oosthuizen and J.T. Paul. Kingston, Ontario. pp. 3-9.

Bert, C.W. (1980) "Composite Materials: A Survey of the Damping Capacity of Fiber Reinforced Composites" In *Damping Applications for Vibrations Control.* Ed. P.J. Torvik. Winter Annual Meeting of ASME Chicago, Illinois. AMD-38:53-63.

Blackwell, R.J. (1986) *Christiaan Huygen's the pendulum clock: Geometric demonstrations concerning the motion of pendula as applied to clocks.* 1st Ed. (Translation of Horologium Oscillatorium). Ames: Iowa State University Press.

Bowell L.J. and C.D. D'Mello (1993) *Dynamics of Structural Systems.* Blackwell Scientific Publications: London.

Brown, R.R. (1987) "An Artificial Neural Network Experiment" in Dr. Dobb's Journal of Software Tools". April:16-26.

Burden, R.L. and J.D. Faires (1985) *Numerical Analysis.* 3rd Ed. PWS Publishers: Boston.

Burns, J.A. (1970) "More on Pumping a Swing" in *Am. J. Phys..* 38:920-922.

Chakraborty G. and Nuguchi. (1997) "Difficulty in Learning vs. Network Size" in *IEEE Inter. Conference on Neural Networks* Houston, Texas. Vol. 3 pp. 2022-2027.

Crawley, E.F. (1994) "Intelligent structures for aerospace: A technology overview and assessment." in *AIAA Journal.* 32(8):1689-99.

Curry, S.M. (1976) "How children swing" in *Am. J. Phys..* 44(10):924-926.

Dai, L. and M.C. Singh. (1998) "Periodic, Quasiperiodic and chaotic behaviour of a driven Froude Pendulum in *Inter. J. of Non-Linear Mech.*. 33(6):947-965.

Dai, L. and M.C. Singh. (1994) "On Oscillatory Motion of Spring-Mass Systems Subjected to Piecewise Constant Forces" in *Inter. J. of Non-Linear Mech.*. 173(2):217-231.

Farrel, O.J. and B. Ross. (1971) *Solved Problems in Analysis.* 1st Ed. Dover Publications Inc.: N.Y.

Forsley, L.P.G. (1993) "Definitions the Extensible Language Newsletter" in *Definitions.* 1(1):1.

Freeman, J.A. and D.M. Skapara. (1991) Neural Networks: Algorithms, Applications and Programming Techniques. Addison-Wesley Publishing Inc.: Reading, Massachuets.

Goldberg, D.E. (1989) *Genetic Algorithms in Search, Optimization and Machine Learning.* 1st Ed. Addison-Wesley Publishing Company: Reading, Massachusetts.

Goldstein, H. (1980) *Classical Mechanics.* Addison-Wesley Publishing Co.: Reading, Massachusetts.

Gore, B.F. (1970) "The Child's Swing". in *Am. J. Phys.*. 38:378-9.

Hassoun, M.H. (1995) *Fundamentals of Artificial Neural Networks.* MIT Press: Cambridge, Massachusetts.

Huang, S. and Y. Huang. (1991) "Bounds on the Number of Hidden Neurons in Multilayer Perceptrons". *in IEEE Trans. on Neural Networks.* 2(1):47-55,

Hayashi, C. (1964) *Nonlinear Oscillations in Physical Systems.* McGraw-Hill Inc.: New York.

Hayashi, C. (1953) *Forced Oscillations in Nonlinear Systems.* Nippon Printing and Publishing Company, Ltd.: Japan.

Haykin, Simon (1994) *Neural Networks: A Comprehensive Foundation.* Macmillan College Publishing Company: New York.

Hirose, Y., K. Yamashita, S. Hijiya (1991) "Back-propagation Algorithms Which Varies the Number of Hidden Units" in *Neural Networks.* 4:61-66.

Henderson, J.P. (1980) "Damping Applications In Aero-propulsion Systems" in *Damping Applications for Vibrations Control.* Ed. P.J. Torvik. Winter Annual Meeting of ASME Chicago, Illinois. AMD-38:145-158.

Holland, J.H. (1975) *Adaptation in Natural and Artificial Systems.* University of Michigan Press: Ann Arbor, MI.

Inman, D.J. (1996) *Engineering Vibration.* Prentice-Hall. Inc.: Upper Saddle River, N.J.

Irwin, J.D. and E.R. Graf. (1979 *Industrial Noise and Vibration Control.* Prentice-Hall Inc.: Englewood Cliffs, N.J. 267ff.

Krishnamoorthy, C.S. and S. Rajeev. (1996) *Artificial Intelligence and Expert Systems for Engineers.* CRC Press: Boca Raton, Florida.

Korenev, B.G. and L.M. Reznikov. (1993) *Dynamic Vibration Absorbers Theory and Technical Applications.* John Wiley & Sons: Chichester, U.K.

Ku, C.C. and K.Y. Lee (1995) "Diagonal Recurrent Neural Networks for Dynamic Systems Control" in *IEEE Trans. on Neural Networks.* 6(1):144-156.

Lanczos, C. (1970) *The Variational Principles of Mechanics.* Toronto: University of Toronto Press.

Lawrence, J. (1990) "Untangling Neural Nets: in *Dr. Dobb's Journal of Software Tools.* April:38-44.

Librescu, L., L. Meirovitch, S. S. Na. (1997) "Control of Cantilever Vibration via Structural Tailoring and Adaptive Materials" in *AIAA Journal.* 35(8):1309-1315.

Lippman, R.P. (1987) "An Introduction to Computing with Neural Nets" in *IEEE Acoustics, Speech, Signal Processing Magazine.* 4(2) pp. 4-22.

Lu, L.Y., S. Utky, B.K. Wada. (1992) "On the placement of active members in adaptive truss structures for vibration control" in *Smart Materials and Structures.* 1(1):8-23.

Marasco, J. (1986a) "Math: A Variable Metric Minimizer" in *Dr. Dobb's Journal of Software Tools.* 11(3):24-34,74-83.

Marasco, J. (1986b) "Math: Variable Metric Minimizer" in Dr. Dobb's Journal of Software Tools. 11(4):84-110.

Masters, T. (1995) *Advanced Algorithms for Neural Networks: C++ Sourcebook*. John Wiley and Sons, Inc.: N.Y.

McLachlan, N. W. (1951) *Theory and Applications of Mathieu Functions*. Oxford University Press: Great Britain.

Michealwicz, Z. (1992) *Genetic Algorithms + Data Structures = Evolution Programs*. 1st Ed. Springer: New York.

Miller, R.K. (1990) *Neural Networks*. Fairmont Press, Inc.: Lilburn, GA. p.16.

Mirchandani, G. and Cao, W. (1989) "On Hidden Nodes for Neural Nets" in *IEEE Trans. of Circuits, Systems*. 36(5)

Miura,K., (1989) "Studies of Intelligent Adaptive Structures", in *Adaptive Structures from the Winter Annual Meeting of ASME*, AD-Vol. 15. pp.88-94.

Neelakanta, P.S. and D.F. De Groff (1994) *Neural Network Modeling: Statistical Mechanics and Cybernetic Perspectives*. CRC Press, Inc.: Boca Raton, Florida.

Nguyen, P.H. and J.H. Ginsberg. (1999) "Vibration Control Using Parametric Excitation. in *Proceedings of the ASME Dynamic Systems and Control Division*. DSC-67:141-148. (pendulum too)

Noble, J.V. (1989) "Scientific Computations in Forth", in *Computers in Physics*, 3(5):31-38.

Noble, J.V. (1988) "Fortran is Dead: Long Live Forth!", *JFAR*, 5(2):261-270.

Ogata, K. (1970) *Modern Control Engineering*. Prentice-Hall, Inc.: Englewood Cliffs, N.Y.

Pham, D.T. and D. Karaboga (1999) "Training Elman and Jordan networks for system Identification Using Genetic Algorithms". in *Artificial Intelligence for Engineering*. 13(2)107-117.

Pinsky, M.A. and A. A. Zevin. (1999) "Oscillations of a pendulum with a periodically varying length and a model of a swing" in *Inter. J. of Non-Linear Mech.*. 34(1):105-109.

Press, W.H., S.A. Teukolsky, W.T. Vetterling, B.P. Flannery. (1992a) *Numerical Recipes in C: The Art of Scientific Computing*. 2nd Ed. . Cambridge University Press: N.Y.

Press, W.H., S.A. Teukolsky, W.T. Vetterling, B.P. Flannery. (1992b) *Numerical Recipes in Fortran: The Art of Scientific Computing.* Cambridge University Press: N.Y.

Qian, Schoenau, Burton and Ukranitz "Measurement Performance of PID and Neural Net Control of a Hydraulic Actuator", Proceedings of the 1998 IMACS Inter. Conference on Circuits, Systems and Computers. Greece, Oct. pp.607-611.

Rahim, N. (1994) *Artificial Neural Networks for Speech Analysis/Synthesis.* Chapman Hall: London.

Relton, F. E. (1965) *Applied Bessel Functions.* Dover Publishing Inc.: N.Y.

Rumelhart, D.E., G.E. Hinton, R.J. Williams. (1986) "Learning Internal Representations by Error Propagation", in *Parallel Distributed Processing: Explorations in the Microstructure of Cognition* (eds. D.E. Rumelhart and J.L. McClelland), 1, MIT Press, Cambridge.

Sànchez-Sinencio, E. and C. Lau. *Artificial Neural Networks: Paradigms, Applications and Hardware Implementations.* IEEE Press: New York.

Sanmartin, J.R. (1984) "O Botafumeiro: Parametric Pumping in the Middle Ages" in *Am. J. Phys.*. 52(10):937-945.

Simpson, P.K. (1992) "Foundations of Neural Networks" *in Artificial Neural Networks: Paradigms, Applications and Hardware Implementations.* eds. Sànchez-Sinencio and Lau. IEEE Press: New York. pp. 3-24.

Soucek, B. (1989) *Neural and Concurrent Real-Time Systems.* John Wiley & Sons: N.Y.

Stilling, D.S.D. (1993a) "Intelligent Structures: Application to Effect Active Vibration Attenuation" in the *Proceedings of the 25th Canadian Congress of Applied Mechanics, CANCAM'93.* Kingston, Ontario. pp. 153-154.

Stilling, D.S.D. (1993b) *Forth for Microcomputer/controller Interfacing Using A New Micros Inc. Single Board Computer (Seminar Participant Handbook)* University of Saskatchewan. for 1993 Association For Computing Machinery Conference in Indianapolis, Indiana.

Stilling, D.S.D. (1991) "System Architecture for Training A Neural Net Controller", in *1991 Rochester Forth Conference: Intelligent Instruments.* Rochester, N.Y. pp.105-107.

Stilling, D.S.D. (1990a) "Attenuation of Vibrations in an Intelligent Structure Using A Neural Net Controller" (unpublished) Ph. D. Comprehensive Report at University of Saskatchewan: Department of Mechanical Engineering.

Stilling, D.S.D. (1990b) "Exploring Dedicated Controllers Through Designing A Portable Hand-Held Game", in *1990 Rochester Forth Conference: Embedded Systems* in Rochester, N.Y. pp.141-143.

Stilling, D.S.D. (1989) *Improving Springboard Diving Through Biomechanical Analyses and Knowledge Based Expert System Applications.* Master of Science Thesis. University of Saskatchewan: Department of Mechanical Engineering. p. 80-1.

Stilling, D.S.D. and L.G. Watson. (1997) "Interaction of A Mass Along A Structure" in *Proceedings of the 27th Canadian Congress of Applied Mechanics, CANCAM'97* Laval, Quebec. pp.235-236.

Stilling, D.S.D. and L.G. Watson. (1994a) "MATMATH: A Matrix Handling Package For Forth" in *Journal of Forth Applications and Research*, Rochester, New York: Institute of Applied Forth Research, Inc.

Stilling, D.S.D. and L.G. Watson. (1994b) "Parametric Amplification Applied to Structural Vibration Attenuation" in *CSCE Engineering Mechanical Symposium.* Winnipeg, Manitoba. pp. 25-30. pp. 25-30.

Stilling, D.S.D. and L.G. Watson. (1993) "Dynamics of a Variable Length Pendulum for Attenuating Vibrational Energy", in *Proceedings of the 25th Canadian Congress of Applied Mechanics, CANCAM'93* Kingston, Ontario. pp. 183-184.

Stilling, D.S.D. and L.G. Watson. (1992) "Review of Microcontroller/computer Interfacing Course", in *1992 Rochester Forth Conference Proceedings: Biomedical Applications* Rochester, N.Y. pp. 95-98.

Stilling, D.S.D. and L.G. Watson. (1991) "Generating Neural Networks", in *1991 Rochester Forth Conference: Intelligent Instruments.* Rochester, N.Y. pp. 135-137.

Stilling, D.S.D. and L.G. Watson. (1990) "Neural Net Control of Intelligent Structures", in *1990 Rochester Forth Conference: Embedded Systems.* Rochester, N.Y. pp. 139-144.

Tea, P.L. and H. Falk. (1968) "Pumping on a Swing" in *Am. J. Phys.*. 36:1165-1166.

Wada, B.K., J.L. Fanson and E.F.Crawley, (1989) "Adaptive Structures", in *Adaptive Structures from the Winter Annual Meeting of ASME*, AD-Vol. 15. pp.1-8.

Walker, J. (1989) "The Amateur Scientist: How To Get The Playground Swing Going: A First Lesson In The Mechanics Of Rotation" in *Sc.*106-109.

Walker, T.C. and R.K. Miller (1990) *Expert Systems Handbook.* Fairmont Press, Inc.: Lilburn, GA.

Warwick, K. (1995) "Neural networks: an Introduction" in *Neural Network Applications in Control.* eds. G.W, Irwin, K. Warwick and K.J. Hunt. The Institution of Electrical Engineers: London.

Waterman, D. R. (1986) *A Guide To Expert Systems.* Reading Massachusetts: Addison-Wesley Publishing Company, Inc.

Watson, L.G. and D.S.D. Stilling. (1992a) "Genetic Algorithms in Forth", in *1992 Rochester Forth Conference Proceedings: Biomedical Applications* Rochester, N.Y. pp. 106-107.

Watson, L.G. and D.S.D. Stilling. (1992b) *Forth for Microcomputer/controller Interfacing Using New Micros Inc. NMIN-0121 Drop Point Card (Seminar Participant Handbook).* University of Saskatchewan: Saskatoon.

Watson, L.G. and D.S.D. Stilling (1991a) "Experiences with Linear Algebra and The Forth Utility Package, MATMATH", in *1991 Rochester Forth Conference: Intelligent Instruments.* Rochester, N.Y. pp. 129-134.

Watson, L.G., and D.S.D. Stilling (1991b) *MATMATH: A Linear Algebra Package -- User's Guide.* Copyright Registation 210620. University of Saskatchewan: Saskatoon.

Watson, L.G. and D.S.D. Stilling (1990) "Number Crunching with Forth", in *1990 Rochester Forth Conference: Embedded Systems.* Rochester, N.Y. pp.152-153.

Widrow, B. and M. A. Lehr (1990) "30 Years of Adaptive Neural Networks: Perceptron, Madaline, and Backpropagation" in *Proc. of IEEE.* 78(9):1415-1442.

Whittaker, E.T. and G. N. Watson. (1927) *A Course of Modern Analysis.* 4th Ed. Cambridge University Press: N.Y.

Wolfgram, D.H,, T.J. Dear, C.S. Galbraith. (1987) *Expert Systems for the Technical Professional.* Toronto: John Wiley & Sons.

Xu, X., W. Xu and J. Genin. (1997) "A Non-linear Moving Mass Problem", in *J. of Sound and Vibrations.* 204(3):495-504.

Yagasaki, K. (1999) "Co-dimension-two bifurcations in a pendulum with feedback control" in Inter. J. of Non-Linear Mech.. 34(6):983-1002.

Yagasaki, K. (1998) "Dynamics of a Pendulum with FeedForward and Feedback Control" in JSME Inter. Journal of Mechanical Systems, Machine Elements and *Manufacturing.* 41(3):545-554.

Yoshida, K. and K. Sato. (1998) "Characterization of Reverse Rotation In Chaotic Response of Mecanical Pendulum" in *Inter. J. of Non-Linear Mech..* 33(5)819-826.

Zbikowski, R. and P.J. Gawthrop (1995) "Fundamentals of neurocontrol: a survey" in *Neural Network Applications in Control,* eds. G.W. Irwin, K. Warwick and K.J. Hunt. The Institute of Electrical Engineers: London.

Zheng, D.Y., Y.K. Cheung, F.T.K. Au and Y.S. Cheng. (1998) "Vibration of Multi-span non-uniform beams under moving loads by Using Modified Beam Vibration Functions" in *J. of Sound and Vibrations.* 212(3):455-467.

APPENDICES

Appendix A: Terminology

A list of the terminology as used within the thesis is presented below. The terms are from structural and vibrational engineering, control engineering, optimization and artificial intelligence technology.

ACTIVE ATTENUATION MECHANISM as proposed in the thesis, consists of motion of a mass either within or along a structure to reduce its vibrational energy; the mass may be an auxiliary unit or intrinsic to the structure. The technique is also termed mass redistribution or mass reconfiguration.

ARTIFICIAL INTELLIGENCE TECHNOLOGY refers to concepts and developments that combine biological processes with computer technology to emulate various human or biological processes; some of the tools that have evolved include artificial neural networks and knowledge based systems.

ARTIFICIAL NEURAL NETWORKS is also referred to as neural networks, neural nets or nets in this work; as employed in this research the net provides a matching between input and output patterns using a parallel set of weighted sums and nonlinear squashing functions.

ATTENUATION refers to the loss of vibrational energy of a structure; it is positive damping that occurs from the active vibration technique.

AUXILIARY MASS is the end mass of the simple pendulum or the sliding mass of the physical pendulum that translates along the system to reconfigure its mass to effect active vibration attenuation.

CLOSED LOOP CONTROL SYSTEM is a control system with output fedback into the controller; the controller maintains a prescribed relation between the reference input and system output by comparing these and using the

difference as a means of effecting control. (See also open loop control system.)

CONTROLLER is the logic that directs the control mechanism to effect the desired objective for the plant by supplying appropriate action or signal.

DAMPING refers to the change in energy of the system.

POSITIVE DAMPING refers to loss or dissipation of energy; in this work it refers to the attenuation of oscillations or the reduction of structural, vibrational energy.

NEGATIVE DAMPING refers to the gain of energy.

EXEMPLARY PATTERNS refers to a set of paired input and output patterns used to train artificial neural networks.

FEEDBACK CONTROL SYSTEM see closed loop control system.

INSTABILITY refers to oscillations that are unbounded; the amplitude of oscillation increases. (See also stability and neutral stable).

KNOWLEDGE BASED SYSTEM or expert system refers to a knowledge base, an inference engine, working memory and interface used to emulate human expertise in a given area.

MASS REDISTRIBUTION see active attenuation mechanism.

MASS RECONFIGURATION see active attenuation mechanism.

MATHEMATICAL PENDULUM see simple pendulum.

MATHIEU-HILL EQUATIONS are linear differential equations with periodic coefficients.

MATMATH is the name of the linear algebra software package that was custom developed in Forth for the thesis research.

NEUTRAL STABILITY refers to oscillations that remain unchanged; no attenuation or growth in amplitude. (See also stability and instability).

OPEN LOOP CONTROL SYSTEM is a control system whereby the output does not affect the control action; the input and output relation of the system is well defined for each reference input and there corresponds fixed operating conditions. Such systems often operate on a time basis and do not operate well in the presence of disturbances. (See also closed loop control system.)

OPTIMIZATION is the process of determining extrema in an objective or cost function; it is determining a "best" solution.

PARAMETRIC RESONANCE vibrations that are characterized by monotonically increasing oscillations; also it is referred to as parametric excitations.

PHYSICAL PENDULUM is a compound or dual mass pendulum system; both the pendulum structure and the sliding or auxiliary mass possess physical properties of mass or inertia.

PLANT refers to the physical object that is to be controlled; that is, the equipment or mechanism(s) that functions to perform a given operation.

PROCESS refers to the progressive, continuous operation of a series of control actions leading to the desired end result or behavior; process is the controlled operation that may be systematically directed, the action to achieve a desired result.

PROPORTIONAL AND DERIVATIVE CONTROL ACTION refers to a type of processing of the feedback signal to the controller; proportional action involves scaling the feedback signal and derivative action involves scaling its derivative.

SEARCH TECHNIQUES refers to methods used to find optimums in an objective function; techniques include: conjugate gradient, coordinate search, evolutionary programs and others.

SELF-TUNING or self adjusting terms refers to parameters that autonomously change; in this thesis, this refers to parameters that adjust to maintain proper coordination between the active attenuation mechanism and the vibrating structure.

SIMPLE PENDULUM is also referred to as a mathematical pendulum and accurately models a variable length pendulum where the pendulum structure, itself, is massless.

STABILITY refers to oscillations that remain bound. (See also instability and neutral stability).

STRUCTURE is the vibrating plant that is controlled; for the research reported herein the structures have consisted of pendula structures.

SYSTEM is the combination of the components that cohesively perform a certain objective; the system is the combination of the controller and plant.

TRAINING SUITE refers to a set of exemplar patterns used to adjust the weights or train an artificial neural network.

VALIDATION SUITE refers to a set of exemplar patterns used to evaluate the training of the artificial neural network.

VIBRATION is the oscillatory behavior of bodies which possess mass and stiffness undergo when disturbed by either an internal or external disturbance.

Angular Vibration refers to rotational oscillations.
Translational Vibrations refer to linear oscillations.

Appendix B: Deriving the Governing Equations for a Physical Pendulum

The physical pendulum system is a dual mass system; both the pendulum and the attenuation device, the slider possess mass. A typical schematic for the simple pendulum is shown below.

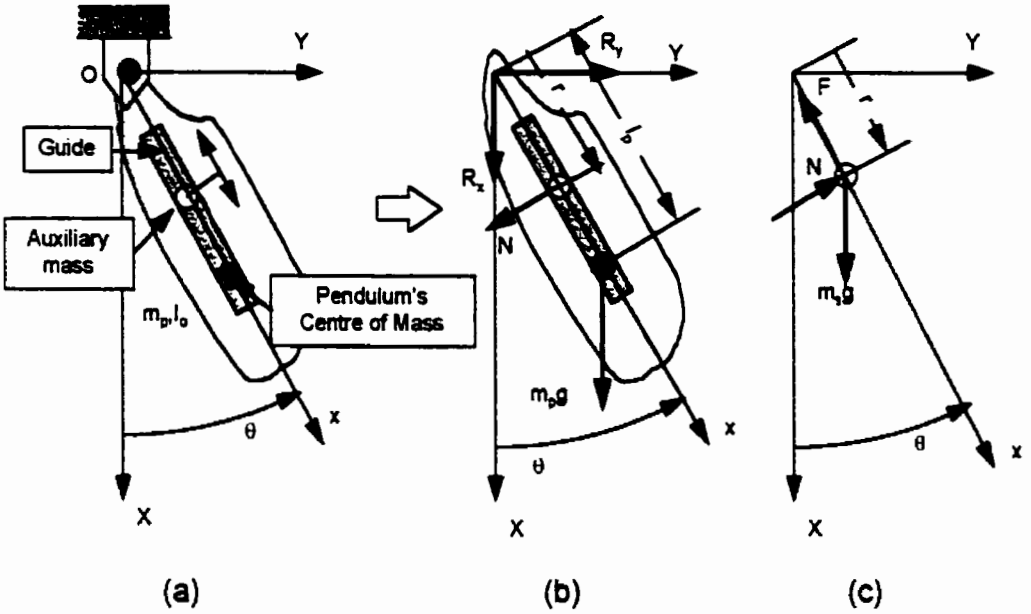

Figure B.1 Physical pendulum system and the free body diagrams of (b) the pendulum and (c) the auxiliary mass components.

Applying Newtonian equilibrium principles, moments of the forces are taken about the pivot to give,

$$I_o\ddot{\theta} = -m_p g l_p \sin\theta - Nr \tag{B.1}$$

where the notation is consistent with Figure B.1 and is defined in the Nomenclature and Abbreviations found on page xviii.

As developed in Section 2.2, the motion of the slider is governed by,

$$m_s\left[\left(\ddot{r}-\dot{\theta}^2 r\right)\hat{i}+\left(\ddot{\theta}r+2\dot{\theta}\dot{r}\right)\hat{j}\right]=-m_s g\left(cos\theta\hat{i}+sin\theta\hat{j}\right)-F\hat{i}+N\hat{j}\,. \qquad \text{(B.2)}$$

This equation in terms of its rectangular components can be expressed as,

$$m_s\left(\ddot{r}-\dot{\theta}^2 r\right)=-m_s g\,cos\theta-F \qquad \text{(B.2a)}$$

and

$$m_s\left(\ddot{\theta}r+2\dot{\theta}\dot{r}\right)=-m_s g\,sin\theta+N\,. \qquad \text{(B.2b)}$$

From Equation B.2b, the interaction force, N, is defined as

$$N=m_s\left(\ddot{\theta}r+2\dot{\theta}\dot{r}+g\,sin\theta\right). \qquad \text{(B.3)}$$

By substituting Equation B.3 into Equation B.1, the planar motion of the pendulum is defined as,

$$\left(I_o+m_s r^2\right)\ddot{\theta}+2m_s r\dot{r}\dot{\theta}+\left(m_p l_p+m_s r\right)g\,sin\theta=0\,. \qquad \text{(B.4)}$$

The force required to move the sliding or auxiliary mass is defined by rearranging Equation B.2a,

$$F=m_s\left(\dot{\theta}^2 r-\ddot{r}+g\,cos\theta\right). \qquad \text{(B.5)}$$

Appendix C:

Using Lagrangian Dynamics, An Energy Formulation, To Derive the Governing Differential Equations

C.1 Introduction

The governing differential equations of motion for the pendulum system and the proposed attenuation device are derived. Newtonian mechanics model systems using forces is quite adequate for analyzing simple systems. However, to formulate the equations of motion for more complex systems, energy principles or Lagrangian Dynamics are often used [Barr, 1993]. Regardless of the modeling approach, the governing differential equations are identical.

A brief introduction to the approach of Lagrangian Dynamics is followed by the derivation of the governing equations for a simple, constant length pendulum, for the variable length pendulum, a physical pendulum with a stationary auxiliary mass and a physical pendulum where the mass traverses the structure. Knowledge of the interaction between the pendulum and the auxiliary mass is not necessary for deriving the differential equations describing the planar oscillations. Lastly, the general equations as derived are discussed.

C.2 Background

Briefly, the energy formulation is based on Hamilton's Principle [Goldstein, 1980]. The dynamics of a system is based on minimizing the time integral of the differences between kinetic (T) and potential (U) energies. The

difference in energy is called the Lagrangian ($\mathcal{L}=T-U$). Using Calculus of Variations [Lanczos, 1970], Hamilton's Principle can be expressed as:

$$\delta\int_0^{\tau}(T-U)\,dt=0\ . \tag{C.1}$$

Therefore, the Euler-Lagrange equations or the Lagrangian equations of motion are defined by:

$$\frac{d}{dt}\left(\frac{\partial\mathcal{L}}{\partial\dot{q}}\right)-\frac{\partial\mathcal{L}}{\partial q}=F_q \tag{C.2}$$

where q represents a generalized coordinate,

the superscript, "$\cdot$", the first time derivative;

∂, partial differential operator; and

F_q, the generalized non-conservative forces.

Additional background and references on Lagrangian Dynamics appears in Section C.8.

C.3 Simple Pendulum

A single mass pendulum as shown in Figure C.1 consists of a constant length pendulum. A mass or bob is located at a fixed distance, r, from the support. Assuming the mass moment of inertia of the bob about its center is significantly less than its inertia about the support and the connection (cable or rod) has negligible constant mass, then the energy of the system can be expressed as follows:

Kinetic Energy: $T=\frac{1}{2}mr^2\dot{\theta}^2$ (C.3)

Potential Energy: $U=mgr(1-cos\theta)$ (C.4)[1]

[1] As potential energy is a relative term, the selected zero reference position correspond to the vertical equilibrium position when $r=R_o$. This convention is followed throughout this appendix.

where m represents the mass of the bob;

r, the radial distance from the pivot to the mass;

θ, the angular displacement measured with respect to the vertical;

g, the acceleration due to gravity and

the superscript, $\dot{}$, represents the first time derivative of the parameter. Note that the potential energy has been defined with respect to the lowest position of the mass.

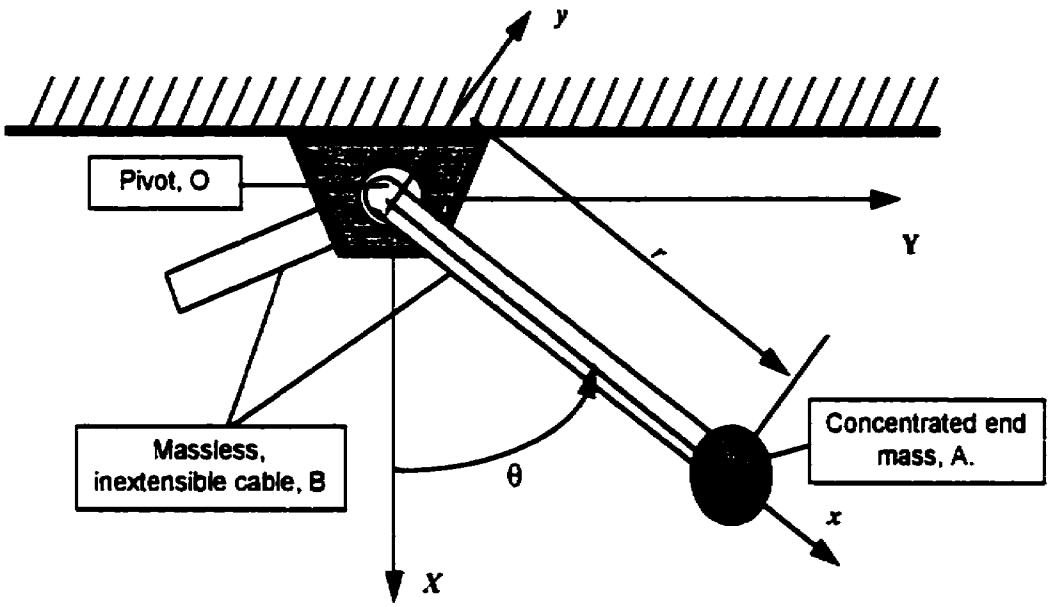

Figure C.1 Model of a variable length pendulum.

For the conservative system, simple pendulum motion based on the Lagrangian formulation (Equation C.2) gives the following governing differential equation where the generalized coordinate is the angular displacement measured with respect to the vertical:

$$mr^2\ddot{\theta} + mgr\sin\theta = 0 \qquad \text{(C.5)}$$

which simplifies to

$$\ddot{\theta}+\omega_n^2 \sin\theta = 0 \tag{C.6}$$

with

$$\omega_n^2 = \frac{g}{r}. \tag{C.6a}$$

C.4 Variable Length Pendulum

Next, the mechanism for active damping which is the lengthening and shortening of the pendulum is considered. To continue with the energy derivation, the change in the position of the mass can be modeled by its translational kinetic energy. The kinetic energy formulation (Equation C.3) is expanded to become

$$T = \frac{1}{2}mr^2\dot{\theta}^2 + \frac{1}{2}m\dot{r}^2 \tag{C.7}$$

with the Lagrangian now expressed as:

$$\mathcal{L} = \frac{1}{2}mr^2\dot{\theta}^2 + \frac{1}{2}m\dot{r}^2 - mg(R_o - r\cos\theta) \tag{C.8}$$

and when differentiated and simplified the governing equation of motion for the oscillations of the pendulum can be expressed as:

$$\ddot{\theta}+2\frac{\dot{r}\dot{\theta}}{r}+\frac{g}{r}\sin\theta = 0 \tag{C.9}$$

The mechanism that decreases or increases the energy of the system is mathematically represented in the coefficient, $2\frac{\dot{r}}{r}$. Depending on the sign of this term, positive or negative "damping" may ensue. Alternately, the governing differential equation can be re-written so that the affects of changing the length can be viewed as the forcing function, mathematically this can be stated as,

$$\ddot{\theta} + \frac{g}{r} sin\theta = p(\theta, r, t) \tag{C.10}$$

$$\text{where } p(\theta, r, t) = -2\frac{\dot{r}\dot{\theta}}{r} \tag{C.10a}$$

The motion of the mass, achieved by increasing or decreasing the length of the pendulum, drives the oscillations of the system. An iterative algorithm for solving Equation C.10 would be required, as the force is a function of the current angular kinematics of the structure.

The force associated with moving the mass can be derived by considering the radial distance between the pivot and the end mass (i.e. the length of the pendulum) as the generalized coordinate. Mathematically, the force to effect a change in mass position can be expressed as:

$$F_r = m\left[\dot{\theta}^2 r - \ddot{r} + g\cos\theta\right] \tag{C.11}$$

where F_r represents the tension in the cable. Approximating the force in the cable is essential for design implementation, such as, component selection, service life predictions and establishing limits for cable operation. By calculating the work associated with moving the end $(F_r \cdot \Delta r)$, a work-energy balance can be used to validate the accuracy of the simulation.

C.5 Physical Pendulum System

The governing differential equations of motion for a pendulum possessing either a concentrated or distributed mass closely parallel those for the simple pendulum as presented in Section C.3. The governing equations increase in complexity when the physical properties of the pendulum are taken into account. The active attenuation mechanism, an auxiliary mass, coexists with the structural mass as appears in the governing differential

equations. Incorporating the active vibration attenuation device can be visualized as augmenting the system with an additional sliding mass; a coupled system results.

To appreciate the physical contribution made by the pendulum, the following configurations for the pendulum were considered:

(a) a pendulum with a concentrated mass located at a fixed distance from the support, and

(b) a pendulum with distributed mass, such as a uniform rod.

Schematically, these systems are illustrated in Figure C.2.

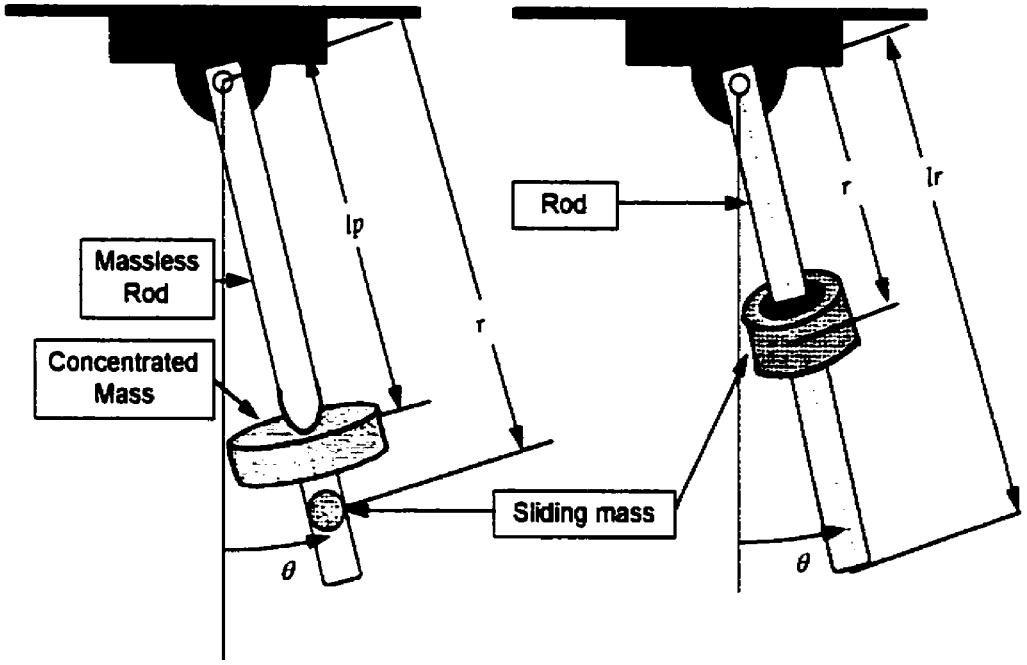

Figure C.2 Pendulum structures with an auxiliary mass or slider: (a) a massless rod with concentrated mass and (b) an uniform rod with rotational inertia.

A key difference between these models is in defining the moments of inertia about the pivot or support; the moments of inertia for each pendulum type are respectively given as:

(a) $I_a = m_p l_p^2$ (C.12a)

(b) $I_b = \frac{1}{3} m_r l_r^2$ (C.12b)

where I refers to the moment of inertia with the subscript indicating the configuration;

m_p, the concentrated mass of the pendulum;

l_p, the radial distance from the pivot to the concentrated mass;

m_r, the distributed mass of the rod; and

l_r, the length of the rod.

By examining only the pendulum, the energy for the two cases are defined as follows:

Kinetic Energy:

(a) $T_a = \frac{1}{2} m_p l_p^2 \dot{\theta}^2$ (C.13a)

(b) $T_b = \frac{1}{6} m_r l_r^2 \dot{\theta}^2$ (C.13b)

Potential Energy:

(a) $U_a = m_p g l_p (1 - \cos\theta)$ (C.14a)

(b) $U_b = \frac{m_r g l_r}{2} (1 - \cos\theta)$ (C.14b)

where θ represents the angular displacement measure with respect to the vertical;

g, the acceleration due to gravity, and

the superscripts, $\dot{}$, the first time derivative of the indicated parameter.

Based on the Lagrangian formulation (Equation C.2), the following governing equations of motion for the two cases can be derived as:

(a) $m_p l_p^2 \ddot{\theta} + m_p g l_p \sin\theta = 0$ (C.15a)

(b) $\frac{1}{3} m_r l_r^2 \ddot{\theta} + \frac{1}{2} m_r g l_r \sin\theta = 0$ (C.15b)

When simplifying these differential equations, the familiar equation describing simple pendulum motion as discussed in Section C.3 ensues with the natural frequencies as noted below:

$$\ddot{\theta} + \omega_n^2 \sin\theta = 0 \quad \text{(C.16)}$$

where

(a) $\omega_n = \sqrt{\frac{g}{l_p}}$ (C.16a)

(b) $\omega_n = \sqrt{\frac{2g}{3l_r}}$ (C.16b)

The essential difference between the two configurations is that the effective length for the uniform rod is

$$l_e = \frac{3}{2} l_r \quad \text{(C.17)}$$

C.6 Physical Pendulum with an Auxiliary Sliding Mass

The attenuation mechanism is an auxiliary sliding mass. The mechanism is not integral to the structure as was the case for the simple or mathematical pendulum system. The affects of the slider to alter the dynamic characteristics of the structure are considered next. Since a dual mass system is formed, applying the energy formulation for deriving the governing differential equation requires accounting for the kinetic energy and potential energy of the slider.

$$T_s = \frac{1}{2} m_s \dot{r}^2 \dot{\theta}^2 \tag{C.18}$$

$$U_s = m_s g(R_o - r\cos\theta) \tag{C.19}$$

where the subscript, s, refers to the auxiliary mass or slider with m referring to mass and r referring to the radial distance between the support and the centroid of the slider.

By combining Equations C.13, C.14, C.18 and C.19, the Lagrangian equations for the pendulum-slider systems can be mathematically stated as:

$$\text{(a)}\ \mathcal{L}_a = \frac{1}{2}\left(m_p l_p^2 + m_s r^2\right)\dot{\theta}^2 + g\left(m_p l_p(1-\cos\theta) + m_s R_o\left(1 - \frac{r}{R_o}\cos\theta\right)\right) \tag{C.20a}$$

$$\text{(b)}\ \mathcal{L}_b = \frac{1}{2}\left(\frac{1}{3} m_r l_r^2 + m_s r^2\right)\dot{\theta}^2 + g\left(\frac{1}{2} m_r l_r(1-\cos\theta) + m_s R_o\left(1 - \frac{r}{R_o}\cos\theta\right)\right) \tag{C.20b}$$

with the simplified, governing differential equations of motion being:

$$\text{(a)}\ \ddot{\theta} + g\left(\frac{m_p l_p + m_s r}{m_p l_p^2 + m_s r^2}\right)\sin\theta = 0 \tag{C.21a}$$

$$\text{(b)}\ \ddot{\theta} + g\left(\frac{\frac{1}{2} m_r l_r + m_s r}{\frac{1}{3} m_r l_r^2 + m_s r^2}\right)\sin\theta = 0 \tag{C.21b}$$

The natural frequency of the pendulum-slider system is a function of the individual parameters of the pendulum and the slider. As expressed mathematically, this characteristic or fundamental frequency is dependent not only on the position but also the magnitude of the mass of the slider:

$$\text{(a)}\ \omega_n = \sqrt{g\left(\frac{m_p l_p + m_s r}{m_p l_p^2 + m_s r^2}\right)} \tag{C.22a}$$

$$\text{(b) } \omega_n = \sqrt{g\left(\frac{\frac{1}{2}m_r l_r + m_s r}{\frac{1}{3}m_r l_r^2 + m_s r^2}\right)} \qquad \text{(C.22b)}$$

By rearranging the equations of motion (Equations C.21a and C.21b) to segregate the effects of the slider, nonhomogeneous equations can be written, wherein the contribution of the external auxiliary mass can be viewed as the forcing function, $p(\theta, r, t)$. Mathematically, the equations of motion may be written as:

$$\text{(a) } m_p l_p^2 \ddot{\theta} + m_p g l_p \sin\theta = p(\theta, r, t) \qquad \text{(C.23a)}$$

$$\text{(b) } \frac{1}{3}m_r l_r^2 \ddot{\theta} + \frac{1}{2}m_r g l_r \sin\theta = p(\theta, r, t) \qquad \text{(C.23b)}$$

$$\text{where } p(\theta, r, t) = -m_s\left(r^2\ddot{\theta} + rg\sin\theta\right) \qquad \text{(C.23c)}$$

The total energy of the system depends on the position of the auxiliary mass, the slider, when the other parameters are held constant.

When the slider is permitted to move, the dynamics become more involved. The translational energy associated with the slider must also be taken into account. The Lagrangian becomes:

$$\text{(a) } \mathcal{L}_a = \frac{1}{2}\left(m_p l_p^2 + m_s r^2\right)\dot{\theta}^2 + \frac{1}{2}m_s \dot{r}^2 + g\left(m_p l_p(1-\cos\theta) + m_s R_o\left(1 - \frac{r}{R_o}\cos\theta\right)\right)$$

(C.24a)

(b) $\mathcal{L}_b = \frac{1}{2}\left(\frac{1}{3}m_r l_r^2 + m_s r^2\right)\dot{\theta}^2 + \frac{1}{2}m_s \dot{r}^2 + g\left(\frac{1}{2}m_r l_r(1-\cos\theta) + m_s R_o\left(1-\frac{r}{R_o}\cos\theta\right)\right)$

(C.24b)

and the ensuing governing differential equations can be expressed as:

(a) $\ddot{\theta} + \left(\frac{2m_s r}{m_p l_p^2 + m_s r^2}\right)\dot{r}_s\dot{\theta} + g\left(\frac{m_p l_p + m_s r}{m_p l_p^2 + m_s r^2}\right)\sin\theta = 0$ (C.25a)

(b) $\ddot{\theta} + \left(\frac{2m_s r}{\frac{1}{3}m_r l_r^2 + m_s r^2}\right)\dot{r}\dot{\theta} + g\left(\frac{\frac{1}{2}m_r l_r + m_s r}{\frac{1}{3}m_r l_r^2 + m_s r^2}\right)\sin\theta = 0$ (C.25b)

Again, by reorganizing the above equations so that the left-hand side of the equations containing terms related to the auxiliary mass, the affects of the auxiliary mass can be viewed as the forcing function for the system:

(a) $m_p l_p^2\ddot{\theta} + m_p g l_p \sin\theta = p(\theta, r, t)$ (C.26a)

(b) $\frac{1}{3}m_r l_r^2\ddot{\theta} + \frac{1}{2}m_r g l_r \sin\theta = p(\theta, r, t)$ (C.26b)

where $p(\theta, r, t) = -m_s\left(r^2\ddot{\theta} + 2r\dot{r}\dot{\theta} + rg\sin\theta\right)$ (C.26c)

The total energy of the system is affected by the work associated with the motion of the slider. The work associated with the translational motion of the slider is the scalar product of the force applied to move the slider and its translational displacement. To derive the required force to displace the slider, the Lagrangian is considered with the radial displacement of the slider being the generalized coordinate, hence the force to move the auxiliary mass along the pendulum can be mathematically expressed as:

$$F_s = m_s\left[\dot{\theta}^2 r - \ddot{r} + g\cos\theta\right] \qquad \text{(C.27)}^2$$

By prescribing various motion patterns for the slider, the dynamic interaction between the structure and slider can be studied.

C.7 Discussion and Summary

First by neglecting the motion of the auxiliary mass, the mathematical modeling of both pendulum structures are characterized by the equation:

$$\ddot{\theta} + \omega_n^2 \sin\theta = 0 \qquad \text{(C.6 or C.16)}$$

with the natural frequency, ω_n, being a function of the mass and its distribution within the structure. For small displacements, the system is classified as being conservative with simple harmonic motion ensuing, if an initial displacement from its equilibrium position is applied. During vibrations, the structural energy transforms between kinetic and potential energy.

When considering the redistribution of mass either within or along the structure, then the general equation is of the form,

$$\ddot{\theta} + c\dot{\theta} + \omega_n^2 \sin\theta = 0 \qquad \text{(C.28)}$$

where c represents the damping coefficient which is a function of the auxiliary mass magnitude, its position and its velocity, as expressed in Equations 3.1, 3.3a, and 3.3b.

Alternately, the governing equation of motion can be expressed so that the effects of the motion of the auxiliary or sliding mass are viewed as the forcing function for the system,

$$A\ddot{\theta} + B\sin\theta = C\,p(r, \theta, t) \qquad \text{(C.29)}$$

---

[2] Note that the equation describing the force to effect the sliding mass motion is consistent; see Equations (2.9), (3.2), (B.5), (C.11) and (C.27).

where the coefficients, A and B are based on the physical parameters of the structure and C is based on those of the auxiliary mass and $p(r,\theta,t)$ is the forcing function that depends on the current kinematic state of the auxiliary mass. The auxiliary mass can be viewed as either a damping term or a forcing function. Different positions and magnitudes of the auxiliary mass can effect the dynamic parameters and behavior of the pendulum systems.

C.8 References on Lagrangian Dynamics

Barr, A.D.S. (1993) "Parametric Vibration In Beams". In *Proceedings of the 14th Engineering Mechanics Symposium.* Eds. P.H. Oosthuizen and J.T. Paul. May 1993 Kingston, Ontario on the Theory of Computing pp. 3-9.

Goldstein, H. (1980) *Classical Mechanics.* Reading, Massachusetts: Addison-Wesley Publishing Company.

Lanczos, C. (1970) *The Variational Principles of Mechanics.* Toronto: University of Toronto Press.

Appendix D: Values for Pendulum Parameters

Mass reconfiguration was investigated using pendulum structures. Both a simple or single mass pendulum and a physical or dual mass pendulum were used. The simple pendulum represents a variable length pendulum as shown in Figure D.1(a). Mass reconfigurability is intrinsic to this system. The physical pendulum consists of a massless rod supporting a concentrated mass 1 m from the pivot with an auxiliary mass that slides along/within the connecting rod, as shown in Figure D.1(b).

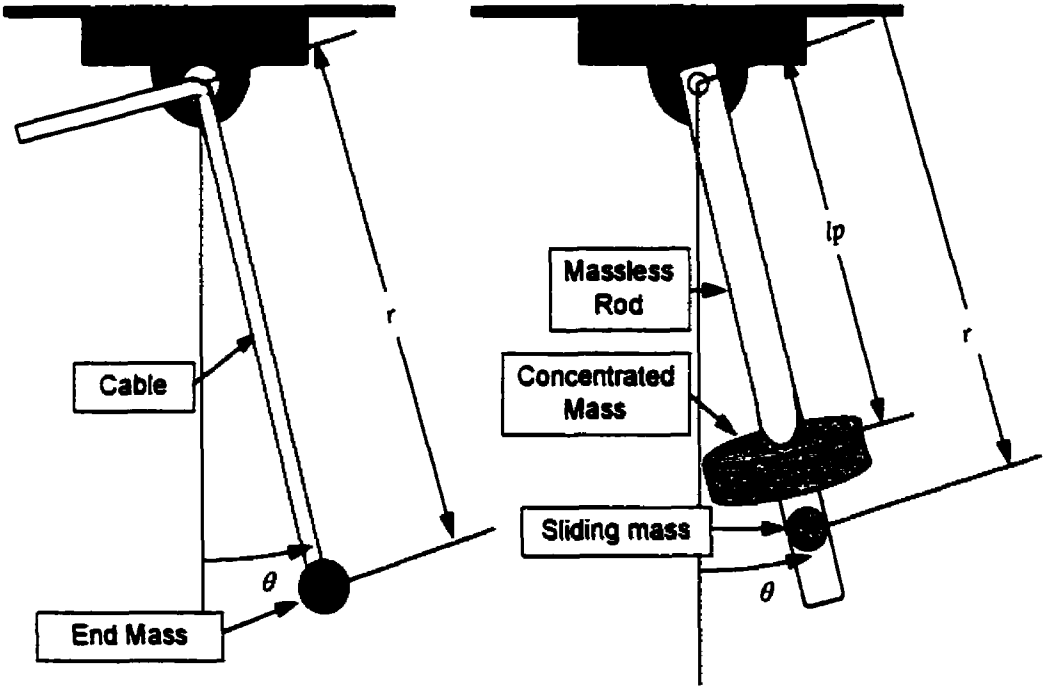

Figure D.1 Simple pendulum and physical pendulum models with mass reconfiguration.

The parameters used in the computer simulations to investigate the dynamics and to effect a controlled system are provide in Table D.1. Note that the parameterization was selected so that the natural frequencies of the systems were approximately equivalent; thus, comparison could be easily made.

Table D.1 Parameter Identification as used in the Simulations

Symbol	Description	Value	Units
θ	angular displacement of the system (measured with respect to the vertical)	variable	radians
θ_o	initial angular displacement of the system	$\frac{\pi}{6}$	radians
$\dot{\theta}$	angular velocity of the system	variable	rad/s
$\dot{\theta}_o$	initial angular velocity of the system	0	rad/s
$\ddot{\theta}$	angular acceleration of the system	variable	rad/s^2
t	time	[0,t]	second
g	acceleration due to gravity	9.81	m/s^2
m_p	mass of pendulum (structure)	7.5	kg
m_s	mass of the slider (auxiliary mass)	0.75	kg
l_p	location of concentrated mass of pendulum (pendulum length)	1.0	m
r	position of the auxiliary mass or force (measured radially from the pivot)	$Al_s(1-cos\omega t)$	m
$\dot{r}$	velocity of the auxiliary mass or force	$Al_s\omega\, sin(\omega t)$	m/s
a	amplitude for displacement profile	0.25	m
ϖ or ω_n	displacement frequency of force/mass profile	3.1321	rad/s

Appendix E: Initial Value Solvers

E.1. Introduction

Initial value solvers time step through a differential equation based on the initial conditions for the problem. Initial value solvers may be classified as:

1. direct methods,
2. multi-step, predictor-corrector or iterative methods, and
3. extrapolation methods.

All three types were programmed to ensure the results were representative of the governing differential equation or the existing physical phenomena and not artifacts of the simulation techniques. A modular style of programming provided ease in changing the initial value solver; however, for this study not all of the equations could be expressed explicitly in time and iterative routines needed to be developed.

Each method is briefly described with details of the algorithm as employed given.

E.2. Direct Methods: Runge-Kutta

The direct methods are one step integration methods that are self-starting and require only initial conditions or current values to begin. A fourth order, Runge-Kutta method was used. Runge-Kutta methods are multipurpose, commonly employed integrators.

Successive values are calculated based on the average slope with agreement to a Taylor series expansion. Each step is identical. The algorithm has a fourth order error associated with it and requires four

evaluation for each time step. In each step, the derivative is calculated at the initial point, twice at the temporary midpoint and at the endpoint. From these derivatives, the final function value is calculated as given by the Runge-Kutta formula:

$$k_1 = hf(x_n, y_n)$$

(E.1)

$$k_2 = hf\left(x_n + \frac{h}{2}, y_n + \frac{k_1}{2}\right) \tag{E.2}$$

$$k_3 = hf\left(x_n + \frac{h}{2}, y_n + \frac{k_2}{2}\right) \tag{E.3}$$

$$k_4 = hf(x_n + h, y_n + k_3)$$

(E.4)

$$y_{n+1} = y_n + \frac{k_1}{6} + \frac{k_2}{3} + \frac{k_3}{3} + \frac{k_4}{6} + O(h^5) \tag{E.5}$$

where f is the derivative defined by the right-hand side of the first order differential equation and h is the step size.

This technique provides solutions at regularly spaced intervals. Note that the high order of this technique does not guarantee high accuracy. To evaluate the accuracy the number of steps should be doubled and the results compared.

E.3. Multi-step Methods: Adams Predictor-Corrector

Multi-step or predictor-corrector methods process data from more than one previous time step using multiple methods to determine the value of the next time step. Two types of methods exist: explicit (or open) methods that define the solution in terms of the previously determined values and implicit (or closed) method which defines the solution using both sides of the value

and require interpolation. These methods are best suited for very smooth functions.

The Adams fourth order predictor-corrector method uses a four step, Adams-Bashforth method as the predictor and a three step Adams-Moulton method as the corrector. The Adams-Bashforth method is explicit. The Adams-Moulton technique is an implicit and provides fourth order accuracy.

The method is initiated with preliminary values of the routine found using the Runge-Kutta technique. The Adams-Bashforth method (Equation E.6) approximates the solution which is corrected by the Adams-Moulton technique (Equation E.7).

$$y_p = y_3 + h\left[55f(x_3, y_3) - 59f(x_2, w_2) + 37f(x_1, y_1) - 9f(x_0, y_0)\right] / 24 \qquad \text{(E.6)}$$

$$y = y_3 + h\left[9f(x, y_p) + 19f(x_3, y_3) - 5f(x_2, w_2) + f(x_1, y_1)\right] / 24 \qquad \text{(E.7)}$$

E.4. Extrapolation Methods

These methods extrapolate a result that would have been obtained if the step size were smaller. Early implementations were Bulirsch-Stoer and Richardson extrapolation methods. These techniques are best suited for smooth functions and those without singularities; however, these methods provided high accuracy solutions with minimal computational efforts.

The extrapolation technique used a variable step size [Burden and Faires, 1985]. Consistency in accuracy is monitored internally by the algorithm; numerical errors are controlled by automatically changing the step size. The variable step size routine essentially calls the algorithm for a smaller step and compares the results. Based on the compatibility with a predetermined accuracy criterion, an appropriate step size and solution is generated. The algorithm was adjusted by imposing that the output be generated at set intervals, yet allowing for the algorithm to initiate smaller step sizes if necessary. This technique used a difference method with error

expansion and an end error correction and is presented as Extrapolation Algorithm 5.6 [Burden and Faires, 1985].

E.5. Discussion

When the function being evaluated is relatively simple and does not require many manipulation extrapolation procedures are most efficient. Predictor-corrector methods are favored when the evaluation of the function is complicated. Runge-Kutta techniques are good general purpose methods. When good accuracy is required, Runge-Kutta should be used to provide good starting values for the advanced methods. As with any numerical approximation, it is desirable to attain sufficiently accuracy with the approximation with minimal effort.

Runge-Kutta Methods have high-order local truncation errors without requiring the computation and evaluation of derivatives of the functions. These techniques are one-step methods as the approximation for the next time interval is based solely on the previous time.

Appendix F: MATMATH—A Linear Algebra Software Package

MATMATH is a software utility package that was created and developed during this thesis project [Stilling and Watson, 1994a; Watson and Stilling 1991b]. The package performs fundamental linear algebra operations and unique element or data manipulation routines. The routines are categorized by function in Table F.1.

The matrix operations are intended for two dimensional arrays with provisions made for vector operations. The gamut of operations include: matrix defining operators, functions for matrix addition, subtraction, multiplication, determinants, inverse, eigenvalues/eigenvectors, norm computations, lower-upper triangular decomposition, solve utilities, copying and partitioning routines, conversion programs, element arithmetic operators and others.

The computations can be performed as either single or double precision arithmetic or short or long IEEE floating point arithmetic. Unique methods of memory management for complex operations enables returning computational resources.

This package was viewed as a major asset for the Forth community. Especially, since operators were state sensitive (that is, the code was accessible in both the interpret and compile states). The package has been developed with several Forth kernels for various computer platforms.

Table F.1: MATMATH Operator Index by Function

Matrix Structure and Type Declaration

MATRIX	DOUBLE#	FLOAT#	INTEGER#

Assignment Operators

BI_MAT	TRI_MAT	UNI_MAT

Matrix Input/Output Utilities

.MAT	123FILL	DIAGONAL	IDENTITY
HILBERT	M!	M@	MEDIT
MFILL	MRANDOM	MZERO	STACK->MAT
STACK->SYMM			

Matrix Operations

DETERMINANT	EIGEN	INVERSE	LUDECOMP
MMINUS	MMULT	MPLUS	SMULT
SOLVE			

Matrix Norm Operators

COL_NORM	E_NORM	NORM	ROW_NORM

Copying and Partitioning Utilities

COL_EXTRACT	COL_INSERT	DIAG->VECT	MCOPY
MEXTRACT	MINSERT	ROW_EXTRACT	MINSERT
ROW_EXTRACT	ROW_INSERT	TRANS_COPY	VECT->DIAG

Temporary or Dynamic Memory Management Operator

TEMP_MATRIX	TEMP_ALLOT	TEMP_DEALLOT

Matrix Parameter Interrogation Commands

?#BYTES	?#COLUMNS	?#ROWS	?DIMENSION
?TYPE	LMAT.NAME	RMAT.NAME	SMAT.NAME

Defining Operator

3ELEMENT_OP:	ELEMENT_OP:

Conversion Utilities

M?>D	M?>F	M?>S	MF>?

Element Arithmetic Operations

M1+	MABSOLUTE	MDIVIDE	MMULTE
MSQROOT			

The procedure for creating functional and readable code involves:

(1) declaring or creating the data structure (matrices);
(2) initializing the data structure;
(3) performing the required computations.

As evident from the equations presented in Chapter 5, neural network computations can be easily postulated in matrix algebra form. The operation as given by the following equation is essentially a series of nested, inner products,

$$y_i = \varphi\left(\sum_{k=0}^{K} w_{ik} \cdot \varphi\left(\sum_{j=0}^{J} w_{jk} \cdot \varphi\left(\sum_{i=0}^{I} w_{ij} \cdot x_i\right)\right)\right) \qquad \text{(F.1)}$$

The MATMATH source code for the operation of a multi-layer feed forward network is given below with non-executable comments following each backslash.

```
FLOAT#                          \ Selecting floating point as operating mode
4 7 MATRIX WJI                  \ Creating matrices for adjustable weighting
7 9 MATRIX WKJ
9 3 MATRIX WLK
4 1 MATRIX INPUT                \ Creating vectors for nodal outputs
7 1 MATRIX HL1
9 1 MATRIX HL2
3 1 MATRIX OUTPUT
' FTANH ELEMENT_OP: SQUASH      \ Creates the logistic squashing function;
                                \ assumes that ftanh defined and fl. pt. only.

: NN                            \ Defining executable program called NN
 TRI_MAT WJI INPUT HL1          \ Identifying matrices to be manipulated
    MMULT                       \ Matrix multiplication (inner product)
 UNI_MAT HL1 SQUASH             \ Apply activation function to each element
TRI_MAT WKJ HL1 HL2 MMULT       \ Identify and multiply for next layer of net
UNI_MAT HL2 SQUASH              \ Perform logistic squashing
TRI_MAT WLK HL2 OUTPUT MMULT    \ Calculations for next layer: inner product
UNI_MAT OUTPUT SQUASH           \ and logistic squashing
;                               \ Terminate program
                                \ To operate a trained net, enter NN
```

The package provided good flexibility in implementing and evaluating several nets [Stilling and Watson, 1991 and 1990]. Also, the package was initially used to solve the second order differential equations using the Runge-Kutta algorithm [Stilling, 1990a].

Appendix G:

Work-Energy Balance for the Pendulum Systems

The freely oscillating, constant length pendulum represents a conservative system. As the pendulum oscillates, energy is transformed between kinetic and potential energy. The total energy of the system remains constant and is equivalent to the initial energy of the system. The energy balance for the system is defined as:

$$(T+U)_{t_1} = (T+U)_{t_2} \tag{G.1}$$

where T represents the kinetic energy;

U, the potential energy, and

t_1 and t_2 represent instances in time.

The pendulum systems with mass reconfiguration is nonconservative. As the mass is moved along the oscillating pendulum, energy is either added or removed from this system. The work done in moving the mass accounts for the change in total structural energy, as indicated in the work-energy balance,

$$(T+U)_{t_1} + W_{1-2} = (T+U)_{t_2} \tag{G.2}$$

where W_{1-2} represents the work done over the time interval from t_1 to t_2.

The work associated with moving the end mass is the product of the force applied to move the mass and the corresponding motion, as given by

$$W_{1-2} = \int_{s_1}^{s_2} \vec{F} \cdot d\vec{s} \tag{G.3}$$

where $\vec{F}$ represents the force applied to the moving mass and

$d\vec{s}$ represents the motion of the mass between the limits s_1 and s_2.

As previously defined in Chapter 2 and 3, the force applied to the end mass is given by

$$F = m_s\left(\dot{\theta}^2 r - \ddot{r} + g\cos\theta\right) \tag{G.4}$$

where m_s is the mass of the sliding or moving mass;

g, the acceleration due to gravity;

θ and $\dot{\theta}$, the angular displacement and velocity of the mass; and

r and $\ddot{r}$, the translational displacement and acceleration of the mass, respectively.

For the case of a variable length pendulum, this force defines the tension in the cable. The force is assumed positive if the cable is to remain taut. Since this force is not constant, the work for the same net displacement may also vary. To account for the change in total energy over an extended time period requires tracking the incremental work done; that is a cumulative sum of the work during the interval must be tallied.

For the variable length pendulum, when the motion of the end mass was defined as being sinusoidal with a tuned frequency, the work-energy balance was monitored. For each time step of the simulation, an average force and the related work were calculated. As the initial value solvers tend to be prone to cumulative error, the work-energy balance was performed over the simulation run as given below,

$$WE = \sum_{1}^{n} W_{(i-1)-i} + T_i + U_i \tag{G.5}$$

where i indicates the current time step;

n, the number of time steps in the simulation run; and

WE, the work-energy sum for the system[1].

When accounting for all forms of energy and work done, the value of WE should remain constant and be equivalent to the initial system energy.

[1] When integrating Equation H.3 using a trapezoidal routine, the integration error was considerably larger than the initial value solver. Thus, smaller time steps were required to maintain the work-energy balance.

This provided a further measure of the accuracy of the numerical simulation. As shown in Figure G.1, the work-energy term (WE) remains constant. Note also that potential and kinetic energy is transformed as the pendulum oscillates and the moving mass performs work to change the net energy state of the system.

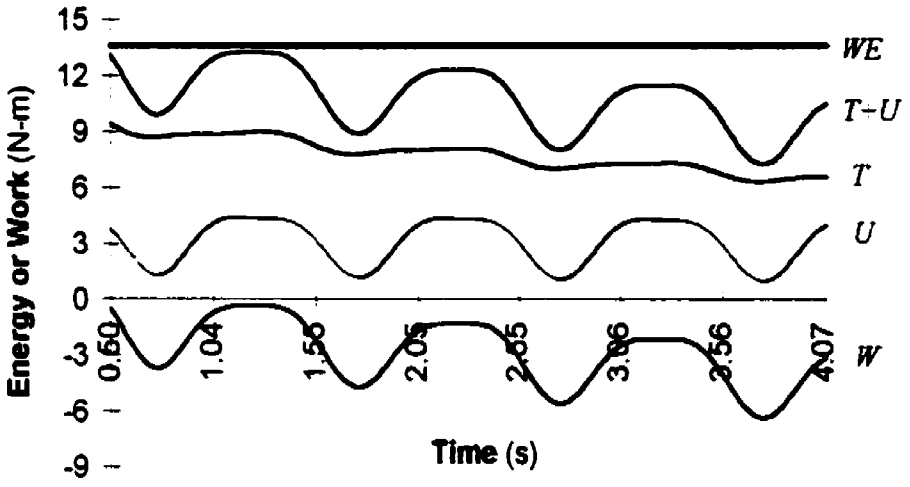

Figure G.1 Work-Energy balance performed when the mass is reconfigured sinusoidally.

Appendix H: Simulating Mathieu's Equations

Mathieu's equation (Equation 3.15) were simulated based on the parameterization for the physical systems as given in Appendix D. Namely, the governing differential equation for the reconfigurable mass pendulum system (Equation 2.10) was reformulated to a fractional order of Mathieu's Equations (Equation 3.19) under the assumptions of small angular oscillations and small harmonic, slider motion at twice the frequency of the angular oscillations.

The displacement profiles were simulated and appear in Figure H.1 with the viscous-equivalent damper (as derived in Section 3.3.3), where the $a = 1$ and $q = 0.125$ for Equation 3.15 and $\bar{a} = 1$, $q = 0.125$ and $\kappa = 0.1875$ for Equation 3.19.

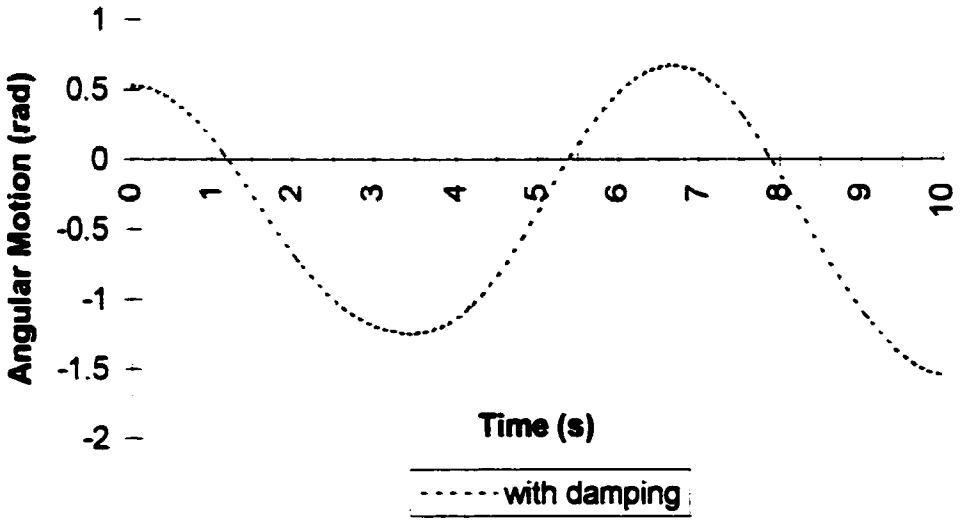

Figure H.1 Angular displacement profile for the first instability zone for Mathieu's Equation of Fractional Order 3.23 (with damping).

Also, frequencies were selected to investigate the second and third instability zone. For these cases, the parameterization for Equation 3.15 were $a = 4$ and $q = 0.25$ for the second zone and $a = 9$ and $q = 0.5625$ for the third zone, and for Equation 3.19 the parameterization were $\bar{a} = 4$, $q = 1$ and $\kappa = 0.375$ for the second zone and were $\bar{a} = 9$, $q = 1.125$ and $\kappa = 0.5625$ for the third zone. The displacement histories for the first few cycles are illustrated in Figures H.2 and H.3, respectively.

The relation between stability and instability are characterized as bounded or oscillatory motion and unbounded (divergent) unlimited growth of the displacement profile. As shown, for the chosen parameterization, the dynamics lie along the characteristic curve and the undamped case exhibits neutral stability.

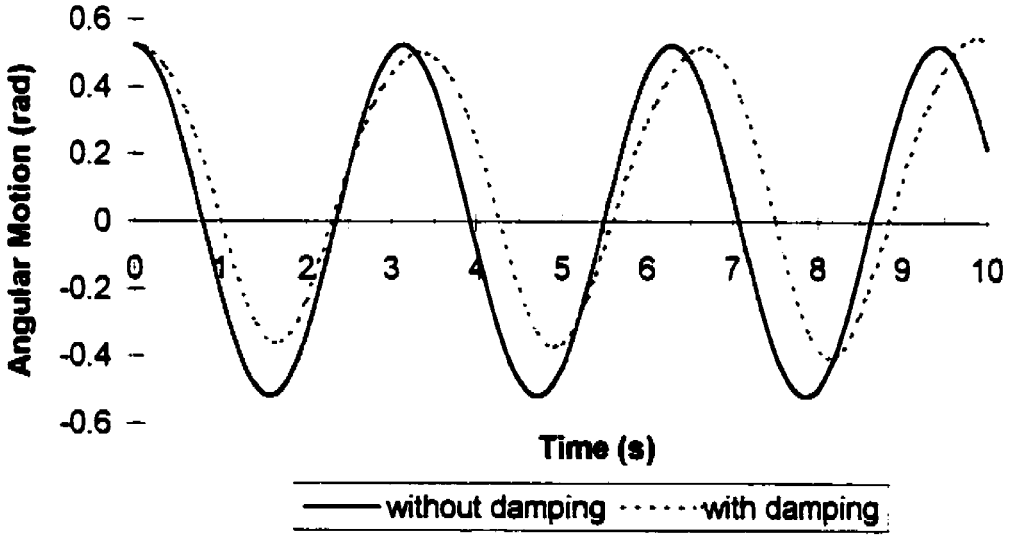

Figure H.2 Angular displacement profile for the second instability zone: Mathieu's Equation 3.15 (without damping) and Mathieu's Equation of Fractional Order 3.19 (with damping).

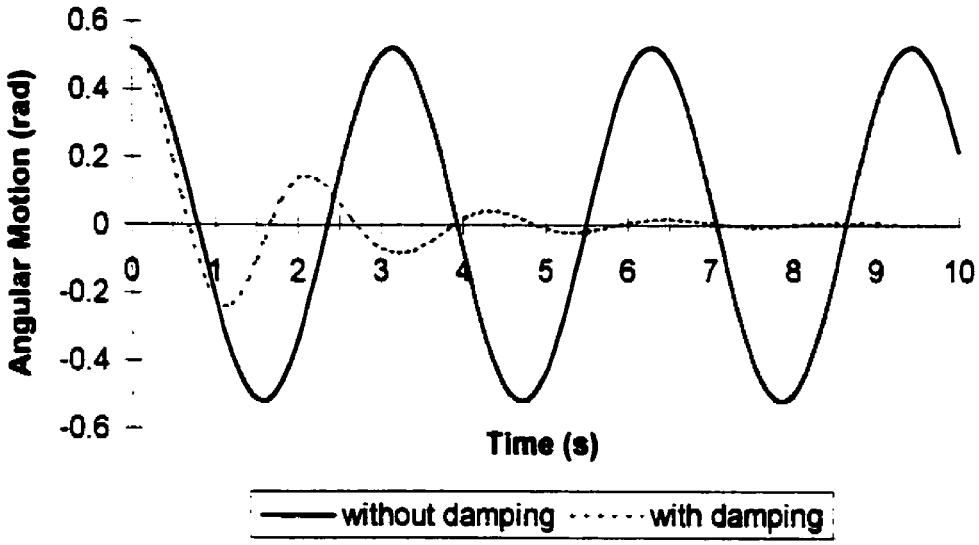

Figure H.3 Angular displacement profile for the third instability zone: Mathieu's Equation 3.15 (without damping) and Mathieu's Equation of Fractional Order 3.19 (with damping).

Appendix I:

Sinusoidal Mass Reconfiguration
(at integer multiples of the structural, natural frequency)

I.1 Introduction

The reconfiguration of the mass at integer multiples of the structural, average natural frequency was simulated. The frequencies of interest were when the mass moved at the same frequency as the structural frequency, at nine (9) and sixteen (16) times the natural frequency. The latter were chosen as they correspond with instability zones predicted by Mathieu's Equations.

The parameterization for the pendulum systems were based on values presented in Appendix D.

I.2 Mass Reconfiguration at the Same Frequency as the Structural, Natural Frequency

The angular displacement of the pendulum as the mass is reconfigured at the same frequency as the average natural frequency of the pendulum is studied. The temporal profiles of the angular motion and the position of the traversing auxiliary mass are shown in Figures I.1 and I.2 when the translational mass motion is initially in phase and out of phase with angular oscillations, respectively. Figure I.3 shows the phase portrait for the initial 50 seconds (~25 time constants).

When the motion is in phase ($\phi = 0$), the resulting angular displacement is symmetric and at the same frequency as shown in Figures I.1 and I.3(a). For the case, where the motion is out of phase ($\phi = \pi/2$ rad), the

motion is antisymmetric, Figures I.2 and I.3(b). The amplitude of angular oscillation is not affected appreciably by the mass motion during the first few periods.

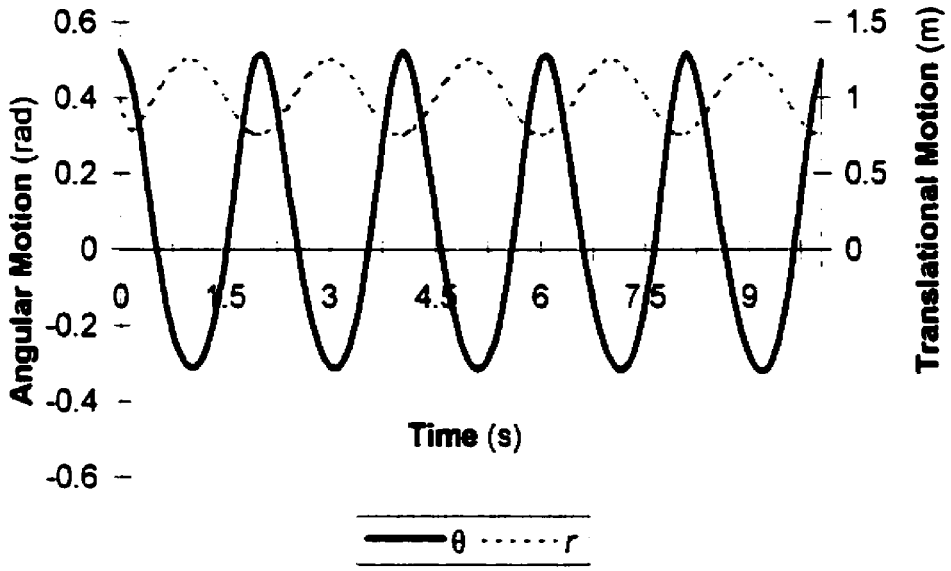

Figure I.1 Coordinated temporal kinematic profiles -- simple pendulum with mass motion of $r(t) = R_o - \Delta r \sin(n\omega t + \phi)$ where $n = 1$ and $\phi = 0$.

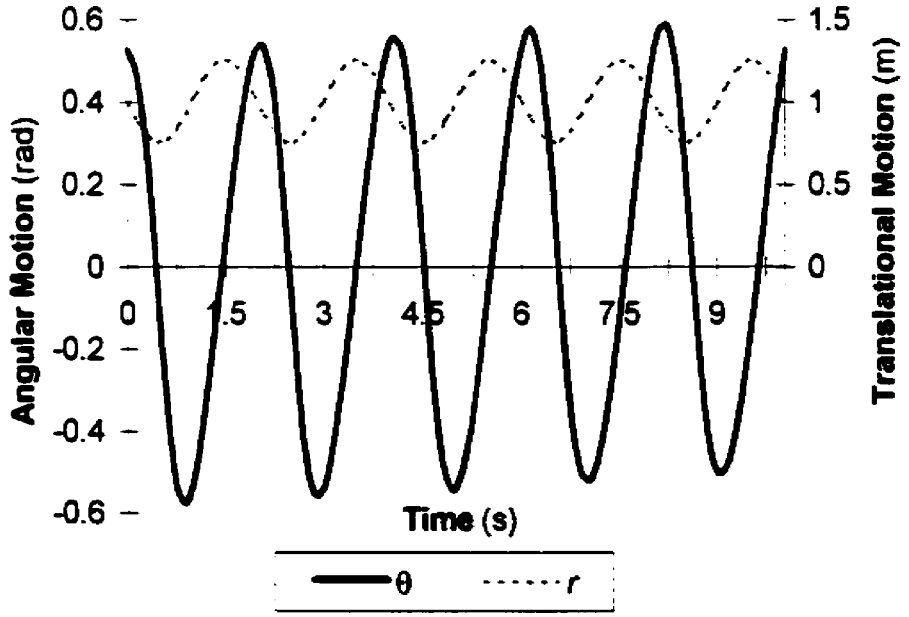

Figure I.2 Coordinated temporal kinematic profiles – simple pendulum with mass motion of $r(t) = R_o - \Delta r \sin(n\omega t + \phi)$ where $n = 1$ and $\phi = \pi/2$.

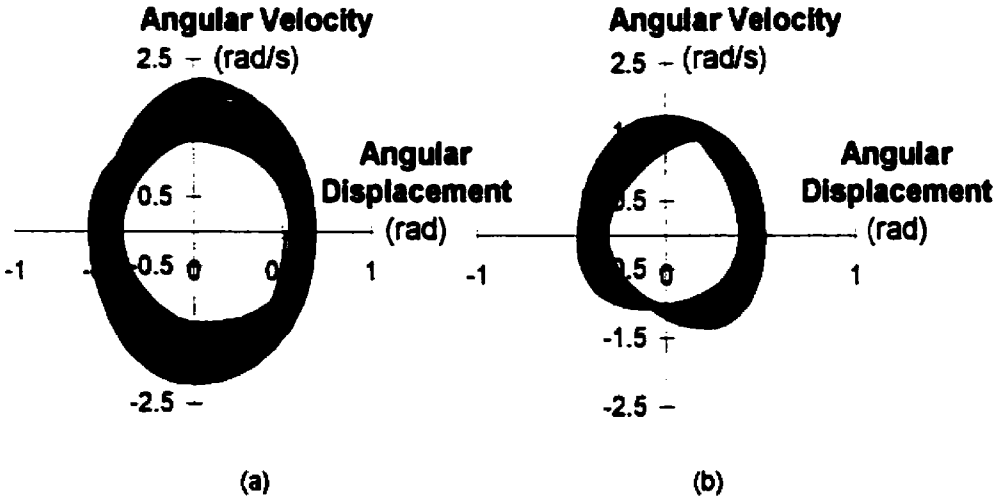

Figure I.3 Phase plane plots of the angular pendulum motion when (a) $\phi = 0$ and (b) $\phi = \pi/2$ for the translational mass displacement.

The forces that are required to generate these sinusoidal motions for the mass are illustrated in Figure I.4. Both profiles are continuous and converge in the steady state.

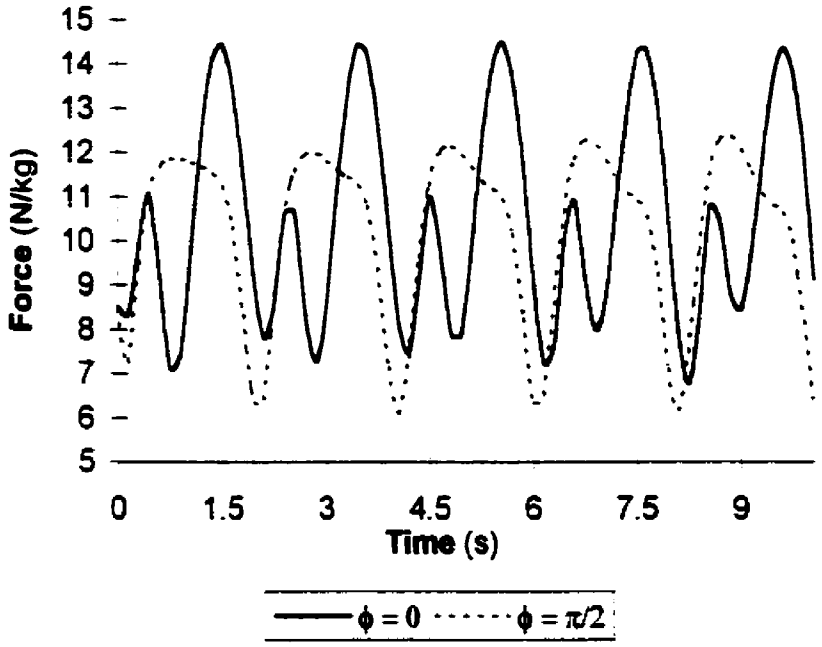

Figure I.4 The driving force to effect sinusoidal auxiliary mass motion.

Similar behavior was observed for the physical pendulum system. However, the motion of the system tended to be more symmetrical than observed for the simple pendulum.

I.3 Mass Reconfiguration at Nine Times the Structural, Natural Frequency

As predicted by Mathieu's equations a zone of instability should occur when the frequency is nine (9) times the natural frequency of the system. The two extreme cases where the mass motion begins either in or out of the phase were simulated for both the simple and physical pendulum. The pendulum dynamics were similar to those of Mathieu's equation as shown in Appendix H; namely, the motion was oscillatory without any unstable, divergent behavior as shown in the phase plot of Figure I.5.

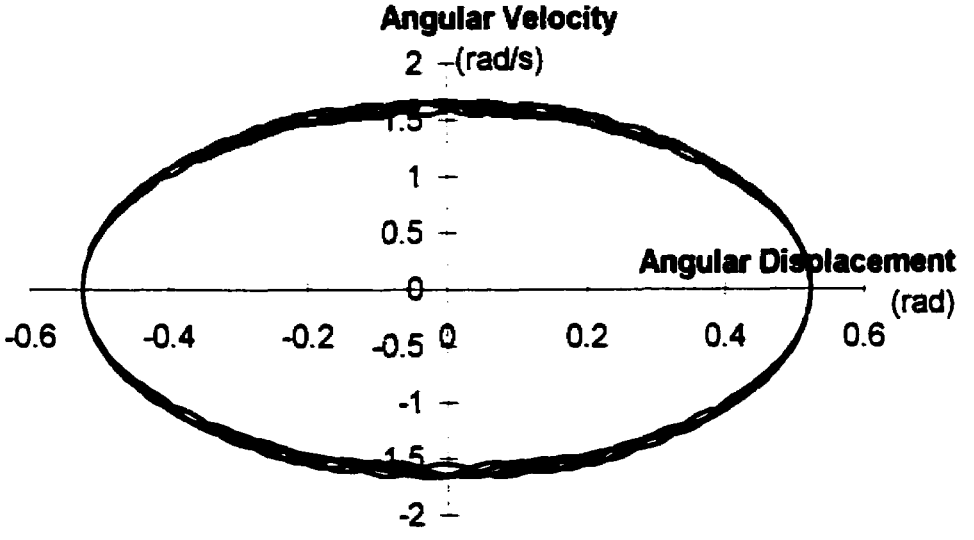

Figure I.5 Oscillatory angular displacement history for ten time constants.

By examining the mass-normalized energy change for this reconfiguration profile (similar to Section 3.3.3) gives

$$\frac{\omega_n^2 \pi \theta_o^2 \varepsilon}{12}\left[15\sin\left(\frac{2}{3}\omega_n t\right) - \frac{9}{4}\sin\left(\frac{4}{3}\omega_n t\right) - \frac{9}{8}\sin\left(\frac{8}{3}\omega_n t\right)\right]\Big|_0^T + O\left(\varepsilon^2\right) \qquad (I.1)$$

Note this expression does not contain a secular term as was the case when the mass reconfiguration was at twice the natural frequency of the angular oscillations.

I.4 Mass Reconfiguration at Sixteen Times the Structural, Natural Frequency

From Mathieu's Equations another instability zone should occur when mass reconfiguration is at sixteen (16) times the structural natural frequency. The coordinated dynamics for the simple pendulum are illustrated in Figure I.6 and those for the physical pendulum are shown in Figure I.7. Note that these simulations were completed with a time step of 0.005s.

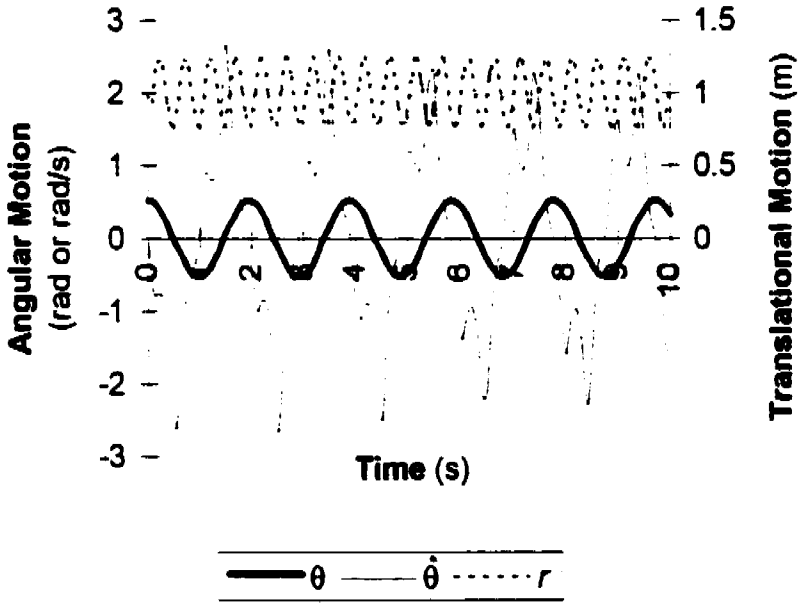

Figure I.6 Coordinated dynamics for simple pendulum with the mass motion of $r(t) = R_o - \Delta r \sin(n\omega t + \phi)$ where $n = 16$ and $\phi = \frac{\pi}{2}$.

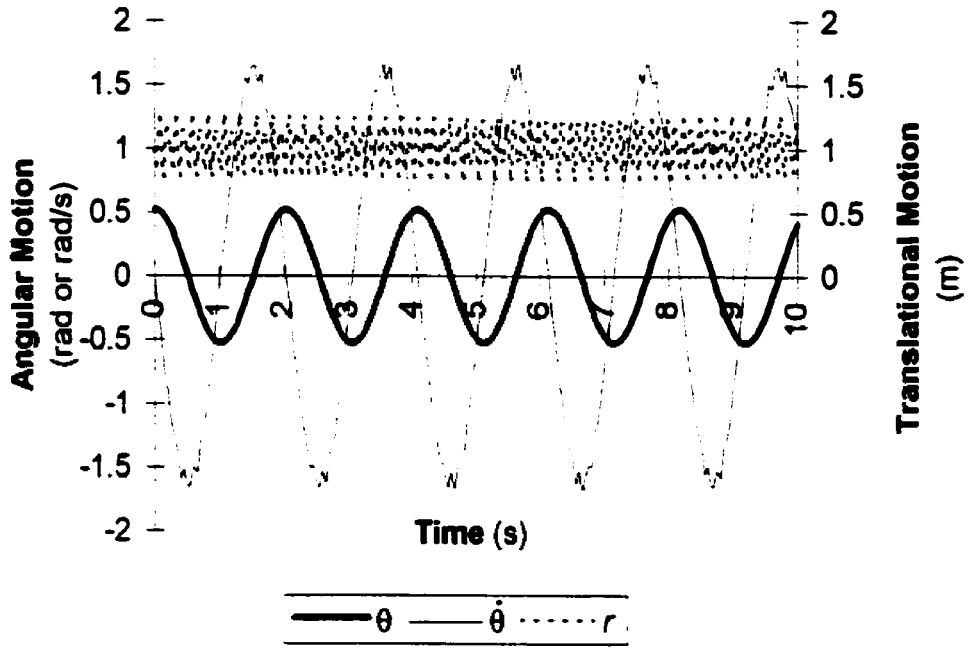

Figure I.7 Coordinated dynamics for physical pendulum with mass motion of $r(t) = R_o - \Delta r \sin(n\omega t + \phi)$ where $n = 16$ and $\phi = \frac{\pi}{2}$.

The kinematic profiles indicate stable, oscillatory motion for these parameters. For the simple pendulum, the energy dissipation over a period can be approximated by the following expression,

$$\frac{\omega_n^2 \theta_o^2 \varepsilon}{4}\left[5\sin\left(\frac{1}{4}\omega_n t\right) - \frac{3}{14}\sin\left(\frac{7}{4}\omega_n t\right) - \frac{1}{6}\sin\left(\frac{9}{4}\omega_n t\right)\right]\Big|_0^T + O\left(\varepsilon^2\right). \qquad (I.2)$$

Note that there is no secular term.

Appendix J: Optimization and ANN Training Algorithms

J.1 Introduction

Optimization has been applied throughout the research. In particular, mass reconfiguration profiles and supervisory training algorithms for the artificial neural networks were developed using optimization techniques. The optimization process and techniques are presented herein with respect to training the neural networks.

J.2 Overview of the Optimization Process

Optimization describes the process of determining the "best" solution or design. As applied in this research, optimization techniques were applied to determine mass reconfiguration profiles that would attenuate the structural vibrational energy (Section 4.6) and to set values of the weighting matrices to train the artificial neural network to learn input-output patterns.

The optimization process essentially determines extrema of an objective or cost function. This function mathematically represents the design problem and through proper parameterization of the design variables a "best" solution is discerned. For the mass reconfiguration problem, the objective function defined the structural energy in terms of the mass reconfiguration; that is, the design variables defined the mass displacement profiles. For the neural net training the objective function was reducing the error between net generated output and desired output values; the design variables were the adjustable weights.

Algorithms that are used to determine optimal solutions may be classified according to the search process. The search process is based on

the objective function and the degree or order of the optimization method is determined by the information used in the objective function. For example, zero order methods require only an evaluation of the function; whereas, first order methods use the first derivative of the objective function.

The techniques used in this research were iterative in nature. Convergence criteria were set based on executing a set number of iterations or evaluating the change in the objective function for design changes.

The optimization methods used included steepest descent, coordinate search, conjugate gradient, Powell, quasi-Newton, evolutionary programming and genetic algorithm methods. Each technique is described as implemented for the neural net training. The majority of the mass reconfiguration optimization was done using evolutionary algorithms. The final training for the neural networks used a direct first order method.

J.3 Optimization for Training the Neural Networks

A very important feature of artificial networks is their adaptive nature; they "learn by example" rather than by traditional pr ogramming. This process is called "training" of the neural network. The training process is presented in Appendix K, whereas, this section discusses the algorithms used to training the network. The training process was viewed as unconstrained minimization where the error[4] represented the cost function and the adjustable weights were the design parameters. For each net, its structure (number and types of nodes and connections, etc.) was predetermined. The design space is defined by the possible values for the design parameters (that is, the adjustable weights and thresholds). Through optimization techniques the

[4] For a single patterm, the error for a particular output node can be defined as $e_l = \left(y_l^d - y_l\right)^2$ where e_l represents the error signal of the lth output; y, an output value; and the superscript, d, indicates the desired output for the given input signal.

value of the adjustable weights are determined, so that the error function is minimized.

Computationally, the optimization algorithms should involve minimal computational effort and not be memory expensive; thus, ideally, the function should be evaluated as few times as possible. Optimization methods find either global (true maximum or minimum values) or local (maximum or minimum values for a given region) extremum; usually finding the global extremum is desirable. Although training trials from different starting points were completed and did produce different weighting values for this control application, finding a global minimum was not ensured.

When this phase of research was conducted, the accepted and popular, general purpose training technique for multi-layer networks was back propagation[5] [Rumelhart et al., 1986; Lippman, 1987]. Due to encountered inefficiencies when training the networks, other optimization techniques were applied; namely, coordinate search, conjugate gradient, Powell method, quasi-Newton methods and evolutionary algorithms. Many of these techniques provided significant acceleration in the training process as compared to the simple pattern or batch modes of back propagation. It should be noted that the application of these optimization strategies for training neural networks was completed independently of those that have since been published in the literature.

J.4 Training Algorithms

As each technique is well-documented elsewhere in the literature, only a brief overview of the algorithms with the specific adjustments for training neural networks follows.

---

5 Rosenblatt in 1959, proposed the training technique for simple nonlinear tasks with perceptron training.

J.4.1 Back Propagation

Back propagation is a gradient search technique applied to supervised, error-based neural network training. Its implementation is attributed to work by Werbos, Parker, Widrow and Hoff and Rumelhart and McClelland [Freeman and Skapara, 1991]. Essentially, this technique is steepest descent optimization method as used in least square curve fitting. This technique was initially used in this research [Stilling, 1990a].

As shown in the flowchart of Figure J.1, the cost function between the desired output and those generated by the net is minimized by adjusting the weights. After initializing the adjustable connections, the process involves repeated presentation of input-output patterns with the weights being adjusted. The process requires the state of all nodes be computed for each presentation of training data, starting from the bottom layer (input) and moving to the top layer (output), then the error is calculated based on the difference between the generated and the desired or target values. The variables of the net are then adjusted by propagating the error backwards through the net. The back propagation algorithm follows the flowchart.

As shown, the output from a node is calculated as the nonlinear weighted sum of the preceding nodes (Block 3 of Figure J.1) or in terms of only the previous layer can be defined as:

$$y_j = \varphi(v_j) \tag{J.1}$$

where $v_j = \sum_{i=0}^{I} w_{ij} y_i$ (J.1a)

and y_i is the input of the ith node;

w_{ij}, the adjustable weight connecting the y_i node to y_j node;

v_j, the weighted sum of the inputs to the jth node;

φ, the nonlinear activation function[6]
(an exponential sigmoid function is assumed);

y_j, the output of the jth node; and

J, is the number of nodes in the jth layer.

[6] The activation function is assumed to be a sigmoid function.

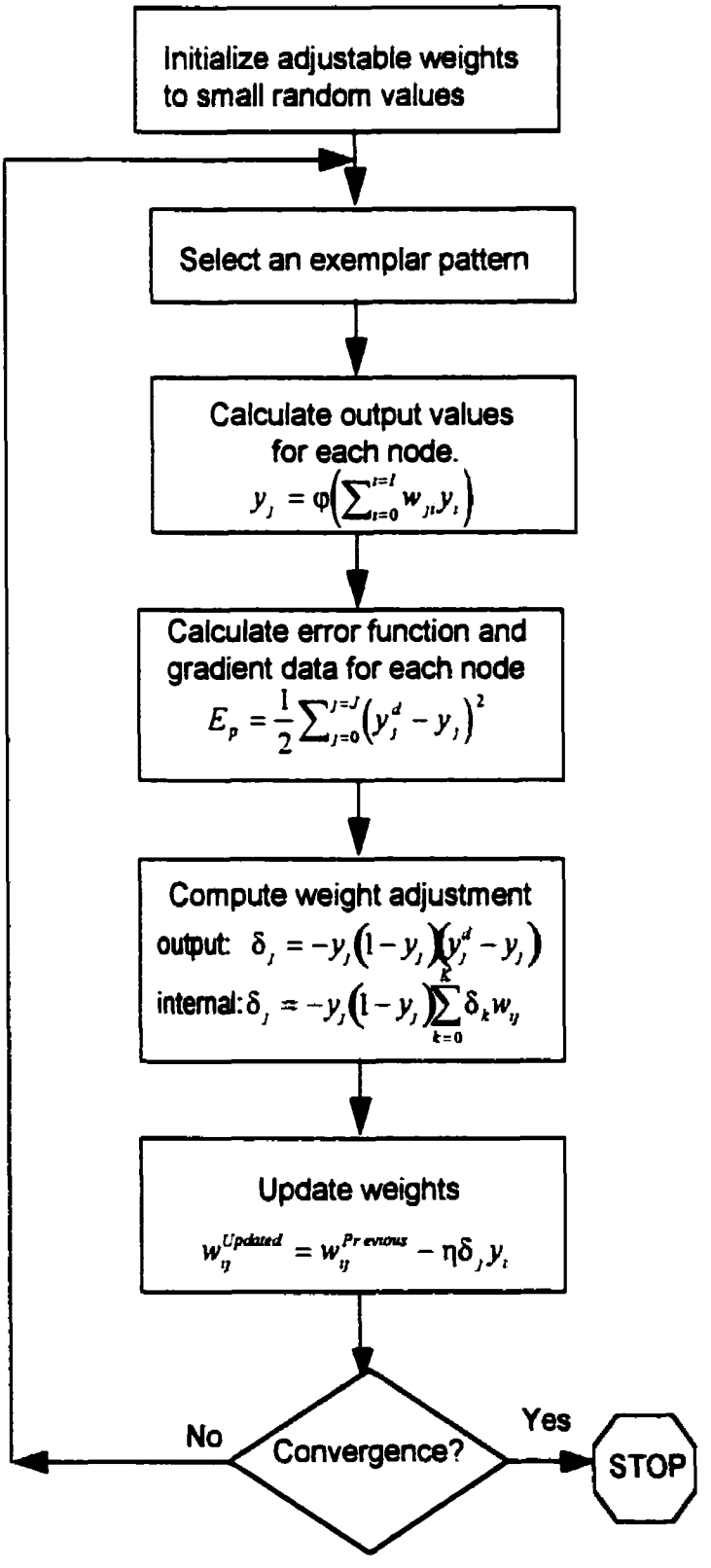

Figure J.1 Flowchart of Back Propagation Algorithm.

Then, the error associated for a given pattern (E_p) for the above node is calculated (Block 4 of Figure J.1) or in terms of the jth layer can be stated as

$$E_p = \frac{1}{2}\sum_{j=0}^{J}\left(y_j^d - y_j\right)^2 \tag{J.2}$$

where the superscript d indicates a desired or target value.

Next, the error corrections are calculated based on derivative of the error by applying the chain rule;

(1) for an output node as

$$\frac{\partial E_p}{\partial w_{ij}} = \frac{\partial E_p}{\partial v_j}\frac{\partial v_j}{\partial w_{ij}} = \frac{\partial E_p}{\partial y_j}\frac{\partial y_j}{\partial v_j}\frac{\partial v_j}{\partial w_{ij}} = \delta_j y_i \tag{J.3}$$

where $\frac{\partial v_j}{\partial w_{ij}} = y_i$ (J.3a)

$$\frac{\partial v_{ij}}{\partial v_j} = y_j\left(1 - y_j\right) \tag{J.3b}$$

$$\frac{\partial E_p}{\partial y_j} = -\left(y_j^d - y_j\right) \tag{J.3c}$$

and

(2) for internal node as

$$\frac{\partial E_p}{\partial y_j} = \sum_{k=0}^{K}\frac{\partial E_p}{\partial v_k}\frac{\partial v_k}{\partial y_j} = \sum_{k=0}^{K}\frac{\partial E_p}{\partial v_k}w_{jk} = \sum_{k=0}^{K}\delta_k w_{jk} \tag{J.4}$$

The adjustment to the weight can be summarized for the output node as,

$$\delta_j = -y_j\left(1 - y_j\right)\left(y_j^d - y_j\right) \tag{J.5}$$

and for the internal nodes as,

$$\delta_j = -y_j\left(1 - y_j\right)\sum_{k=0}^{K}\delta_k w_{ij} \tag{J.6}$$

The weight adjustment equation (Block 6 of Figure J.1) can now be defined as

$$w_{ij}^{Updated} = w_{ij}^{Previous} - \eta\frac{\partial E}{\partial w_{ij}} = w_{ij}^{Previous} - \eta\delta_j y_i \tag{J.7}$$

where η is the learning rate or step size associated with the weight adjustment.

To summarize, this gradient search technique defines the error as the difference between desired and net generated output. Weights are initially selected as small random numbers that are adjusted based on gradient information. The error is propagated backwards from the top layer back to the input layer. This algorithm is vulnerable to local minimums and often converges slowly near a minimum requiring small steps.

J.4.2 Coordinate Search Method

The coordinate search method searches the possible solution domain or the design space by repeatedly finding minimums for each variable's direction. For the neural net application one weight is adjusted while the remainder are fixed until a minimum value is reached. Then, the next weight is adjusted with the other weights being held constant. These independent single variable optimizations are continued until all the variable (weights) have been independently adjusted. Then, the process is repeated until convergence to a minimum or an acceptable value has been reached. This method requires only functional evaluations throughout in seeking a minimum value. The single variable optimization method used was Brent's method [Press et al., 1992a&b].

J.4.3 Conjugate Gradient Technique

With this technique, the search directions are conjugate gradients of each other (orthogonal and conjugate to one another)[5]. For a set of N linearly independent, mutually conjugate directions, N line minimization will converge

---

[5] Given the vectors, $g_{i+1} = g_i - \lambda_i A \cdot h_i$
$h_{i+1} = g_{i+1} + \gamma_i h_i$
where $i = 0,1,2...$; λ and γ are scalars, and A is a matrix, and $h_o = g_o$, the vectors are considered conjugate and orthogonal if they satisfy the following:
$g_i \cdot g_j = 0 \quad h_i \cdot A \cdot h_j = 0 \quad g_i \cdot h_j = 0 \quad i \neq j$.

to the minimum for a quadratic function. If the function is not quadratic the minimization process requires repeated cycling though the N line searches.

To determine a conjugate direction to the preceding search (and previous searches), the derivative of the function is calculated at each point from where the search is initiated. The technique as programmed was a combination of the Fletcher-Reeve and Polak-Ribiere versions of the conjugate gradient [Press et al., 1992b]. In training the neural networks, the derivatives were approximated numerically. A one-dimensional, sub-minimization routine was applied along each search method; for this research the Brent method was used [Press et al., 1992a&b].

By using the conjugate gradient to determine search directions, noninterfering directions are followed and convergence to the minimum is quicker than gradient information. However, in calculating the derivative information additional computations are required. Generally, the computational savings in the rate of convergence exceeds the extra functional calculations of the conjugate directions.

J.4.4 Powell Method

The Powell method is also a direction set method for multi-dimensions. The technique does not require the calculation of derivative information which can become quite involved for the neural network error function. This method uses one-dimensional search techniques to bracket and converge to the solution. The technique through repeated iterations has been shown to generate conjugate gradient search directions for multi-design variables for quadratic functions.

Basically, the process for the Powell method involves searching along the basis vectors which correspond to the direction of each design variable (that is, the direction associated with each adjustable weight is searched until a minimum is found for that direction). Then by combining these previous searches, a new set of directions are generated. After several iterations, the

directions generated will be mutually conjugate, if the function is quadratic [Press, et al., 1992b]. Otherwise, the search sequence is repeated.

To summarize the procedure is as follows:

(a) select the basis vector (direction of each adjustable weight) as the set of search directions;

(b) search a direction (along the weight direction) until a minimum is reached;

(c) record the distance traveled in this direction;

(d) then, repeat steps (b) and (c) for each search direction;

(e) create a new search direction based on the vector summation of the distance traveled along the search direction;

(f) search along this "conjugate direction";

(g) discard the first search direction;

(h) using the newly generated set of search directions repeat steps (b) through (h) to reach the minimum of the function (error function).

A known fault of this method is that searching may result in parallel search directions (linearly dependent) being generated which requires the process be restarted or adjusted.

For the research reported herein, the line search steps (referred to in step (b)) used the Brent Method [Press, et al., 1992a&b]. The majority of the results for the artificial neural networks were trained using this method. These algorithms with source code appear in Numerical Recipes in Fortran [Press, et al., 1992a] and Numerical Recipes in C [Press et al., 1992b]. For this study, the algorithms were programmed in the Forth language.

J.4.5 Other Search Methods

Variable Metric Methods were also applied to train neural networks. These techniques are called quasi-Newton methods. Similar to conjugate gradient methods, data from successive line minimization are accumulated. These techniques require the computation of the actual gradients and cumulatively store updated information. The algorithms used included

Davidon-Fletcher-Powell and the Broyden-Fletcher-Goldfarb-Shanno technique [Marasco, 1986a&b]. These techniques were successfully applied to the benchmark problem (see Appendix K); however, the memory requirements were viewed as being extensive and was not applied to the control problem being studied.

J.4.6 Evolutionary Algorithms

These optimization methods are zero order, random search methods that are based on the "principles of evolution" or "survival of the fittest". The methods are classified as either genetic algorithms or evolutionary programs. The primary difference is that genetic algorithms searches several directions in parallel as multiple solutions are being optimized collectively; whereas, evolutionary programming operates by comparing two solutions. Also, historically, the original genetic algorithm proposal [Holland, 1975; Goldberg, 1989; Michealwicz, 1992] requires the set of design parameters be binary encoded.

Basically, the genetic algorithm process can be summarized by the flowchart of Figure J.2.

When applied to neural networks training, this optimization examines the net globally rather than examining the single weights using gradient or conjugate gradient information as the previous techniques do. The first step was to represent the adjustable connecting weights as genetic code; this was done by representing the weights as a floating point vector. The second adjustment was to transform the error minimization to a maximization problem to create a fitness evaluation; this was done by negating the error function.

The fitness function was defined as

$$F(\ ) = \begin{cases} -E(\ ) & \text{if } E(\ ) \geq 0 \\ 0 & \text{otherwise} \end{cases} \tag{J.8}$$

Note that the error was calculated for the entire training suite. Another technique to transform weights selection to a minimization problem can be formed from

$$F(\ ) = \frac{F_{MAX} - F_{MIN}/a}{F(w_t) - F_{MIN}/a} \tag{J.9}$$

where F_{MAX} and F_{MIN} are the evaluated fitness functions maximum and minimum values, and a is a control parameter selected between 1.01 to 1.001.

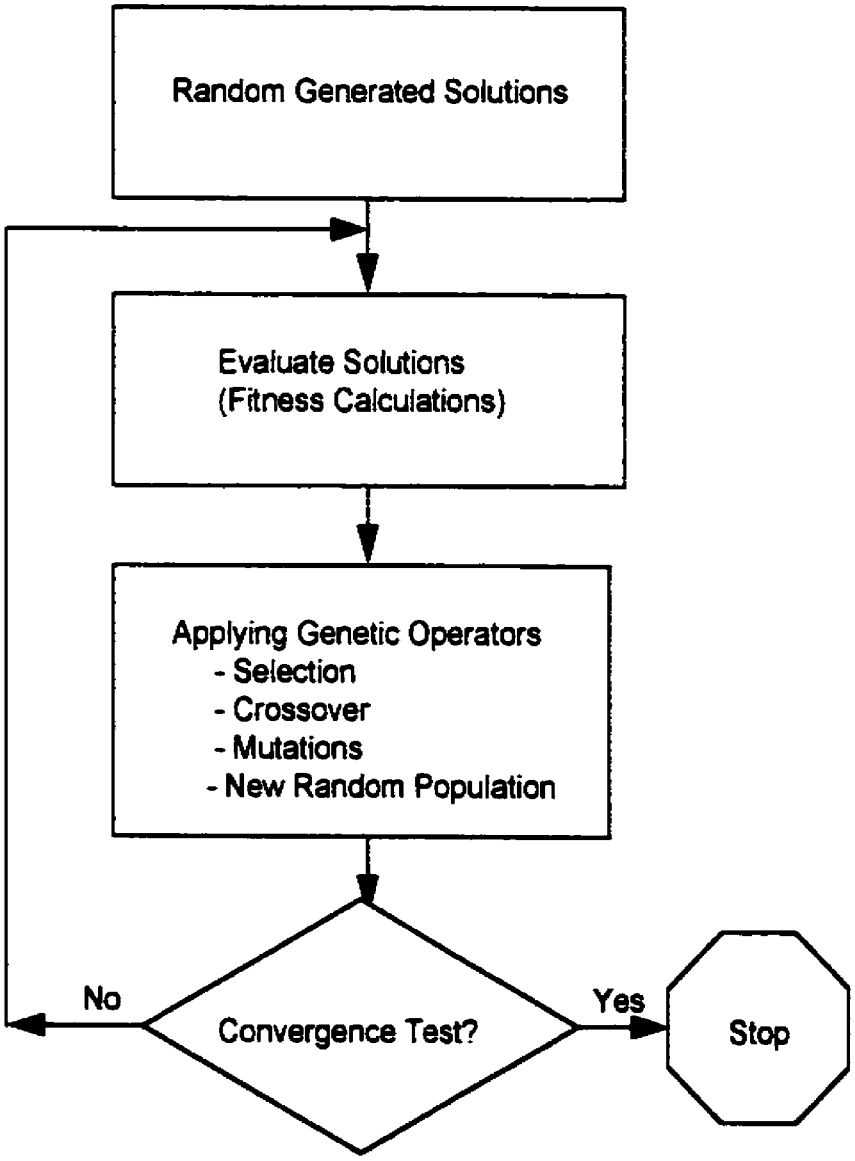

Figure J.2 Flowchart for a genetic training algorithm.

Next, the genetic operators that emulate biological evolution processes of selection, reproduction (or cross-over) and mutation are applied iteratively.

First, the selection process allows the best solutions to be retained; those solutions with higher fitness have a greater chance of reproducing.

$$Population\ Selection = \frac{F(w_i)}{\sum_{j=1}^{N} F(w_j)} \qquad (J.10)$$

where w_i and w_j are adjustable weight vectors within the population; N, the number of vectors in population set; and $F(\ )$, fitness value.

The cross-over operation is effective at the beginning of the search process. To perform cross-over, the weighted strings from the population set are "spliced", the parts are exchanged, then rejoined as shown pictorially in Figure J.3, the adjustable weights being represented by lower case letters. The cross-over point (place where the splice occurs) may be fixed, flexible (or randomly chosen) or multiple based on a given mask.

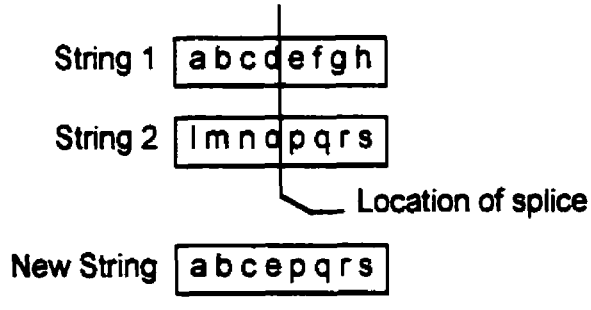

Figure J.3 Illustration of the cross-over genetic operation.

The mutation operator provides additional randomness as a few weights are adjusted by small random amounts. This process avoids premature convergence to local optimal by introducing diversity. Also, a few new solutions may be randomly generated and added to the set. Then, the process is repeated until convergence to a suitable solution is obtained.

Appendix K: Artificial Neural Networks

K.1 Introduction

Artificial neural networks can be defined simply as an interconnected system of parameterized functions. In this appendix an overview of the artificial neural networks with the various considerations made in developing the neural network as the control unit are presented. The details associated the architecture and topology (or the type of interconnections), its operation and the training considerations.

K.2 Net Morphology: The Neuron Model

The basic computation element[6] of the artificial neural net was selected to be a nonlinear, weighted sum model that contained a bias or threshold parameter. This model, a weighted summation with threshold, has become commonplace in defining and implementing neural networks. Mathematically, each neuron performs the following operation:

$$y = \varphi\left(w_o x_o + \sum_{i=1}^{I} w_i x_i \right) = \varphi\left(\sum_{i=0}^{I} w_i x_i \right) \tag{K.1}$$

where the variables have been previously defined in Equations 5.2 and 5.3 with a bias parameter being included as a new synapse with fixed input, $x_o = 1$ and value given by the weight, w_o. The generated output value is then passed to subsequent neurons.

The activation function provides scaling of the output and were illustrated in Figure 5.8 and can be described as, being

---

[6] These fundamental elements of an artificial neural network are also called processing elements, computation units, neurons or nodes.

(a) a signum threshold function (Figure 5.8(a)) described by

$$\begin{aligned} &\text{if } v > 0 \quad \text{then } \varphi(v) = 1 \\ &\text{if } v = 0 \quad \text{then } \varphi(v) = 0 \\ &\text{if } v < 0 \quad \text{then } \varphi(v) = -1 \end{aligned} \tag{K.2}$$

Note that when the activation function range is from 0 to 1, this type of neuron has an all-or-none firing properties as described by the McCulloch-Pitts model[7];

(b) a piece-wise linear (ramp) function (Figure 5.8(b)) described by

$$\begin{aligned} &\text{if } v \geq v_a \quad \text{then } \varphi(v) = 1 \\ &\text{if } v_b < v < v_a \quad \text{then } \varphi(v) = av \\ &\text{if } v < v_b \quad \text{then } \varphi(v) = -1 \end{aligned} \tag{K.3}$$

where a is the amplification factor of the linear mapping region; and

(c) a sigmoid function (Figure 5.8(c)) which may have several forms

$$\text{(I) } \varphi(v) = \frac{1}{1 + exp(-av)} \tag{K.4a}$$

(Note that when the slope parameter, a, approaches infinity the function becomes a threshold function.);

$$\text{(ii) } \varphi(v) = tanh\left(\frac{v}{2}\right) = \frac{1 - exp(-v)}{1 + exp(-v)} \tag{K.4b}$$

which represents a hyperbolic tangent function, or

$$\text{(iii) } \varphi(v) = \frac{v^2}{1 + v^2} \tag{K.4c}$$

which represents a parametric relation [Simpson, 1992]. The sigmoid functions are the most popular since they are continuous, differentiable monotonically increasing function that exhibits smoothness and asymptotic properties. Note that the hyperbolic tangent function as previously defined in Equation K.4b.

---

[7] The McCulloch-Pitt neuron is an *n*-input, single output element with a signum nonlinearity.

K.3 Net Architecture

When this research commenced, very little information for net synthesis was available. Since design principles did not exist, this section summarizes some of the considerations made when designing the neural networks for this application. The selection of inputs, the consideration of using dynamic nets[8], the selection of output parameters, the connection topography and the number of nodes and layers are discussed in this section.

The first consideration was selecting input parameters. The angular displacement and translational displacement of the reconfigurable mass were chosen as the relation between these parameters are coupled (as given in Table 3.1). The coordination between the mass reconfiguration and the angular displacement ultimately determines the success in attenuating vibrations. Furthermore, including the translational displacement variable enables constraint information to be incorporated into the net. Because the interaction between the attenuation device and the angular oscillations is second order the time derivative data were also considered as inputs.

The connections may be within a layer and/or among nonadjacent levels/elements. Typically, the feedback connection incorporates derivative information or a time delay ($\frac{d}{dt}$ or z^{-1}). The feedback connection may operate in several ways as shown in Figure K.1; time-delayed feedback from the input nodes supplement the input layer with derivative information of the external inputs; time-delayed feedback from the hidden layer creates additional, internal input nodes[9]; time-delayed feedback from the output layer also creates internal input nodes[10], and/or a combination of these option. Another topography for nets is that connections may be local creating a partially connected network.

---

[8] Ibid.
[9] This is called an Elman network [Pham and Karaboga, 1999].
[10] This is called a Jordan network [Pham and Karaboga, 1999].

Feed forward nets with appropriate time delay elements have been successfully applied to identify dynamic systems [Pham and Karaboga, 1999]; however, they are plagued by requiring a large number of input nodes which infers extensive computations and training requirements; these networks are susceptible to noise. Furthermore, training these types of net as an independent simulator are difficult. Recurrent nets have been applied to dynamic systems without these drawbacks [Ku and Lee, 1995] and are especially popular in real-time control applications.

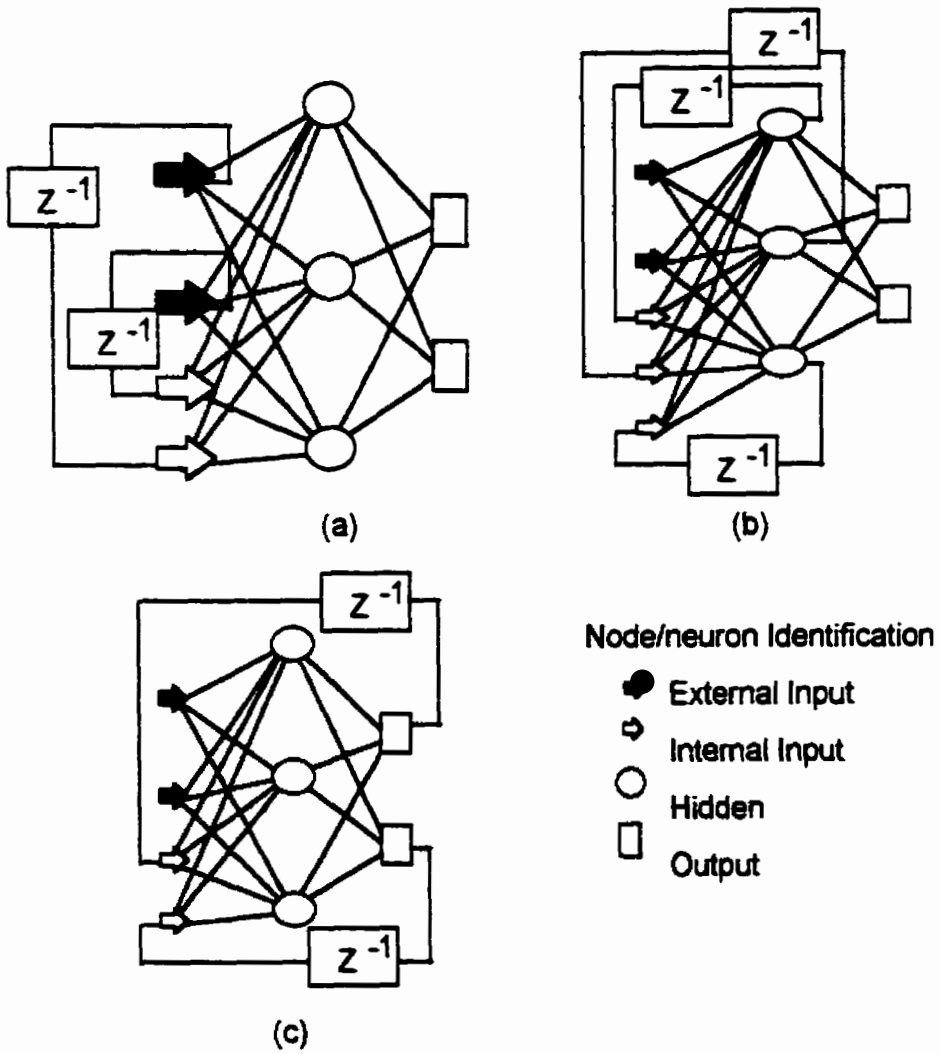

Figure K.1 Various types of recurrent networks include (a) nodal, (b) Elman and (c) Jordan.

Consideration was given to implement a recurrent or dynamic net. A trial net was created where time-delays were introduced for the input displacements as illustrated in Figure K.2. Other types of recurrent or feedback action within the net were not considered. Since hidden layers typically contain more nodes than an input layer, adding recurrence to these levels would create a larger net that would increase the storage or memory requirements and related computations.

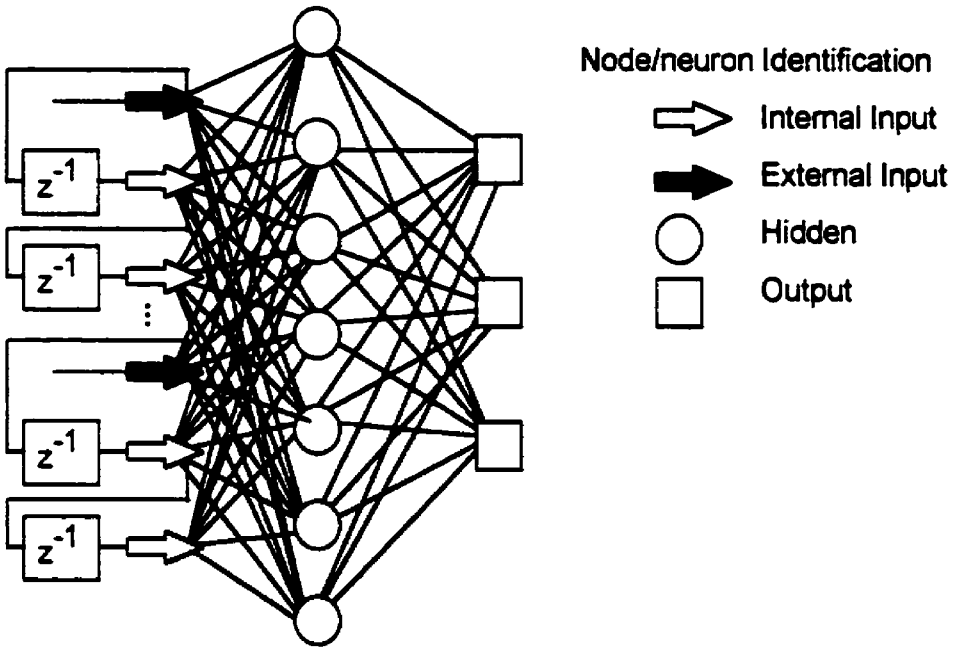

Figure K.2 Prototype neural networks with recurrent input nodes.

As an alternative to adding time delays to the input nodes, both the instantaneous displacement and velocity values for the input parameters were added as input parameters. This has similar effects as a time delayed neural network. This net was as easily trained to learn input-output relations and required less computational resources as the recurrent net (Figure K.2). At the time of developing the net morphology [Stilling, 1991 and 1990a; Stilling and Watson, 1991 and 1990], providing appropriate dynamic input parameters was believed to free the net from storing time dependent operations (such as calculating derivatives or integrals) and other calculated

information (such as products) internally. Providing dynamic input parameters, especially integral relations, has since become accepted practice in control applications [Qian et al., 1998].

The output parameters as presented in Sections 5.6.3 and 8.3.1 were either the kinematic parameters ($\theta(t), \dot{\theta}(t), r(t)$ and $\dot{r}(t)$) or three tri-state values. The net used as a controller was either an *I-J-K-4* or an *I-J-K-3*. For either case, the output data was post processed prior to being fed to the control mechanism (or simulation package that implements the control action). For the *I-J-K-4* network, the output nodes corresponding to the translational velocity of the attenuation mechanism required only a unity gain as the post processor, as the value was readily incorporated into the simulation package of the controlled system. For the three parameter output, the norm of the output vector was compared to preset limits (as discussed in Section 8.3.4.2).

The size of the net affects its computational ability and as described in Section 8.3.1 the net size was established by having the neural network learn a time based inverse of the controlled system which was believed to be a superset of the desired control action. The result was a network with three sets of adjustable weights with the number of nodes being 4 input nodes, 13 and 11 nodes in the first and second hidden layer and either 3 or 4 nodes in the output layer. Also a bias node was added to each input layer. Thus the number of connecting or adjusting weights were 252 or 241, respectively.

To conclude, the net selected for this investigation was a feed-forward, multi-layer, static net[11]. The processing capabilities of each neuron was described by Equation K.1. The net topology consisted of fully interconnected neurons between adjacent layers, with no interconnections within a layer. The data processing was contiguous whereby information was passed through to consecutive layers; that is, the output of the preceding layer formed

[11] A static network has only feed forward connections; there is no recurrence. In contrast a dynamic net has both feed forward and feed backward connections. [Zbikowski and Gawthrop, 1995].

the input of the current layer which was then processed and passed to the next layer. The vector for the input layer represents the kinematic state of the structure containing both position and derivative information. Two hidden layers were chosen to provide intermediate mapping which gave the net three layers of adjustable weights. The output layer provided the generated control response. The net provided a matching of the kinematic sensory data to the control response that was required for attenuating vibrations. The selected nets appeared mathematically tractable and would not tax available memory resources, yet appeared to be practical and to provide good flexibility.

K.3 Neural Network Training

"Training" of the neural network refers to adjusting the interconnecting weights so that the input-output relation can be learned. The artificial neural network controller was to provide predictive control action by imitating a controlled mass-pendulum system. Regardless of the system to be imitated, the net essentially functions as a "smart" function generator where the input parameters of $\theta(t), \dot{\theta}(t), r(t)$ and $\dot{r}(t)$ were used to generate output vectors that were processed to give an appropriate control signal ($m(t)$). To provide the time-dependent sensitivity, the parameters contained derivative data and input-output patterns were time delayed. The development of the neural net controller involved training the net, validating the training and implementing the net. This section discusses the training process. Sample training and validation suites are given in Appendix L. The energy reduction associated when the net was implemented as a controller appears in Chapter 8.

The mode of training was "supervisory" where the net generated output was compared to a desired or target output to generate an error value that is minimized by adjusting the interconnecting weights. An "off-line" error- driven training process where exemplar patterns were generated by periodically sampling a controlled mass-pendulum system was used. However, initially,

an external rule base was used to monitor and select appropriate control in an "on-line" training mode. With the "on-line" training, the learning was *in situ* and completed pattern by pattern as the patterns were being generated by the rule base monitor. When "off-line" training was completed, the training was primarily, in batch mode[12] where the entire set of input-output patterns were generated *a priori* to the initiation of training. Details of these training modes are discussed concurrently with the generation of the exemplar patterns.

Supervised training algorithms, for both pattern and batch modes of training, were used to train the artificial neural networks. The training process is represented in the flowchart of Figure K.3. Initially, small random values were assumed for the adjustable connections. A comparison between the expected response and the net generated response was formulated as an expected error function that was defined as either a sum of squares or a mean square sum.

The error associated with a particular output node for a single pattern was defined as

$$e_l = \left(y_l^d - y_l\right)^2 \tag{K.5}$$

where e_l represents the error signal of the lth output;

y, an output value; and

the superscript, d, indicates the desired, corresponding output.

The expected error function for the output layer for a given pattern was expressed as an averaged sum of the output errors,

$$E_p = \frac{1}{2L}\sum_{l=1}^{L}\left(y_l^d - y_l\right)^2 \tag{K.6}$$

where E_p is the error over the output vector for a single pattern, p, and

L is the number of nodes in the output layer.

[12] Batch mode training will also be referred to as epoch training.

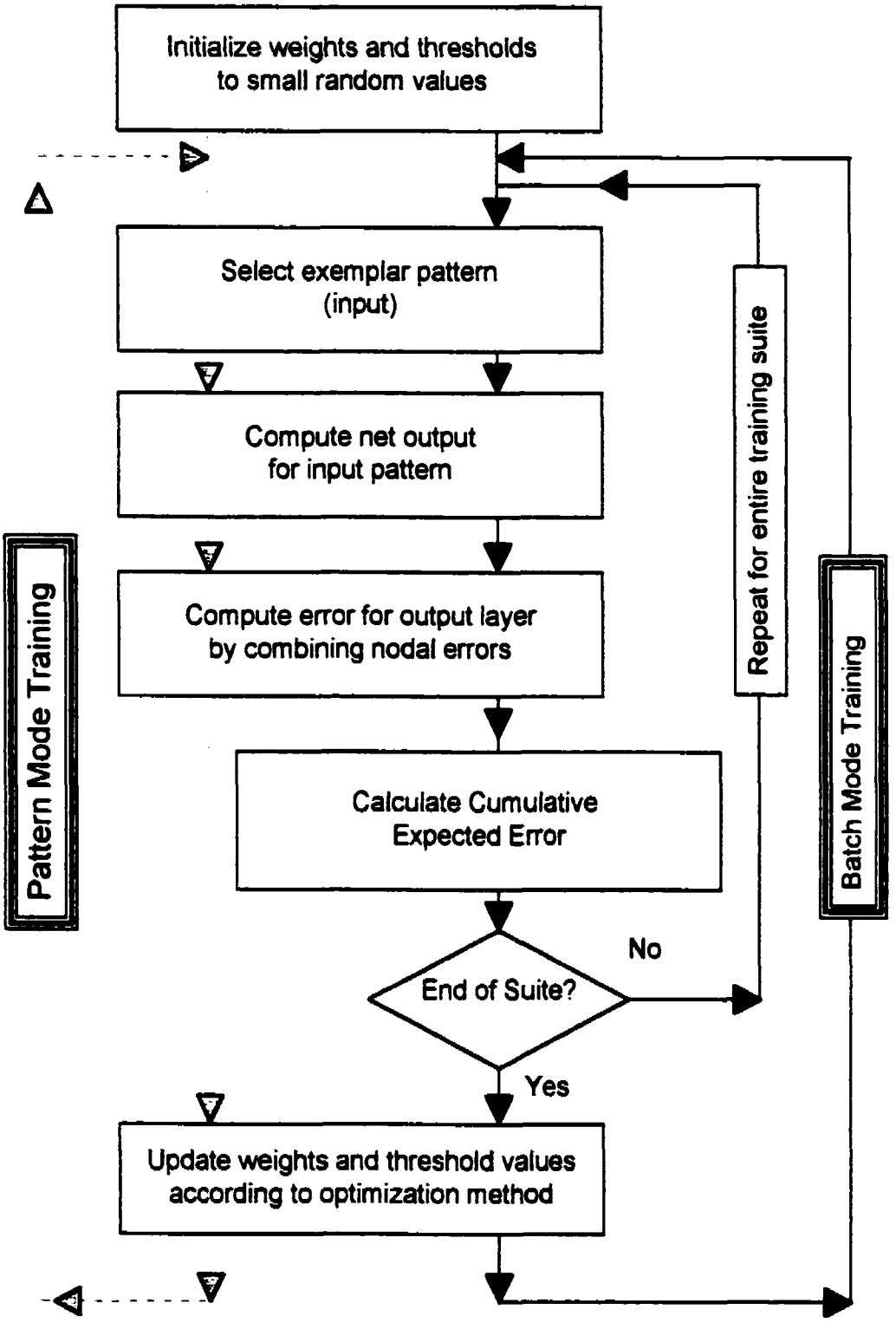

Figure K.3 Flowchart representing both pattern (dashed lines) and batch mode (solid lines) supervised, error correction training.

For the batch training mode, the expected error function was defined by summing the output layer error over the training suite[13], as given by

$$E = \frac{1}{P}\sum_{p=1}^{P} E_p \qquad \text{(K.7)}$$

where P is the number of patterns in the training suite.

Since the supervised training process was viewed as an unconstrained minimization problem. Various optimization techniques (such as, coordinate search, conjugate gradient, Powell, evolutionary algorithms and others) for adjusting the weights were implemented to minimize the error function. A brief overview of the algorithms appear in Appendix J.

Computationally, the optimization algorithms should involve minimal computational effort and not be memory expensive; thus, ideally, the function should be evaluated as few times as possible. Convergence criteria were established based on the magnitude of the error function. Optimization methods find either global (true maximum or minimum values) or local (maximum or minimum values for a given region) extremum; usually finding the global extremum is desirable. Although training trials from different starting points were completed and did produce different weighting values for this control application, finding a global minimum was not ensured.

For minimization problems, a set of criteria to terminate the training process was established. Ideally, the output as generated by the net matches the target for a given input pattern. The convergence criteria were based on the error (cost) function reaching preset limits. Regardless of the training mode, the error averaged over the entire training suite was less than a set value and no one pattern could have an error greater than a set limit. A level of confidence was defined in terms of the norm of the target output vector for the training suite for the trinomial output net.

---

[13] The training suite refers to the entire set of exemplar patterns used for setting the connecting weights of a network.

Despite training to a global minimum being intuitively desirable, convergence to a global minimum resulted in "overtraining" which did not always produce the best functioning net for this application. When training convergence was relaxed the net operation was more general and appropriate for a wider set of operating conditions in comparison to nets with lower convergence limits. This concept has since been reported by others who have shown that an "overtrained" neural networks do not tolerate variations to the input when generating a corresponding output .

The training scheme first implemented was Back Propagation using a pattern training mode [Stilling, 1990a]. However, during the training, previously trained patterns appeared to be "forgotten". To enhance the pattern training mode, patterns were introduced randomly rather than in the same sequence. Then, eventually, a batch training mode was adopted. The change was that the error and its gradient were tallied over the entire training suite.

Early efforts using training techniques developed by implementing the various optimization techniques were done as an on-line training methods where the paired input-output patterns were generated by assessing three possible control actions; namely, motion of the mass towards the pivot, motion of the mass away from the pivot and no motion of the mass. The change of structural energy for each possibility was examined and the control action corresponding to the maximum reduction in energy was chosen. As this assessment was done at discrete time steps, the *pattern training* format was applied after each set of evaluations [Stilling, 1990a]. Alternately, the patterns could be stored for off-line *batch training*. The second method of generating a training suite was to sample simulations of the system as it was being controlled; for example, training suites were generated as a human performed the control, when a proportional and derivative control action was employed or when the knowledge based controller was used. These exemplar patterns were used for off-line, batch training mode. Appendix L

contains a sample set of exemplar patterns used for training and validated the neural network.

These other optimization techniques were evaluated using benchmark systems. The two systems chosen were the XOR mapping and a binary encoding system. For the XOR problem the net that was trained was a 2-3-3-1 feed forward weighted sum network. The binary encoding sequence used as 5-7-7-5 network. Good convergence (error minimization) was achieved for the XOR case, for all training algorithms, as this problem can be viewed as an identification problem that has a unique solution. Also, the patterns for the binary encoded sequence were trained using each method.

The back propagation technique had an average number of computations per iteration and was easily programmed using linear algebra. It provided good initial convergence but was slow during the final reduction of the sum of square errors. The coordinate search method performance was dependent on the line search method; it required few computations per each training iteration and provided improved convergence over the back propagation method. The conjugate gradient and the Powell method produced similar results. The Powell method was computationally less intense per training iteration but tended to require more training iterations to reduce the sum of square errors. The convergence with the conjugate gradient method tended to "jump" to improved states. Both of the evolutionary programs were relatively slow to converge. Because the genetic algorithm performs several parallel searches the computations per training iteration was large. These results were summarized by ordinal ranking of the computational intensity per training iteration, the convergence rate (the number of training iterations required to reduce the sum of square errors) and the likelihood of whether or not the training was towards a local or global minimum with results tabulated in Chapter 5.6.2. Comparable results were obtained when Powell and conjugate gradient training algorithms were used,

the latter was chosen due to its ease in implementing in both software languages.

K.4 SUMMARY

The neural network selected was a multiple layer, feed forward net. The input signals were time dependent, continuous values that represented the state of the dynamic system. The output signal provides control action; the output was either the same as the input parameters at a time step later or the control action was mapped to a tri-valued output set. Two hidden layers were creating either approximately 240-250 adjustable weights in the entire net. Training was done, primarily, in a supervisory, error-reduction mode to create a "proxy" controller for attenuating vibrational energy of the mass-pendulum system. As artificial neural networks were in their infancy at the time of initiating this phase of the research, many software tools were developed. Developments included training algorithms using optimization techniques, determining net size based on the inverse problem and using time derivative data to provide dynamics to the network. The training and evaluation of the neural network involved an assessment of the training using a validation suited which was followed by implementing the net at the controller in the mass-pendulum system.

Appendix L: Artificial Neural Network Training and Validation Data

The artificial neural network controllers were trained to be "proxies" of other control systems, such as the human operator system, the rule base system and others. The training data was sampled from the pendulum system when the control action produced effective vibration attenuation.

The exemplar patterns were paired input-output data. Both the training and validation suites were generated from the same simulation; sampling was done at slightly different times. The training suite was used to set the weights of the artificial neural network controller; whereas the validation suite evaluated the training of the neural network controller. The input data contained the angular displacement and velocity of the pendulum and the translational position and the velocity of the auxiliary or sliding mass. The matched output data was either the same kinematic parameters sampled at a time step, Δt, later or a three value output vector ([111], [000] or [-1-1-1]) based on the translational velocity of the reconfigurable mass.

The training suite and the validation suite each contained approximately 100 samples and believed to span the operating range for the system. Also, the "pristine values as generated from the simulation were used; that is, the patterns did not contain any artifact or noise

For the human operator controller, as presented in Chapter 7, the control motion for the auxiliary mass was a relay action characterized by piece-wise constant velocity motion. The user selected whether the mass should be moved towards or away from the pivot or no motion at all with the corresponding velocity being -1 m/s , 1 m/s or 0 m/s. The input-output data

was sampled at 12.5 Hz which corresponds to the simulation time step of 0.08 seconds. The corresponding training suite appears in Table L.1 and the validation suite follows in Table L.2. Note that due to the relay action the kinematic output data for the translational velocity of the auxiliary mass matches the tri-value output data.

Table L.1 Training Suite Data from Human Operator Controlled System

Input Data				Output Data Set 1				Output Data Set 2		
θ	$\dot{\theta}$	r	$\dot{r}$	θ	$\dot{\theta}$	r	$\dot{r}$			
0.5256	0	1	0	0.498	-0.5369	0.95	-1	-1	-1	-1
0.463	-0.8673	0.9	-1	0.4105	-1.2357	0.85	-1	-1	-1	-1
0.3386	-1.6406	0.8	-1	0.2456	-2.078	0.75	-1	-1	-1	-1
0.1383	-2.2031	0.75	0	0.0333	-1.9924	0.8	1	1	1	1
-0.0606	-1.7628	0.85	1	-0.1429	-1.5241	0.9	1	1	1	1
-0.2131	-1.2843	0.95	1	-0.2715	-1.0494	1	1	1	1	1
-0.3183	-0.824	1.05	1	-0.3542	-0.6112	1.1	1	1	1	1
-0.382	-0.4958	1.05	-1	-0.4032	-0.3504	1	-1	-1	-1	-1
-0.4164	-0.172	0.95	-1	-0.4197	0.0422	0.9	-1	-1	-1	-1
-0.4114	0.2954	0.85	-1	-0.3894	0.5902	0.8	-1	-1	-1	-1
-0.3515	0.9288	0.75	-1	-0.2997	1.1386	0.75	0	0	0	0
-0.2382	1.3128	0.75	0	-0.1734	1.2759	0.8	1	1	1	1
-0.1111	1.211	0.85	1	-0.0526	1.1253	0.9	1	1	1	1
0.0012	1.0251	0.95	1	0.0497	0.9152	1	1	1	1	1
0.0926	0.8	1.05	1	0.1297	0.6828	1.1	1	1	1	1
0.161	0.5665	1.15	1	0.1865	0.4531	1.2	1	1	1	1
0.2064	0.3444	1.25	1	0.2216	0.2609	1.25	0	0	0	0
0.2328	0.1875	1.2	-1	0.2401	0.1	1.15	-1	-1	-1	-1
0.2426	-0.0022	1.1	-1	0.2395	-0.1197	1.05	-1	-1	-1	-1
0.2303	-0.2527	1	-1	0.214	-0.4011	0.95	-1	-1	-1	-1
0.1898	-0.5644	0.9	-1	0.1572	-0.7412	0.85	-1	-1	-1	-1
0.1154	-0.9295	0.8	-1	0.0674	-0.9856	0.8	0	0	0	0
0.0174	-1.0117	0.8	0	-0.0367	-1.1501	0.75	-1	-1	-1	-1
-0.0899	-0.9777	0.8	1	-0.1346	-0.8076	0.85	1	1	1	1
-0.1708	-0.6437	0.9	1	-0.1992	-0.4888	0.95	1	1	1	1
-0.22	-0.3448	1	1	-0.2339	-0.2129	1.05	1	1	1	1
-0.2415	-0.0938	1.1	1	-0.2435	0.0123	1.15	1	1	1	1
-0.2406	0.1054	1.2	1	-0.2324	0.2197	1.15	-1	-1	-1	-1
-0.2183	0.3452	1.1	-1	-0.1977	0.4813	1.05	-1	-1	-1	-1

Input Data				Output Data Set 1				Output Data Set 2		
-0.17	0.6267	1	-1	-0.1348	0.7795	0.95	-1	-1	-1	-1
-0.0963	0.7589	1	1	-0.0592	0.7244	1.05	1	1	1	1
-0.024	0.679	1.1	1	0.0085	0.6254	1.15	1	1	1	1
0.0384	0.566	1.2	1	0.0651	0.5028	1.25	1	1	1	1
0.0895	0.4724	1.25	0	0.1122	0.4329	1.25	0	0	0	0
0.1327	0.3848	1.25	0	0.1506	0.3293	1.25	0	0	0	0
0.1661	0.2907	1.2	-1	0.1794	0.2405	1.15	-1	-1	-1	-1
0.1899	0.1775	1.1	-1	0.1969	0.1009	1.05	-1	-1	-1	-1
0.1997	0.0097	1	-1	0.1976	-0.0969	0.95	-1	-1	-1	-1
0.1897	-0.2196	0.9	-1	0.1753	-0.3586	0.85	-1	-1	-1	-1
0.1535	-0.5138	0.8	-1	0.1236	-0.6845	0.75	-1	-1	-1	-1
0.0897	-0.6652	0.8	1	0.0573	-0.6311	0.85	1	1	1	1
0.0268	-0.5862	0.9	1	-0.0011	-0.5337	0.95	1	1	1	1
-0.0264	-0.4762	1	1	-0.0488	-0.416	1.05	1	1	1	1
-0.068	-0.3548	1.1	1	-0.0843	-0.294	1.15	1	1	1	1
-0.0975	-0.2347	1.2	1	-0.1078	-0.1779	1.25	1	1	1	1
-0.1156	-0.1341	1.25	0	-0.1212	-0.0876	1.25	0	0	0	0
-0.1244	-0.0395	1.25	0	-0.1251	0.0093	1.25	0	0	0	0
-0.1234	0.0581	1.25	0	-0.1191	0.1148	1.2	-1	-1	-1	-1
-0.1118	0.1768	1.15	-1	-0.1013	0.2434	1.1	-1	-1	-1	-1
-0.0874	0.3142	1.05	-1	-0.0698	0.388	1	-1	-1	-1	-1
-0.0485	0.4635	0.95	-1	-0.026	0.4367	1	1	1	1	1
-0.0049	0.4038	1.05	1	0.0142	0.3666	1.1	1	1	1	1
0.0316	0.3265	1.15	1	0.0469	0.2849	1.2	1	1	1	1
0.0601	0.2427	1.25	1	0.0716	0.2168	1.25	0	0	0	0
0.0817	0.1867	1.25	0	0.0902	0.153	1.25	0	0	0	0
0.097	0.1162	1.25	0	0.102	0.0839	1.2	-1	-1	-1	-1
0.1052	0.0454	1.15	-1	0.1064	0.0003	1.1	-1	-1	-1	-1
0.1051	-0.0515	1.05	-1	0.1011	-0.1102	1	-1	-1	-1	-1
0.094	-0.1756	0.95	-1	0.0834	-0.2476	0.9	-1	-1	-1	-1
0.0707	-0.2606	0.95	1	0.0575	-0.2656	1	1	1	1	1
0.0442	-0.2641	1.05	1	0.0312	-0.2572	1.1	1	1	1	1
0.0186	-0.2459	1.15	1	0.0066	-0.2311	1.2	1	1	1	1
-0.0044	-0.2137	1.25	1	-0.015	-0.2099	1.25	0	0	0	0
-0.0253	-0.2019	1.25	0	-0.0352	-0.19	1.25	0	0	0	0
-0.0443	-0.1744	1.25	0	-0.0525	-0.1553	1.25	0	0	0	0
-0.0598	-0.1332	1.25	0	-0.0658	-0.1086	1.25	0	0	0	0
-0.0708	-0.0889	1.2	-1	-0.0746	-0.0645	1.15	-1	-1	-1	-1

Input Data				Output Data Set 1				Output Data Set 2		
-0.0771	-0.0352	1.1	-1	-0.0781	-0.0006	1.05	-1	-1	-1	-1
-0.0771	0.0393	1	-1	-0.074	0.0849	0.95	-1	-1	-1	-1
-0.0685	0.1361	0.9	-1	-0.0603	0.1928	0.85	-1	-1	-1	-1
-0.0504	0.201	0.9	1	-0.0403	0.2031	0.95	1	1	1	1
-0.0302	0.2002	1	1	-0.0203	0.1932	1.05	1	1	1	1
-0.0109	0.1831	1.1	1	-0.002	0.1704	1.15	1	1	1	1
0.006	0.156	1.2	1	0.0134	0.1402	1.25	1	1	1	1
0.0203	0.1336	1.25	0	0.0268	0.1243	1.25	0	0	0	0
0.0327	0.1126	1.25	0	0.038	0.0987	1.25	0	0	0	0
0.0425	0.0829	1.25	0	0.0464	0.0711	1.2	-1	-1	-1	-1
0.0496	0.0561	1.15	-1	0.052	0.0377	1.1	-1	-1	-1	-1
0.0533	0.0157	1.05	-1	0.0535	-0.0102	1	-1	-1	-1	-1
0.0522	-0.0402	0.95	-1	0.0493	-0.0743	0.9	-1	-1	-1	-1
0.0447	-0.1125	0.85	-1	0.038	-0.1547	0.8	-1	-1	-1	-1
0.0302	-0.1561	0.85	1	0.0225	-0.1532	0.9	1	1	1	1
0.0149	-0.1471	0.95	1	0.0078	-0.1383	1	1	1	1	1
0.0011	-0.1277	1.05	1	-0.0049	-0.1158	1.1	1	1	1	1
-0.0103	-0.103	1.15	1	-0.0152	-0.0897	1.2	1	1	1	1
-0.0193	-0.0762	1.25	1	-0.0229	-0.0679	1.25	0	0	0	0
-0.0261	-0.0583	1.25	0	-0.0287	-0.0475	1.25	0	0	0	0
-0.0308	-0.0357	1.25	0	0.0324	-0.0253	1.2	-1	-1	-1	-1
-0.0333	-0.013	1.15	-1	-0.0336	0.0014	1.1	-1	-1	-1	-1
-0.0331	0.0179	1.05	-1	-0.0318	0.0366	1	-1	-1	-1	-1
-0.0294	0.0575	0.95	-1	-0.026	0.0803	0.9	-1	-1	-1	-1
-0.0219	0.084	0.95	1	-0.0176	0.0852	1	1	1	1	1
-0.0134	0.0844	1.05	1	-0.0092	0.0819	1.1	1	1	1	1
-0.0052	0.078	1.15	1	-0.0014	0.0731	1.2	1	1	1	1
0.002	0.0673	1.25	1	0.0053	0.0659	1.25	0	0	0	0
0.0086	0.0631	1.25	0	0.0116	0.0591	1.25	0	0	0	0
0.0145	0.054	1.25	0	0.017	0.0478	1.25	0	0	0	0
0.0192	0.0406	1.25	0	0.0211	0.0327	1.25	0	0	0	0
0.0225	0.0241	1.25	0	0.0235	0.0151	1.25	0	0	0	0
0.024	0.0057	1.25	0	0.0236	-0.0142	1.2	-1	-1	-1	-1

The validation process involved presenting the set of exemplar patterns to the net and calculating the cumulative error. The validation process provied a single measure for the training that had been achieved.

Table L.2 Validation Suite Data from Human Operator Controlled System

Input Data				Output Data Set 1				Output Data Set 2		
θ	$\dot{\theta}$	r	$\dot{r}$	θ	$\dot{\theta}$	r	$\dot{r}$			
0.498	-0.537	0.95	-1	0.463	-0.867	0.9	-1	-1	-1	-1
0.4105	-1.236	0.85	-1	0.3386	-1.641	0.8	-1	-1	-1	-1
0.2456	-2.078	0.75	-1	0.1383	-2.203	0.75	0	0	0	0
0.0333	-1.992	0.8	1	-0.061	-1.763	0.85	1	1	1	1
-0.143	-1.524	0.9	1	-0.213	-1.284	0.95	1	1	1	1
-0.272	-1.049	1	1	-0.318	-0.824	1.05	1	1	1	1
-0.354	-0.611	1.1	1	-0.382	-0.496	1.05	-1	-1	-1	-1
-0.403	-0.35	1	-1	-0.416	-0.172	0.95	-1	-1	-1	-1
-0.42	0.0422	0.9	-1	-0.411	0.2954	0.85	-1	-1	-1	-1
-0.389	0.5902	0.8	-1	-0.352	0.9288	0.75	-1	-1	-1	-1
-0.3	1.1386	0.75	0	-0.238	1.3128	0.75	0	0	0	0
-0.173	1.2759	0.8	1	-0.111	1.211	0.85	1	1	1	1
-0.053	1.1253	0.9	1	0.0012	1.0251	0.95	1	1	1	1
0.0497	0.9152	1	1	0.0926	0.8	1.05	1	1	1	1
0.1297	0.6828	1.1	1	0.161	0.5665	1.15	1	1	1	1
0.1865	0.4531	1.2	1	0.2064	0.3444	1.25	1	1	1	1
0.2216	0.2609	1.25	0	0.2328	0.1875	1.2	-1	-1	-1	-1
0.2401	0.1	1.15	-1	0.2426	-0.002	1.1	-1	-1	-1	-1
0.2395	-0.12	1.05	-1	0.2303	-0.253	1	-1	-1	-1	-1
0.214	-0.401	0.95	-1	0.1898	-0.564	0.9	-1	-1	-1	-1
0.1572	-0.741	0.85	-1	0.1154	-0.93	0.8	-1	-1	-1	-1
0.0674	-0.986	0.8	0	0.0174	-1.012	0.8	0	0	0	0
-0.037	-1.15	0.75	-1	-0.09	-0.978	0.8	1	1	1	1
-0.135	-0.808	0.85	1	-0.171	-0.644	0.9	1	1	1	1
-0.199	-0.489	0.95	1	-0.22	-0.345	1	1	1	1	1
-0.234	-0.213	1.05	1	-0.242	-0.094	1.1	1	1	1	1
-0.244	0.0123	1.15	1	-0.241	0.1054	1.2	1	1	1	1
-0.232	0.2197	1.15	-1	-0.218	0.3452	1.1	-1	-1	-1	-1
-0.198	0.4813	1.05	-1	-0.17	0.6267	1	-1	-1	-1	-1
-0.135	0.7795	0.95	-1	-0.096	0.7589	1	1	1	1	1
-0.059	0.7244	1.05	1	-0.024	0.679	1.1	1	1	1	1
0.0085	0.6254	1.15	1	0.0384	0.566	1.2	1	1	1	1
0.0651	0.5028	1.25	1	0.0895	0.4724	1.25	0	0	0	0
0.1122	0.4329	1.25	0	0.1327	0.3848	1.25	0	0	0	0
0.1506	0.3293	1.25	0	0.1661	0.2907	1.2	-1	-1	-1	-1
0.1794	0.2405	1.15	-1	0.1899	0.1775	1.1	-1	-1	-1	-1
0.1969	0.1009	1.05	-1	0.1997	0.0097	1	-1	-1	-1	-1

Input Data				Output Data Set 1				Output Data Set 2		
0.1976	-0.097	0.95	-1	0.1897	-0.22	0.9	-1	-1	-1	-1
0.1753	-0.359	0.85	-1	0.1535	-0.514	0.8	-1	-1	-1	-1
0.1236	-0.685	0.75	-1	0.0897	-0.665	0.8	1	1	1	1
0.0573	-0.631	0.85	1	0.0268	-0.586	0.9	1	1	1	1
-0.001	-0.534	0.95	1	-0.026	-0.476	1	1	1	1	1
-0.049	-0.416	1.05	1	-0.068	-0.355	1.1	1	1	1	1
-0.084	-0.294	1.15	1	-0.098	-0.235	1.2	1	1	1	1
-0.108	-0.178	1.25	1	-0.116	-0.134	1.25	0	0	0	0
-0.121	-0.088	1.25	0	-0.124	-0.04	1.25	0	0	0	0
-0.125	0.0093	1.25	0	-0.123	0.0581	1.25	0	0	0	0
-0.119	0.1148	1.2	-1	-0.112	0.1768	1.15	-1	-1	-1	-1
-0.101	0.2434	1.1	-1	-0.087	0.3142	1.05	-1	-1	-1	-1
-0.07	0.388	1	-1	-0.049	0.4635	0.95	-1	-1	-1	-1
-0.026	0.4367	1	1	-0.005	0.4038	1.05	1	1	1	1
0.0142	0.3666	1.1	1	0.0316	0.3265	1.15	1	1	1	1
0.0469	0.2849	1.2	1	0.0601	0.2427	1.25	1	1	1	1
0.0716	0.2168	1.25	0	0.0817	0.1867	1.25	0	0	0	0
0.0902	0.153	1.25	0	0.097	0.1162	1.25	0	0	0	0
0.102	0.0839	1.2	-1	0.1052	0.0454	1.15	-1	-1	-1	-1
0.1064	0.0003	1.1	-1	0.1051	-0.052	1.05	-1	-1	-1	-1
0.1011	-0.11	1	-1	0.094	-0.176	0.95	-1	-1	-1	-1
0.0834	-0.248	0.9	-1	0.0707	-0.261	0.95	-1	-1	-1	-1
0.0575	-0.266	1	1	0.0442	-0.264	1.05	1	1	1	1
0.0312	-0.257	1.1	1	0.0186	-0.246	1.15	1	1	1	1
0.0066	-0.231	1.2	1	-0.004	-0.214	1.25	1	1	1	1
-0.015	-0.21	1.25	0	-0.025	-0.202	1.25	0	0	0	0
-0.035	-0.19	1.25	0	-0.044	-0.174	1.25	0	0	0	0
-0.053	-0.155	1.25	0	-0.06	-0.133	1.25	0	0	0	0
-0.066	-0.109	1.25	0	-0.071	-0.089	1.2	-1	-1	-1	-1
-0.075	-0.065	1.15	-1	-0.077	-0.035	1.1	-1	-1	-1	-1
-0.078	-6E-04	1.05	-1	-0.077	0.0393	1	-1	-1	-1	-1
-0.074	0.0849	0.95	-1	-0.069	0.1361	0.9	-1	-1	-1	-1
-0.06	0.1928	0.85	-1	-0.05	0.201	0.9	1	1	1	1
-0.04	0.2031	0.95	1	-0.03	0.2002	1	1	1	1	1
-0.02	0.1932	1.05	1	-0.011	0.1831	1.1	1	1	1	1
-0.002	0.1704	1.15	1	0.006	0.156	1.2	1	1	1	1
0.0134	0.1402	1.25	1	0.0203	0.1336	1.25	0	0	0	0
0.0268	0.1243	1.25	0	0.0327	0.1126	1.25	0	0	0	0
0.038	0.0987	1.25	0	0.0425	0.0829	1.25	0	0	0	0
0.0464	0.0711	1.2	-1	0.0496	0.0561	1.15	-1	-1	-1	-1

Input Data				Output Data Set 1				Output Data Set 2		
0.052	0.0377	1.1	-1	0.0533	0.0157	1.05	-1	-1	-1	-1
0.0535	-0.01	1	-1	0.0522	-0.04	0.95	-1	-1	-1	-1
0.0493	-0.074	0.9	-1	0.0447	-0.113	0.85	-1	-1	-1	-1
0.038	-0.155	0.8	-1	0.0302	-0.156	0.85	1	1	1	1
0.0225	-0.153	0.9	1	0.0149	-0.147	0.95	1	1	1	1
0.0078	-0.138	1	1	0.0011	-0.128	1.05	1	1	1	1
-0.005	-0.116	1.1	1	-0.01	-0.103	1.15	1	1	1	1
-0.015	-0.09	1.2	1	-0.019	-0.076	1.25	1	1	1	1
-0.023	-0.068	1.25	0	-0.026	-0.058	1.25	0	0	0	0
-0.029	-0.048	1.25	0	-0.031	-0.036	1.25	0	0	0	0
-0.032	-0.025	1.2	-1	-0.033	-0.013	1.15	-1	-1	-1	-1
-0.034	0.0014	1.1	-1	-0.033	0.0179	1.05	-1	-1	-1	-1
-0.032	0.0366	1	-1	-0.029	0.0575	0.95	-1	-1	-1	-1
-0.026	0.08	0.9	-1	-0.022	0.08	1	1	1	1	1
-0.018	0.0852	1	1	-0.013	0.0844	1.05	1	1	1	1
-0.009	0.0819	1.1	1	-0.005	0.078	1.15	1	1	1	1
-0.001	0.0731	1.2	1	0.002	0.0673	1.25	1	1	1	1
0.0053	0.0659	1.25	0	0.0086	0.0631	1.25	0	0	0	0
0.0116	0.0591	1.25	0	0.0145	0.054	1.25	0	0	0	0
0.017	0.0478	1.25	0	0.0192	0.0406	1.25	0	0	0	0
0.0211	0.03	1.3	0	0.0225	0.02	1.3	0	0	0	0
0.0235	0.0151	1.25	0	0.024	0.0057	1.25	0	0	0	0